International Doctorate Program in Molecular Oncology and Endocrinology

Doctorate School in Molecular Medicine

XXII cycle - 2006–2009

Coordinator: Prof. Giancarlo Vecchio

Functional role of the CXCR4 chemokine receptor in thyroid cancer

Elvira Avilla

University of Naples Federico II
Dipartimento di Biologia e Patologia Cellulare e Molecolare
"L. Califano"

Administrative Location

Dipartimento di Biologia e Patologia Cellulare e Molecolare "L. Califano"
Università degli Studi di Napoli Federico II

Partner Institutions

Italian Institutions
Università degli Studi di Napoli "Federico II", Naples, Italy
Istituto di Endocrinologia ed Oncologia Sperimentale "G. Salvatore", CNR, Naples, Italy
Seconda Università di Napoli, Naples, Italy
Università degli Studi di Napoli "Parthenope", Naples, Italy
Università del Sannio, Benevento, Italy
Università di Genova, Genoa, Italy
Università di Padova, Padua, Italy
Università degli Studi "Magna Graecia", Catanzaro, Italy
Università degli Studi di Firenze, Florence, Italy
Università degli Studi di Bologna, Bologna, Italy
Università degli Studi del Molise, Campobasso, Italy
Università degli Studi di Torino, Turin, Italy
Università di Udine, Udine, Italy

Foreign Institutions
Université Libre de Bruxelles, Brussels, Belgium
Universidade Federal de Sao Paulo, Brazil
University of Turku, Turku, Finland
Université Paris Sud XI, Paris, France
University of Madras, Chennai, India
University Pavol Jozef Šafàrik, Kosice, Slovakia
Universidad Autonoma de Madrid, Centro de Investigaciones Oncologicas (CNIO), Spain
Johns Hopkins School of Medicine, Baltimore, MD, USA
Johns Hopkins Krieger School of Arts and Sciences, Baltimore, MD, USA
National Institutes of Health, Bethesda, MD, USA
Ohio State University, Columbus, OH, USA
Albert Einstein College of Medicine of Yeshiwa University, N.Y., USA

Supporting Institutions
Ministero dell'Università e della Ricerca
Associazione Leonardo di Capua, Naples, Italy
Dipartimento di Biologia e Patologia Cellulare e Molecolare "L. Califano", Università degli Studi di Napoli "Federico II", Naples, Italy
Istituto Superiore di Oncologia (ISO), Genoa, Italy
Università Italo-Francese, Torino, Naples, Italy
Università degli Studi di Udine, Udine, Italy
Agenzia Spaziale Italiana
Istituto di Endocrinologia ed Oncologia Sperimentale "G. Salvatore", CNR, Naples, Italy

Italian Faculty

Giancarlo Vecchio, MD, Co-ordinator

Salvatore Maria Aloj, MD

Francesco Saverio Ambesi Impiombato, MD

Francesco Beguinot, MD

Maria Teresa Berlingieri, MD

Angelo Raffaele Bianco, MD

Bernadette Biondi, MD

Francesca Carlomagno, MD

Gabriella Castoria, MD

Angela Celetti, MD

Mario Chiariello, MD

Lorenzo Chiariotti, MD

Vincenzo Ciminale, MD

Annamaria Cirafici, PhD

Annamaria Colao, MD

Alma Contegiacomo, MD

Sabino De Placido, MD

Gabriella De Vita, MD

Monica Fedele, PhD

Pietro Formisano, MD

Alfredo Fusco, MD

Michele Grieco, MD

Massimo Imbriaco, MD

Paolo Laccetti, PhD

Antonio Leonardi, MD

Paolo Emidio Macchia, MD

Barbara Majello, PhD

Rosa Marina Melillo, MD

Claudia Miele, PhD

Francesco Oriente, MD

Roberto Pacelli, MD

Giuseppe Palumbo, PhD

Silvio Parodi, MD

Nicola Perrotti, MD

Giuseppe Portella, MD

Giorgio Punzo, MD

Antonio Rosato, MD

Guido Rossi, MD

Giuliana SalvatoreMD,

Massimo Santoro, MD

Giampaolo Tortora, MD

Donatella Tramontano, PhD

Giancarlo Troncone, MD

Giuseppe Viglietto, MD

Roberta Visconti, MD

Mario Vitale, MD

Foreign Faculty

Université Libre de Bruxelles, Belgium
Gilbert Vassart, MD
Jacques E. Dumont, MD

Universidade Federal de Sao Paulo, Brazil
Janete Maria Cerutti, PhD
Rui Monteiro de Barros Maciel, MD PhD

University of Turku, Turku, Finland
Mikko Laukkanen, PhD

Université Paris Sud XI, Paris, France
Martin Schlumberger, MD
Jean Michel Bidart, MD

University of Madras, Chennai, India
Arasambattu K. Munirajan, PhD

University Pavol Jozef Šafàrik, Kosice, Slovakia
Eva Cellárová, PhD
Peter Fedoročko, PhD

Universidad Autonoma de Madrid - Instituto de Investigaciones Biomedicas, Spain
Juan Bernal, MD, PhD
Pilar Santisteban, PhD

Centro de Investigaciones Oncologicas, Spain
Mariano Barbacid, MD

Johns Hopkins School of Medicine, USA
Vincenzo Casolaro, MD
Pierre A. Coulombe, PhD
James G. Herman MD
Robert P. Schleimer, PhD

Johns Hopkins Krieger School of Arts and Sciences, USA
Eaton E. Lattman, MD

National Institutes of Health, Bethesda, MD, USA
Michael M. Gottesman, MD
J. Silvio Gutkind, PhD
Genoveffa Franchini, MD
Stephen J. Marx, MD
Ira Pastan, MD
Phillip Gorden, MD

Ohio State University, Columbus, OH, USA
Carlo M. Croce, MD
Ginny L. Bumgardner, MD PhD

Albert Einstein College of Medicine of Yeshiwa University, N.Y., USA
Luciano D'Adamio, MD
Nancy Carrasco, MD

Functional role of the CXCR4 chemokine receptor in thyroid cancer

TABLE OF CONTENTS

LIST OF PUBLICATIONS

This dissertation is based upon the following publications:

I. De Falco V, Guarino V, **Avilla E**, Castellone MD, Salerno P, Salvatore G, Faviana P, Basolo F, Santoro M, Melillo RM. Biological role and potential therapeutic targeting of the chemokine receptor CXCR4 in undifferentiated thyroid cancer. *Cancer Res 2007 Dec 15;67(24):11821-9.*

II. Guarino V, Castellone MD, **Avilla E**, Melillo RM. Thyroid cancer and inflammation. *Molecular and Cellular Endocrinology 2009 Oct 14 (Epub ahead of print).*

III. Melillo RM, Guarino V, **Avilla E**, Galdiero MR, Liotti F, Prevete N, Rossi FW, Basolo F, Ugolini C, de Paulis A, Santoro M and Marone G. Mast cells play a protumorigenic role in human thyroid cancer. *Submitted to Oncogene.*

IV. **Avilla E**, Guarino V, Visciano C, Liotti F, Svelto M, Krisnamoorty G, Franco R and Melillo RM. Activation of TYRO3/AXL tyrosine kinase receptors in thyroid cancer. *Manuscript in preparation.*

ABSTRACT

Thyroid cancer is the most common endocrine malignancy and its incidence is increasing worldwide. We previously found that normal rat thyroid cells, transduced with papillary thyroid cancer (PTC)-related oncogenes, display an inflammatory signature, that includes cytokines, chemokines and their receptors (Melillo at al., 2005). One of the chemokine receptors we identified, CXCR4, is frequently up-regulated in thyroid cancer and the chemokine SDF-1, a CXCR4 ligand, induces proliferation, survival and invasive ability of PTC cells; moreover, CXCR4 blocking compounds inhibit thyroid cancer growth (Castellone et al., 2004; De Falco et al., 2007).

In order to better understand the molecular mechanisms of the biological effects of CXCR4/SDF-1α in thyroid carcer, we performed a global genome expression profile, through DNA microarrays, of CXCR4-expressing human papillary thyroid carcinoma cells (TPC-1) treated or not with SDF-1α. We identified, as transcriptional targets of CXCR4/SDF-1α**,** two tyrosine-kinase receptors: TYRO3 and AXL. These proteins belong to a small Protein Tyrosine Kinase (PTK) subfamily of receptors that includes three members: TYRO3, AXL and MER, from which this family is named TAM; they can be activated by two ligands, GAS6 and Protein S, are involved in the regulation of immune response, and are overexpressed in some epithelial cancers (Linger et al., 2008). We found that TPC-1 cells, derived from a human PTC, constitutively express TYRO3 and AXL receptors, but SDF-1α stimulation increased their protein level and tyrosine phosphorylation. We found that most of the available thyroid cancer cell lines express both the receptors, albeit to different extent, and AXL was always much more abundant than TYRO3. In most cell lines, the two receptors display high levels of tyrosine-phosphorylation, due to constitutive expression of GAS6. An exception to this rule was the TPC-1 cell line, in which AXL was highly phosphorylated despite the fact that GAS6 is absent. AXL and its ligand GAS6 are also overexpressed in human thyroid carcinoma samples with respect to normal thyroid, as assessed by IHC. The inhibition of TYRO3 and AXL by blocking reagents or RNA interference targeting each receptor or the ligand decreased cell proliferation and resistance to apoptotic stimuli in different thryoid cancer cell lines. In cell lines that expressed both receptors and ligand, the simultaneous blockade of these molecules dramatically affected cell viability. Accordingly, we showed that the stimulation of GAS6-negative TPC-1 cells with exogenous GAS6 increased their proliferation and survival. Finally, we found that the blockade of AXL receptor consistently impaired thyroid carcinoma cell line invasiveness through Matrigel and, moreover, it inhibited tumor growth in nude mice.

In this thesis project, we provide evidences that targeting CXCR4/SDF-1 or TYRO3/AXL/GAS6 axis might be exploited as novel anticancer therapyes for human thyroid carcinomas.

1. BACKGROUND

1.1 Thyroid cancer

The thyroid gland develops in the embryo as a tubular evagination of the pharyngeal endoderm at the basis of the tongue. It is located in the neck, beside the trachea. The functional thyroid unit consists of the follicle, a hollow spheroid lined by a single layer of columnar epithelial (follicular) cells, filled with colloid containing thyreoglobulin secreted by these cells. A small minority of follicles includes a second epithelial cell type, the C or parafollicular cells, which arise from the neuroectoderm of the neural crest and produce calcitonin.

Thyroid cancer is the most frequent endocrine malignancy with an incidence of about 9-100.000 cases/year; moreover, the incidence increases with age, reaching a plateau at 50 years. Thyroid cancer can derive from both the follicular and the parafollicular cells.

1.1.1 Classification, etiopathogenesis, clinical features of thyroid carcinoma

Thyroid carcinoma is responsible for about 60% of deaths secondary to endocrine cancer (Sherman 2003). Malignant thyroid tumors can derive from any of the gland cell populations, although those deriving from the epithelial cells are most frequent. The most common carcinomas deriving from thyroid follicular cells are: (1) the well-differentiated thyroid carcinomas (WDTC), including the papillary carcinoma (PTC), and the follicular carcinoma (FTC); (2) the recently identified poorly differentiated carcinomas, (PDC), hystologically between the un- and the differentiated tumors; (3) the undifferentiated or anaplastic carcinomas (ATC) (Rosai 2004).

PTC is the most common thyroid malignancy; it accounts for 75 to 80% of all thyroid cancers, showing an incidence peak at 40-50 years. A well-established cause of PTC is the exposure to ionizing radiations, especially in the neck region; in fact, about 2-4% of the patients irradiated to treat deseases such as acne or enlarged thymus, develop a differentiated thyroid carcinoma after about 20-30 years. Accordingly, the frequency of PTC is dramatically increased in the children exposed to the massive release of radionuclides that followed the explosion of the nuclear reactor in Chernobyl in 1986. Immunohistochemically, PTC features distinctive architectural pattern and cell nuclei morphology, and is usually associated with good therapeutic response and prognosis. However, PTC can usually metastasize to the cervical lymphonodes; distant metastasis are uncommon, but lung and bone are the most frequent sites. The solid/follicular, tall-cell and diffuse/follicular variants of PTC have been associated with increased malignancy (Rosai et al. 1992).

FTC is less frequent than PTC and represents about 10-30% of thyroid cancers; it is particularly linked to dietary iodine deficiency (Williams et al.,

1997) and both iodine and iodine deficiency and genetic influences could account for its link with a history of nodular goiter (Ron E et al., 1987).

ATC is one of the most aggressive solid tumors in humans. ATC cancer cells are extremely undifferentiated and spread rapidly to other parts of the body; ATC makes up only about 1% of all thyroid cancers. Metastasis to regional lymph-nodes are quite common as well as distant ones; no effective therapy is available for ATC and prognosis is extremely negative, with a mean survival of six months after diagnosis (Giuffrida et al. 2000).

Finally, the medullary thyroid carcinoma (MTC) derives from the calcitonin-secerning parafollicular C cells. About 5 to 7% of all thyroid cancers are medullary; of the four types of thyroid cancers, only MTC has a clear genetic predisposition that can be passed on in families; in fact, together with pheochromocytoma, parathyroid adenoma and other tumor types, MTC can be inherited in the context of autosomal dominant MEN 2 (multiple endocrine neoplasia type 2) syndromes, MEN 2A and MEN 2B, and FMTC (familial medullary thyroid carcinoma) (Cote et al. 2003).
(Fig.1)

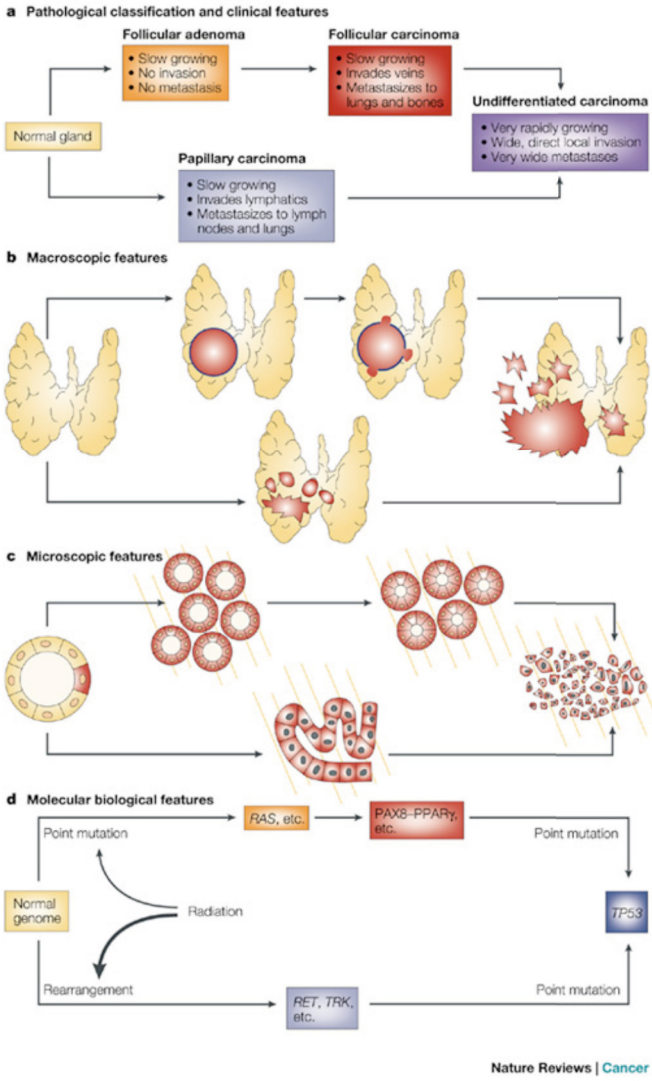

Figure 1: Features of thyroid tumors (Modified from Williams 2002).

1.1.2 Molecular genetics of thyroid tumors

PTC

Several studies on thyroid tumors have allowed the identification of many genetic alterations. In particular, four genetic lesions, at the somatic level, are associated with PTC. They include chromosomal aberrations targeting the RET or TRKA tyrosine kinase receptors and point mutations in RAS or BRAF genes.

In a sizeable fraction of papillary thyroid carcinomas, the kinase domain of the tyrosine kinase receptor for the GDNF (Glial-Derived Neurotrophic Factor), c-Ret (REarranged during Transfection), is fused with the N-terminal region of constitutively expressed, heterologous genes, such as H4 (in RET/PTC1) or RFG (in RET/PTC3) (Manie et al., 2001). In RET/PTC rearrangements, fusion with protein partners, possessing protein-protein interaction domains, provides RET/PTC proteins with coiled-coil domains, thereby resulting in ligand-independent activation of c-Ret tyrosine kinase activity (Santoro et al. 1995). RET/PTC1, the H4-RET fusion, and RET/PTC3, the RFG-RET fusion, are the most prevalent variants. RET/PTC3 is frequently found in radiation-associated-PTC occurred after the Chernobyl accident (Fagin 2002). RET/PTC-transgenics develop PTC, proving that RET/PTC oncogenes are able to initiate thyroid carcinogenesis (Santoro et al., 1996). RET/PTC oncogenes are detected with a high frequency in clinically-silent small PTC, confirming that they can be early events in thyroid tumorigenesis (Fusco et al. 2002). Similar rearrangements of the high affinity receptor for NGF (Nerve Growth Factor), TRKA, can be also found, at a low prevalence in human PTC (Alberti et al., 2003). As a member of the tyrosine kinases receptor family (RTK), and thanks to its intrinsic kinase activity, RET activates many intracellular signaling pathways. Upon binding to ligand, it dimerizes and autophosphorylates various cytoplasmic tyrosines. The phosphorylated tyrosines thus become binding sites for intracellular molecules containing phosphotyrosine-binding motifs, thereby initiating a diverse array of signaling pathways (Santoro et al. 2004). In RET/PTC rearrangements, the fusion with protein partners possessing protein-protein interaction motifs provides RET/PTC kinases with dimerizing interfaces, thereby resulting in ligand-independent autophosphorylation. The RET intracellular domain contains at least 12 autophosphorylation sites, 11 of which are maintained in RET/PTC proteins (Kawamoto et al. 2004). Phosphorilated tyrosine 905 (Y905) is a binding site for SH2-containing proteins, such as Grb7/10 adaptors (Pandey et al. 1996). Phosphorilated tyrosines 1015 and 1096 are responsible for binding of phospholipase Cγ and GRB2, respectively (Borrello et al. 1996, Jhiang S.M. 2000; Hansford et al. 2000; Airaksinen M.S. et al. 1999; van Weering et al. 1998), and phosphorilated tyrosine 981 for c-Src (Encinas et al. 2004). The multi-docking site tyrosine 1062 is the binding site for several proteins including the Shc family proteins (Shc and N-Shc/RAI), IRS1/2, FRS2, DOK1/4/5 and Enigma (Ichihara et al. 2004). Binding to Shc and FRS2 mediates recruitment of Grb2-SOS complexes, leading to GTP exchange on RAS and RAS/ERK stimulation (Asai et al. 1996; Melillo et al. 2001); moreover, it is responsible for the activation of the phosphatidylinositol 3-kinase (PI3K)/AKT and the c-Jun amino-terminal protein kinase (JNKs) and the p38MAPK (Jhiang S.M. 2000; Hansford et al. 2000; van Weering et al. 1998).
(Fig. 2).

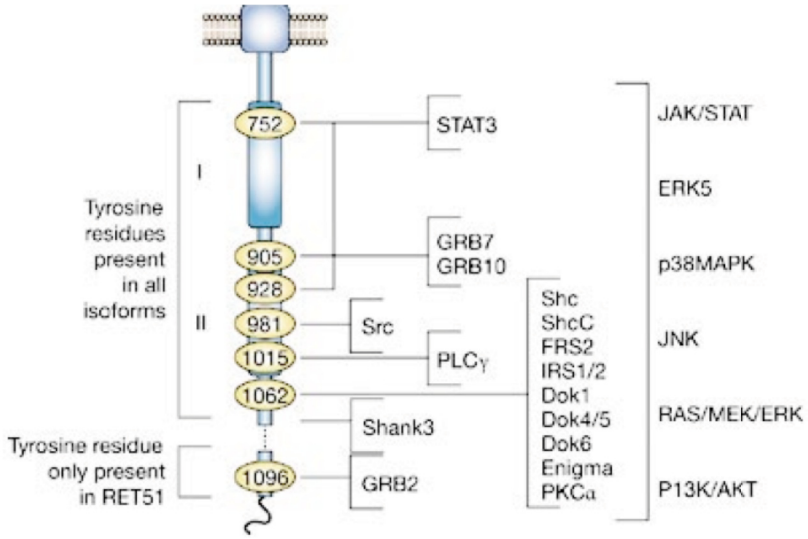

Figure 2: Signaling pathways activated by RET (modified by Drosten 2006).

Activating point mutations in RAS small GTPases are found roughly in 10% of PTC, mainly in those belonging to the follicular variant (PTC-FV) (Zhu et al. 2003). Point mutations in BRAF are the most common genetic lesions found in PTC (up to 50% of the cases) (Kimura et al. 2003; Xu et al. 2003; Soares et al. 2003; Fukushima et al. 2003; Cohen et al. 2003). BRAF is a member of the RAF family of serine/threonine kinases and it is a component of the RAF-MEK-ERK signaling module. Activation of the RAF proteins is mediated through binding of RAS in its GTP-bound state. Once activated, RAF kinases phosphorylate MEK which in turn phosphorylates and activates ERK (Malumbres et al. 2003). A Glutamine for Valine substitution at residue 600 (V600E) in the activation segment accounts for more than 90% mutations of BRAF in PTC (Kimura et al. 2003; Cohen et al. 2003; Soares et al. 2003). This mutation enhances BRAF activity through disruption of the autoinhibited state of the kinase. (Fig. 3).

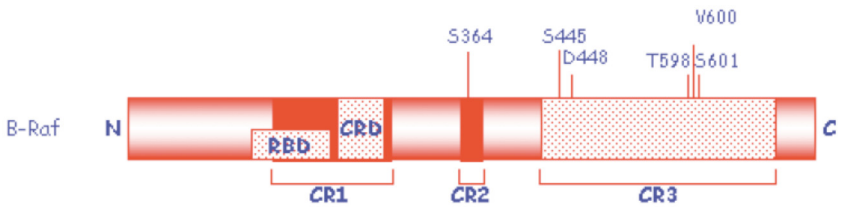

Figure 3. Structure of BRAF gene. CR: conserved regions; triangles denote the common oncogenic mutations. RBD: Ras Binding Domain. CRD: Cystein Rich Domain. (Modified from Cohen 2003).

In human PTC, the genetic alterations of RET/PTC, RAS and BRAF are mutually exclusive, suggesting the existence of a common signaling cascade; moreover, mutations at more than one of these sites are unlikely to provide an additional biological advantage (Kimura et al. 2003, Cohen et al. 2003, Soares et al. 2003).

FTC

Follicular thyroid carcinoma (FTC) is also a well-differentiated cancer developing from thyroid cells. In this carcinoma the presence of K-, H-, and N-RAS mutations is quite common. More recently, it has been shown that a quite high proportion of FTC carries the PAX8/PPARγ rearrangement (Nikiforova MN et al. 2003). PAX8 encodes a thyroid-specific transcription factor, while PPARγ is a nuclear receptor involved in lipid metabolism and tumorigenesis. The resulting fusion protein has dominant negative activity on wild type PPARγ (Kroll et al. 2000).

PDC and ATC

Point mutations in the RAS oncogene and in the tumor suppressor p53 have been described in PDC and ATC (Garcia-Rostan et al. 2003, Donghi et al. 1993, Fagin 1993). It is well known that p53 safeguards the cell cycle, the DNA repair and the apoptotic processes; thus, mutations in its sequence can account for the progression from a more differentiated to an anaplastic carcinoma, according to a model already described for the colon carcinoma by Vogelstein (Vogelstein et al., 1988). Garcia-Rostan and colleagues found somatic mutations within the PI3K catalytic subunit in 23% of analyzed ATC as well as activating point mutations of β-catenin (Garcia-Rostan et al. 2005). Mutations of BRAF gene have been detected in anaplastic carcinomas, suggesting that some ATC may arise from a preexisting WDTC, while others may arise *de novo* (Nikiforova MN et al. 2003).

MTC

Germline point mutations in RET cause the dominantly inherited cancer syndromes: multiple endocrine neoplasia (MEN) 2A and 2B, and familial medullary thyroid carcinoma (FMTC). MEN2 patients are invariably affected

by Medullary Thyroid Carcinoma (MTC), a malignant tumour arising from calcitonin-secerning C cells of the thyroid. Additional features can be present in MEN2A (pheochromocytoma and parathyroid adenoma) and MEN2B (pheochromocytoma, mucosal neuroma and ganglioneuroma of the intestine) (Brandi et al. 2001). Most MEN2B patients carry the M918T substitution in the P+1 loop in the kinase domain. In MEN2A and most FMTC patients, mutations affect one cysteine of the extracellular cysteine-rich domain of RET (609, 611, 618, 620, 630, 634) that can change to different residues. A significant genotype-phenotype correlation is observed. In particular, about 90% of MEN2A patients have Cys634 mutation, and this mutation is highly predictive of the presence of pheochromocytoma and parathyroid hyperplasia. (Santoro et al. 1995; Carlomagno et al. 1997). RET activation by mutations targeting the intracellular domain is less understood (Santoro et al. 1995, Iwashita et al. 1999) but it can be envisaged that a modification of the structure of the kinase may switch on its enzymatic function.

1.2 Inflammation and cancer

Inflammation is a physiological, protective response organized by the organism in response to tissue damages. Several chemical signals initiate and sustain the inflammatory response whose aim is repairing the damage. Several cells migrate in the sites of tissue damage, thanks to the action of chemotactic and adhesion proteins, including the integrin and selectin family members (Coussens et al., 2002). Resident cells, such as macrophages and mast cells, and migrating cells, such as neutrophils, secrete ROS, vasoactive proteins, such as histamine and leukotrienes, and several other factors, such as cytokines, chemokines and proteases that remodel the extracellular matrix (de Visser et al., 2006).
(Fig. 4)

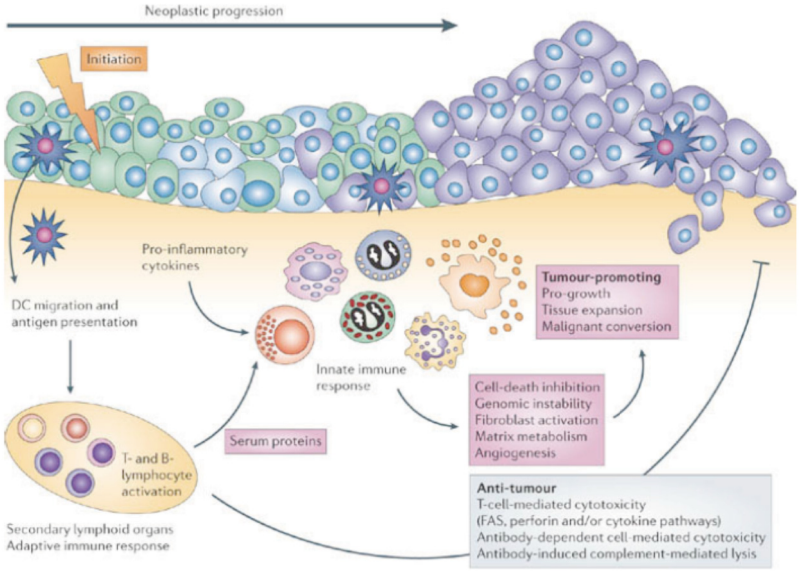

Figure 4 A **model of innate and adaptative immune-cell function during inflammation-associated cancer development** (modified from De Visser 2006).

Inflammation is an auto-limiting process; however, the abnormal persistence of the stimuli that first induced the inflammatory response or the failure of the mechanisms determining its termination cause chronic inflammation (Coussens et al., 2002). A functional relationship between chronic inflammation and cancer has been envisaged long ago. In 1863, Virchow hypothesized that the origin of cancer was at sites of chronic inflammation (Virchow 1863), in part based on the hypothesis that some classes of irritants, together with the tissue injury and ensuing inflammation they cause, enhance cell proliferation (Balkwill and Mantovani 2001). Although it is now clear that proliferation of cells alone does not cause cancer, sustained cell proliferation in an environment rich in inflammatory cells, growth factors, activated stroma, and DNA-damage-promoting agents, certainly potentiates and/or promotes neoplastic risk. Leukocytes physiologically secrete ROS and RNS, to eliminate the pathogens. However, these highly reactive metabolites induce the production of peroxynitrite and other mutagenic agents; therefore, they can induce "DNA damage", i.e. mutations in proliferating cells (Coussens et al., 2002). Thus, in the case of a persistent tissue damage of O_2 and N highly reactive metabolites secreted by the inflammatory cells induce point mutations, rearrangements and double strand breaks in the DNA of proliferating cell. This results in a higher probability of oncogene activation or tumor suppressor loss of function (Colotta et al., 2009).

1.3 Thyroid cancer and inflammation

An association between Hashimoto's thyroiditis (HT) and thyroid cancer has been reported in about the 30% of the cases (Di Pasquale, 2001; Wirtschafter.et al., 1997; Mechler et al., 2001; Segal et al., 1985; Eisemberg et al., 1989; Ott et al., 1987; Sclafani et al., 1993; Pisanu et al., 2003) and the increased incidence of carcinomas in patients with thyroiditis suggests it might be a precancerous condition. The vast majority of thyroiditis-associated carcinomas are papillary; however, also follicular and anaplastic, medullary carcinomas have been reported (Guarino et al., 2009). Hashimoto thyroiditis is an autoimmune disorder in which the immune system is activate to react against a variety of thyroid antigens. HT is characterized by a progressive depletion of thyroid epithelial cells (thyrocytes), mononuclear cell infiltration and fibrosis, which ultimately leads to thyroid functional insufficience. Sensitization of autoreactive CD4+ T-helper cells to thyroid antigens appears to be the initiating event, but multiple immunological mechanisms might contribute to thyreocyte death in HT. This disease is also characterized by proliferating nodules as well as cytological alterations and nuclear modifications similar to those of the papillary carcinomas (Weetman et al., 2004). The thyroid follicular cells in HT may have chromosomal defects, such as the RET/PTC1 rearrangement, the hallmark of many papillary thyroid carcinomas. Several other evidences suggest a role for RET/PTC in the association between thyroiditis and cancer. In fact, patients exposed to radiation from the Chernobyl nuclear power plant disaster often develop not only RET/PTC-induced papillary tumors but also an associated autoimmune thyroiditis (Williams et al 2002). Transgenic mice engineered to express RET/PTC develop papillary carcinomas and chronic thyroiditis (Powell et al. 1998). Finally, Wirtschafter and colleagues have detected RET/PTC expression in about the 90% of the HT they have analyzed (Wirtschafter et al., 1997). These data are, however, partially in contrast with the report by Rhoden and colleagues. These authors have found only few follicular cells expressing very low levels of the rearranged PTC protein in HT, thus suggesting that RET/PTC expression does not necessarily predicts the development of a papillary carcinoma in patients with thyroiditis (Rhoden et al., 2006). Two models have been hypothesized to explain the association between Hashimoto's thyroiditis and RET/PTC. The first one suggests that inflammation might facilitate the rearrangement. According to this hypothesis, free radicals production, cytokine secretion, cellular proliferation as well as other phenomena correlated with inflammation might predispose to the rearrangement in follicular cells. Another hypothesis suggests that it is the rearrangement that promotes thyroid inflammation. Accordingly, RET/PTC induces a severe inflammatory response in animal models and the synthesis of many inflammatory proteins in epithelial

thyroid cells (Powell et al., 2003; Melillo et al., 2005; Puxeddu et al., 2003; Guarino et al., 2009).

1.4 Chemokines and chemokine receptors

Chemokines are a group of small (~8-14 KDa) secretory proteins; they belong to a family of chemotactic cytokines which possess a relatively high degree of specificity for chemoattraction of specific leukocyte populations; they are involved in the recruitment of downstream effector cells and dictate the natural evolution of the inflammatory response. The profile of cytokine/chemokines persisting at an inflammatory site is important in the development of chronic disease. Chemokines can be produced not only by leukocytes but also by fibroblasts, endothelial and epithelial cells. Chemokine production is induced by inflammatory cytokines and growth factors (Mantovani et al. 2004; Balkwill 2004). More than 50 chemokines and 18 chemokine receptors have been discovered. They are subdivided into four groups based on the relative position of cysteine residues: CC, CXC, XC and CX3C, with the CC and CXC groups being by far the most common ones.
(Fig. 5).

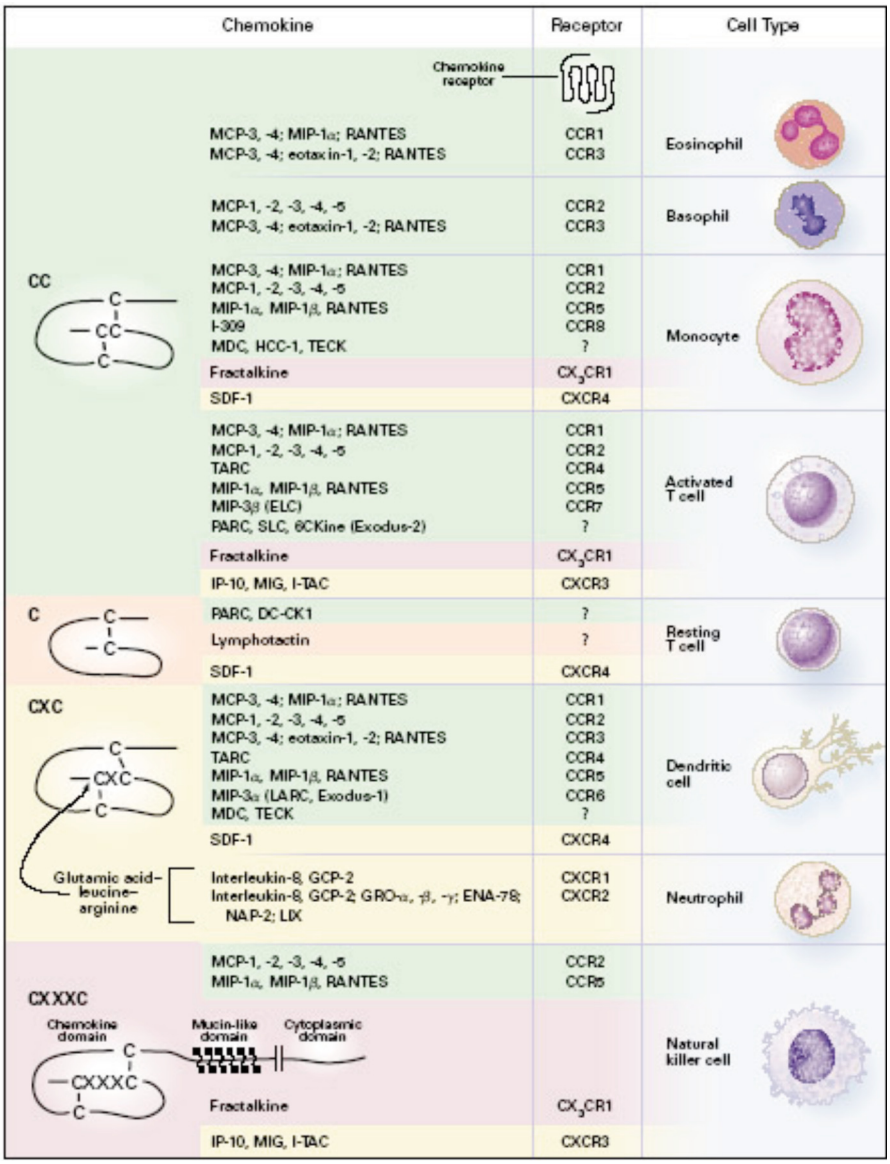

Figure 5: Chemokine families (From Luster 1998).

Corresponding groups of CCR, CXCR, XCR and CX3CR receptors of the GPCR (G protein coupled receptor) family (seven-transmembrane receptors) mediate the functions of those chemokines on their target cells. Several chemokines can bind the same receptor and one chemokine can bind to several receptors, creating multiple combinations and, therefore, multiple biological outcomes (Balkwill 2004).
(Fig. 6).

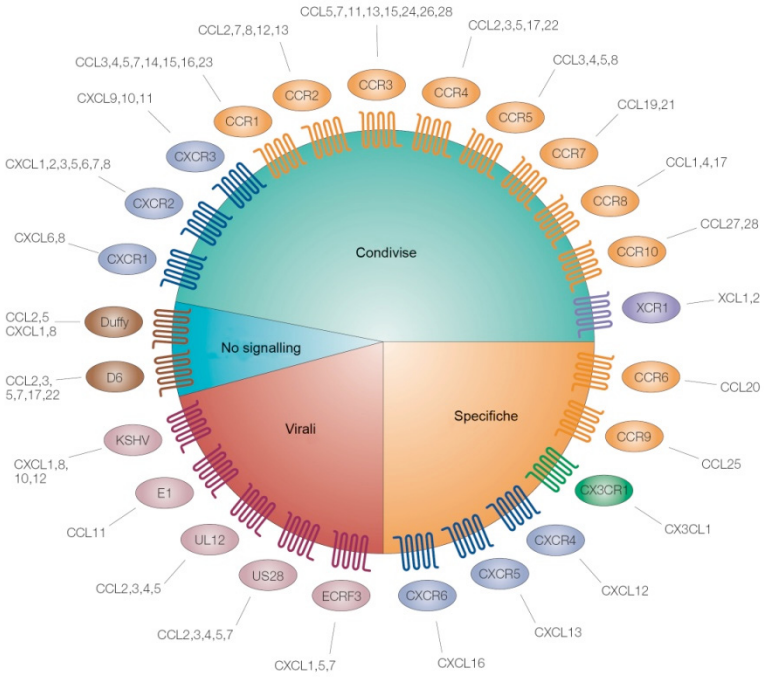

Figura 6: The chemokine wheel. This illustration explains the ligand-binding patterns of the seven-transmembrane domain G-protein-coupled human chemokine receptors. Receptors CXCR1–CXCR3, CCR1–CCR5, CCR7, CCR8, CCR10 and CXCR1 all bind several chemokines. By contrast, CCR6, CCR9, CX3CR1 and CXCR4–CXCR6 bind only one ligand each. Duffy and D6 are considered to be 'deceptors', as they bind ligands but do not signal, thereby acting as a negative feedback for chemokine responses.(Modified by Balkwill, 2004).

Chemokine receptors are coupled to heterotrimeric G proteins of the Gαi class and can be inhibited by *Bordetella pertussis* toxin (PTX). Their activation leads to a cascade of cellular events, including the generation of diacylglycerol and inositol triphosphate, release of intracellular calcium, inhibition of adenyl cyclase, and activation of several signaling proteins including Janus tyrosine kinase/signal transducers and activators of transcription (Jak/STAT), protein kinase C, phospholipase C, phosphatidylinositol 3-kinase (PI3K) and small GTPases of the Ras and Rho families. This results in activation of AKT and ERK and in cell polarization, adhesion and migration (Luster et al. 1998).
(Fig. 7).

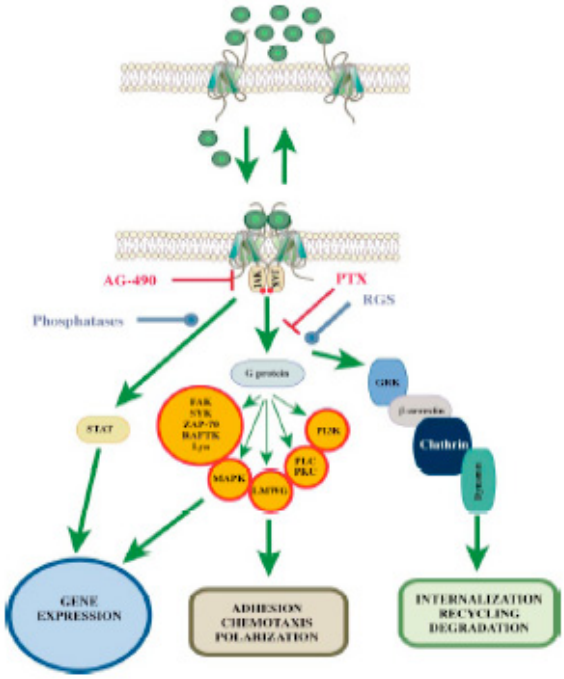

Figure 7: Signaling pathways activated by chemokines binding to their receptors and promoted biological activities (Modified from Mellado et al. 2001).

1.4.1 Chemokines and cancer

Initially, chemokines have been functionally defined as soluble factors able to control the directional migration of leukocytes, in particular during infection and inflammation. Although originally identified on leukocytes, functional chemokine receptors are also found on epithelial cells, particularly on those that have undergone malignantly transformation. Therefore it appears that the biological effects mediated by chemokines are by far more complex and that virtually all cells, including many tumor cell types, can express chemokines and chemokine receptors (Rollins 1997; Rossi et al. 2000). Accordingly, one of the most interesting aspects of the relationship between inflammation and cancer is the fact that several tumors may use molecules of the innate immune sytem, such as chemokines and their receptors, not only to recruit leukocytes, but also for growth, survival and metastasis (Balkwill and Mantovani 2001). It can be envisaged that a mixture of chemokines are produced in the tumor microenvironment and act in an autocrine or paracrine fashion on neighboring homotypic cells.

New informations indicate that chemokines can influence metastatic potential and site-specific spread of cancer cells (Muller et al. 2001; Kang et al. 2003). Therefore, chemokines can have a two-sided effect in cancer as they can influence both leukocyte infiltration in tumor sites and the malignant phenotype of neoplastic cells. It is becoming now clear that different

chemokines produced locally in the tumor can strongly influence the composition of inflammatory infiltrate that can be composed by macrophages, endothelial cells, fibroblasts, but also by mast cells, NK and B cells (Brigatti et al., 2002; Coussens et al., 2002; Poliard et al 2004). In particular, we observed that mast cells are present into thyroid carcinomas and that they can promote proliferation, survival and invasive ability of thyroid cancer cells in culture (Melillo et al., submitted to *Oncogene*). These evidences suggest that leukocytic tumoral infiltrate is able to promote cancer progression; furthermore, the local production of chemokines, that are the typical and most important chemotactic proteins for leukocytes in the tumoral site, can be considered as a very poor prognostic factor (Luboshits et al., 1999; Azenshteen et al., 2002; Saji et al., 2001).

1.4.2 Role of CXCR4 in human cancer

CXCR4 is one of the chemokine receptors higly expressed in tumors of epithelial and non epithelial origin. CXCR4 is the receptor for the chemokine CXCL12/SDF-1α (Stromal Derived Factor-1). It is broadly expressed in cells of both the immune and the central nervous system and can induce migration of CXCR4-positive cells in response to its ligand. Mice lacking CXCR4 exhibit hematopoietic and cardiac defects identical to those of SDF1-deficient mice (Nagasawa et al., 1996), suggesting that CXCR4 may be the only receptor for SDF-1. SDF-1 is a chemokine that belongs to the CXC family, characterized by the presence of 4 conserved cysteines, which form 2 disulfide bonds. The SDF-1 protein is produced in two forms, SDF-1α and SDF-1β by alternate splicing of the same gene. These chemokines activate leukocytes and are often induced by proinflammatory stimuli such as lipopolysaccharide, TNF or IL1. SDF-1 is generally expressed at high levels by tumoral stroma, thus generating a paracrine loop which sustains the malignant phenotype of cancer cells (Orimo et al., 2006). Several studies have demonstrated the implication of CXCR4/SDF-1α couple in tumor progression. In particular, the chemokine receptor CXCR4 and its ligand SDF-1/CXCL12 have been implicated in the metastatic spread of breast cancer cells. SDF-1 induces endothelial expression of VEGF-A; VEGF-A in turn upregulates CXCR4 on endothelial cells (Homey et al. 2002). Studies by Muller and co-workers (2001) suggest that chemokine expression is particularly high in target organs for breast cancer metastasis (Muller et al., 2001). The involvement of CXCR4 in metastasis is not limited to breast cancer, as CXCR4 is expressed in several tumour cell lines (for example, prostate carcinomas, B-cell lymphomas, astrogliomas and chronic lymphocytic leukaemias) that also respond to SDF-1 (Moore 2001). Moreover, it has been shown that the CXCR4-SDF-1 axis has an important role in promoting cell growth, invasiveness and survival in thyroid cancer cell cultures (Castellone et al., 2004). These data suggest that CXCR4 is one of the most important chemokine receptor for cancer cells.

1.5 TAM receptors

In a screening for SDF-1-induced genes in thyroid cancer cells, we identified Tyro3 and Axl, two tyrosine kinase receptors (RTK). These receptors belong to a small Protein Tyrosine Kinase (PTK) subfamily of receptors, that includes three members, Tyro3, Axl and Mer, from which this family was named TAM. The three TAM receptors were identified as a distinct receptor PTK subfamily in 1991. They share a common structure, that includes an extracellular, ligand-binding region which contains two immunoglobulin-related domains and two fibronectin type III repeats, each in tandem; a single-pass transmembrane domain; a catalytically competent, cytoplasmic PTK domain (Lemke and Rothlin, 2008). The TAM receptors are most closely related to RON (also known as CD136), the PTK receptor for macrophage-stimulating protein, and to MET, the hepatocyte growth-factor receptor (Manning et al., 2002). Similar to all others RTKs, the TAMs seem to function as dimers (Sasaki et al., 2006). TAM receptors are frequently co-expressed in vascular, reproductive, nervous and mature immune system in adults, but they seem to have a pivotal role in innate immunity; TAM receptors inhibit inflammation in dendritic cells and macrophages, promote the phagocytosis of apoptotic cells and membranous organelles, and stimulate the maturation of natural killer (NK) cells (Lemke and Rothlin, 2008). Their expression is not indispensable for life, since knockout of each receptor produces viable and fertile mice. Interestingly, when all the three receptors are deleted, several phenotypes arise few weeks after birth. Indeed, TAM-deficient mice are unfertile (Lu et al., 1999), display retinal degeneration, and develop a systemic autoimmune disease (Lu et al., 2001).

1.5.1 TAM receptors and their ligands

TYRO3 (also named Tif/Sky/Dtk/Rse/Brt) was first cloned from a human myelogenous leukemia cell line. Its expression is widely distributed, but it appears to be higher in the central nervous system (Funakoshi et al., 2002) and brain (Ohashi et al., 1994); TYRO3 is also overexpressed in osteoclasts in bone, indicating a role in bone resorption (Nakamura et al., 1998).

AXL (alternatively named Ufo/Ark/Tyro7) was originally identified in patients with chronic mielogenous leukemia (Liu et al., 1988) and chronic myeloproliferative disorder (Janssen et al., 1991; O'Bryan et al., 1991); it is ubiquitously expressed, being detected in cell lines of epithelial, mesenchymal and haematopoietic origins. It is also overexpressed in several cancer types and its levels correlate with cancer progression in some epithelial neoplasia.

MER (alternatively named Eyk/Nym/Tyro12) was firstly identified as the homologue of the avian retroviral *v-eyk* oncogene (Jia et al., 1994). Human MER is named after its original reported expression pattern (monocytes and epithelial and reproductive tissues) (Graham et al., 1994). It displays tissue

specific expression, almost exclusively in the monocytic cell lineage, and has a role in the phagocytosis of apoptotic cells by macrophages and in the homeostasis of the retina and of the immune system; finally, MER appears able to induce the cytoskeletal remodelling that is required for engulfment during phagocytosis (Todt et al., 2004; Jennings et al., 2005).

The two physiological ligands that bind to and activate the TAM receptors are two closely related proteins, GAS6 (Growth-Arrest-Specific 6) (Manfioletti et al., 1993) and Protein S (Stitt et al., 1995). Both of them are highly similar vitamin K-dependent proteins. Gas6 was identified as a gene up-regulated in NIH3T3 fibroblasts upon serum deprivation and can bind, with distinct affinities, the three receptors (Nagata et al., 1996). Protein S has been identified as a negative regulator of the blood coagulation process (Rezende et al., 2004) and has a role in the engulfment of apoptotic bodies by phagocytic cells. It has been shown that Protein S can act as an agonist for Tyro3 and Mer, while there are no data available sustaining Axl/Protein S interaction; moreover, it is not clear whether ligands can bind as heterodimers and how receptor homo-heterodimers eventually respond to different combinations of ligands. The two ligands display 42% aminoacid identity; each protein has a ~60 aminoacid Gla domain at its amino terminus, a region rich in glutamic acid residues that are γ-carboxylated in a vitamin-K-dependent reaction (Gla-domain-containing proteins are prominent components of the blood coagulation cascade). These Gla domains bind the phospholipid phosphatidylserine on apoptotic cells (Huang et al., 2003) and this is an important feature of the *in vivo* function of GAS6 and Protein S (Nakano et al., 1997; Anderson et al., 2003). The Gla domain is followed by a loop region constituted by four epidermal growth factor (EGF)-like-repeats and by a C-terminal globular sex hormone binding globulin (SHGB)-like domain (Sasaki et al., 2006). This last region is both necessary and sufficient for receptor activation and biological activity (Sasaki et al., 2002).
(Fig. 8).

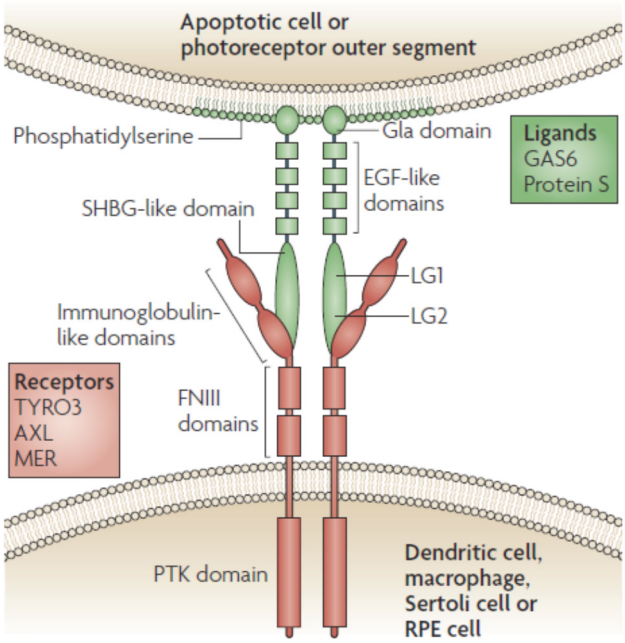

Figure 8: **TAM receptors and their ligands.** Tam receptors dimers bind to their ligands, GAS6 and Protein S, through interaction between the two N-terminal immunoglobulin-like domains of the receptors and the SHBG (Sex Hormon Binding Globulin) domain of the ligands. Via their N-terminal Gla domains, GAS6 and Protein S can bind to phosphatidylserine that is dispayed on the extracellular surface of the plasma membranes of apoptotic cells or on the outer segment of photoreceptors. EGF: epidermal growth factor; FNIII: fibronectine type III. (Modified from Greg Lemke and Carla V. Rothlin 2008).

1.5.2. TAM receptors and cancer

It has been highlighted that TAM receptors are endowed with transforming ability and also play an important role in cancer development and progression; together, these receptors regulate many processes, such as cell proliferation, survival, cell adhesion, migration, inflammation and cytokine release, thus suggesting their implication in human cancerogenesis (Linger et al., 2008).

Axl was originally identified as a transforming gene in chronic myeloid leukemia patients and in a chronic myeloproliferative disorder wherein it was suggested to be capable of transforming cells without intrinsic activating mutations (Liu et al., 1991). Moreover, Axl has been shown to be overexpressed and to have mitogenic and prosurvival roles in a broad spectrum of human malignancies, including colon (Craven et al., 1995), oesophageal (Nemoto et al., 1997), thyroid (Ito et al., 2002), breast (Zantek et al., 2001), lung (Shieh et al., 2005), renal (Gustafsson et al., 2009) and ovarian (SunW et al., 2004) carcinomas. Recently, Axl was shown to mediate glioma cell proliferation, migration, and invasion (Vajkoczy et al., 2006), and in human gliomas, both Axl and its ligand Gas6 are frequently overexpressed and this predicts poor prognosis (Hutterer et al., 2008). Moreover, Axl affects multiple

cellular behaviors required for neovascularization, such as endothelial cell proliferation, migration, survival, and tube formation *in vitro*, and regulates angiogenesis *in vivo* (Holland et al., 2005).

Although able to induce cell transformation experimentally (Lan et al., 2000), information about TYRO3 expression in human cancer is still scant. To date, TYRO3 has been detected in several human leukaemic cell lines and blasts of acute myeloid leukaemia patients (Crosier et al., 1995), and overexpressed in myeloma cells compared to autologous B-lymphoblastoid cell lines (De Vos et al., 2001).

As with TYRO3, very little has been reported about the expression/activity of MER in cancer. Experimentally, both the transforming and antiapoptotic abilities of this receptor have been observed through at least its intracellular region (Georgescu et al., 1999). One microarray study has shown MER to be overexpressed in an ACTH-secreting adenomas compared with normal pituitary gland (Evans et al., 2001). Also, since its original detection in neoplastic B- and T-cell lines (Graham et al., 1999), MER up-regulation has been observed in mantle cell lymphomas as compared to normal B cells (Ek et al., 2002). Finally, Gas6 is frequently co-expressed with Axl or Tyro3 in cancer cells; in some cancer types its expression levels correlate with a poor prognosis (Hutterer et al., 2008).

2. AIM OF THE STUDY

This thesis project was aimed at understanding the biological role of chemokines and chemokine receptors in thyroid cancerogenesis. In particular we analyzed the role of the CXCR4/SDF1α receptor/ligand couple in thyroid cancer. Moreover, we studied the role of two CXCR4/SDF-1 transcriptional targets, the tyrosine kinase receptors Tyro3 and Axl, in thyroid cancer. Specifically, our focus was as follows:

1. Evaluation of the the biological role of CXCR4 and of its ligand SDF-1α in thyroid cancer.

2. Identification of SDF-1α–induced transcriptional targets in thyroid cancer cells.

3. Study of the biological role of the tyrosine kinase receptors AXL and TYRO3 in thyroid cancer cells through deletion and overexpression approaches.

3.MATERIALS AND METHODS

3.1 Cell cultures

Human primary cultures of normal thyroid and ATC cells were obtained from F. Curcio (Dipartimento di Patologia e Medicina Sperimentale e Clinica, University of Udine, Udine, Italy;) P5, P5-2N, P5-3N, P5-4N (hereafter "NT") and U-HTH83/U-HTH7, and cultured as described previously (Salvatore et al., 2006). Human thyroid papillary cancer cell lines TPC1 , BcPAP and NIM have been described previously (Carlomagno et al., 2003; Inokuchi et al., 1995). TPC1 cells harbor a RET/PTC1 rearrangement; BCPAP cells harbor a BRAF(V600E) mutation in homozygosis; NIM cells harbor a BRAF(V600E) mutation in heterozygosis. The anaplastic cells FB1 cells harbor a BRAF(V600E) mutation in heterozygosis; 8505C and FRO harbor a BRAF(V600E) mutation in homozygosis (Salvatore et al., 2006); CAL62 cells express wild-type BRAF but mutant NRAS allele (Q61K); U-HTH83 cells express wild-tipe BRAF but mutant HRAS allele (Q61R) ; C643 cells express wild-type BRAF but mutant HRAS allele (G13R); SW1736 cells harbor a BRAF(V600E); U-HTH7 cells express wild-type BRAF but mutant NRAS allele (Q61R); OCUT-1 cells harbor a BRAF(V600E) mutation in heterozygosis; ACT-1 cells express a wild-type BRAF but mutant NRAS (Q61K). (Guida et al., 2005). Continuous cell lines were maintained in DMEM supplemented with 10% fetal bovine serum, 1% penicillin-streptomycin, and 1% glutamine. PC Cl 3 (hereafter "PC") is a differentiated thyroid follicular cell line derived from 18-month-old Fischer rats. PC cells were cultured in Coon's modified Ham F12 medium supplemented with 5% calf serum and a mixture of 6 hormones (6H), including thyrotropin (TSH, 10 mU/ml), hydrocortisone (10 nM), insulin (10 μg/ml), apo-transferrin (5 μg/ml), somatostatin (10 ng/ml) and glycyl-histidyl-lysine (10 ng/ml) (Sigma Chemical Co., St. Louis, MO) (Fusco et al 1987).

3.2 Tissue samples and immunohistochemistry

Retrospectively-collected archival thyroid tissue samples from patients affected by ATCs were retrieved from the files of the Pathology Department of the University of Pisa, on informed consent, and tested for CXCR4 expression with a mouse monoclonal antibody against CXCR4 (clone 12G5; R&D Systems). Retrospectively-collected archival frozen thyroid tissue samples from 26 patients affected by thyroid carcinomas (8 PTCs, 10 FTCs and 8 PDCs/ATCs) were retrieved from the files of the Struttura Complessa di Anatomia Patologica, Istituto Nazionale Tumori, Fondazione G. Pascale, of Naples, upon informed consent, and analysed for AXL and GAS6 expression, by using anti-AXL (R&D Systems) and anti-GAS6 antibodies for the staining(R&D Systems). Sections (4-8 μM thick) of paraffin-embedded samples were

stained with hematoxylin and eosin for histological examination to ensure that the samples fulfilled the diagnostic criteria required for the identification of PTC, FTC, PDC/ATC. Normal thyroid tissue samples were also retrieved from the Pathology Department of the University of Pisa and from Struttura Complessa di Anatomia Patologica, Istituto Nazionale Tumori, Fondazione G. Pascale of Naples, as well.

3.3 RNA interference

Small inhibitor duplex RNAs targeting human CXCR4 were chemically synthesized by Proligo. Transfection was performed using 5 to 15 μg of duplex RNA and 6 μL of Oligofectamine reagent (Invitrogen). For silencing of Axl, Tyro3 and Gas6, the *SMART*pool (custom-synthesized siRNA) system by Dharmacon was used. As transfection reagent, Dharma*FECT* was used. Transfection was performed by using 100nM of *SMART*pool and 6 μl of Dharma*FECT* (Dharmacon).

3.4 RNA extraction and reverse transcription polymerase chain reaction

Total RNA was isolated by the RNeasy Kit (Qiagen, Crawley, West Sussex, UK) and subjected to on-column DNase digestion with the RNase-free DNase set (Qiagen) according to the manufacturer's instructions. The quality of RNA was verified by electrophoresis through 1% agarose gel and visualized with ethidium bromide. Random-primed first strand cDNA was synthesized in a 50 μl reaction volume starting from 2 μg RNA by using the GeneAmp RNA PCR Core Kit (Applied Biosystems, Warrington, UK). Quantitative (real-time) reverse transcription polymerase chain reactions (QRT- PCR) were performed by using the SYBR Green PCR Master mix (Applied Biosystems) in the iCycler apparatus (Bio-Rad, Munich, Germany). Fluorescent threshold values were measured in triplicate and fold changes were calculated by the formula: 2-(sample 1 ΔCt - sample 2 ΔCt), where Δ*Ct* is the difference between the amplification fluorescent thresholds of the mRNA of interest and the ß actin mRNA.

3.5 Generation of stable shRNA-expressing cell lines

We obtained 5 lentiviral constructs (pLKO.1*puro*) containing custom synthesized, 21-mer short hairpin RNA (shRNA) directed to various coding region of AXL cDNA and with puromycin resistance locus (Mission shRNA, pLKO.1 *puro*) from Sigma-Aldrich, Inc. (Stewart et al., 2003). We transfected 8505-C the plasmid shAxl pool or a pool of non-targeting vectors (control, shCTR) by electroporation. Stable transfectants were clonally selected in medium with 500ng/ml puromycin for 15 days, and cell colonies were screened for Axl silencing by Western blot analysis.

3.6 Protein studies

Protein extractions and immunoblotting experiments were performed according to standard procedures. Briefly, cells were harvested in lysis buffer (50 mM HEPES, pH7.5, 150 mM NaCl, 10% glycerol, 1% Triton X-100, 1 mM EGTA, 1.5 mM MgCl2, 10 mM NaF, 10 mM sodium pyrophosphate, 1 mM Na3VO4, 10 μg of aprotinin/ml, 10 μg of leupeptin/ml) and clarified by centrifugation at 10,000 x g for 30 min. Protein concentration was estimated with a modified Bradford assay (Bio-Rad, Munich, Germany). Immune complexes were detected with the enhanced chemiluminescence kit (ECL, Amersham). Recombinant human SDF-1α was from Peprotech (Princeton Business Park, Rocky Hill, NJ). Anti-AXL for Western Blot and immunoprecipitation analysis was from Santa Cruz Biotechnology, Inc. (Santa Cruz, CA); anti-phosphorilated AXL, specific for the active AXL phosphorilated at tyrosine 779, was from R&D Systems; anti-GAS6 for Western Blot was from R&D Systems. Anti-TYRO3 (NB 100-2311) for Western Blot and immunoprecipitation was from Novus Biologicals. Anti-CXCR4 was from Abcam Ltd. Anti-AKT and antiphosphoAKT, specific for the active AKT phosphorylated at serine 473, were from Cell Signaling (Beverly, MA). Anti-phosphorylated p44/42 MAPK, specific for the active MAPK phosphorilated at threonins 202 and 204, and anti-p44/42 MAPK were from Cell Signaling (Beverly, MA). Monoclonal anti-αtubulin was from Sigma Chemical Co. Secondary anti-mouse and anti-rabbit antibodies coupled to horseradish peroxidase were from Bio-Rad; secondary antibodies coupled to horseradish peroxidase were from Santa Cruz Biotechnology, Inc. (Santa Cruz, CA) and from Biorad. Anti-phosphotyrosine antibodies were from Upstate Biotechnology Inc., (Lake Placid, NY, USA).

3.7 Flow cytometric analysis.

Subconfluent cells were detached from culture dishes with a solution of 0.5 mmol/L EDTA and then washed thrice in PBS buffer. After saturation with 1 μg of human IgG/10^5 cells, cells were incubated for 20 min on ice with phycoerythrin (PE)-labeled antibodies specific for human CXCR4 (R&D Systems) or isotype control antibody. After incubation, unreacted antibody was removed by washing cells twice in PBS buffer. Cells resuspended in PBS were analyzed on a FACSCalibur cytofluorimeter using the CellQuest software (Becton Dickinson). Analyses were performed in triplicate. In each analysis, a total of 10^4 events were calculated.

3.8 ELISA assay

Thyroid cells plated in 6-well dishes were allowed to grow to 70% confluency and then serum-deprived for 24h. Gas6 levels in culture

supernatants were measured using a quantitative immunoassay ELISA kit (QuantiKine colorimetric Sandwich assay ELISA, R&D Systems, UK), following the manufacturer's instructions. Triplicated samples were analyzed at 490 nM with an ELISA reader (Model 550 microplate reader, Bio-Rad). ELISA results were validated on cell lysates by Western Blotting analysis by using an anti-GAS6 antibody (R&D Systems).

3.9 Matrigel invasion

In vitro invasiveness through Matrigel was assayed using transwell cell culture chambers according to described procedures. Briefly, confluent cell monolayers were harvested with trypsin/EDTA and centrifuged at 800x*g* for 10 min. The cell suspension ($1x10^5$ cells/well) was added to the upper chamber of a pre-hydrated polycarbonate membrane filter of 8 μM pore size (Costar, Cambridge, MA, USA) coated with 35 μg Matrigel (Collaborative Research Inc., Bedford, MA, USA). The lower chamber was filled with complete medium or 2.5% FCS (as indicated). After having plated stably-AXL-silenced cells on matrigel, cells were then incubated at 37°C in a humidified incubator in 5% CO2 and 95% air for 24h and 48h. Nonmigrating cells on the upper side of the filter and Matrigel were wiped off and migrating cells on the reverse side of the filter were stained with 0.1% crystal violet in 20% methanol for 15 min, and photographed. The stained cells were lysed in 10% acetic acid. Triplicated samples were analyzed at 570 nM with an ELISA reader (Model 550 microplate reader, Bio-Rad). The results were expressed as the percentage of 8505-C sh-Axl migrating cells with respect to the controls.

3.10 Cell proliferation

S-phase entry was evaluated by BrdU incorporation and indirect immunofluorescence. Cells were serum deprived for 12 h and BrdU was added at a concentration of 10 μM for the last 2h before the reaction was stopped. Subsequently, cells were fixed in 3% paraformaldehyde and permeabilized with 0.2% Triton X-100. BrdU-positive cells were revealed with Texas-Red-conjugated secondary antibodies (Jackson Immuno Research Laboratories, Inc. Philadelphia, PA). Cell nuclei were identified by Hoechst staining. Fluorescence was visualized with a Zeiss 140 epifluorescent microscope.
For growth curves, cells were plated at a density of 0.5×10^5 with complete medium or in low serum conditions (2.5%) (as shown) and counted at the indicated time-points.

3.11 TUNEL assay

For terminal deoxynucleotidyl transferase-mediated. deoxyuridine triphosphate nick end-labeling (TUNEL), an equal number (5×10^3) of thyroid

carcinoma cells from the different lines was seeded onto single-well Costar glass slides. Cells were fixed in 4% (w/v) paraformaldehyde and permeabilized by the addition of 0.1% Triton X-100/0.1% sodium citrate. Slides were rinsed twice with PBS, air-dried and subjected to the TUNEL reaction (Roche). All coverslips were counterstained in PBS containing Hoechst 33258, rinsed in water and mounted in Moviol on glass slides. The fluorescent signal was visualized with an epifluorescent microscope (Axiovert 2, Zeiss) (equipped with a 100X objective) interfaced with the image analyzer software KS300 (Zeiss).

3.12 Tumorigenesis in immunodeficient mice

Mice were housed in barrier facilities and in 12-hour light-dark cycles and received food and water ad libitum at the Dipartimento di Biologia e Patologia Cellulare e Molecolare (University of Naples "Federico II", Naples, Italy). This study was conducted in accordance with Italian regulations for experimentation on animals. All manipulations were performed while mice were under isoflurane gas anesthesia. No mouse showed signs of wasting or other signs of toxicity. BHT101 cells (5 x 10^6 per mouse) were inoculated s.c. into the right dorsal portion of 4-week-old male BALB/c nu/nu mice (The Jackson Laboratory). When tumors measured 40 mm3, mice were randomized to receive AMD3100 (n = 10; 1.25 mg/kg/twice daily) or vehicle alone (n = 10; PBS) by i.p. injection for 5 consecutive days per week for 3 to 4 weeks. Moreover, three groups of mice (4-week-old male BALB/c nu/nu mice, Jackson Laboratories, Bar Harbor, ME) were inoculated subcutaneously into the right dorsal portion with 8505-C shCTR cells (10x10^6/mouse), 8505-C shAXL CL1(1x10^6/mouse), 8505-C shAXL CL2 (1x10^6/mouse). Tumor diameters were measured at regular intervals with a caliper. Tumor volumes (V) were calculated with the formula: V= A x B2/2 (A=axial diameter; B= rotational diameter). Tumors were excised and fixed overnight in neutral buffered formalin and processed by routine methods.

4.RESULTS and DISCUSSION

4.1 CXCR4 is overexpressed in surgical samples of human ATC.

To evaluate CXCR4 expression in ATC, we analysed a set of human samples (n = 13) and normal thyroids (n=6) by quantitative Real-Time PCR. As shown in Fig. 9A, CXCR4 mRNA was found to be up-regulated in most of the tumor samples (10 of 13) with respect to samples of normal thyroid tissue. The statistical analysis showed that the differences in the expression levels of CXCR4 between tumors and normal thyroid tissues were statistically significant (P = 0.0084; Fig. 9A). Then, we performed a Western Blot analysis to verify whether CXCR4 overexpression also resulted in an increase in the protein levels; to this aim, we used protein extracts from a different set of human ATC samples and three normal thyroid tissues and analysed CXCR4 protein levels by using a CXCR4-specific antibody. As shown in Fig. 9B, CXCR4 protein levels were higher in ATC samples than in normal thyroid. As a positive control for CXCR4 expression, we used a human colon carcinoma cell line, the ARO cells, which were previously shown to feature high CXCR4 levels (Hwang et al., 2003). Finally, we evaluated CXCR4 expression, by immunohistochemical experiments, in a set of 33 ATC samples and in normal thyroid tissues. As shown in Fig. 9C, we found that normal thyroid tissues were completely negative for CXCR4 expression, but 13 (39%) of the ATC samples presented a strong positivity for CXCR4. These data suggest that a relevant fraction of human ATCs features the overexpression of CXCR4 receptor and that this overexpression is probably due to a transcriptional mechanism.
(Fig 9).

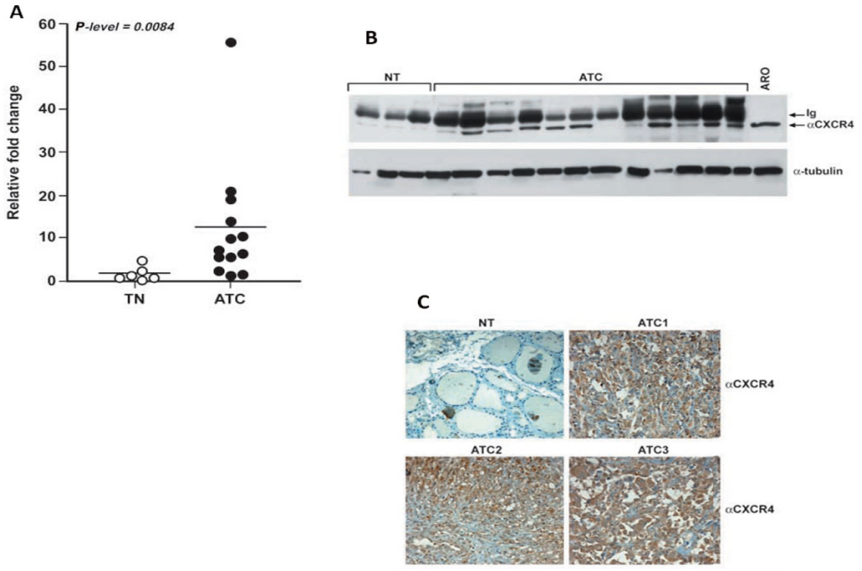

Figure 9. A) Expression levels of CXCR4 in human ATC samples versus six normal thyroid tissues by real-time RT-PCR. CXCR4 expression levels of tumors (Y axis) are calculated relative to the mean CXCR4 level of normal human thyroid tissues (NT). All experiments have been performed in triplicate and the average value of the results was plotted

on the diagram. P value was calculated with the two-tailed, non-parametric Mann-Whitney test. **B)** Protein lysates (100 μg) extracted from the indicated samples underwent Western blotting with anti-CXCR4-specific antibodies. Immunocomplexes were revealed by enhanced chemiluminescence. Equal protein loading was ascertained by anti-tubulin immunoblot. **C)** Immunohistochemical staining for CXCR4 of formalin-fixed, paraffin-embedded ATCs. Tissue samples from normal thyroid (NT) or ATC were incubated with a mouse monoclonal anti-CXCR4 antibody. ATCs show a strong immunoreactivity for CXCR4,whereas normal thyroid tissue is negative. Representative pictures of normal and pathologic positive samples are shown. Isotype control was also performed (data not shown).

4.2 CXCR4 is overexpressed in thyroid cancers of transgenic mice.

Several transgenic mice model of thyroid cancer are available, developed by using various oncogenes under the transcriptional control of the thyroid-specific thyroglobulin bovine promoter. Carcinomas developed by these mice, according to the specific transgene, can be assimilated to human PTC, FTC or ATC, both cytologically and histologically. In particular, mice expressing either RET/PTC3 (TGPTC3) or TRK/T1 (TGTRK) oncogene develop PTC-like tumors (Powell et al., 1998; Russell et al., 2000). NRAS transgene expression induces follicular tumors that progress to poorly differentiated carcinomas (TGNRAS; Vitagliano et al., 2006). Finally, animals expressing the SV40 large T antigen (TGSV) feature aggressive thyroid cancer very similar to human ATC (Ledent et al., 1991). We decided to evaluate the expression of CXCR4 in carcinomas developed in these animal models by performing Western blot analysis with anti-CXCR4 antibodies. As shown in Fig. 10, all tumors derived by transgenic mice expressed CXCR4, but, it was much more expressed in ATC models with respect to well-differentiated thyroid cancer models. These data, together with previously published data (Hwang et al., 2003; Castellone et al., 2004), suggest that CXCR4 up-regulation is a frequent event in thyroid tumorigenesis and that, in the mice models, there is a strong correlation between the malignancy of lesions and the overexpression of CXCR4.

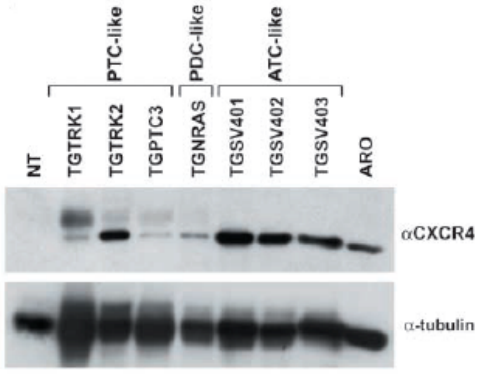

Figure 10. The expression levels of CXCR4 protein were analyzed in thyroid tumor samples from transgenic mice models. Tumor tissues were snap frozen and immediately homogenized by using the Mixer Mill apparatus in lysis buffer. Equal amounts of proteins were immunoblotted and stained with anti-CXCR4 polyclonal antibodies (Abcam). ATC-like samples displayed a more intense immunoreactivity for CXCR4. As a control for equal loading,the anti-a-tubulin monoclonal antibody was used.

4.3 CXCR4 is overexpressed in human ATCs cell lines

We analysed a panel of different human ATC cell lines; as shown in Fig. 11A and B, normal thyroid cultures displayed undetectable CXCR4 expression levels. PTC cell lines expressed CXCR4, but most (7 of 10) of ATC cell lines expressed high levels of the receptor both at the protein and at the mRNA levels, as verified by Western blot (Fig 11A and B) and quantitative Real-Time PCR analysis (Fig. 11C). We then asked whether this receptor was expressed on the cell surface. To this aim, we performed flow cytometry experiments using a PE-conjugated mouse monoclonal anti-CXCR4 antibody. We determined the percentage of CXCR4-positive cells. Normal thyroid cells did not express CXCR4 as analyzed by FACS analysis (data not shown), while almost all the ATC cell lines tested, with the exception of the FB1, expressed CXCR4; the ARO cells were used as a positive control (Fig 12). Interestingly, SDF-1, the CXCR4 ligand, was not expressed by ATC cells as assessed by quantitative PCR or ELISA assay (data not shown).

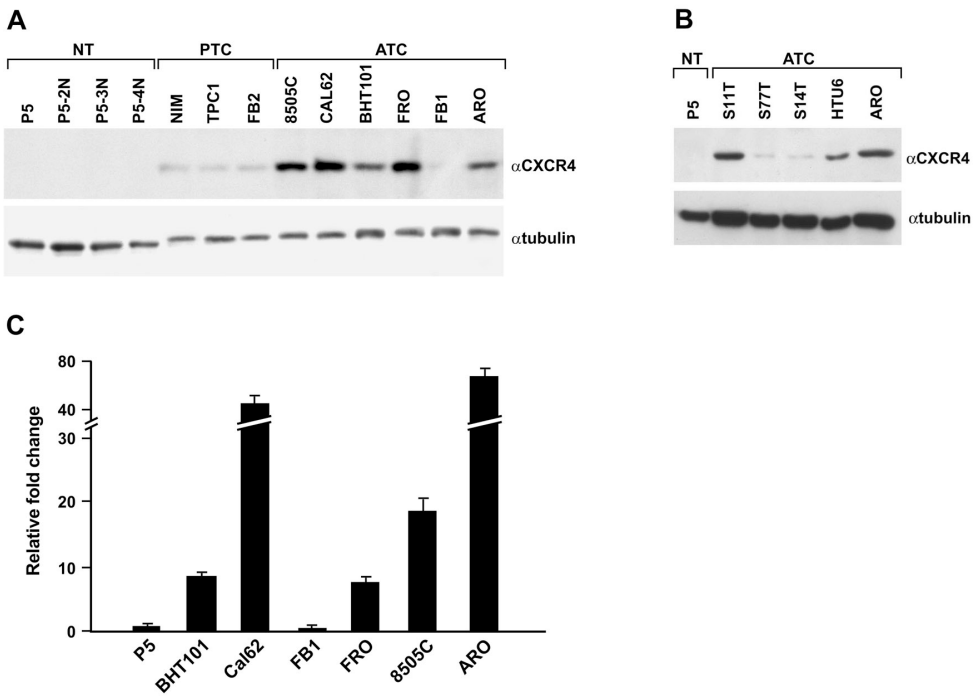

Figure 11. Overexpression of CXCR4 in human ATC cell lines. A) CXCR4 up-regulation in cell lines derived from human thyroid carcinomas was evaluated by Western Blot with a polyclonal anti-CXCR4 antibody. The expression levels of CXCR4 protein were analyzed in the P5 human primary thyroid cells and in the indicated cell lines derived from human PTCs (NIM,TPC1, FB2) or from human ATCs (8505C, CAL62, BHT101, FRO and FB1). ARO cells, a CXCR4-expressing human colon carcinoma cell line, was used as positive control **B)** ATC-derived (S11T,S77T, S14T, HTU8) and normal thyroid primary cultures (P5) were screened for CXCR4 expression by Western blot analysis with the polyclonal anti-CXCR4 antibody. As a control for equal loading, the anti-tubulin monoclonal antibody was used. **C)** Expression levels of CXCR4 mRNA in human ATC cells versus the P5 normal thyroid culture were evaluated by real-time RT-PCR analysis. CXCR4 expression levels of ATC cell lines (Y axis) are calculated relative to the expression level in the normal human cell culture P5. All experiments were performed in triplicate, and the average value of the results was plotted on the diagram. SDs were smaller than 25% in all cases (data not shown).

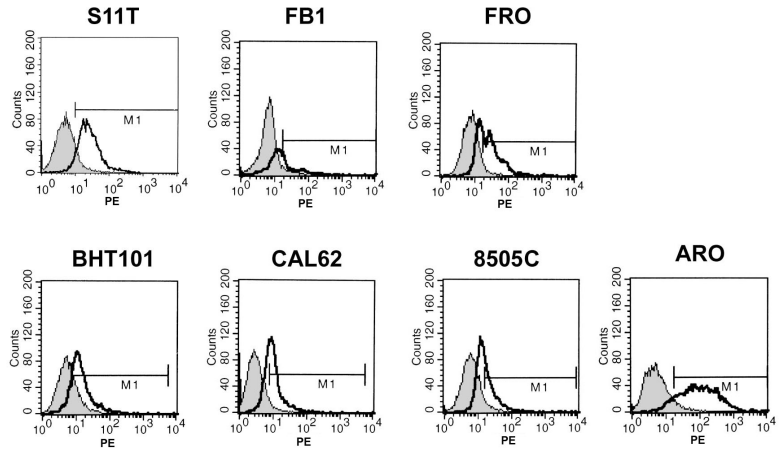

Figure 12. FACS (fluorescence-activated cell sorting analysis) of surface-expressed CXCR4 in ATC cells. Subconfluent cells were detached from culture dishes and incubated with PE-labeled antibodies specific for human CXCR4. ARO cells were used as positive control of CXCR4 expression.

4.4 CXCR4 is activated by SDF-1α in human ATC cells

It is already known that the stimulation of CXCR4 is able to induce the activation of different kinase cascades, specifically through the activation of the G subunit of the Gi protein (Gangu et al., 1998; Peng et al., 2005). We asked whether CXCR4 receptor was also functional in human thyroid carcinoma cell lines. Particularly, we tested the phosphorylation of two downstream effectors, extracellular signal-regulated kinase (ERK) 1/2 and AKT, using specific phosphorylated antibodies. To this aim, we selected S11T and BHT101 cells. Cells were serum deprived for 12 h and then stimulated with SDF-1α for different time-points. As shown in Fig. 13A and B, the activation of ERK1/2 both in S11T and BHT101 was evident from the first minute after the stimulation with SDF-1α and proceeded in a time-dependent way; instead, AKT activation was a later event of the stimulation with SDF-1α and was less pronounced in S11T cells. Taken together, these data indicate that CXCR4 is a functional receptor in ATC cells. Activation of ERK1/2 and AKT was observed in virtually all the ATC cell lines expressing CXCR4, whereas normal thyroid cells, which do not express CXCR4, did not display these effects (data not shown).

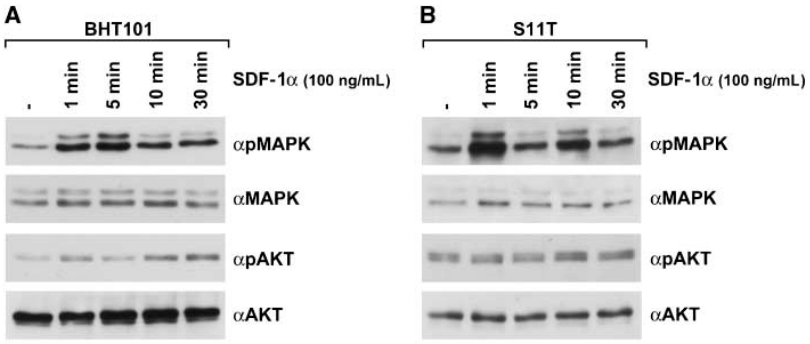

Figure 13. **A) and B)** protein extracts from the indicated cell lines were subjected to immunoblotting with anti-phosphorylated p44/42 MAPK (apMAPK) and with anti-phosphorylated AKT (apAKT) antibodies. The blots were reprobed with anti-p44/42 and anti-AKT antibodies for normalization.

4.5 CXCR4 induces S-phase entry of human ATC cell lines.

In order to evaluate whether SDF-1α was able to induce cell proliferation in ATC cells, we performed BrdU incorporation assays on BHT101 and S11T. Cells were maintained in low-serum (2.5%) growth conditions for 24 h and then either left untreated or stimulated with SDF-1α for 12 h. As a measure of DNA synthesis, we counted BrdU-positive cells on a 1-h BrdU pulse. As shown in Fig. 14 A, both the cell lines presented an increased percentage of BrdU incorporation under SDF-1α treatment. We then used a specific CXCR4 inhibitor, AMD3100, to block this effect. AMD3100 is a competitive antagonist of SDF-1α, but it also displays partial agonist activity (De Clerq, 2005). Normal thyroid cells were insensitive to SDF-1α stimulation and to the effect of AMD3100 (data not shown). As shown in Fig. 14A, in the presence of AMD3100, SDF-1α–mediated DNA synthesis in ATC cells was blocked. To evaluate whether SDF-1α could stimulate ATC cell growth, we also performed growth curves in low-serum (2.5%) conditions. As shown in Fig. 14B, the stimulation of BHT101 with SDF-1α increased their proliferation rate, and AMD3100 reverted this effect. SDF-1α was also able to increase the proliferative rate of different ATC cell lines, which express CXCR4, BHT101 and CAL62, but was unable to do so on FB1 cells, which we previously reported to be devoid of CXCR4; AMD3100 alone did not have any effect on ATC cells (data not shown). To exclude off-target effects of AMD3100 and to directly determine the role of CXCR4 on ATC cell proliferation, we used small duplex RNA oligos to knock down CXCR4. We then transfected CXCR4 siRNAs into BHT101, CAL62, and 8505C cells. CXCR4 RNA interference was verified by Western blot analysis in BHT101 cells (Fig. 15A and B). CXCR4 silencing substantially impaired SDF-1α–induced S-phase entry in all the ATC cells but had no effect on BrdU incorporation in the absence of the chemokine, as shown in Fig. 15. When we used the control scrambled siRNA,

this inhibitory effect was not observed. Furthermore, scrambled oligos had no effect on CXCR4 protein levels (Fig. 15A). These data confirm the role of CXCR4 and of its specific ligand SDF-1α, in the proliferation of human ATC cells, thus suggesting the possibility to neutralize this pro-proliferative effect by inhibiting this chemokine receptor.

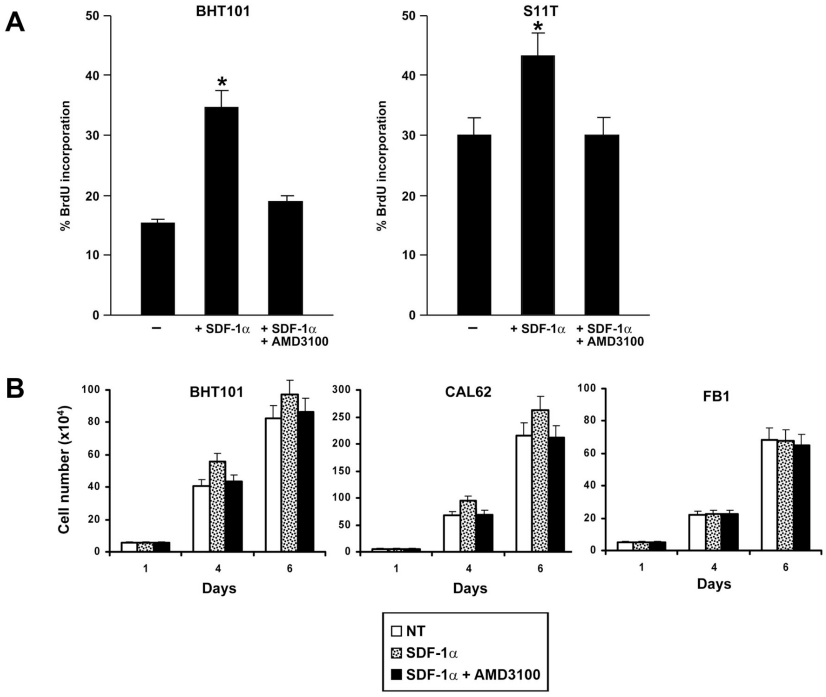

Figure 14. **A)** BrdU incorporation was measured to evaluate S-phase entry of BHT101 and S11T cells treated with SDF-1α in the presence or absence of the CXCR4 inhibitor AMD3100. Columns, average results of three independent experiments; bars, SD. $P < 0.05$. **B)** The indicated cell lines were plated at the same density (5×10^4) in 2.5% serum, harvested, and counted at the indicated time points. Columns, average results of at least three independent determinations; bars, SD.

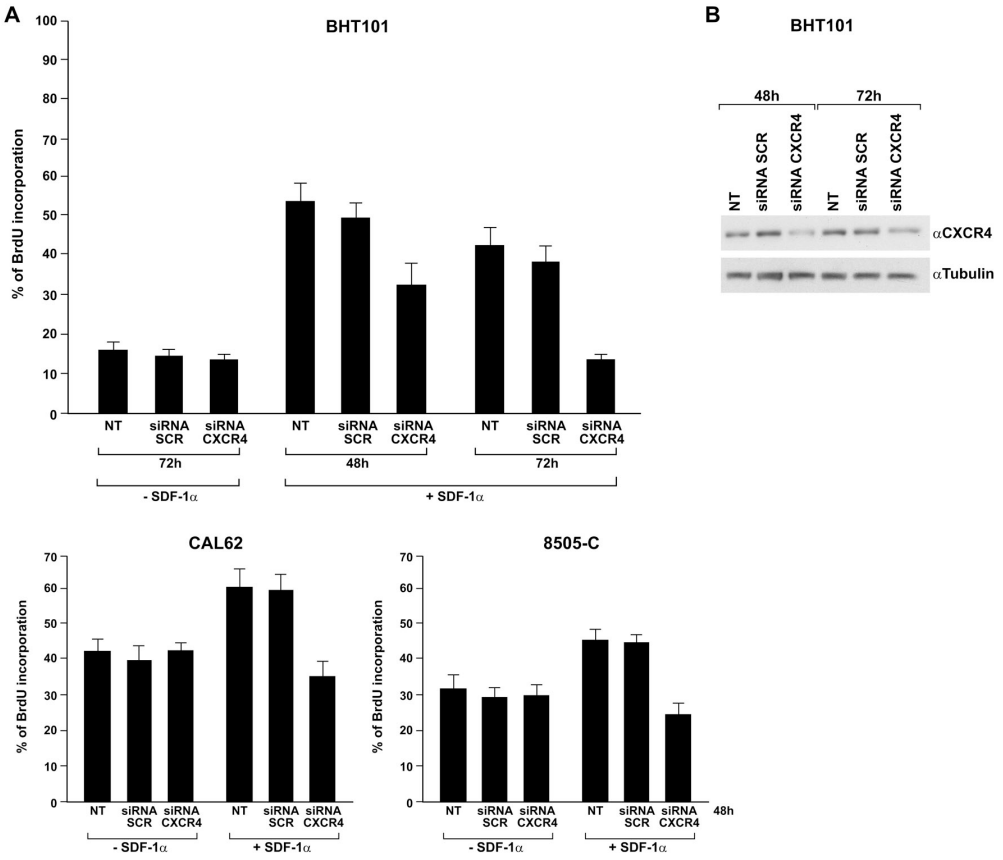

Figure 15. A) CXCR4 RNA interference was used to transiently suppress CXCR4 expression in ATC cells. BHT101, CAL62 and 8505C cells were transfected with siRNAs against CXCR4 (siRNA CXCR4) or control non-specific small duplex RNA containing the same nucleotides, but in scrambled fashion (siRNA SCR), and harvested 48 and 72 h later. CXCR4 RNA interference (siRNA CXCR4) inhibited SDF-1α–stimulated S-phase entry as evaluated by BrdU incorporation assay. Control siRNA (siRNA SCR) did not inhibit DNA synthesis. Unstimulated cells were not affected by siRNA transfection. **B)** Protein lysates were subjected to immunoblotting with anti-CXCR4 and anti-tubulin antibodies. Control siRNA did not affect CXCR4 protein levels.

4.6 CXCR4 reduces the growth of ATC xenografts in nude mice.

It has been previously shown that the CXCR4/SDF-1 axis plays an important role in the growth and in the metastatic ability of several epithelial cancers (Balkwill et al., 2004). According to our *in vitro* results regarding the possibility to reduce the proliferation of human anaplastic cell lines by blocking CXCR4 with its specific antagonist, AMD3100, and because it has been shown that this chemokine is secreted by stromal tumoral cells (Orimo et al., 2005), we hypothized that the drug could represent a real therapeutical possibility for the treatment of human ATCs. In order to demonstrate that, we selected BHT101 cells for their ability to respond to SDF-1α and their ability to form tumors in vivo with high efficiency. We then injected nude mice, s.c., with 5 x 10^6 cells. After about 10 days, when tumors measured 40 mm^3, we

randomized mice (n = 20) in two groups to receive AMD3100 (1.25 mg/kg/twice daily i.p.) or vehicle 5 days per week for 3 to 4 weeks. We measured tumor diameters at regular times with caliper. After 21 days, the mean volume of BHT101 tumors in mice treated with AMD3100 was 48 mm^3, whereas that of mice treated with vehicle was 620 mm^3. No mice expressed signs of toxicity due to the drug. We show representative experiments in Fig. 16A and B. These data confirmed the critical role of CXCR4 in the tumoral growth and, most importantly, suggest the possibility to consider CXCR4 as potential therapeutical target for the treatment of human anaplatic thyroid carcinoma, that represents one of the most aggressive human malignancy.

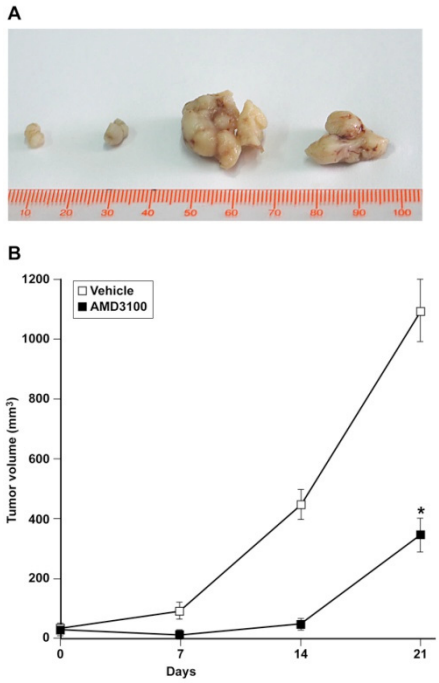

Figure 16. Antitumorigenic effects of AMD3100 in BHT101 xenografts. A) Excised and photographed tumors. Two representative examples of BHT101 xenografts untreated (right) or AMD3100 treated (left) are shown. **B)** Antitumorigenic effects of AMD3100 in BHT101xenografts. BHT101 cells (5 x 10^6 per mouse) were injected s.c. into the right dorsal portion of BALB/c athymic mice. When tumors measured 40 mm3, mice were randomized to two groups to receive AMD3100 or vehicle (PBS) by i.p. injection. Treatment was given for 5 consecutive days per week for 3 to 4 wk (day 1 is the treatment starting day). Tumor diameters were measured with calipers and tumor volumes were calculated. Unpaired Student's t test (normal distributions and equal variances) was applied. All P values were two sided, and differences were statistically significant at $P < 0.05$(*).

4.7 The Tyro3 and Axl receptors are transcriptional targets of the CXCR4/SDF-1α axis and are overexpressed in thyroid cancer cells.

To characterize the molecular mechanisms of the SDF-1/ CXCR4 biological activity in thyroid cancer cells, we performed a global gene expression profiling experiment, by using, as a model system, TPC1 cells, a human PTC-derived cell line that has been previously characterized for the expression and the functional activity of CXCR4 (Castellone et al., 2004).

Cells were serum-deprived and then stimulated for 24 h with human recombinant SDF-1α (100ng/ml). To perform microarray analysis, the GE Healthcare software and the codelink gene expression bioarray platform (based on an oligonucleotide array representing the entire human genome) was used. Statistical analysis on triplicate experiments, data mining and differential expression were evaluated by using the GeneSpring analysis platform. Several groups of SDF-1α-regulated genes were identified based on statistical analysis, whose activity, according to data available in literature, is related to different biological processes. Consistent with the biological activities of SDF-1α, genes involved in cell adhesion and motility, cell proliferation, survival and signal transduction resulted up-regulated. Genes with functions related to interferon activity, mRNA processing and ribosome biosynthesis were also identified. Genes with at least 1,5 fold change and a P value < 0.05 were considered.

Among the different genes induced by SDF-1α, we found TYRO3 and AXL, two tirosine kinase receptors belonging to the TAM family. To confirm these data, we first analysed Tyro3 and Axl levels both at mRNAs and protein levels respectively by Real-time (RT-PCR) (data not shown) and by Western blot analysis in TPC1 cells treated with SDF-1α. Tyro3 basal levels were much lower than those of Axl in TPC1 cells, but under SDF-1α treatment , both Axl and Tyro3 protein levels increased, as shown by the time-course experiments in fig. 17A. SDF-1α treatment also increased their tyrosine phosphorylation levels (data not shown). Then, Tyro3 and Axl protein levels were evaluated by Western blot analysis in a panel of thyroid cancer cell lines and in primary cultures of thyroid normal cells. As shown in Fig. 17B, Tyro3 and Axl protein levels were not expressed in normal thyroid cells, but most of the cancer cell lines presented high levels of the two receptors, being Axl consistently more expressed than Tyro3. This was also confirmed by RT-PCR experiments (data not shown). We also analysed the expression of both the receptors in a rat thyroid cell line (PC Cl3) and in PC Cl3-derived cell lines transduced with different oncogenes. While we could not detect endogenous Tyro3, we were able to show that two RET/PTC isoforms, RET/PTC1 and RET/PTC3, the cooperation between E1A and RAF, and the v-mos oncogenes were able to induce Axl overexpression in these cells. Since it has been reported that TAM receptors are activated in different cancer histotypes (Craven et al.,1995; Nemoto et al., 1997; Ito 2002; Zantek et al., 2001; Shieh et al., 2005; Gustafsson et al., 2009), we asked whether Axl receptor was also tyrosine-phosphorylated in our cell lines. To verify this, we performed immunoprecipitation experiments by using an anti-Axl antibodies followed by Western blot analysis with either anti-phosphotyrosine antibodies or an anti-phospho-Axl antibody, which specifically recognizes phosphorylated Tyr 779 (Y779), a residue of the carboxy-terminal tail that is phosphorylated upon Axl stimulation. As shown in fig. 17C, we found that all the cell lines tested displayed Axl activation, being phosphorylation levels higher in Cal62, 8505-C and NIM with respect to OCUT-1 and ACT1. The TPC1 cells, derived from a human PTC featuring a spontaneous RET/PTC1 rearrangement, showed the

highest levels of phospho-Axl relative to total Axl. We also evaluated Axl activation in Axl-expressing PC Cl3 rat cell lines, PC PTC3, PC663 and PC E1A RAF. As shown in fig. 17C, Axl phosphorylation was very low in PC663 and PC E1A/RAF, while PC PTC3, consistently, displayed the highest levels. (Fig. 17).

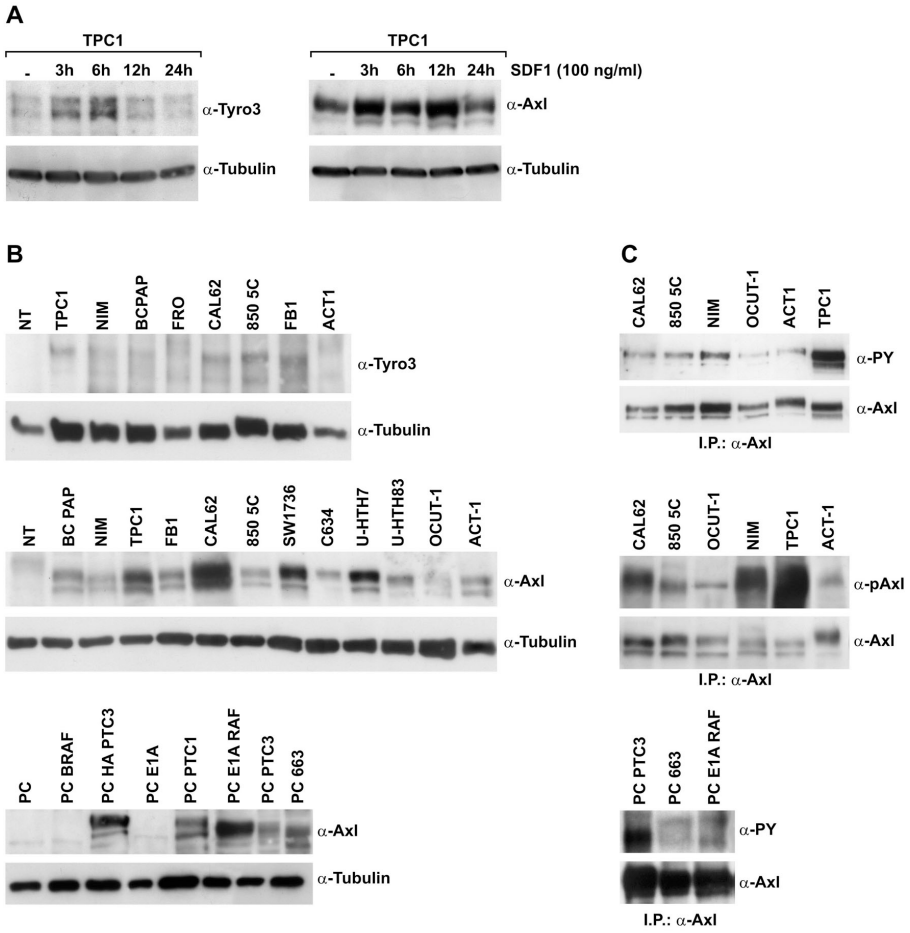

Figure 17: A) Analysis of Tyro3 and Axl protein levels by western blot analysis on TPC1 cells stimulated with SDF-1α at different time-points. **B**) Evaluation of Tyro3 and Axl protein levels by western blot in a panel of human thyroid cancer cell lines and in primary cultures of thyroid normal cells (NT). Axl levels were also evaluated in PC rat thyroid cell lines transduced with the indicated oncogenes. Equal amounts of proteins (50 μg) were immunoblotted with anti-TYRO3 and anti-AXL polyclonal antibodies. Anti-tubulin monoclonal antibody was used as a control for equal loading. **C)** Analysis of Axl tyrosine-phosphorylation by anti-phosphotyrosine and phospho-AXL western blot in a panel of human PTC and ATC cell lines. AXL-phosphorylation levels were evaluated.

These data show that thyroid cancer cells express both Axl and Tyro3 receptors. Moreover, in most cell lines Axl is also activated, as demonstrated by the high levels of phosphotyrosine content of the receptor.

4.8 Thyroid cancer cell lines express Gas6, one of the Tyro3/Axl ligands.

Since it has been reported that Axl activation in tumor cells is due to autocrine or paracrine loops, we asked whether thyroid cancer cell lines expressed one of the Axl/Tyro3 ligands, Gas6 and Protein S. We first performed RT-PCR experiments to evaluate whether our cells expressed these ligands and we found that only Gas6, but not Protein S, was produced (data not shown). To confirm these results, we analysed Gas6 levels by using both ELISA immunoassay and Western blot analysis. As shown in Fig. 18A, among the cell lines we tested, 8505-C, NIM, CAL62 and SW1736, produced detectable levels of Gas6, while OCUT-1 and TPC1 did not. When we performed a Western blot analysis with a specific anti-Gas6 antibody, we found again that all the cell lines produced Gas6, with the exception of TPC1. Recombinant human Gas6 was used as a positive control. Silencing of Gas6 in NIM cells (NIM siGAS6) and overexpression of Gas6 in OCUT-1 cells (OCUT-1 Gas6) were used to confirm antibody specificity (Fig. 18B).
(Fig. 18).

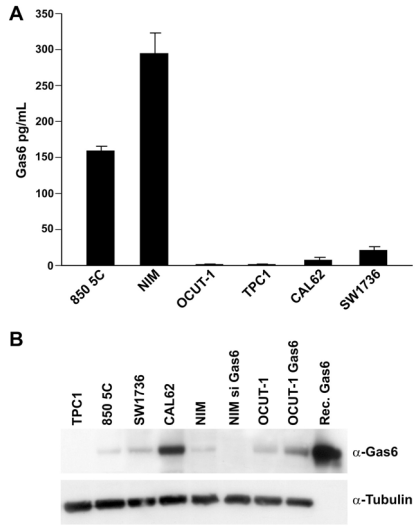

Figure 18: A) Evaluation of Gas6 levels by using ELISA immunoassay. **B**) Western blot analysis with specific anti-Gas6 antibody. Anti-tubulin monoclonal antibody was used as a control for equal protein loading.

In summary, with these experiments, we identified cell lines, such as CAL62and SW1736, that produce Gas6, but inefficiently release it in the culture medium; cell lines, such as NIM and 8505-C, that produce and secrete high levels of Gas6; cell lines, such as TPC1, that did not produce detectable levels of Gas6, but, despite this, display high levels of Axl phosphorylation. Taken together, these data suggest that receptor activation is probably due to an autocrine effect, since all the cell lines, with the exception of the TPC1, express variable levels of the ligand, Gas6.

4.9 Human thyroid cancer specimens express Axl and its ligand Gas6

To confirm our results, we evaluated Axl and Gas6 expression in human thyroid cancer specimens. We analysed a panel of 26 thyroid carcinoma samples (8 PTCs, 10 FTCs and 8 PDC/ATCs) and 2 normal thyroid by using immunohistochemical staining with specific anti-human Axl and Gas6 antibodies. The 73% (19/26) of all the tested carcinoma presented positivity for Axl expression (Table 1).

Sample	% Axl positivity	% Gas6 positivity
PTC	60%	ND
PTC	20%	20%
PTC	60%	40%
PTC	40%	10%
PTC	0%	10%
PTC	30%	40%
PTC	80%	30%
PTC	10%	10%
PTC	40%	0%
FTC	0%	0%
FTC	30%	0%
FTC	20%	0%
FTC	60%	20%
FTC	60%	10%
FTC	0%	0%
FTC	0%	20%
FTC	0%	20%
FTC	10%	10%
FTC	10%	10%
PDC	10%	30%
ATC	60%	50%
ATC	40%	60%
ATC	0%	30%
PDC	0%	40%
PDC	30%	0%
PDC	30%	30%
ATC	10%	60%

Table 1: This Table summarizes the percentage of AXL and GAS6 positivity in the panel of human thyroid cancer specimens analysed by immunohistochemistry.

As shown in Fig.19, Axl positivity was observed mainly in the epithelial tumoral cells. Most of the samples showed membrane positivity, but a small number of specimens were characterized by cytosolic staining. In the last case, Axl was particularly found in the perinuclear vescicles probably representing the Golgi apparatus, pattern that is sometimes observed for overexpressed proteins. Tumoral stroma and non tumoral adjacent tissues were negative for Axl staining, with the exception of endothelial and red blood cells, that were strongly recognized by anti-Axl antibody, as previously reported (Tang et al., 2009). To confirm whether thyroid carcinomas feature autocrine/paracrine loops involving Axl and its ligand, we also performed IHC experiments to evaluate Gas6 expression in the same human sample set. As summarized in

Table 1 and shown in fig. 19, 74% of analysed samples scored positive for Gas6 expression and 55% of these were positive for both receptor and ligand expression. Gas6 staining was cytosolic and was mainly found in carcinoma cells; some samples also presented stromal positivity, suggesting that ligand can also be provided by other cells of the tumor microenvironment.
(Fig. 19).

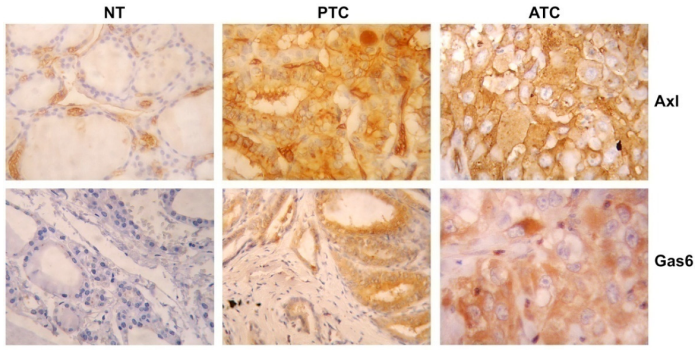

Figure 19: Immunohistochemistry on human thyroid cancer specimens with anti-AXL and anti-GAS6 antibodies. Axl positivity was observed mainly in tumoral cells. Gas6 staining was cytosolic and was mainly found in carcinoma cells but also a stromal positivity was observed.

4.10 Axl/Tyro3-Gas6 axis blockade inhibits papillary thyroid cancer (PTC) cell proliferation.

To investigate whether the Axl/Gas6 axis could influence thyroid cancer cell proliferation, we performed BrdU-incorporation experiments. To this aim, we first selected two PTC cell lines, TPC-1 and NIM. As shown above, TPC1 cells express high levels of activated Axl in the absence of the ligand; NIM cells express both Axl receptor and Gas6 ligand. We analysed the levels of DNA synthesis by BrdU incorporation assays both in basal conditions (serum deprivation) and in the presence of exogenous Gas6. As shown in Fig. 20A, under serum-deprivation, 10% of TPC1 incorporated BrdU; when Gas6 was added, the percentage of BrdU incorporation increased to 20%. Then, we used a blocking compound, a chimaeric protein (Dtk/FC) which is composed by the extracellular domain of Tyro3 receptor fused to the FC portion of an IgG that is able to sequester and then to inhibit Gas6-mediated biological effects. In the presence of Dtk/Fc, we found that the percentage of BrdU-positive cells after Gas6 stimulation decreased. To confirm the role of Axl in TPC1 cell proliferation, we decided to silence the receptor by using transient RNA interference. Axl silencing was verified by Western blot analysis (Fig 20C). As shown in Fig. 20B, when Axl was silenced, there was only a modest reduction of BrdU incorporation in basal conditions. This reduction was more dramatic in the presence of Gas6: the percentage of BrdU-positive cells strongly decreased from 27% to 13%. Consistently, Gas6 silencing did not modify TPC1 DNA synthesis, as we expected, according to the observation that Gas6 is not

produced by TPC1 cells (data not shown). Since the additon of Gas6 partially recovered the effects of Axl blockade in this cell line, we evaluated whether Tyro3 was responsible for this effect. To this aim, Tyro3 was silenced in TPC1 cells through RNA interference and DNA synthesis was evaluated. As shown in Figure 20B, Tyro3 silencing also induced a reduction of BrdU incorporation, but when we silenced both Tyro3 and Axl receptors, we obtained a dramatic decrease of the percentage of BrdU-positive cells to 5%; finally, Gas6 treatment did not modify the effect of the double silencing. Tyro3 and Axl silencing was confirmed by Western blot analysis (Fig 20C).

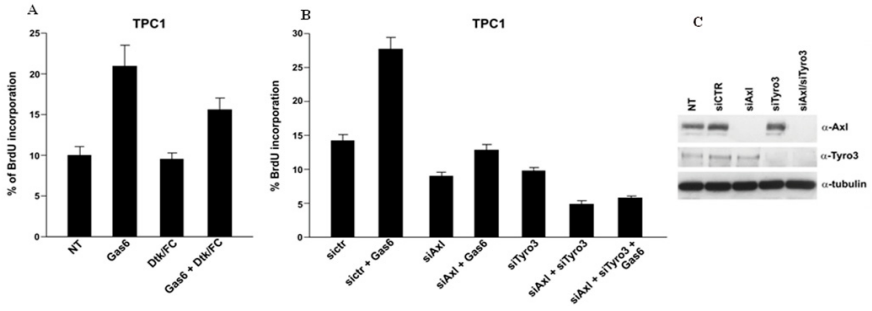

Figure 20. Axl/Tyro3 blockade inhibits TPC1 cell proliferation. A) TPC1 cells were serum-deprived and, where indicated, treated with GAS6 (200ng/ml) and/or the blocking chimaeric protein Dtk/FC for 24h. The results are expressed as percentage of BrdU incorporation with respect to NT (untreated) TPC1 cells. Gas6 stimulated BrdU incorporation of TPC1 cells and this effect was blocked by the Dtk/FC protein. The average results and the standard deviations of three independent experiments in which at least 400 cells were counted are reported. **B)** TPC1 were silenced for AXL or TYRO3 receptors; after 24h of silencing, cells were serum-deprived for 12h and treated or not with GAS6. AXL and TYRO3 silencing inhibited TPC1 BrdU incorporation. The results are expressed as percentage of BrdU incorporation with respect to sictr-silenced TPC1 cells (sictr). **C**) Western blot analysis with anti-AXL and anti-TYRO3 antibodies was peformed to verify Axl- Tyro3 silencing. Anti-tubulin monoclonal antibody was used as a control for equal protein loading.

Moreover, we performed similar experiments by using another PTC cell line, NIM, that, as already shown above, expresses both Axl and Gas6. As indicated in Fig 21, the addition of exogenous ligand did not modify BrdU incorporation. Instead, the blockade of both endogenous Axl and Gas6 by using Dtk/FC or RNAi inhibited NIM DNA synthesis (Fig 21A and B), and exogenous Gas6 addition partially reverted these effects. These data suggested that the presence of Tyro3 could also affect NIM proliferation. In fact, as shown in Fig 21B, Tyro3 silencing induced a reduction of BrdU incorporation; Tyro3/Axl silencing was more effective than single knockdown. In this condition, exogenous Gas6 was not able to modify the percentage of BrdU incorporation. Gas6 silencing was as effective as Axl/Tyro3 double silencing. Gas6, Tyro3 and Axl knockdown was verified by Western blot analysis (Fig 21).

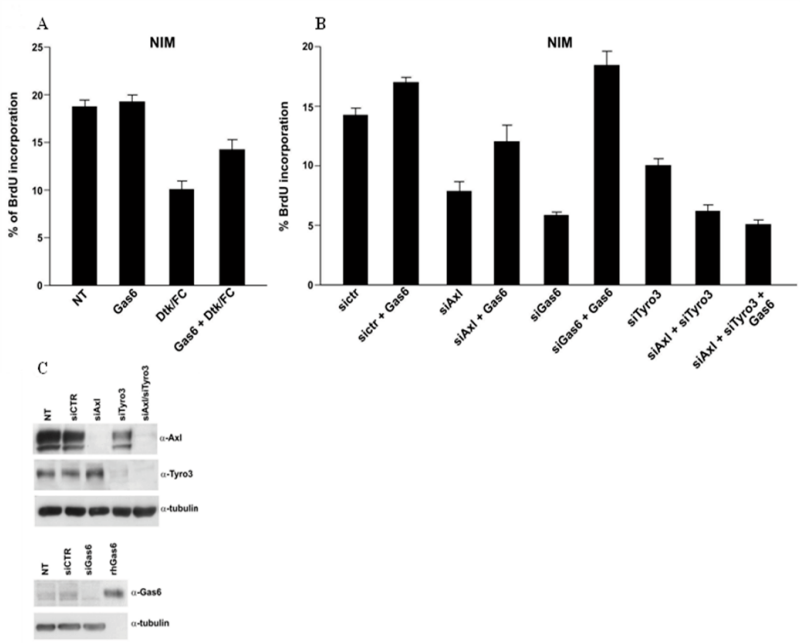

Figure 21. Axl/Tyro3 blockade inhibits NIM cell proliferation. A) NIM cell lines were serum-deprived and then treated with GAS6 and Dkt/FC as indicated. BrdU incorporation was evaluated in presence or absence of human recombinant GAS6. Dtk/FC inhibited DNA synthesis of NIM cells. **B)** AXL, Gas6 and TYRO3 silencing affected NIM BrdU incorporation. **C**) Western blot analysis verified Axl, Tyro3, GAS6 silencing. Anti-tubulin monoclonal antibody was used as a control for equal protein loading.

4.11 Axl/Tyro3-Gas6 axis blockade inhibits papillary thyroid cancer cell survival.

To evaluate whether Axl/Tyro3-Gas6 axis blockade could also influence PTC cell lines resistance to apoptotic stimuli, we performed TUNEL assays, both in basal conditions or in the presence of exogenous Gas6. To this aim, we used again TPC1 and NIM cells. In these experiments, we first induced apoptosis by exposing cells to a pro-apoptotic substance, DEM (DiEthylMaleate), or to serum-deprivation. As shown in Fig 22A, upon DEM treatment, 48% of TPC1 cells displayed TUNEL positivity, that was dramatically decreased in the presence of exogenous Gas6. The blockade of exogenous Gas6 with Dtk/FC completely reverted this effect. Consistently, Dtk/FC did not modify the percentage of apoptotic cells when used in the absence of Gas6. We also performed apoptosis assays after Axl- or Gas6-silencing. In this case, apoptosis was induced by 24h of serum deprivation. In this condition, 10% of apoptotic cells were observed. This percentage decreased to 5% when Gas6 was added. Axl silencing dramatically increased the rate of apoptotic cells to 30%. Interestingly, when Gas6 was added to Axl-silenced cells, the pro-apoptotic effects of Axl silencing were consistently inhibited (Fig 22B). These results can be considered as a further confirm that the other tyrosine-kinase receptor, Tyro3, can contribute to Axl biological

functions. In fact, when Tyro3 was knocked down in TPC1 cells through RNA interference, we found an increase of apoptotic rate and, particularly, the silencing of the two receptors together resulted in further decrease of TPC1 survival, not modified by the addition of exogenous Gas6 (Fig 22B). Finally, again Gas6 silencing did not modify TPC1 apoptosis rate both in presence and in absence of Gas6 (data not shown). Axl and Tyro3 silencing was verified by Western blot analysis (Fig 22C).

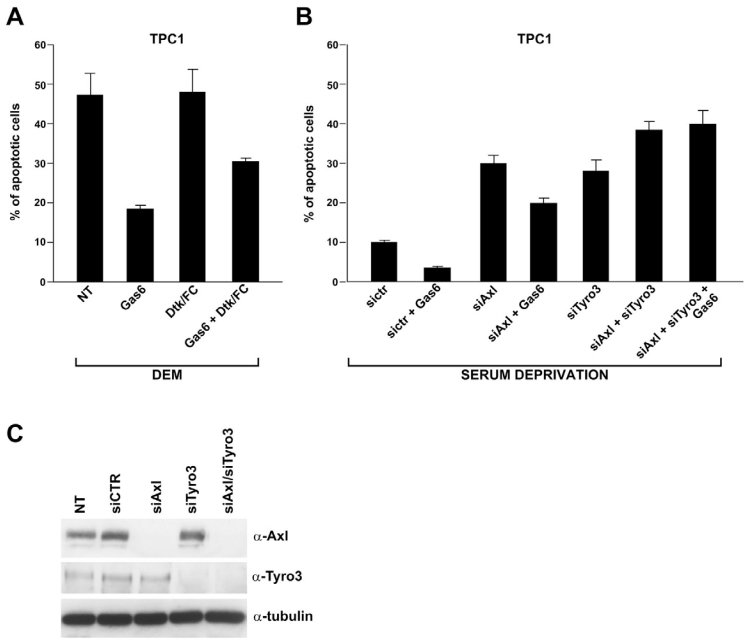

Figure 22. Axl/Tyro3 blockade inhibits TPC1 cell survival. A) TPC1 cell line was treated with a proapoptotic sunstance DEM (DiEthylMaleate) for 12h and then with Gas6 and/or Dtk/FC. Gas6 decreased the percentage of TPC1 apoptotic cells and Dtk/FC reverted this effect. The percentage of apoptotic cells was evaluated with the TUNEL reaction. The average results and S.D. of three independent experiments in which at least 400 cells were counted is reported. **B)** TPC1 were serum-deprived and AXL, TYRO3 or both were silenced. In these conditions, the percentage of apoptotic cells increased. **C**) Western blot analysis with anti-AXL and anti-TYRO3 antibodies was perfprmed to verify Axl- Tyro3 silencing. Anti-tubulin monoclonal antibody was used as a control for equal protein loading.

We obtained similar results when we performed TUNEL assays on NIM cell lines. As shown in Fig 23A, DEM treatment of NIM cells induced 40% of apoptotic cells, and the blockade of Gas6 with DtkFC increased to 62% this percentage; when cells were serum deprived (Fig 23B), we observed 18% of apoptotic cells. This percentage was slightly changed by Gas6 treatment. Axl or Gas6 silencing strongly enhanced NIM apoptotic rate, and these effects were again reverted by exogenous Gas6. Tyro3 silencing also affected NIM survival. The silencing of the two receptors resulted in a dramatic increase of the apoptotic rate, and the addition of Gas6 could not revert this phenotype.
(Fig 23).

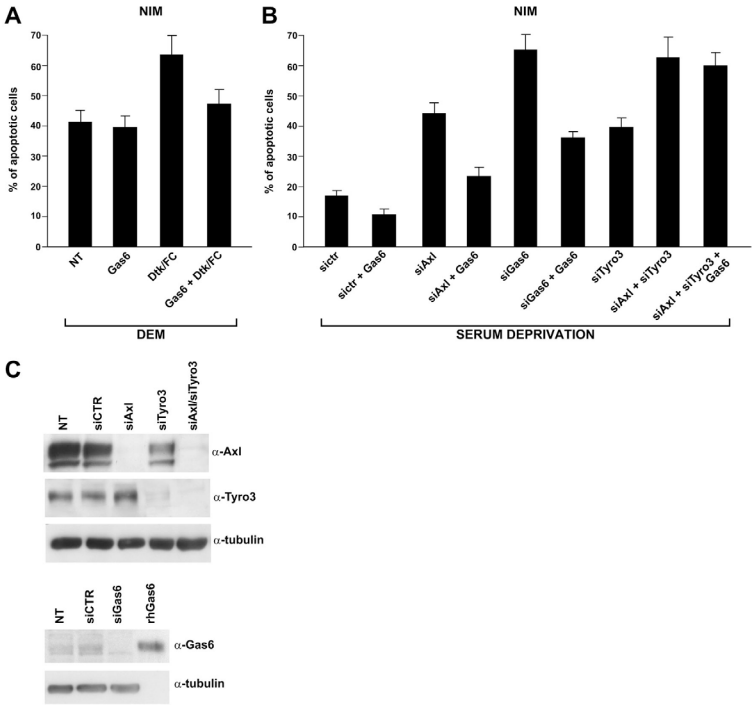

Figure 23. Axl/Tyro3 blockade inhibits NIM cell survival. A) NIM cell line was treated with the proapoptotic substance DEM (DiEthylMaleate) for 12h and then with Gas6 and Dtk/FC. The percentage of apoptotic cells was evaluated with the TUNEL reaction. The average results and S.D. of three independent experiments in which at least 400 cells were counted is reported. Gas6, as expected, did not modify NIM apoptotic rate, while the Dtk/FC protein increased the percentage of apoptotic cells and the addition of exogenous Gas6 reverted this effect. **B)** NIM cells were serum deprived after AXL, TYRO3 (individually or together) and Gas6 silencing. In these conditions,the perncentage of apoptotic cells increased and exogenous Gas6 reverted this effect. **C**) Western blot analysis was performed to verify Axl, Tyro3, GAS6 silencing. Anti-tubulin monoclonal antibody was used as a control for equal protein loading.

4.12 Axl/Tyro3-Gas6 axis blockade inhibits anaplastic thyroid cancer (ATC) cell proliferation and survival

To verify whether Axl knockdown could impair proliferation and survival of human ATC cell lines, we also used siRNA directed against Axl. To this aim, we used 8505-C cells, derived from human ATCs. As shown in figure 24A and B, Gas6 stimulated cell proliferation and inhibited apoptosis of 8505-C. Consistently, Axl silencing inhibited BrdU incorporation and enhanced apoptotic rate of 8505C and exogenous Gas6 partially reverted these effects. Axl silencing was verified by Western blot analysis. We obtained the similar results when another ATC cell line, Cal62, was used (data not shown). (Fig 24).

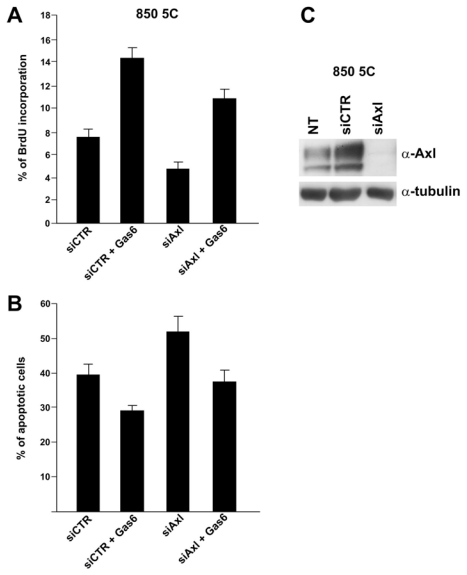

Figure 24. **Axl/Tyro3-Gas6 axis blockade also inhibits 8505-C cell proliferation and survival**. **A)** 8505-C were silenced for AXL and BrdU incorporation was evaluated. Gas6 stimulated 8505C BrdU incorporation while siAXL inhibeted. Gas6 reverted this effect. **B)** 8505C cells were subjected to AXL silencing and serum-deprivation. The percentage of apoptotic cells was evaluated with the TUNEL reaction. AXL silencing increased the percentage of apoptotic cells and Gas6 reverted this effect. **C)** Western blot analysis was performed to verify Axl silencing with an anti-AXL antibody. Anti-tubulin monoclonal antibody was used as a control for equal protein loading.

4.13 Stable silencing of Axl reduces growth, proliferation, survival and invasiveness of 8505-C.

To confirm that Axl silencing effectively inhibited the viability of thyroid cancer cells, we stably transfected 8505-C cells with two pools of vectors expressing, respectively, five different shRNAs directed to Axl or five different control non-targeting shRNAs. After antibiotic selection, cell clones were isolated and screened by Western blot analysis for Axl expression. As shown in Fig. 25A, we identified several clones in which Axl expression was strongly reduced (shAxl Cl 1-2) or completely repressed (shAxl Cl3-6). We first verified whether Axl knockdown could impair cell growth both in optimal serum (10% FCS) or in low serum (2,5% FCS) conditions by performing growth curves. As shown in Fig. 25B, shRNA-mediated Axl silencing showed mild effects on cell proliferation in complete culture medium, while it was significantly more effective in low serum conditions. To assess whether reduced cell growth was due to decreased DNA synthesis or increased cell death, 8505c shAxl clones 3-6 were selected. Cells were serum-starved for 12h and we evaluated the percentage of BrdU- and TUNEL-positive cells. As shown in Fig 25C, all shAxl clones displayed a significant reduction of BrdU incorporation and a significant increase in apoptosis when compared to control clones.

(Fig. 25).

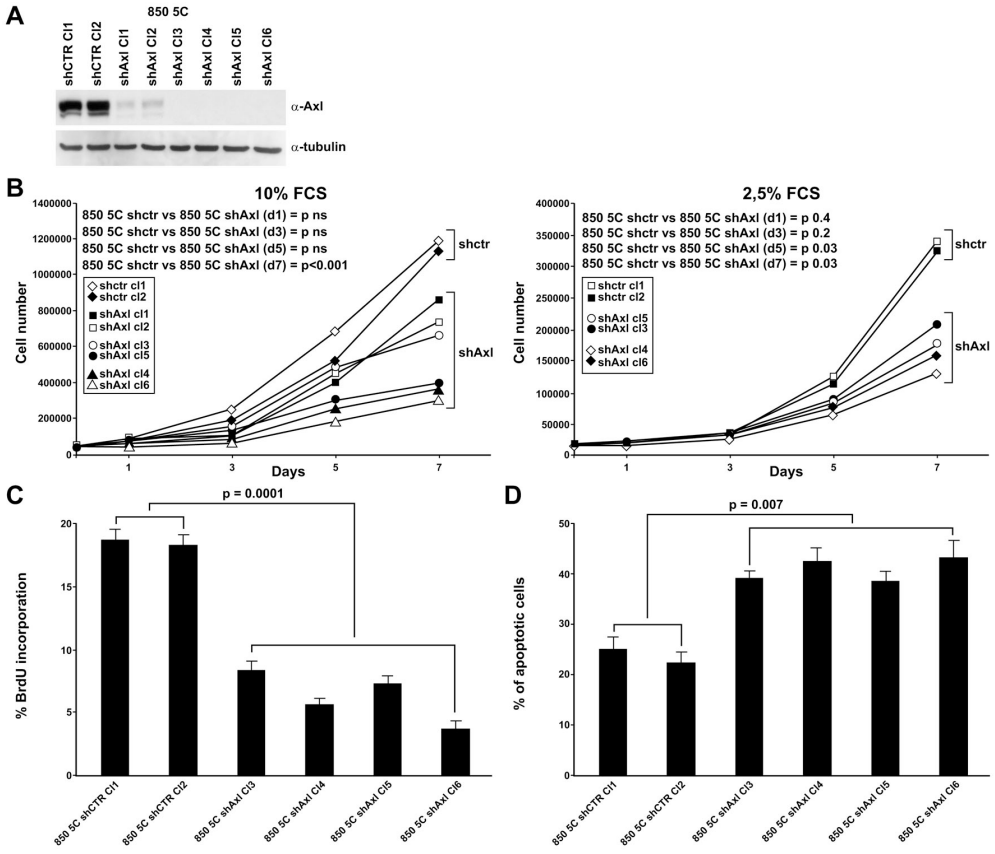

Figure 25. Biological effects of stable silencing of Axl in 8505-C ATC cells. A) Screening of cell clones (8505-C shAXL) by Western blot analysis with an anti-AXL antibody. **B)** Growth curves on 8505-C shAXL and shCTR clones. Cells were plated at a density of 0.5 x 10^5 in complete (10% FCS) (left panel) or in low serum conditions (2.5% FCS) (right panel), harvested and counted at the indicated time points. The average results of at least three independent determinations were reported. **C)** BrdU-incorporation was measured to evaluate S-phase entry of stably silenced clones. AXL silencing decreased the percentage of BrdU-positive cells. **D)** TUNEL reaction was performed on cell clones to evaluated the proapoptotic effect of AXL stable silencing. Cells were serum-deprived for 12h and then processed for TUNEL assay. AXL silencing increased the percentage of apoptotic cells.

Moreover, we asked whether stable AXL silencing on ATC cell lines could impair cell invasiveness through Matrigel. Invasive ability of cells was verified both in optimal (10%FCS) or in low-serum (2,5%FCS) conditions. As indicated in Fig. 26, shAXL clones showed a clear decrease of invasive ability with respect to shCTR, but only in low-serum conditions (Fig. 26).

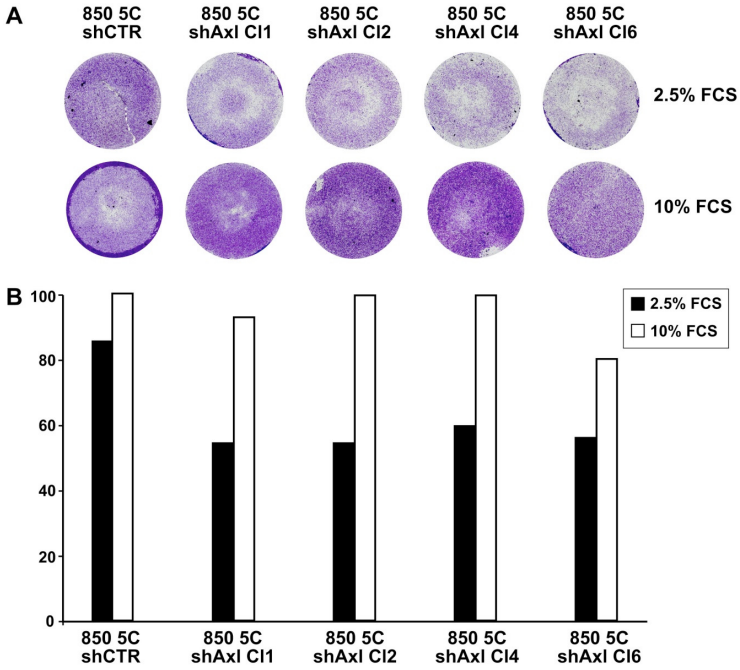

Figure 26. Matrigel invasion on 8505-C shAXL. A) Cells were added to the upper chamber of a pre-hydrated polycarbonate membrane filter of 8 μM pore size coated with Matrigel. The lower chamber was filled with complete medium or 2.5% FCS (as indicated). Triplicated samples were analyzed at 570 nM with an ELISA reader (Model 550 microplate reader, Bio-Rad). The results were expressed as percentage of migrating cells with respect to the unsilenced ones. **B)** Densitometric analysis of Matrigel invasion assay was reported. AXL silencing inhibited Matrigel invasion in low-serum conditions.

4.14 Axl silencing inhibits experimental tumor growth

Finally, we evaluated the role of Axl in tumor growth by using xenografts of ATC cells into (*nu/nu)* immunodeficient mice. To this aim, we choose 8505-C as a model cell line because it expresses Axl and it is able to efficiently form tumors when injected into nude mice. To study the role of Axl in tumor growth, we injected animals with parental, shCTR-transfected (shCTR Cl1) and shAxl (shAxl CL4 and CL6) 8505-C cell lines, and compared their growth rate. Parental cells formed tumors with the same efficiency as shCTR-transfected cells did (data not shown). As shown in Fig. 28, the tumorigenicity of 8505-C shAxl CL4 and CL6 was dramatically reduced when compared with 8505-C shCTR cells. At three weeks, shCTR tumor median volume was 34 mm^3, while shAXL was < 10 mm^3. At four, five and six weeks, shCTR tumors continued to grow, reaching a final median volume of ~150 mm^3. shAXL tumors did not grow or regressed. At the end of the experiment, no shAXL tumors were available. This precluded histological analysis.
(Fig. 27).

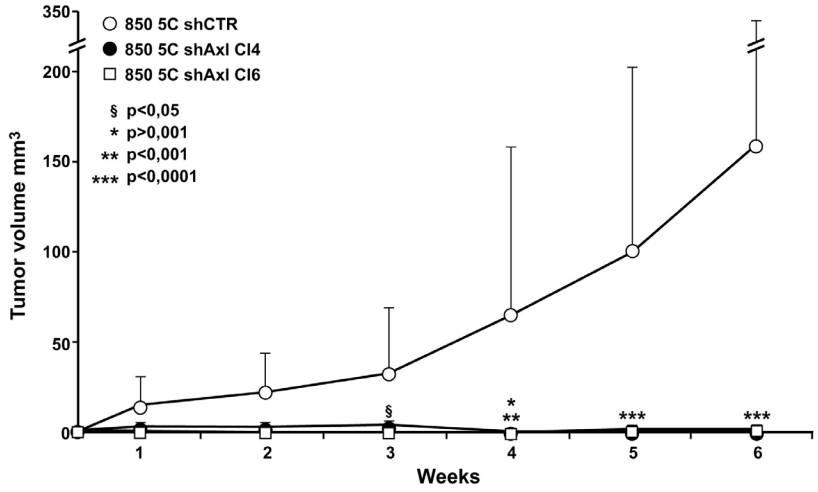

Figure 27.**Tumorigenicity of 8505-C shCTR and shAxl clones in ATC cell xenografts.** Three groups of mice (4-week-old male BALB/c nu/nu mice) were inoculated subcutaneously into the right dorsal portion with 8505-C shCTR cells ($10x10^6$/mouse), 8505-C shAXL CL1 ($10x10^6$/mouse) or 8505-C shAXL CL2 ($10x10^6$/mouse), respectively. Tumor diameters were measured at regular intervals with a caliper. Tumor volumes (V) were calculated with the formula: V= A x B2/2 (A=axial diameter; B= rotational diameter). 8505C tumor growth was strongly impaired in shAXL clones with respect to shCTR. Unpaired Student's T test (normal distributions and equal variances) was applied. All P values were two sided, and differences were statistically significant at $P < 0.05$.

5.CONCLUSIONS

In this thesis, we show that CXCR4, receptor for the chemokine SDF-1α, is involved in the pathogenesis and progression of human anaplastic thyroid carcinoma and can also be considered a potential therapeutical target for this disease. We previously reported functional expression of CXCR4 in human papillary thyroid carcinomas (Castellone et al., 2004). In this report, we observed that CXCR4 is overexpressed in human anaplastic thyroid carcinoma samples and also in a large panel of human ATC established and primary cell cultures, both at the mRNA and at the protein level. Neither normal thyroid tissue samples nor normal thyroid cell cultures expressed this chemokine receptor. In contrast, SDF-1 was not detected in cancer cells. We also show that the CXCR4 expressed on ATC cell lines is functional. In fact, stimulation of ATC cells with human recombinant SDF-1α activated ERK1/2 and AKT pathways. Moreover, stimulation with SDF-1α was able to increase S-phase entry of ATC cells, feature that has also been observed in small cell lung cancer cells (Kijima et al., 2002). By using a small CXCR4 inhibitor, AMD3100 (De Clerq, 2003), it is possible to revert this phenotype. We found that the treatment of immunodeficient mice with AMD3100 significantly suppressed the development of tumors in different xenograft models of ATC cells. These data suggest the possibility to use CXCR4 inhibitors in thyroid cancer therapy and eventually to potentiate the effects of conventional anti-cancer therapies (Muller et al., 2001; Rubin et al., 2003).

Then, we identified two tyrosine-kinase receptors, Tyro3 and Axl, as transcriptional targets of the CXCR4/SDF-1 axis in thyroid cancer. We showed that both the receptors, were expressed at basal levels in TPC-1 cells, but under SDF-1 stimulation, their protein level and tyrosine phosphorylation increased. We found that most of the thyroid cancer cell lines available express both the receptors, being AXL more expressed than TYRO3. In particular, in most cell lines we tested, AXL receptor was also activated, as demonstrated by an increase of tyrosine phosphorilation levels, and this phosphorilation was mainly due to the presence of endogenous GAS6. The only exception to this rule was represented by TPC-1 cell line, in which AXL was highly phosphorylated despite the fact that GAS6 is absent. All these *in vitro*-expression results were confirmed by IHC on human thyroid carcinoma samples; in fact, we found that most of the human samples we analysed presented a strong positivity for AXL and its ligand GAS6, with respect to normal thyroid. Then, we showed that the inhibition of TYRO3 and AXL by using blocking reagents or RNA interference targeting each receptor or the ligand decreased the two main properties of malignant thyroid cells, cell proliferation and resistance to apoptotic stimuli. In particular, we found that cell lines that expressed both receptors and ligand, after the simultaneous blockade of these molecules, presented a dramatic reduction of their cell viability. Accordingly, we show that the stimulation of GAS6-negative TPC-1 cells with exogenous GAS6 increased their proliferation and survival.

Moreover, we found that stable silencing of Axl reduces thyroid cancer cells invasiveness and inhibits experimental tumor growth in nude mice. These results suggest that TYRO3 and AXL play a critical role in promoting proliferation and survival of these neoplasias. For these reasons, targeting the Axl-Tyro3/Gas6 axis may represent an important new therapeutic strategy for the treatment of thyroid cancer.

6. ACKNOLEDGEMENTS

This study has been performed at the University of Naples Federico II, Italy, Department of Molecular and Cellular Biology and Pathology and "Istituto di Endocrinologia ed Oncologia Sperimentale" (IEOS) "G.Salvatore". This work has been supervised by Professor Rosa Marina Melillo.

I wish to present my sincere gratitude to all contributors in my PhD thesis. Fisrt of all, a special thank goes to my supervisor Prof. Rosa Marina Melillo for having encouraged my interest in research and whose passion and enthusiasm I had the privilege to appreciate since I started taking part of her group. I would like to thank all the members of Rosa Marina Melillo's research group, Dr. Federica Liotti and Dr. Gnanaprakasam Krishnamoorty, and in particular Dr. Carla Visciano that actively contributed to all the phases of this project, since she was a younger student. My thanks go to Dr. Valentina Guarino that has been my first guide in my scientific way. I would also like to thank the IEOS research groups of Rosa Marina Melillo, Francesca Carlomagno and Angela Celetti, for their precious and stimulating suggestions and to all my collegues and friends of "LAB11" for their scientific and moral help.

I acknowledge with gratitude Prof. Giancarlo Vecchio, coordinator of this International Doctorate Program, for giving me the beautiful opportunity to attend his Doctorate School. My thanks also go to Prof. Massimo Santoro and his working group at the University of Naples for their support during my PhD years.

I would like to thank Prof. Fulvio Basolo's group from Pathology Department of the University of Pisa for providing human thyroid carcinoma samples for CXCR4-immunohistochemistry experiments and Dr. Renato Franco's group from Istituto Nazionale Tumori, Fondazione G. Pascale of Naples for AXL and GAS6 staining on human PTC and ATC samples. My thanks go to Prof. Marone's group for his friendly collaboration.

Finally, I would like to express my sincere thanks to Prof Luciano D'Adamio of Albert Einstein College of Medicine of Yeshiwa University, N.Y., USA, where I had a very pleasant work experience, for the kind hospitality of his laboratory and also for his continuous encouragement and the exiting exchange of ideas.

7.REFERENCES

Airaksinen MS, Titievsky A, Saarma M.GDNF family neurotrophic factor signaling: four masters, one servant? *Mol Cell Neurosci*. 1999 May;13(5):313-25.

Alberti L, Carniti C, Miranda C, Roccato E, Pierotti MA. RET and NTRK1 proto-oncogenes in human diseases. *J Cell Physiol*. 2003 May;195(2):168-86. Anderson, H. A. *et al.* Serum-derived protein S binds to phosphatidylserine and stimulates the phagocytosis of apoptotic cells. *Nature Immunol.* 4, 87–91 (2003).

Asai N, Murakami H, Iwashita T, Takahashi M. A mutation at tyrosine 1062 in MEN2A-Ret and MEN2B-Ret impairs their transforming activity and association with shc adaptor proteins. J Biol Chem 1996;271:17644-9.

Azenshtein E, Luboshits G, Shina S, Neumark E, Shahbazian D, Weil M, Wigler N, Keydar I, Ben-Baruch A. The CC chemokine RANTES in breast carcinoma progression: regulation of expression and potential mechanisms of promalignant activity. Cancer Res 2002;62:1093-102.

Balkwill F, Cancer and the chemokine network. Nat Rev Cancer 2004; 4, 540-550

Balkwill F and Mantovani A. Inflammation and cancer: back to Virchow? Lancet 2001;357: 539-545.

Borrello MG, Alberti L, Arighi E, Bongarzone I, Battistini C, Bardelli A, Pasin B, Piutti C, Rizzetti MG, Mondellini P, Radice MT, Pierotti MA. The ful oncogenic activity of Ret/ptc2 depends on tyrosine 539, docking site for phospholipase Cgamma. Mol Cell Biol 1996;16:2151-63.

Brigati C., Noonan, D. M., Albini, A. & Benelli, R. Tumors and inflammation infiltrates: friends or foes? *Clin. Exp. Metastatis* 2002:19,247-258.

Carlomagno F, Vitagliano D, Guida T, et al. Efficient inhibition of RET/papillary thyroid carcinoma oncogenic kinases by 4-amino-5-(4-chloro-phenyl)-7-(t-butyl)- pyrazolo[3,4-d]pyrimidine (PP2). J Clin Endocrinol Metab 2003;88:1897–902.

Castellone MD, Guarino V, De Falco V, Carlomagno F, Basolo F, Faviana P, Kruhoffer M, Orntoft T, Russell JP, Rothstein JL, Fusco A, Santoro M, Melillo RM. Functional expression of the CXCR4 chemokine receptor is induced by RET/PTC oncogenes and is a common event in human papillary thyroid carcinomas. Oncogene 2004; Aug 5; 23(35):5958-67.

Cohen Y, Xing M, Mambo E, Guo Z, Wu G, Trink B, Beller U, Westra WH, Ladenson PW, Sidransky D. BRAF mutation in papillary thyroid carcinoma. J Natl Cancer Inst 2003;95:625-7.

Colotta F, Allavena P, Sica A, Garlanda C, Mantovani A. Cancer-related inflammation, the seventh hallmark of cancer: link sto genetic instability. *Carcinogenesis*2009.Jul;30(7):1073-81. (Review).

Cote GJ, Gagel RF. Lessons learned from the management of a rare genetic cancer. *N Engl J Med*. 2003 Oct 16;349(16):1566-8.

Craven RJ, Xu LH, Weiner TM, et al. Receptor tyrosine kinases expressed in metastatic colon cancer. Int J Cancer 1995;60:791–7.

Crosier PS, Hall LR, Vitas MR, Lewis PM, Crosier KE. Identification of a novel receptor tyrosine kinase expressed in acute myeloid leukaemic blasts. Leukemia Lymphoma 1995;18:443–9.

Coussens LM, Werb Z. Inflammation and cancer. *Nature*. 2002 Dec 19-26;420(6917):860-7.

Curcio F, Ambesi-Impiombato FS, Perrella G, Coon HG. Long-term culture and functional characterization of follicular cells from adult normal human thyroids. Proc Natl Acad Sci U S A. 1994 Sep 13;91(19):9004-8.

De Clerq Erik. *Nature*. 2:581-587 (Review).

De Clercq E. Potential clinical applications of the CXCR4 antagonist bicyclam AMD3100. Mini RevM ed Chem 2005;5:805–24.

De Falco V, Guarino V, Avilla E, Castellone MD, Salerno P, Salvatore G, Faviana P, Basolo F, Santoro M, Melillo RM. Biological role and potential therapeutic targeting of the chemokine receptor CXCR4 in undifferentiated thyroid cancer. *Cancer Res. 2007 Dec 15;67(24):11821-9.*

De Visser KE, Eichten A, Coussens LM. Paradoxical roles of the immune system during cancer development, Nat Rev Cancer 2006; 6: 24 – 37.

De Vos J, Couderc G, Tarte K, et al. Identifying intercellular signalling genes expressed in malignant plasma cells by using complementary DNA arrays. Blood 2001;98:771–80.

Di Pasquale M, Rothstein JL, Palazzo JP. Pathologic features of Hashimoto'sassociated papillary thyroid carcinoma. Hum Pathol 2001; 32: 24-30

Donghi R, Longoni A, Pilotti S, Michieli P, Della Porta G, Pierotti MA. Gene p53 mutations are restricted to poorly differentiated and undifferentiated carcinomas of the thyroid gland. J Clin Invest. 1993 Apr;91(4):1753-60.

Drosten M, Pützer BM. Mechanisms of Disease: cancer targeting and the impact of oncogenic RET for medullary thyroid carcinoma therapy. Nat Clin Pract Oncol. 2006 Oct;3(10):564-74. Review.

Eisenberg BL, Hensley SD. Thyroid cancer with coexistent Hashimoto's thyroiditis. Clinical assessment and management. Arch Surg 1989; 124: 1045-7.

Ek S, Hogerkorp CM, Dictor M, Ehinger M, Borrebaeck CA. Mantle cell lymphomas express a distinct genetic signature affecting lymphocyte trafficking and growth regulation as compared with subpopulations of normal human B cells. Cancer Res 2002;62:4398–405.

Encinas M, Crowder RJ, Milbrandt J, Johnson EM Jr. Tyrosine 981, a novel Ret autophosphorylation site, binds c-Src to mediate neuronal survival. J Biol Chem 2004;279:18262-9.

Evans CO, Young AN, Brown MR, et al. Novel patterns of gene expression in pituitary adenomas identified by complementary deoxyribonucleic acid

microarrays and quantitative reverse transcriptionpolymerase chain reaction. J Clin Endocrinol Metab 2001;86:3097–107.

Fagin JA, Matsuo K, Karmakar A, Chen DL, Tang SH, Koeffler HP. High prevalence of mutations of the p53 gene in poorly differentiated human thyroid carcinomas. J Clin Invest. 1993 Jan;91(1):179-84.

Fagin JA. Perspective: lessons learned from molecular genetic studies of thyroid cancer--insights into pathogenesis and tumor-specific therapeutic targets. Endocrinology 2002;143(6):2025-8.

Fukushima T, Suzuki S, Mashiko M, Ohtake T, Endo Y, Takebayashi Y, Sekikawa K, Hagiwara K, Takenoshita S. BRAF mutations in papillary carcinomas of the thyroid. Oncogene 2003;22(41):6455-7.

Funakoshi H, Yonemasu T, Nakano T, Matumoto K, Nakamura T. Identification of Gas6, a putative ligand for Sky and Axl receptor tyrosine kinases, as a novel neurotrophic factor for hippocampal neurons. J Neurosci Res 2002;68:150–60.

Fusco A, Berlingieri MT, Di Fiore PP, Portella G, Grieco M, Vecchio G. Oneand two-step transformations of rat thyroid epithelial cells by retroviral oncogenes. Mol Cell Biol. 1987 Sep;7(9):3365-70.

Fusco A, Chiappetta G, Hui P, Garcia-Rostan G, Golden L, Kinder BK, Dillon DA, Giuliano A, Cirafici AM, Santoro M, Rosai J, Tallini G. Assessment of RET/PTC oncogene activation and clonality in thyroid nodules with incomplete morphological evidence of papillary carcinoma: a search for the early precursors of papillary cancer. Am J Pathol 2002;160(6):2157-67.

Ganju RK, Brubaker SA, Meyer J, et al. The achemokine, stromal cell-derived factor-1a, binds to the transmembrane G-protein-coupled CXCR-4 receptor and activates multiple signal transduction pathways. J Biol Chem 1998;273:23169–75.

García-Rostán G, Costa AM, Pereira-Castro I, Salvatore G, Hernandez R, Hermsem MJ, Herrero A, Fusco A, Cameselle-Teijeiro J, Santoro M. Mutation of the PIK3CA gene in anaplastic thyroid cancer. Cancer Res. 2005 Nov 15;65(22):10199-207

Garcia-Rostan G, Zhao H, Camp RL, Pollan M, Herrero A, Pardo J, Wu R, Carcangiu ML, Costa J, Tallini G. ras mutations are associated with aggressive tumor phenotypes and poor prognosis in thyroid cancer. J Clin Oncol. 2003 Sep 1;21(17):3226-35.

Georgescu MM, Kirsch KH, Shishido T, Zong C, Hanafusa H. Biological effects of c-Mer receptor tyrosine kinase in hematopoietic cells depend on the Grb2 binding site in the receptor and activation of NF-kB. Mol Cell Biol 1999;19:1171–81.

Giuffrida D, Gharib H. Anaplastic thyroid carcinoma: current diagnosis and treatment. Ann Oncol 2000;11(9):1083-9.

Graham DK, Dawson TL, Mullaney DL, Snodgrass HR, Earp HS. Cloning and mRNA expression analysis of a novel human protooncogene, c-mer. Cell Growth Differ 1994;5:647–57.

Guarino V, Castellone MD, Avilla E, Melillo RM. Thyroid cancer and inflammation. *Molecular and Cellular Endocrinology. 2009 Oct 14 (Epub ahead of print)*. (Review).

Guida T, Salvatore G, Faviana P, Giannini R, Garcia-rostan, Provitera L, Basolo F, Fusco A, Carlomagno F, Santoro M. Mitogenic effects of the up-regulation of minichromosome maintenance proteins in anaplastin thyroid carcinoma. 2005. *The J Clin Endoc. Metab.* 90:4703-4709.

Gustafsson A, Bostrom AK, Ljungberg B, Axelson H, Dehlback B. Gas6 and the receptor tyrosine kinase AXL in clear cell renal cell carcinoma. *PLOS One* 2009. Oct 30;4(10):e7575.

Holland SJ,PowellMJ, Franci C, et al.Multiple roles for the receptor tyrosine kinase axl in tumor formation. Cancer Res 2005;65:9294-303.

Homey B, Muller A, Zlotnik A. Chemokines: agents for the immunotherapy of cancer? *Nat Rev Immunol*. 2002 Mar;2(3):175-84.

Huang, M. *et al.* Structural basis of membrane binding by Gla domains of vitamin K‑dependent proteins. *Nature Struct. Biol.* **10**, 751–756 (2003).

Hutterer M, Knyazev P, Abate A, et al. Axl and growth arrest-specific gene 6 are frequently overexpressed in human gliomas and predict poor prognosis in patients with glioblastoma multiforme. Clin Cancer Res 2008;14:130- 8.

Hwang JH, Hwang JH, Chung HK, et al. CXC chemokine receptor 4 expression and function in human anaplastic thyroid cancer cells. J Clin Endocrinol Metab 2003;88:408–16.

Ichihara M, Murakumo Y, Takahashi M. RET and neuroendocrine tumors. Cancer Lett 2004;204:197-211.

Inokuchi N, Zeki K, Morimoto I, et al. Stimulatory effect of interleukin-1a on proliferation through a Ca2+/ calmodulin-dependent pathway of a human thyroid carcinoma cell line, NIM 1. Jpn J Cancer Res 1995;86:670–6.

Ito M, NakashimaM, Nakayama T, et al. Expression of receptor-type tyrosine kinase, Axl, and its ligand, Gas6, in pediatric thyroid carcinomas around chernobyl. Thyroid 2002;12:971–5.

Iwashita T, Kato M, Murakami H, Asai N, Ishiguro Y, Ito S, Iwata Y, Kawai K, Asai M, Kurokawa K, Kajita H, Takahashi M. Biological and biochemical properties of Ret with kinase domain mutations identified in multiple endocrine neoplasia type 2B and familial medullary thyroid carcinoma. Oncogene. 1999 Jul 1;18(26):3919-22.

Janssen JW, Schulz AS, Steenvoorden AC, et al. A novel putative tyrosine kinase receptor with oncogenic potential. Oncogene 1991;6:2113^20.

Jennings JH, Linderman DJ, Hu B, Sonstein J, Curtis JL. Monocytes recruited to the lungs of mice during immune inflammation ingest apoptotic cells poorly. Am J Respir Cell Mol Biol 2005;32:108–17.

Jhiang S.M. The RET proto-oncogene in human cancers. Oncogene. 2000; 19; 5590-5597.

Jia R, Hanafusa H. The proto-oncogene of v-eyk (v-ryk) is a novel receptor-type protein tyrosine kinase with extracellular Ig/GN-III domains. J Biol Chem 1994;269:1839–44.

Kang Y, Siegel PM, Shu W, Drobnjak M, Kakonen SM, Cordon-Cardo C, Guise TA, Massague J. A multigenic program mediating breast cancer metastasis to bone. *Cancer Cell*. 2003 Jun;3(6):537-49.

Kawamoto Y, Takeda K, Okuno Y, Yamakawa Y, Ito Y, Taguchi R, Kato M, Suzuki H, Takahashi M, Nakashima I. Identification of RET autophosphorylation sites by mass spectrometry. J Biol Chem2004;279:1421324.

Kijima T, Maulik G, Ma PC, Tibaldi EV, Turner RE, Rollins B. Regulation of cellular proliferation, cytoskeletal function, and signal transduction through CXCR4 and c-Kit in small cell lung cancer cells. *Cancer Res* 2002;62:6304-11.

Kimura ET, Nikiforova MN, Zhu Z, Knauf JA, Nikiforov YE, Fagin JA. High prevalence of BRAF mutations in thyroid cancer: genetic evidence for constitutive activation of the RET/PTC-RAS-BRAF signalling pathway in papillary thyroid carcinoma. Cancer Res. 2003; 63;1454-1457.

Kroll TG, Sarraf P, Pecciarini L, Chen CJ, Mueller E, Spiegelman BM, Fletcher JA. PAX8-PPARgamma1 fusion oncogene in human thyroid carcinoma. Science 2000;289(5483):1357-60.

Lan Z, Wu H, Li W, et al. Transforming activity of receptor tyrosine kinase tyro3 is mediated, at least in part, by the PI3 kinase-signalling pathway. Blood 2000;95:633–8.

Lemke and Rothlin. *Nature* 2008;(8):327-336 (Review).

Ledent C, Dumont J, Vassart G, Parmentier M. Thyroid adenocarcinomas secondary to tissue-specific expression of simian virus-40 large T-antigen in transgenic mice. Endocrinology 1991;129:1391–401.

Linger RM, Keating AK, Earp HS, Graham DK. TAM receptor tyrosine kinases: biologic functions, signaling, and potential therapeutic targeting in human cancer. Adv Cancer Res 2008;100:35^83.

Liu E, Hjelle B, Bishop JM. Transforming genes in chronic myelogenous leukemia. Proc Natl Acad Sci US A1988;85:1952^6.

Lu, Q. *et al.* Tyro‑3 family receptors are essential regulators of mammalian spermatogenesis. *Nature* 398, 723–728 (1999)

Lu, Q. & Lemke, G. Homeostatic regulation of the immune system by receptor tyrosine kinases of the Tyro 3 family. *Science* 293, 306–311 (2001).

Luboshits, G et al. Elevated expression of CC chemokine regulated on activation, normal T cell expressed and secreted (RANTES) in advanced brest carcinoma. *Cancer Res.*59, 4681-4687 (1999).

Luster AD. Chemokines--chemotactic cytokines that mediate inflammation. N Engl J Med 1998;338(7):436-45.

Malumbres M, Barbacid M. RAS oncogenes: the first 30 years. Nat Rev Cancer 2003;3(6):459-65.

Manfioletti G, Brancolini C, Avanzi G, Schneider C. The protein encoded by a growth arrest-specific gene (gas6) is a new member of the vitamin K-dependent proteins related to protein S, a negative coregulator in the blood coagulation cascade. Mol Cell Biol 1993; 13:4976–85.

Manie S, Santoro M, Fusco A, Billaud M. The RET receptor: function in development and dysfunction in congenital malformation. *Trends Genet.* 2001;17:580–589.

Manning, G., Whyte, D. B., Martinez, R., Hunter, T. Sudarsanam, S. The protein kinase complement o the human genome. *Science* 298, 1912–1934 (2002).

Mantovani A, Allavena P, Sozzani S, Vecchi A, Locati M, Sica A. Chemokines in the recruitment and shaping of the leucocyte infiltrate of tumors. Semin Cancer Biol 2004; 14: 155-60.

Mechler C, Bounacer A, Suarez H, Saint Frison M, Magois C, Aillet G, Gaulier A. Papillary thyroid carcinoma: 6 cases from 2 families with associated lymphocytic thyroiditis harbouring RET/PTC rearrangements. *Br J Cancer*. 2001 Dec 14;85(12):1831-7.

Melillo RM, Santoro M, Ong SH, Billaud M, Fusco A, Hadari YR,Schlessinger J, Lax I. Docking protein FRS2 links the protein tyrosine kinase RET and its oncogenic forms with the mitogen-activated protein kinase signaling cascade. Mol Cell Biol. 2001 Jul;21(13):4177-87.

Melillo R.M, Castellone, M.D, Guarino, V, De Falco V, Cirafici AM, Salvatore G, Chiazzo F, Basolo F, Giannini R, Kruhoffer M, Orntoft T, Fusco A. and Santoro M. The RET/PTC-RAS-BRAF linear signalling cascade mediates the motile and mitogenic phenotype of thyroid cancer cells. J Clin Invest 2005; 115: 1068-108.

Moore MA. The role of chemoattraction in cancer metastases. Bioessays 2001;23(8):674-6.

Müller A, Homey B, Soto H, Ge N, Catron D, Buchanan ME, McClanahan T, Murphy E, Yuan W, Wagner SN, Barrera JL, Mohar A, Verástegui E, Zlotnik A. Involvement of chemokine receptors in breast cancer metastasis. Nature. 2001 Mar 1;410(6824):50-6.

Nagasawa et al., 1996b. Molecular cloning and characterization of a murine pre-B-cell growth-stimulating factor stromal cell-derived factor 1 recptor, a murine homolog of the human immunodeficiency virus 1 entry coreceptor fusin. *Pro. Nat I Acad. SCI U.S.A*;93:14726-14729.

Nagata, K. *et al.* Identification of the product of growth arrest-specific gene 6 as a common ligand for Axl, Sky, and Mer receptor tyrosine kinases. *J. Biol.Chem.* 271, 30022–30027 (1996).

Nakamura YS, Hakeda Y, Takakura N, et al. Tyro 3 receptor tyrosine kinase and its ligand, Gas6, stimulate the function of osteoclasts. Stem Cells 1998;16:229–38.

Nakano T, Ishimoto Y, Kishino J, et al. Cell adhesion to phosphatidylserine mediated by a product of growth arrest-specific gene 6. J Biol Chem 1997;272:29411–4.

Nemoto T, Ohashi K, Akashi T, Johnson JD, Hirokawa K. Overexpression of protein tyrosine kinases in human oesophageal cancer. Pathobiology 1997;65:195–203.

Nikiforova MN, Kimura ET, Gandhi M, Biddinger PW, Knauf JA, Basolo F, Zhu Z, Giannini R, Salvatore G, Fusco A, Santoro M, Fagin JA, Nikiforov YE. BRAF mutations in thyroid tumors are restricted to papillary carcinomas and anaplastic or poorly differentiated carcinomas arising from papillary carcinomas. J Clin Endocrinol Metab 2003;88(11):5399-404.

O'Bryan, J. P. *et al. axl*, a transforming gene isolated from primary human myeloid leukemia cells, encodes a novel receptor tyrosine kinase. *Mol. Cell. Biol.* **11**, 5016–5031 (1991).

Ohashi K, Mizuno K, Kuma K, Miyata T, Nakamura T. Cloning of the cDNA for a novel receptor tyrosine kinase, Sky, predominantly expressed in brain. Oncogene 1994;9:699–705.

Orimo A, Gupta PB, Sgroi DC, Arenzana-Seisdedos F, Delaunay T, Naeem R, Carey VJ, Richardson AL, Weinberg RA. Stromal fibroblasts present in invasive human breast carcinomas promote tumor growth and angiogenesis through elevated SDF-1/CXCL12 secretion. Cell. 2005 May 6;121(3):335-48.

Ott RA, McCall AR, Jarosz H, Armin A, Lawrence AM, Paloyan E. The incidence of thyroid carcinoma in Hashimoto's thyroiditis. Am Surg 1987; 53: 442-44.

Pandey A, Liu X, Dixon JE, Di Fiore PP, Dixit VM. Direct association between the Ret receptor tyrosine kinase and the Src homology 2-containing adapter protein Grb7. J Biol Chem 1996;271:10607-10.

Peng SB, Peek V, Zhai Y, et al. Akt activation, but not extracellular signal-regulated kinase activation, is required for SDF-1a/CXCR4-mediated migration of epitheloid carcinoma cells. Mol Cancer Res 2005;3:227–36.

Pisanu A, Piu S, Cois A, Uccheddu A. Coexisting Hashimoto's thyroiditis with differentiated thyroid cancer and benign thyroid disease: indications for thyroidectomy. Chir Ital 2003; 55: 365-372

Poliard, J. W. Tumour-educated macrophafges promote tumour progression and metastatis. *Nature Rev. Cancer* 4, 71-78 (2004).

Powell DJ Jr, Russell J, Nibu K, Li G, Rhee E, Liao M, Goldstein M, Keane WM, Santoro M, Fusco A, Rothstein JL. The RET/PTC3 oncogene: metastatic solid-type papillary carcinomas in murine thyroids. Cancer Res. 1998 Dec 1;58(23):5523-8.

Powell DJ, Eisenlohr LC, Rothstein JL. A thyroid tumor-specific antigen formed by the fusion of two self proteins. J Immunol 2003; 170: 861-869

Puxeddu E, Knauf JA, Sartor M.A, Mitsutake N, Smith EP. Medvedovic M, Tomlinson CR., Moretti S, Fagin JA. RET/PTC-induced gene expression in thyroid PCCL3 reveals early activation of genes involved in regulation of the immune response. Endocr Relat Cancer 2005; 12: 319-334.

Rezende, S. M., Simmonds, R. E. & Lane, D. A. Coagulation, inflammation, and apoptosis: differen roles for protein S and the protein S–C4b binding protein complex. *Blood* **103**, 1192–1201 (2004).

Rhoden KJ, Unger K, Salvatore G, Yilmaz Y, Vovk V, Chiappetta G, Qumsiyeh MB, Rothstein JL, Fusco A, Santoro M, Zitzelsberger H, Tallini G. RET/papillary thyroid cancer rearrangement in nonneoplastic thyrocytes: follicular cells of Hashimoto's thyroiditis share low-level recombination events with a subset of papillary carcinoma. J Clin Endocrinol Metab. 2006 Jun;91(6):2414-23. Epub 2006 Apr 4.

Rollins BJ. Chemokines. *Blood*. 1997 Aug 1;90(3):909-28. Review.

Ron E, Kleinerman RA, Boice JD Jr, LiVolsi VA, Flannery JT, Fraumeni JF Jr. A population-based case-control study of thyroid cancer. J Natl Cancer Inst. 1987 Jul;79(1):1-12.

Rosai J. The 1991 Fred W. Stewart Award. 14th recipient of the Fred W. Stewart Award: Javier Arias Stella, M.D. Am J Surg Pathol. 1992 Jun;16(6):632.

Rosai J. Poorly differentiated thyroid carcinoma: introduction to the issue, its landmarks, and clinical impact. Endocr Pathol 2004;15:293–6.

Rossi D, Zlotnik A. The biology of chemokines and their receptors. *Annu Rev Immunol*. 2000;18:217-42.

Rubin JB, Kung AL, Klein RS, Chan JA, Sun Y, Schmidt K. Systemic delivery of a small molecule inhibitor of CXCR4 blocks the growth of intracranial xenografts of glioblastoma multiforme. *Proc Am Assoc Cancer* 2003;44:544.

Saji, H et al. Significant correlation of monocyte chemoattractant protein-1 expression with neovascularization and progression of breast carcinoma. *Cancer* 92, 1085-1091 (2001).

Salvatore G, De Falco V, Salerno P, et al. BRAF is a therapeutic target in aggressive thyroid carcinoma. Clin Cancer Res 2006;12:1623–9.

Santoro M, Carlomagno F, Romano A, Bottaro DP, Dathan NA, Grieco M, Fusco A, Vecchio G, Matoskova B, Kraus MH, et al. Activation of RET as a dominant transforming gene by germline mutations of MEN2A and MEN2B. Science. 1995 Jan 20;267(5196):381-3.

Santoro M, Grieco M, Melillo RM, Fusco A, Vecchio G. Molecular defects in thyroid carcinomas: role of the RET oncogene in thyroid neoplastic transformation. Eur J Endocrinol. 1995 Nov;133(5):513-22. Review

Santoro M, Melillo RM, Carlomagno F, Vecchio G, Fusco A. Minireview: RET: Normal and Abnormal Functions. Endocrinology 2004; 145(12):5448-51.

Sasaki T, Knyazev PG, Cheburkin Y, et al. Crystal structure of a Cterminal fragment of growth arrest-specific protein Gas6. Receptor tyrosine kinase activation by laminin G-like domains. J Biol Chem 2002;277:44164–70.

Sasaki, T. *et al.* Structural basis for Gas6–Axl signalling. *EMBO J.* 25, 80–87 (2006).

Sclafani AP, Valdes M, Cho H. Hashimoto's thyroiditis and carcinoma of the thyroid: optimal management. Laryngoscope 1993; 103: 845-849

Segal K, Ben-Bassat M, Avraham A, Har-El G, Sidi J. Hashimoto's thyroiditis and carcinoma of the thyroid gland. Int Surg 1985; 70: 205-209.

Sherman SI. Thyroid carcinoma. Lancet 2003;8;361(9356):501-11.

Shieh YS, Lai CY, Kao YR, et al. Expression of axl in lung adenocarcinoma and correlation with tumour progression. Neoplasia 2005;7:1058–64.

Soares P, Trovisco V, Rocha AS, Lima J, Castro P, Preto A, Maximo V, Botelho T, Seruca R, Sobrinho-Simoes M. BRAF mutations and RET/PTC rearrangements are alternative events in the etiopathogenesis of papillary thyroid carcinoma. Oncogene 2003; 22; 4578-4580.

Stewart, S.A., et al., Lentivirus-delivered stable gene silencing by RNAi in primary cells. RNA, 9, 493-501 (2003).

Stitt, T. N. *et al.* The anticoagulation factor protein S and its relative, Gas6, are ligands for the Tyro 3/Axl family of receptor tyrosine kinases. *Cell* 80, 661–670 (1995).

SunW, FujimotoJ,TamayaT. Coexpression of Gas6/Axl in human ovarian cancers. Oncology 2004;66:450-7.

Tang H, Chen S, Wang H, Wu H, Lu Q, Han D. *Haematoliga* 2009 Mar;94(3):326-334.

Todt JC, Hu B, Curtis JL. The receptor tyrosine kinase MerTK activates phospholipase C gamma2 during recognition of apoptotic thymocytes by murine macrophages. J Leukoc Biol 2004;75:705–13.

Vajkoczy P, Knyazev P, Kunkel A, et al. Dominantnegative inhibition of the Axl receptor tyrosine kinase suppresses brain tumor cell growth and invasion and prolongs survival. Proc Natl Acad Sci USA 2006;103:5799-804.

Van Weering DH. and Bos JL. Signal transduction by the receptor tyrosine kinase Ret. Recent Results Cancer Res. 1998; 154; 271-281.

Vitagliano D, Portella G, Troncone G, et al. Thyroid targeting of the N-ras(Gln61Lys) oncogene in transgenic mice results in follicular tumors that progress to poorly differentiated carcinomas. Oncogene 2006;25:5467–74.

Virchow R. Aetologie der neoplastichen Geschwulste/ Pathogenie der neoplastischen Geschwulste. Die Krankhaften Geschwulste. Berlin: Verlag von August Hirschwald 1863; 57–101.

Vogelstein B, Fearon ER, Hamilton SR, Kern SE, Preisinger AC, Leppert M, Nakamura Y, White R, Smits AM, Bos JL. Genetic alterations during colorectal-tumor development. N Engl J Med. 1988 Sep 1;319(9):525-32.

Williams ED, Doniach I, Bjarnason O, Michie W. Thyroid cancer in an iodide rich area: a histopathological study. Cancer. 1977 Jan;39(1):215-22.

Williams D. Cancer after nuclear fallout: lessons from the Chernobyl accident. Nat Rev Cancer. 2002 Jul;2(7):543-9. Review.

Wirtschafter, A, Schmidt R, Rosen, D, Kundu N, Santoro M, Fusco A, Multhaupt H, Atkins JP, Rosen MR, Keane WM, Rothstein JL.

Expression of the RET/PTC fusion gene as a marker for papillary carcinoma in Hashimoto's thyroiditis. Laryngoscope 1997; 107: 95-100

Xu B Yoshimoto K, Miyauchi A, Kuma S, Mizusawa N, Hirokawa M, Sano T. Cribiform-morular variant of papillary thyroid carcinoma: a pathological and molecular genetic study with evidence of frequent somatic mutations in exon 3 of the beta-catenin gene. J Pathol. 2003; 199; 58-67.

Zantek ND, Walker-Daniels J, Stewart J, et al. MCF-10A-NeoST: a new cell system for studying cell-ECM and cell–cell interactions in breast cancer. Clin Cancer Res 2001;7:3640–8.

Zhu Z, Gandhi M, Nikiforova MN, Fischer AH, Nikiforov YE. Molecular profile and clinical-pathologic features of the follicular variant of papillary thyroid carcinoma. An unusually high prevalence of ras mutations. Am J Clin Pathol 2003;120(1):71-7.

Biological Role and Potential Therapeutic Targeting of the Chemokine Receptor CXCR4 in Undifferentiated Thyroid Cancer

Valentina De Falco,[1] Valentina Guarino,[1] Elvira Avilla,[1] Maria Domenica Castellone,[1] Paolo Salerno,[1] Giuliana Salvatore,[2] Pinuccia Faviana,[3] Fulvio Basolo,[3] Massimo Santoro,[1] and Rosa Marina Melillo[1]

[1]Dipartimento di Biologia e Patologia Cellulare e Molecolare c/o Istituto di Endocrinologia ed Oncologia Sperimentale del CNR "G. Salvatore," Facolta' di Medicina e Facolta' di Scienze Biotecnologiche dell'Universita' "Federico II"; [2]Dipartimento di Studi delle Istituzioni e dei Sistemi Territoriali, Universita' "Parthenope," Naples, Italy; and [3]Dipartimento di Chirurgia, Universita' di Pisa, Pisa, Italy

Abstract

Anaplastic thyroid carcinoma (ATC) is a rare thyroid cancer type with an extremely poor prognosis. Despite appropriate treatment, which includes surgery, radiotherapy, and chemotherapy, this cancer is invariably fatal. CXCR4 is the receptor for the stromal cell–derived factor-1 (SDF-1)/CXCL12 chemokine and it is expressed in a variety of solid tumors, including papillary thyroid carcinoma. Here, we show that ATC cell lines overexpress CXCR4, both at the level of mRNA and protein. Furthermore, we found that CXCR4 was overexpressed in ATC clinical samples, with respect to normal thyroid tissues by real-time PCR and immunohistochemistry. Treatment of ATC cells with SDF-1 induced proliferation and increase in phosphorylation of extracellular signal–regulated kinases and protein kinase B/AKT. These effects were blocked by the specific CXCR4 antagonist AMD3100 and by CXCR4 RNA interference. Moreover, AMD3100 effectively reduced tumor growth in nude mice inoculated with different ATC cells. Thus, we suggest that CXCR4 targeting is a novel potential strategy in the treatment of human ATC. [Cancer Res 2007;67(24):11821–9]

Introduction

Thyroid cancer accounts for the majority of endocrine neoplasms worldwide (1). Malignant tumors derived from the thyroid gland include well-differentiated thyroid carcinomas (WDTC; papillary and follicular) and undifferentiated or anaplastic thyroid carcinomas (ATC). Another group of cancers falls between these two types, the so-called poorly differentiated thyroid carcinomas (PDC). WDTC represents >90% of all thyroid cancers, whereas ATC accounts for approximately 2% to 5% of them (2–4). WDTC management requires surgery and adjuvant radioactive iodine (5, 6). Whereas most of the patients with WDTC have an excellent prognosis, those that present with PDC or ATC have a poor prognosis. PDC displays intermediate biological and clinical features between WDTC and ATC. Indeed, these tumors display high propensity to recur and metastasize. Furthermore, they tend to a progressive dedifferentiation, which leads to the decrease in the levels of the sodium iodide symporter. As a consequence of this, these tumors are unable to concentrate iodine and become resistant to radiometabolic therapy (4, 7). ATC is the most malignant thyroid tumor and one of the more fatal human malignancy with a median survival from the time of diagnosis of only 4 to 12 months (8, 9). ATC is more frequent in iodine-deficient areas and can be associated with other thyroid disorders. These tumors arise at a mean age of 55 to 65 years, are more common in women, and present usually as a rapidly growing mass, localized in the anterior neck area, which rapidly metastasizes at lungs, bone, and brain. Treatment of ATC with surgery, radiotherapy, and chemotherapy, alone or in combination, shows little or no effect on patient's survival (10). For these reasons, novel treatment strategies are urgently needed. Unlike the WDTC, the molecular mechanisms underlying the development of human ATC are largely unknown. Genetic rearrangements of the RET and TRKA tyrosine kinase receptors, point mutations of the BRAF serine-threonine kinase or, less frequently, RAS mutations, are typically found in papillary thyroid carcinoma (PTC). Rearrangements of PPARγ or RAS point mutations are instead found in human FTC (11, 12). Among these genetic alterations, RAS or BRAF point mutations are detected at low frequency in ATC, suggesting that some ATC may arise from a preexisting WDTC, whereas others arise *de novo* (12, 13). Inactivating point mutations of the *p53* tumor suppressor and activating point mutations of the *β-catenin* or the *PIK3CA* are also found in ATC (13–15).

In the attempt to better characterize human ATC at the molecular level, we aimed to study the involvement of chemokine and chemokine receptors in these tumors. Chemokines are small secretory proteins that were initially reported to control the recruitment and the activation of immune cells in inflammation (16). These molecules exert their action through binding to a group of seven-transmembrane G protein–coupled receptors. All chemokine receptors initiate signal transduction by activating a member of the Gi family of G proteins which, on receptor activation, dissociates into α and βγ subunits. The Gα subunit inhibits adenylyl cyclase, whereas the Gβγ dimer activates the phospholipase Cβ and the phosphatidylinositol 3-kinase pathways, with the activation of downstream signaling. It has becoming clear recently that chemokines are also involved in cancer cell migration, survival, and growth (17). Not only chemokines regulate some important features of cancer cells but are also involved in the regulation of tumor angiogenesis and leukocyte recruitment (17). In particular, the chemokine receptor CXCR4 and its ligand stromal cell-derived factor-1 (SDF-1)/CXCL12 have been implicated in the metastatic spread of breast cancer cells (18). CXCR4 is one of the

Requests for reprints: Rosa Marina Melillo, Istituto di Endocrinologia ed Oncologia Sperimentale del CNR, via S. Pansini 5, 80131 Naples, Italy. Phone: 39-081-7463603; Fax: 39-081-7463603; E-mail: rosmelil@unina.it.

doi:10.1158/0008-5472.CAN-07-0899

most important chemokine receptors for cancer cells. Indeed, it is expressed in a great number of human solid and hematologic cancers, including breast, prostate, brain, colon, and lung cancer (19, 20). We and others previously reported the overexpression and functional activity of CXCR4 in thyroid cancer (21, 22). In this report, we show that human ATC cells express high levels of CXCR4 and that the CXCR4-SDF-1/CXCL12 axis sustains the growth of ATC cells. Finally, we provide evidences that targeting CXCR4 might be exploited as a novel anticancer therapy for human ATC.

Materials and Methods

Cell lines. Human primary cultures of normal thyroid and ATC cells were obtained from F. Curcio (Dipartimento di Patologia e Medicina Sperimentale e Clinica, University of Udine, Udine, Italy; P5, P5-2N, P5-3N, P5-4N, and HTU8) and H. Zitzelsberger (Institute of Molecular Radiobiology, GSF-National Research Center for Environment and Health GmbH, Neuherberg, Germany; S11T, S77T, and S14T) and cultured as described previously (23). Primary cultures of ATC were also a kind gift of H. Zitzelsberger. Of these, only the S11T displays a BRAF(V600E) mutation in heterozygosis.[4] Human thyroid papillary cancer cell lines TPC1, FB2, and NIM have been described previously (24–26). TPC1 and FB2 cells harbor a RET/PTC1 rearrangement. NPA87 cells derive from a PDC and harbor a BRAF(V600E) mutation in homozygosis (23). The anaplastic cells ARO, KAT4, BHT101, and FB1 cells harbor a BRAF(V600E) mutation in heterozygosis; 8505C and FRO harbor a BRAF(V600E) mutation in homozygosis (23); and CAL62 cells express wild-type BRAF but mutant NRAS allele. Continuous cell lines were maintained in DMEM supplemented with 10% fetal bovine serum, 1% penicillin-streptomycin, and 1% glutamine.

RNA extraction and reverse transcription PCR. Total RNA was isolated by the RNeasy kit (Qiagen) and subjected to on-column DNase digestion with the RNase-free DNase set (Qiagen) according to the manufacturer's instructions. The quality of RNA was verified by electrophoresis through 1% agarose gel and visualized with ethidium bromide. RNA (1 μg) from each sample was reverse transcribed with the QuantiTect Reverse Transcription (Qiagen) using an optimized blend of oligo(dT) and random primers according to the manufacturer's instructions. To design a quantitative reverse transcription-PCR (RT-PCR) assay, we used the Human ProbeLibray system (Exiqon). Briefly, Exiqon provides 90 human prevalidated Taqman probes (8–9 nucleotides long) that recognize ~99% of human transcripts in the RefSeq database at the National Center for Biotechnology Information. The ProbeFinder assay design software (available online)[5] was used to design primer pairs and probes. All fluorogenic probes were dual labeled with FAM at 5′-end and with a black quencher at the 3′-end. Primer pairs and PCR conditions are available on request. Quantitative RT-PCR was performed in a Chromo 4 Detector (MJ Research) in 96-well plates using a final volume of 20 μL. For each PCR, 8 μL of 2.5× RealMasterMix Probe ROX (Eppendorf AG), 200 nmol/L of each primer, 100 nmol/L probe, and cDNA generated from 50 ng of total RNA were used. PCRs were performed in triplicate and fold changes were calculated with the following formula: $2^{-(\text{sample 1 } \Delta Ct \,-\, \text{sample 2 } \Delta Ct)}$, where ΔCt is the difference between the amplification fluorescent thresholds of the mRNA of interest and the mRNA of RNA polymerase 2 used as an internal reference.

Immunohistochemistry. Retrospectively collected archival thyroid tissue samples from patients affected by ATCs were retrieved from the files of the Pathology Department of the University of Pisa on informed consent. Sections (4 μm thick) of paraffin-embedded samples were stained with H&E for histologic examination to ensure that the samples fulfilled the diagnostic criteria required for the identification of ATC. Normal thyroid tissue samples were also retrieved from the files of the Pathology Department of the University of Pisa.

For immunohistochemistry, paraffin sections (3–5 μm) were dewaxed in xylene, dehydrated through graded alcohols, and blocked with 5% nonimmune mouse serum in PBS with 0.05% sodium azide for 5 min. Mouse monoclonal antibody against CXCR4 (clone 12G5; R&D Systems) was added at 1:1,000 dilution for 15 min. After incubation with biotinylated anti-mouse secondary antibody for 15 min followed by streptavidin-biotin complex for 15 min (Catalyzed Signal Amplification System, DAKO), sections were developed for 5 min with 0.05% 3,3′-diaminobenzidine tetrahydrochloride and 0.01% hydrogen peroxide in 0.05 mol/L Tris-HCl buffer (pH 7.6), counterstained with hematoxylin, dehydrated, and mounted.

Protein studies. Immunoblotting experiments were performed according to standard procedures. Briefly, cells were harvested in lysis buffer [50 mmol/L HEPES (pH 7.5), 150 mmol/L NaCl, 10% glycerol, 1% Triton X-100, 1 mmol/L EGTA, 1.5 mmol/L $MgCl_2$, 10 mmol/L NaF, 10 mmol/L sodium pyrophosphate, 1 mmol/L Na_3VO_4, 10 μg/mL aprotinin, 10 μg/mL leupeptin] and clarified by centrifugation at 10,000 × *g*. For protein extraction from human tissues, snap-frozen samples were immediately homogenized in lysis buffer by using the Mixer Mill apparatus (Qiagen). Protein concentration was estimated with a modified Bradford assay (Bio-Rad). Antigens were revealed by an enhanced chemiluminescence detection kit (Amersham). Anti-CXCR4 antibodies were from Abcam Ltd. For the evaluation of mitogen-activated protein kinase (MAPK) and AKT activity on SDF-1α triggering, BHT101 and S11T cells were serum deprived for 12 h and then stimulated with human recombinant SDF-1α (R&D Systems) for the indicated time. Anti-phosphorylated p44/42 MAPK, anti-p44/42 MAPK, anti-phosphorylated AKT, and anti-AKT antibodies were from New England Biolabs. Anti-tubulin monoclonal antibody was from Sigma Chemical. Secondary anti-mouse and anti-rabbit antibodies coupled to horseradish peroxidase were from Bio-Rad.

Flow cytometric analysis. Subconfluent cells were detached from culture dishes with a solution of 0.5 mmol/L EDTA and then washed thrice in PBS buffer. After saturation with 1 μg of human IgG/10^5 cells, cells were incubated for 20 min on ice with phycoerythrin (PE)-labeled antibodies specific for human CXCR4 (R&D Systems) or isotype control antibody. After incubation, unreacted antibody was removed by washing cells twice in PBS buffer. Cells resuspended in PBS were analyzed on a FACSCalibur cytofluorimeter using the CellQuest software (Becton Dickinson). Analyses were performed in triplicate. In each analysis, a total of 10^4 events were calculated.

Cell proliferation. S-phase entry was evaluated by bromodeoxyuridine (BrdUrd) incorporation and indirect immunofluorescence. Cells were grown on coverslips, kept in 2.5% serum for 24 h, and then treated with recombinant SDF-1α (100 ng/mL) for 48 h. BrdUrd was added at a concentration of 10 μmol/L for the last 1 h. Subsequently, cells were fixed in 3% paraformaldehyde and permeabilized with 0.2% Triton X-100. BrdUrd-positive cells were revealed with Texas red–conjugated secondary antibodies (Jackson ImmunoResearch Laboratories, Inc.). Cell nuclei were identified by Hoechst staining. Fluorescence was visualized with a Zeiss 140 epifluorescent microscope.

For growth curves, cells were plated at a density of 0.5 × 10^5 in low-serum conditions (2.5%) and counted at the indicated time points.

RNA interference. Small inhibitor duplex RNAs targeting human CXCR4 have been described previously and were chemically synthesized by Proligo. Sense strand for human CXCR4 small interfering RNA (siRNA) targeting was the following: 5′-GAGGGGAUCAGCAGUAUAUAC-3′.

Small duplex RNAs containing the same nucleotides, but in scrambled fashion (siRNA SCR), were used as a negative control. For siRNA transfection, ATC cells were grown under standard conditions. The day before transfection, cells were plated in six-well dishes at 50% to 60% confluency. Transfection was performed using 5 to 15 μg of duplex RNA and 6 μL of Oligofectamine reagent (Invitrogen). Cells were harvested at 48 and 72 h after transfection and analyzed for protein expression and biological activity.

Xenografts in nude mice. Mice were housed in barrier facilities and 12-h light-dark cycles and received food and water *ad libitum* at the Dipartimento di Biologia e Patologia Cellulare e Molecolare (University of Naples "Federico II", Naples, Italy). This study was conducted in accordance with Italian regulations for experimentation on animals. All manipulations were performed while mice were under isoflurane gas anesthesia. No mouse

[4] G. Salvatore, unpublished observation.
[5] http://www.probelibrary.com

showed signs of wasting or other signs of toxicity. BHT101, ARO, or KAT4 cells (5×10^6 per mouse) were inoculated s.c. into the right dorsal portion of 4-week-old male BALB/c *nu/nu* mice (The Jackson Laboratory). When tumors measured 40 mm^3, mice were randomized to receive AMD3100 (n = 10; 1.25 mg/kg/twice daily) or vehicle alone (n = 10; PBS) by i.p. injection for 5 consecutive days per week for 3 to 4 weeks. Tumor diameters were measured at regular intervals with calipers. Tumor volumes (V) were calculated with the following formula: $V = A \times B^2 / 2$ (A = axial diameter; B = rotational diameter). Tumors were excised and fixed overnight in neutral buffered formalin and processed by routine methods.

Statistical analysis. To compare CXCR4 mRNA levels in normal thyroid tissues versus ATC samples, we used the Mann-Whitney nonparametric test and the GraphPad Instat software, v.3.0b. To compare ATC xenograft growth in AMD3100-treated versus untreated animals, we used the unpaired Student's t test (normal distributions and equal variances) and the GraphPad Instat software, v.3.0b. All P values were two sided, and differences were considered statistically significant at $P < 0.05$.

Results

CXCR4 is overexpressed in surgical samples of human ATC. We compared CXCR4 mRNA levels in a set of ATC samples (n = 13) versus different samples of normal thyroid tissue (n = 6). As shown in Fig. 1*A*, CXCR4 mRNA was found to be up-regulated in most of the tumor samples (10 of 13). When we performed statistical analysis, the differences in the expression levels of CXCR4 between tumors and normal thyroid tissues were statistically significant (P = 0.0084; Fig. 1*A*).

To verify whether CXCR4 mRNA overexpression resulted in an increase in the protein levels, we used protein extracts from a different set of ATC samples and three normal thyroid tissues in an immunoblot experiment with CXCR4-specific antibodies. As shown in Fig. 1*B*, CXCR4 protein levels were higher in ATC samples than in normal thyroid. As a positive control for CXCR4 expression, the ATC cell line ARO was used.

Finally, CXCR4 antibodies were used in immunohistochemical experiments. We evaluated CXCR4 expression in normal thyroid tissues and a set of ATC samples (n = 33). Whereas no CXCR4 expression was detected in normal thyroid tissues, 13 (39%) of the ATC samples scored positive for CXCR4. A representative CXCR4 immunostaining is shown in Fig. 1*C*. These data indicate that a significant fraction of human ATCs, similarly to other epithelial

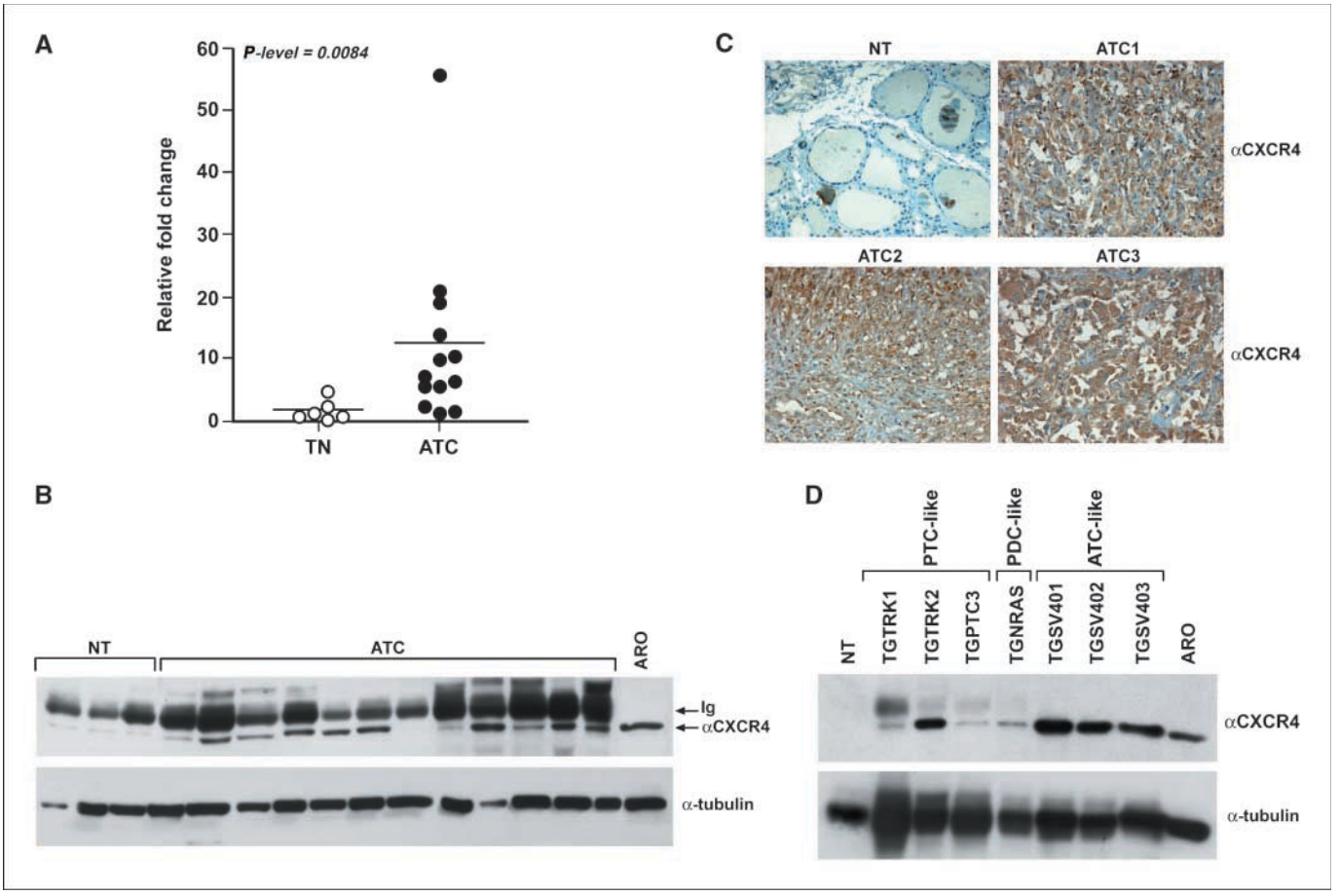

Figure 1. *A,* expression levels of CXCR4 in human ATC samples versus six normal thyroid tissues by real-time RT-PCR. CXCR4 expression levels of tumors (*Y axis*) are calculated relative to the mean CXCR4 level of normal human thyroid tissues (*NT*). All experiments have been performed in triplicate, and the average value of the results was plotted on the diagram. *P* value was calculated with the two-tailed, nonparametric Mann-Whitney test. *B,* protein lysates (100 μg) extracted from the indicated samples underwent Western blotting with anti-CXCR4-specific antibodies. Immunocomplexes were revealed by enhanced chemiluminescence. Equal protein loading was ascertained by anti-tubulin immunoblot. *C,* immunohistochemical staining for CXCR4 of formalin-fixed, paraffin-embedded ATCs. Tissue samples from normal thyroid or ATC were incubated with a mouse monoclonal anti-CXCR4 antibody. ATCs show a strong immunoreactivity for CXCR4, whereas normal thyroid tissue is negative. Representative pictures of normal and pathologic positive samples are shown. Isotype control was also performed (data not shown). *D,* the expression levels of CXCR4 protein were analyzed in thyroid tumor samples from transgenic mice models. Tumor tissues were snap frozen and immediately homogenized by using the Mixer Mill apparatus in lysis buffer. Equal amounts of proteins were immunoblotted and stained with anti-CXCR4 polyclonal antibodies (Abcam). ATC-like samples displayed a more intense immunoreactivity for CXCR4. As a control for equal loading, the anti-α-tubulin monoclonal antibody was used.

cancers, features high expression levels of the CXCR4 receptor. Furthermore, they suggest that the increase in CXCR4 levels occurs at the transcriptional level.

CXCR4 is highly expressed in animal models of ATC. Several transgenic mice model of thyroid cancer have been developed by using various oncogenes under the transcriptional control of the thyroid-specific thyroglobulin bovine promoter. Depending on the specific transgene, these mice develop carcinomas that resemble, for cytologic and histologic features, human PTC, FTC, or ATC. In particular, mice expressing either *RET/PTC3* (TGPTC3) or *TRK/T1* (TGTRK) oncogene develop PTC-like tumors (27, 28). *NRAS* transgene expression results in follicular tumors that progress to poorly differentiated carcinomas (TGNRAS; ref. 29). Finally, animals expressing the *SV40* large T antigen (TGSV) present aggressive thyroid cancer with features similar to human ATC (30). To evaluate the expression of CXCR4 in these animal models, we extracted proteins from different tumor samples of the different transgenic lines and performed Western blot analysis with CXCR4 antibodies. Histologic diagnosis of the thyroid lesions was verified before processing of the samples. As shown in Fig. 1*D*, CXCR4 levels were higher in ATC models than in normal mouse thyroid tissue. PTC samples displayed intermediate levels of CXCR4. These data, together with previously published data (21, 22), suggest that CXCR4 up-regulation is a frequent event in thyroid tumorigenesis and that it correlates with the malignancy of the disease.

CXCR4 is a functional receptor in human ATC cells. To study the role of CXCR4 in human ATC, we first needed to identify a suitable cell model. To this aim, various normal thyroid and ATC-derived primary cultures and continuous cell lines were tested for CXCR4 expression by Western blot analysis. As shown in Fig. 2*A* and *B*, whereas normal thyroid cultures displayed low or undetectable CXCR4 expression levels, several ATC cell lines featured high levels of the CXCR4 receptor. In particular, of 10 ATC cell lines, 7 displayed high expression levels of CXCR4. In the case of ATC cells, the increased levels of CXCR4 proteins were associated to an increase in CXCR4 mRNA levels as assessed by quantitative PCR analysis (Fig. 2*C*). We then asked whether this receptor was expressed on the cell surface. To this aim, we performed flow cytometry experiments using a PE-conjugated mouse monoclonal anti-CXCR4 antibody. The percentage of CXCR4-positive cells was

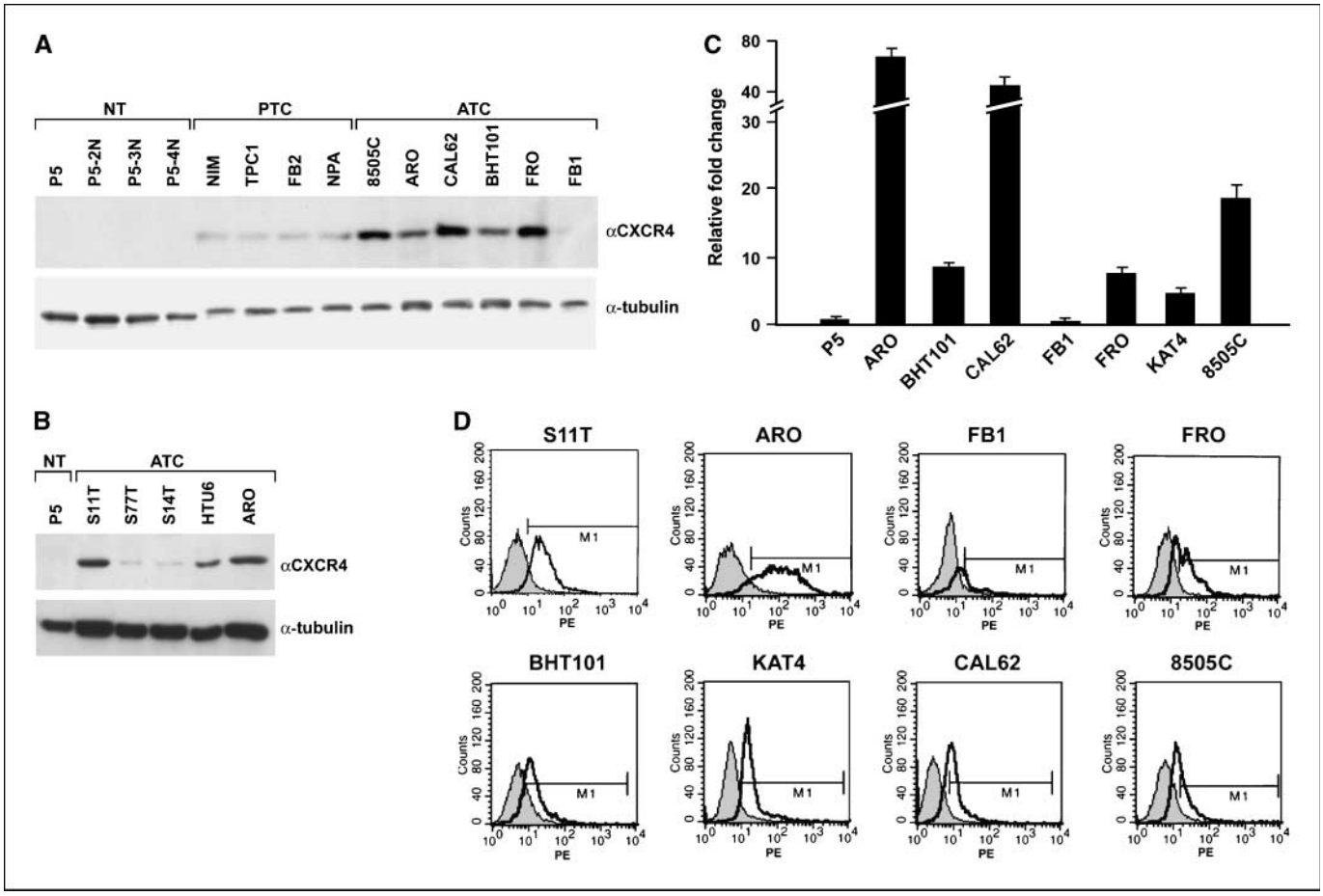

Figure 2. *A,* CXCR4 up-regulation in cell lines derived from human thyroid carcinomas was evaluated by immunoblot with a polyclonal anti-CXCR4 antibody. The expression levels of CXCR4 protein were analyzed in the P5 human primary thyroid cells, and in the indicated cell lines derived from human PTCs (NIM, TPC1, FB2, and NPA) or from human ATCs (8505C, ARO, CAL62, BHT101, FRO, and FB1). *B,* ATC-derived (S11T, S77T, S14T, HTU8 and ARO) and normal thyroid primary cultures (P5) were screened for CXCR4 expression by Western blot analysis with the polyclonal anti-CXCR4 antibody. As a control for equal loading, the anti-α-tubulin monoclonal antibody was used. *C,* expression levels of CXCR4 in human ATC cells versus the P5 normal thyroid culture were evaluated by real-time RT-PCR analysis. CXCR4 expression levels of ATC cell lines (*Y axis*) are calculated relative to the expression level in the normal human cell culture P5. All experiments were performed in triplicate, and the average value of the results was plotted on the diagram. SDs were smaller than 25% in all cases (data not shown). *D,* flow cytometric analysis (fluorescence-activated cell sorting) of surface-expressed CXCR4 in ATC cells. Subconfluent cells were detached from culture dishes and incubated with PE-labeled antibodies specific for human CXCR4.

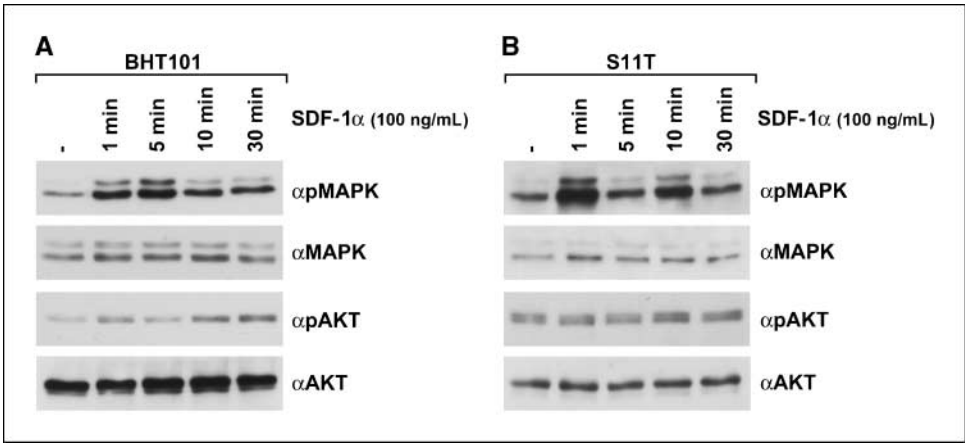

Figure 3. *A* and *B,* protein extracts from the indicated cell lines were subjected to immunoblotting with anti-phosphorylated p44/42 MAPK (*αpMAPK*) and with anti-phosphorylated AKT (*αpAKT*) antibodies. The blots were reprobed with anti-p44/42 and anti-AKT antibodies for normalization.

determined. As shown in Fig. 2*D*, CXCR4 was expressed in almost all the ATC cell lines tested, with the exception of the FB1 cells. The ARO cells, which in a previous report were shown to feature high CXCR4 levels (21), were included as a positive control. In contrast, normal thyroid cells did not express CXCR4 (data not shown). SDF-1, the CXCR4 ligand, was not expressed by ATC cells as assessed by quantitative PCR or ELISA assay (data not shown).

We selected two cell lines, S11T and BHT101, for further experiments. First, we tested the ability of recombinant SDF-1α to stimulate signal transduction in ATC cells. It has been previously reported that stimulation of CXCR4 induces the activation of several kinase cascades mainly through the activation of the Gβγ subunit of the Gi protein (31, 32). We therefore tested the phosphorylation of two downstream effectors, extracellular signal-regulated kinase (ERK) 1/2 and AKT, using phosphorylated-specific antibodies. To this aim, cells were serum starved for 12 h and then stimulated with SDF-1α for different time points. As shown in Fig. 3*A* and *B*, SDF-1α induced rapid and sustained activation of ERK1/2 in both cell lines. AKT activation was also achieved in BHT101 cells on SDF-1α treatment, whereas it was less evident in S11T cells. Together, these data indicate that CXCR4 is functional in ATC cells. Activation of ERK1/2 and AKT was observed in virtually all the ATC cell lines expressing CXCR4, whereas normal thyroid cells, which do not express CXCR4, did not display these effects (data not shown).

Biological activity of CXCR4 in ATC cells. To further test the functional responsiveness of CXCR4 in ATC, we stimulated these cells with SDF-1α and evaluated its ability to induce cell proliferation. To this aim, BHT101 and S11T cells were maintained in low-serum (2.5%) growth conditions for 24 h and then either left untreated or stimulated with SDF-1α for 12 h. As a measure of DNA synthesis, we counted BrdUrd-positive cells on a 1-h BrdUrd pulse. As shown in Fig. 4, SDF-1α consistently enhanced DNA synthesis in both BHT101 and S11T cells. We then used a specific CXCR4 inhibitor, AMD3100, to block this effect. AMD3100 is a competitive antagonist of SDF-1α, but it also displays partial agonist activity (33). Normal thyroid cells were insensitive to SDF-1α stimulation and to the effect of AMD3100 (data not shown). As shown in Fig. 4*A*, AMD3100 inhibited SDF-1α–mediated BrdUrd incorporation in ATC cells. The positive effect of SDF-1 on cell proliferation, measured as S-phase entry, was also observed in other ATC cell lines (Fig. 5*C*). To evaluate whether SDF-1α could stimulate ATC cell growth, we also performed growth curves in low-serum (2.5%) conditions. As shown in Fig. 4*B*, the stimulation of BHT101 with SDF-1α increased their proliferation rate, and AMD3100 reverted this effect. SDF-1α was also able to increase the proliferation rate of three different ATC cell lines, KAT4, CAL62, and ARO, which express CXCR4, but was unable to do so on FB1 cells, which we previously reported to be devoid of CXCR4 (Fig. 4*B*). AMD3100 alone did not have any effect on ATC cells (data not shown).

To exclude off-target effects of AMD3100 and to directly determine the role of CXCR4 on ATC cell proliferation, we used small duplex RNA oligos to knock down CXCR4. CXCR4 RNA interference was verified by Western blot analysis in BHT101 cells (Fig. 5*A*). We then transfected CXCR4 siRNAs into BHT101, KAT4, CAL62, and 8505C cells. CXCR4 silencing substantially impaired SDF-1α–induced S-phase entry in all the ATC cells but had no effect on BrdUrd incorporation in the absence of the chemokine, as shown in Fig. 5. When we used the control scrambled siRNA, this inhibitory effect was not observed. Furthermore, scrambled oligos had no effect on CXCR4 protein levels (Fig. 5*A*).

AMD3100 inhibits ATC tumor formation in nude mice. It has been previously shown that the CXCR4/SDF-1 axis plays an important role in the growth and in the metastatic ability of several epithelial cancers (20). Because we had shown that CXCR4 inhibition blocked SDF-1α–mediated ATC cell growth in culture, and because it has been shown that this chemokine is secreted by stromal tumoral cells (34), we reasoned that SDF-1α-CXCR4 axis blockade by AMD3100 might inhibit ATC tumor growth. To this aim, we selected BHT101, ARO, and KAT4 cells for their ability to respond to SDF-1α and their ability to form tumors *in vivo* with high efficiency. Nude mice were injected s.c. with 5×10^6 cells. When tumors measured ~40 mm^3, mice ($n = 20$ for each cell line) were randomized to receive AMD3100 (1.25 mg/kg/twice daily i.p.) or vehicle 5 days per week for 3 to 4 weeks. Tumor diameters were measured at regular intervals with caliper. After 21 days, the mean volume of BHT101 tumors in mice treated with AMD3100 was 48 mm^3, whereas that of mice treated with vehicle was 620 mm^3. Representative experiments are shown in Fig. 6*A* and *B*. Tumors induced by ARO and KAT4 reached the volume of 40 mm^3 in only 1 week. In addition, in this case, AMD3100 was able to inhibit tumor growth, although to a lesser extent. In fact, ARO-induced tumor mean volume at the end of treatment with AMD3100 was 220 mm^3, whereas that of mice treated with vehicle was 625 mm^3. Similar results were also obtained when KAT4 cells were used. In this case, the difference between the mean volume of AMD3100-treated versus vehicle-treated tumors was not statistically significant after 3 weeks. However, when treatment

was extended for 1 additional week, AMD3100-treated tumor mean volume was 180 mm^3, whereas that of mice treated with vehicle was 690 mm^3, and the *P* value was 0.039 (Fig. 6*A*). These data, taken together, show that treatment with AMD3100 strongly inhibits ATC tumor growth.

Discussion

Despite ATC is a rare disease, it is one of the most aggressive human cancers (9). Although various therapeutic strategies have been exploited to slow down the growth of this tumor, none of these treatments improved survival (10). The molecular pathways implicated in this disease are poorly understood, and this hampers the application of novel rational therapeutic strategies. Genetic alterations found in ATC are inactivating mutations of the *p53* tumor suppressor and activating mutations of *β-catenin, RAS, BRAF,* and *PIK3CA* (11). Recently, molecular genetic alterations of *FHIT* have been also detected in ATC (35). Among the genes involved in ATC, BRAF serine-threonine kinase has been exploited as a potential therapeutic target (23).

Most epithelial cancers feature high levels of expression of the chemokine receptor CXCR4 (20). This receptor has been widely

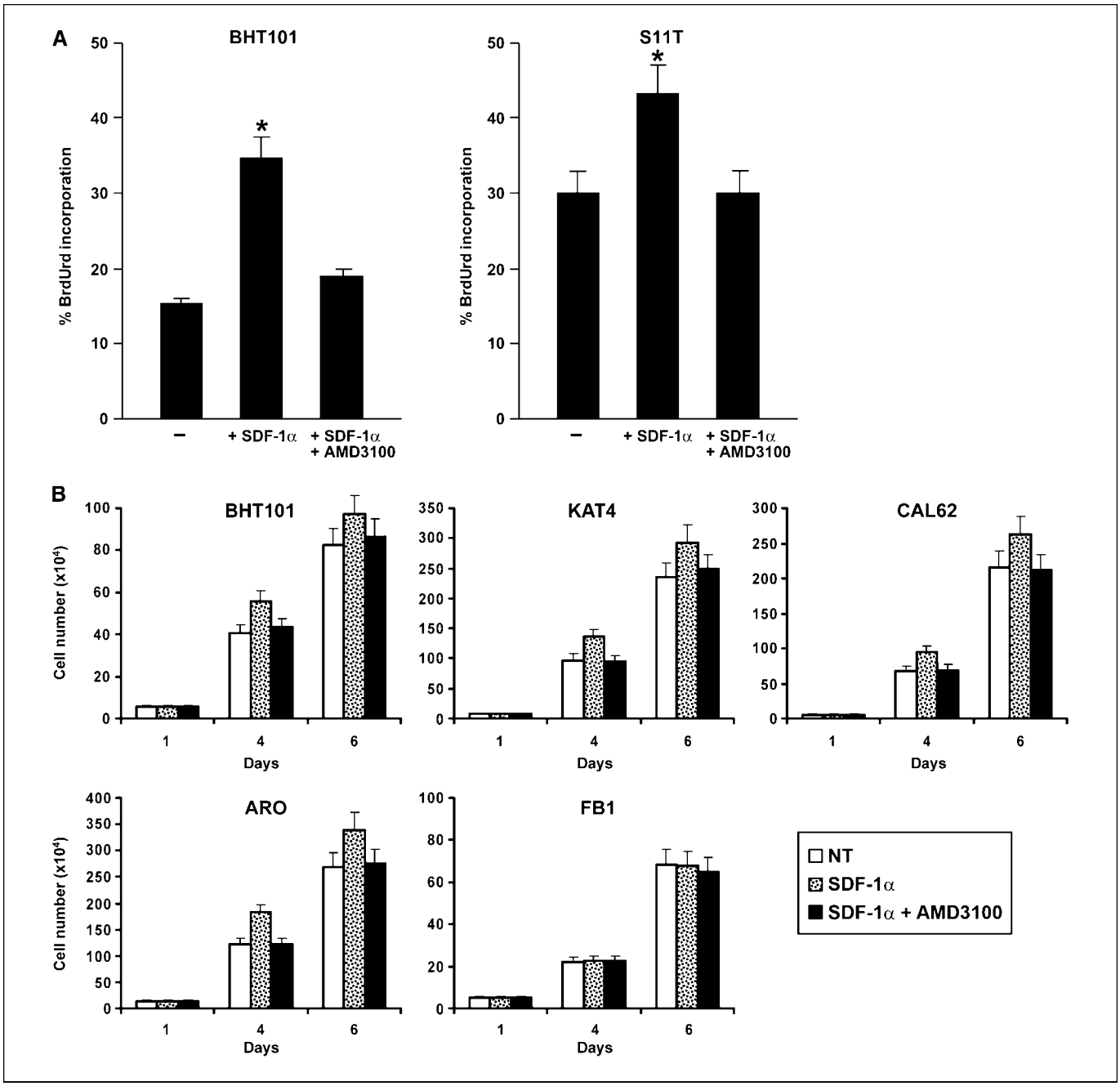

Figure 4. *A,* BrdUrd incorporation was measured to evaluate S-phase entry on treatment of BHT101 and S11T cells with SDF-1α in the presence or absence of the CXCR4 inhibitor AMD3100. *Columns,* average results of three independent experiments; *bars,* SD. $P < 0.05$. *B,* the indicated cell lines were plated at the same density (5×10^4) in 2.5% serum, harvested, and counted at the indicated time points. *Columns,* average results of at least three independent determinations; *bars,* SD.

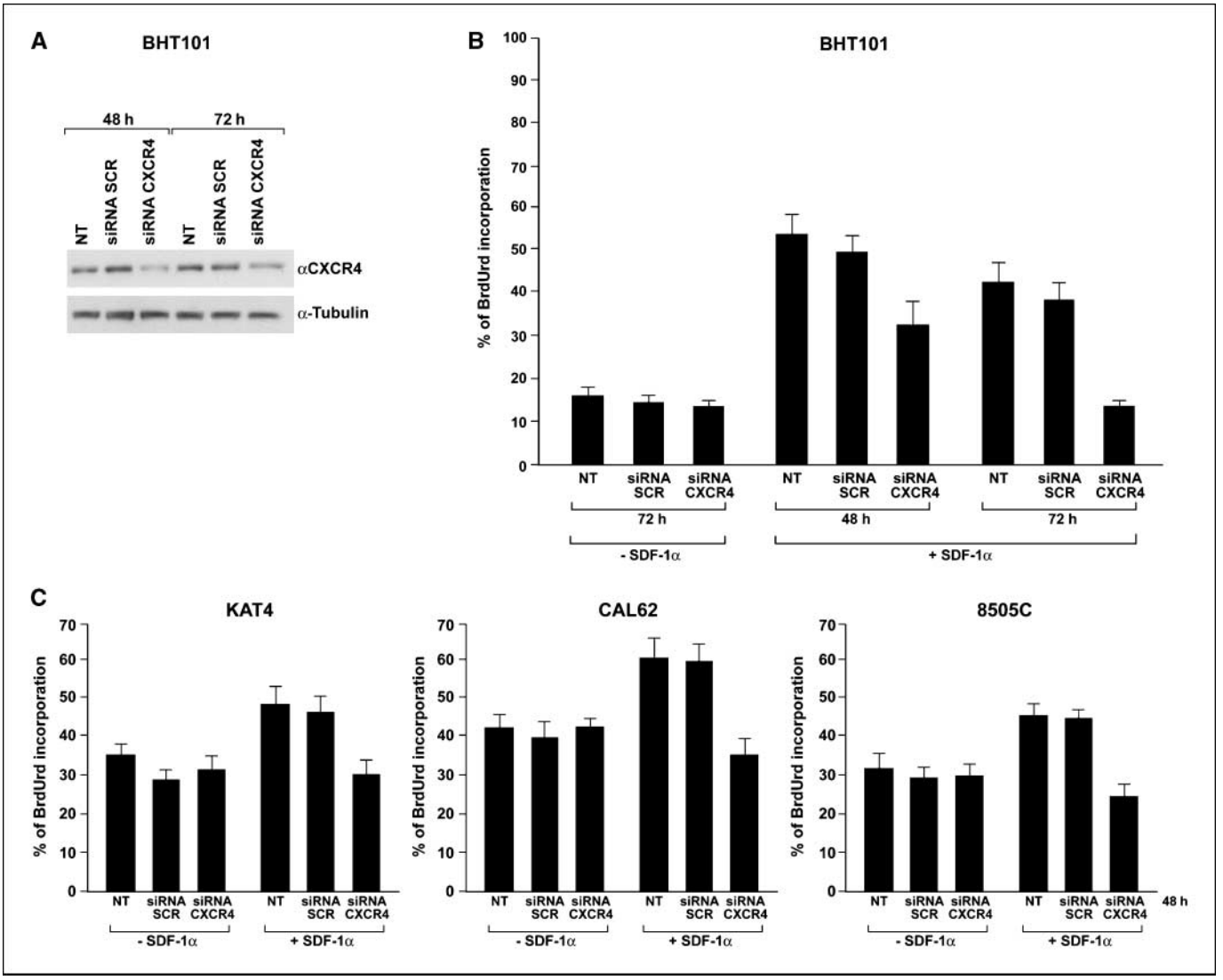

Figure 5. *A,* CXCR4 RNA interference was used to transiently suppress CXCR4 expression in BHT101 cells. BHT101 cells were transfected with siRNAs against CXCR4 (*siRNA CXCR4*) or control nonspecific small duplex RNA containing the same nucleotides, but in scrambled fashion (*siRNA SCR*), and harvested 48 and 72 h later. Protein lysates were subjected to immunoblotting with anti-CXCR4 and anti-tubulin antibodies. Control siRNA did not affect CXCR4 protein levels. *B,* CXCR4 RNA interference (*siRNA CXCR4*) in BHT101 cells inhibited SDF-1α–stimulated S-phase entry as evaluated by BrdUrd incorporation assay. Control siRNA (*siRNA SCR*) did not inhibit DNA synthesis. Unstimulated BHT101 cells were not affected by siRNA transfection. *C,* CXCR4 RNA interference (*siRNA CXCR4*) inhibited S-phase entry in SDF-1α–stimulated KAT4, CAL62, and 8505C. ATC cells were transfected with siRNAs against CXCR4 (*siRNA CXCR4*) or control siRNA (*siRNA SCR*) and harvested 48 h later. Control siRNA did not inhibit DNA synthesis. Unstimulated cells were not affected by siRNA transfection.

studied because its expression contributes to several phenotypes of cancer cells, such as the ability to grow, survive, and spread throughout the body. On the contrary, most epithelial cancers do not express SDF-1, the unique CXCR4 ligand, whereas SDF-1 is produced in high amounts in specific body districts. It has been suggested that the role of this chemokine in cancer is mainly to attract cancer cells to these districts (18). In support of this hypothesis, it has been shown that SDF-1 is produced in several metastatic sites. Recently, it has also been suggested that tumoral stroma secretes high amounts of SDF-1, supporting the concept that this chemokine is pivotal in sustaining local protumorigenic events, such as growth and survival of cancer cells (34). Furthermore, the expression of SDF-1 by stromal cancer cells directly recruits endothelial progenitors that are required for tumor angiogenesis (19). As most epithelial and hematopoietic malignancies, also thyroid cancer expresses high levels of CXCR4.

We previously reported functional expression of CXCR4 in human papillary thyroid cancer (22). Furthermore, Hwang et al. (21) showed that an anaplastic cell line, ARO, expressed high levels of functional CXCR4. In this report, we analyzed human ATC samples for CXCR4 expression. We also screened a large panel of human ATC established and primary cell cultures for CXCR4 expression. We show that, both at the mRNA and at the protein level, this receptor is overexpressed in ATC with respect to normal thyroid samples. In contrast, SDF-1 was not detected. The molecular mechanisms underlying CXCR4 up-regulation in ATC are currently unknown. Because we had previously shown that CXCR4 expression was under the control of the RET/PTC-RAS-BRAF-ERK pathway in PTCs (22), and because this pathway is also activated in ATC, we asked whether CXCR4 expression correlated with the BRAF status in ATC. The ATC cell lines that we used in this study had been previously characterized for *BRAF* mutations.

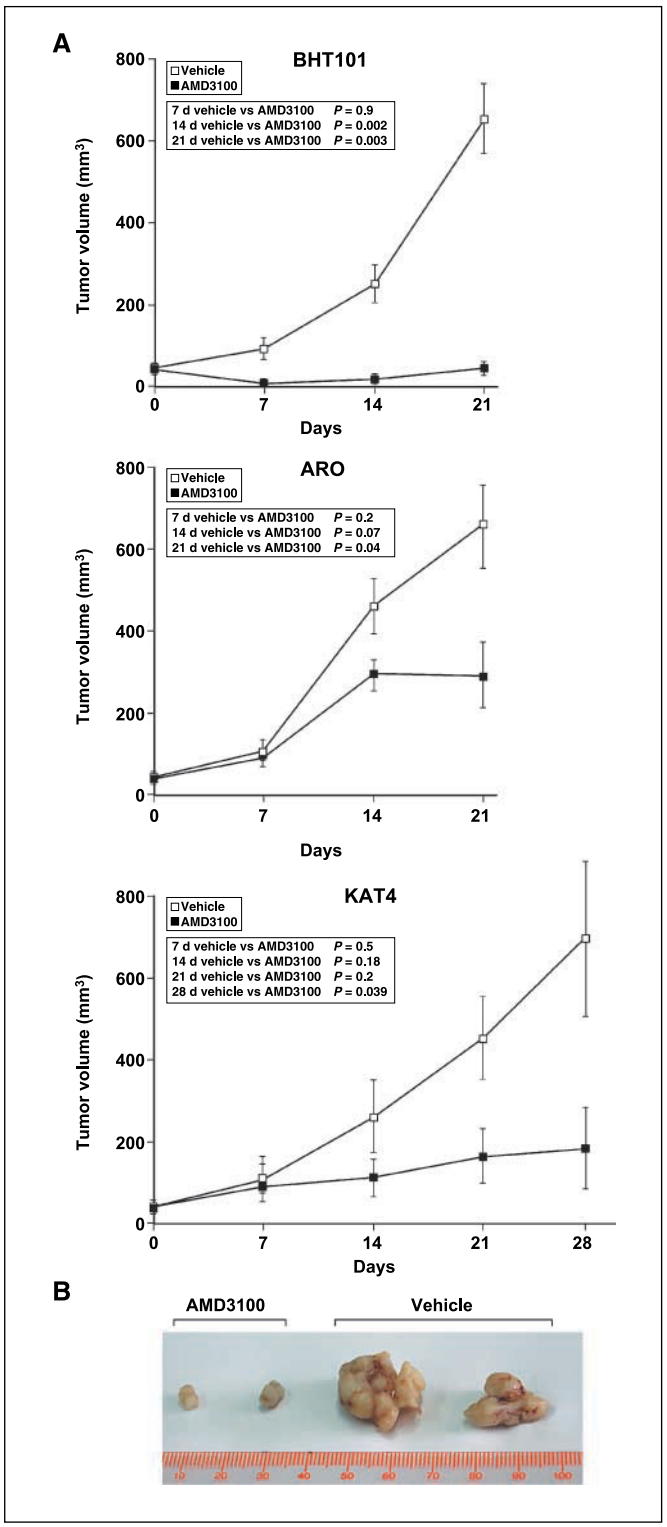

Figure 6. *A,* antitumorigenic effects of AMD3100 in ATC cell xenografts. BHT101, ARO, and KAT4 cells (5×10^6 per mouse) were injected s.c. into the right dorsal portion of BALB/c athymic mice. When tumors measured 40 mm^3, mice were randomized to two groups (10 mice per group) to receive AMD3100 or vehicle (PBS) by i.p. injection. Treatment was given for 5 consecutive days per week for 3 to 4 wk (day 1 is the treatment starting day). Tumor diameters were measured with calipers and tumor volumes were calculated. Unpaired Student's *t* test (normal distributions and equal variances) was applied. All *P* values were two sided, and differences were statistically significant at $P < 0.05$. *B,* tumors were excised and photographed. Two representative examples of BHT101 xenografts are shown.

Furthermore, human ATC samples were screened for the presence of *BRAF* mutations.[6] We found that most of the samples expressed CXCR4, and this expression was present in both the BRAF-positive and in the BRAF-negative tumors and cell lines. These data suggest that CXCR4 up-regulation in ATC is not necessarily linked to the BRAF pathway and that it can be possibly achieved through different mechanisms. The mechanisms of CXCR4 up-regulation in cancer thus far described are various and complex. It has been shown that nuclear factor-κB (NF-κB) positively regulates the expression of CXCR4 (36) in breast cancer cells. Interestingly, NF-κB is activated in human thyroid cancer cells (37, 38). Transduction of human thyroid cancer cells with the mutant *BRAF*(*V600E*) allele induced an increase in NF-κB DNA-binding activity (39). Thus, it is possible that CXCR4 expression in ATC is sustained by high NF-κB activity, which can be the result either of BRAF activation or of the activation of other still undiscovered pathways.

We also show that the CXCR4 expressed on the ATC cell surface is able to transduce biochemical signals into the cell. Indeed, stimulation of ATC cells with recombinant human SDF-1α activated ERK1/2 and, less consistently, AKT pathways in ATC cells. Moreover, we found that SDF-1α stimulated cell growth of different ATC cell cultures, which was inhibited by the small CXCR4 inhibitor AMD3100. Given the high rate of mortality of this cancer and the lack of effective therapies, we focused our efforts in the identification of novel potential therapeutic targets in ATC. We found that the treatment with AMD3100 significantly suppressed the development of tumors in different xenograft models of ATC cells in nude mice.

The more dramatic biological effects of CXCR4 inhibition observed in the animals with respect with those observed in cell culture could be explained by the fact that SDF-1 can act, in tumor microenvironment, at multiple levels. Indeed, tumoral stromal cells, such as fibroblasts and bone marrow–derived cells, express high levels of SDF-1 (34), which can directly enhance the growth of epithelial tumoral cells and can recruit endothelial progenitors, thus favoring angiogenesis. However, when we analyzed xenograft tumors for CD31-positive tumor capillaries, we found that there were no differences in vessel density of AMD3100-treated versus untreated tumors. Preliminary data suggest that AMD3100 activity in xenografts correlates better with a proapoptotic than with an antiproliferative activity.[7] Our findings are in accord with previous reports about the use of CXCR4 inhibitors in brain tumor models (40, 41). Although treatment of ATC xenografts with AMD3100 did not induce a complete regression of tumors, we observed a strong reduction in growth rate, which was more dramatic in the case of BHT101 xenografts. It is conceivable that the combination of conventional anticancer therapies with CXCR4 targeting would display a stronger antineoplastic effect. Given the strong antitumor activity of AMD3100, newer-generation compounds have been developed, such as AMD3465. This compound differs from the bicyclam AMD3100 in that it is a monocyclam endowed with greater solubility in water, higher affinity for CXCR4, and a potent antitumor activity (41). Although these compounds are effective in inhibiting various cancers, long-term sustained dosing of

[6] F. Basolo and P. Faviana, unpublished observations.
[7] V. Guarino et al., unpublished observation.

AMD3100 displayed a certain toxicity (42). For this reason, further studies, aimed at understanding the effects of long-term administration of CXCR4 inhibitors, must be pursued. Despite these considerations, our data, together with several other reports, strongly indicate that the inhibition of this pathway should be actively evaluated as a novel anticancer therapy.

In conclusion, in this report, we identify CXCR4 as another potential target of ATC anticancer therapy and suggest that AMD3100, or other specific CXCR4 inhibitors, should be developed and tested for the therapy of human ATC.

Acknowledgments

Received 3/7/2007; revised 7/26/2007; accepted 9/28/2007.

Grant support: Associazione Italiana per la Ricerca sul Cancro and E.C. Contract 03695 (GenRisk-T). V. De Falco was a fellow of the Dipartimento di Biologia e Patologia Cellulare e Molecolare of the University of Naples. V. Guarino was a fellow of the Associazione Italiana per la Ricerca sul Cancro.

The costs of publication of this article were defrayed in part by the payment of page charges. This article must therefore be hereby marked *advertisement* in accordance with 18 U.S.C. Section 1734 solely to indicate this fact.

We thank F. Curcio for the P5 and HTU8 cells; H. Zitzelsberger for the S11T, S77T, and S147T; J. Dumont for animals expressing the SV40 transgene; and S. Sequino for excellent assistance in animal care and manipulation.

References

1. De Lellis RA, Williams ED. Thyroid and parathyroid tumors. In: De Lellis RA, Lloyd RV, Heitz PU, Eng C, editors. World Health Organization classification of tumors: tumors of the endocrine organs. Lyons (France): IARC Press; 2004. p. 51–6.
2. Sherman SI. Thyroid carcinoma. Lancet 2003;361:501–11.
3. Slough CM, Randolph GW. Workup of well-differentiated thyroid carcinoma. Cancer Control 2006;13:99–105.
4. Rosai J. Poorly differentiated thyroid carcinoma: introduction to the issue, its landmarks, and clinical impact. Endocr Pathol 2004;15:293–6.
5. Vini L, Harmer C. Management of thyroid cancer. Lancet Oncol 2002;3:407–14.
6. Pacini F, Schlumberger M, Dralle H, Elisei R, Smit JW, Wiersinga W; European Thyroid Cancer Taskforce. European consensus for the management of patients with differentiated thyroid carcinoma of the follicular epithelium. Eur J Endocrinol 2006;154:787–803.
7. Patel KN, Shaha AR. Poorly differentiated and anaplastic thyroid cancer. Cancer Control 2006;13:119–28.
8. Pasieka JL. Anaplastic thyroid cancer. Curr Opin Oncol 2003;15:78–83.
9. Are C, Shaha AR. Anaplastic thyroid carcinoma: biology, pathogenesis, prognostic factors, and treatment approaches. Ann Surg Oncol 2006;13:453–64.
10. Veness MJ, Porter GS, Morgan GJ. Anaplastic thyroid carcinoma: dismal outcome despite current treatment approach. ANZ J Surg 2004;74:559–62.
11. Kondo T, Ezzat S, Asa SL. Pathogenetic mechanisms in thyroid follicular-cell neoplasia. Nat Rev Cancer 2006;6:292–306.
12. Nikiforov YE. Genetic alterations involved in the transition from well-differentiated to poorly differentiated and anaplastic thyroid carcinomas. Endocr Pathol 2004;15:319–27.
13. Garcia-Rostan G, Costa AM, Pereira-Castro I, et al. Mutation of the PIK3CA gene in anaplastic thyroid cancer. Cancer Res 2005;65:10199–207.
14. Garcia-Rostan G, Tallini G, Herrero A, D'Aquila TG, Carcangiu ML, Rimm DL. Frequent mutation and nuclear localization of β-catenin in anaplastic thyroid carcinoma. Cancer Res 1999;59:1811–5.
15. Quiros RM, Ding HG, Gattuso P, Prinz RA, Xu X. Evidence that one subset of anaplastic thyroid carcinomas are derived from papillary carcinomas due to BRAF and p53 mutations. Cancer 2005;103:2261–8.
16. Rossi D, Zlotnik A. The biology of chemokines and their receptors. Annu Rev Immunol 2000;18:217–42.
17. Zlotnik A. Chemokines and cancer. Int J Cancer 2006;119:2026–9.
18. Muller A, Homey B, Soto H, et al. Involvement of chemokine receptors in breast cancer metastasis. Nature 2001;410:50–6.
19. Burger JA, Kipps TJ. CXCR4: a key receptor in the crosstalk between tumor cells and their microenvironment. Blood 2006;107:1761–7.
20. Balkwill F. The significance of cancer cell expression of the chemokine receptor CXCR4. Semin Cancer Biol 2004;14:171–9.
21. Hwang JH, Hwang JH, Chung HK, et al. CXC chemokine receptor 4 expression and function in human anaplastic thyroid cancer cells. J Clin Endocrinol Metab 2003;88:408–16.
22. Castellone MD, Guarino V, De Falco V, et al. Functional expression of the CXCR4 chemokine receptor is induced by RET/PTC oncogenes and is a common event in human papillary thyroid carcinomas. Oncogene 2004;23:5958–67.
23. Salvatore G, De Falco V, Salerno P, et al. BRAF is a therapeutic target in aggressive thyroid carcinoma. Clin Cancer Res 2006;12:1623–9.
24. Carlomagno F, Vitagliano D, Guida T, et al. Efficient inhibition of RET/papillary thyroid carcinoma oncogenic kinases by 4-amino-5-(4-chloro-phenyl)-7-(*t*-butyl)-pyrazolo[3,4-*d*]pyrimidine (PP2). J Clin Endocrinol Metab 2003;88:1897–902.
25. Basolo F, Giannini R, Toniolo A, et al. Establishment of a non-tumorigenic papillary thyroid cell line (FB-2) carrying the RET/PTC1 rearrangement. Int J Cancer 2002;97:608–14.
26. Inokuchi N, Zeki K, Morimoto I, et al. Stimulatory effect of interleukin-1α on proliferation through a Ca^{2+}/calmodulin-dependent pathway of a human thyroid carcinoma cell line, NIM 1. Jpn J Cancer Res 1995;86:670–6.
27. Powell DJ, Jr., Russell J, Nibu K, et al. The RET/PTC3 oncogene: metastatic solid-type papillary carcinomas in murine thyroids. Cancer Res 1998;58:5523–8.
28. Russell JP, Powell DJ, Cunnane M, et al The TRK-T1 fusion protein induces neoplastic transformation of thyroid epithelium. Oncogene 2000;19:5729–35.
29. Vitagliano D, Portella G, Troncone G, et al. Thyroid targeting of the N-ras(Gln61Lys) oncogene in transgenic mice results in follicular tumors that progress to poorly differentiated carcinomas. Oncogene 2006;25:5467–74.
30. Ledent C, Dumont J, Vassart G, Parmentier M. Thyroid adenocarcinomas secondary to tissue-specific expression of simian virus-40 large T-antigen in transgenic mice. Endocrinology 1991;129:1391–401.
31. Ganju RK, Brubaker SA, Meyer J, et al. The α-chemokine, stromal cell-derived factor-1α, binds to the transmembrane G-protein-coupled CXCR-4 receptor and activates multiple signal transduction pathways. J Biol Chem 1998;273:23169–75.
32. Peng SB, Peek V, Zhai Y, et al. Akt activation, but not extracellular signal-regulated kinase activation, is required for SDF-1α/CXCR4-mediated migration of epitheloid carcinoma cells. Mol Cancer Res 2005;3:227–36.
33. De Clercq E. Potential clinical applications of the CXCR4 antagonist bicyclam AMD3100. Mini Rev Med Chem 2005;5:805–24.
34. Orimo A, Gupta PB, Sgroi DC, et al. Stromal fibroblasts present in invasive human breast carcinomas promote tumor growth and angiogenesis through elevated SDF-1/CXCL12 secretion. Cell 2005;121:335–48.
35. Pavelic K, Dedivitis RA, Kapitanovic S, et al. Molecular genetic alterations of FHIT and p53 genes in benign and malignant thyroid gland lesions. Mutat Res 2006;599:45–57.
36. Helbig G, Christopherson KW II, Bhat-Nakshatri P, et al. NF-κB promotes breast cancer cell migration and metastasis by inducing the expression of the chemokine receptor CXCR4. J Biol Chem 2003;278:21631–8.
37. Visconti R, Cerutti J, Battista S, et al. Expression of the neoplastic phenotype by human thyroid carcinoma cell lines requires NFκB p65 protein expression. Oncogene 1997;15:1987–94.
38. Pacifico F, Mauro C, Barone C, et al. Oncogenic and anti-apoptotic activity of NF-κB in human thyroid carcinomas. J Biol Chem 2004;279:54610–9.
39. Palona I, Namba H, Mitsutake N, et al. BRAFV600E promotes invasiveness of thyroid cancer cells through nuclear factor κB activation. Endocrinology 2006;147:5699–707.
40. Rubin JB, Kung AL, Klein RS, et al. A small-molecule antagonist of CXCR4 inhibits intracranial growth of primary brain tumors. Proc Natl Acad Sci U S A 2003;100:13513–8.
41. Yang L, Jackson E, Woerner BM, Perry A, Piwnica-Worms D, Rubin JB. Blocking CXCR4-mediated cyclic AMP suppression inhibits brain tumor growth *in vivo*. Cancer Res 2007;67:651–8.
42. Hendrix CW, Collier AC, Lederman MM, et al; AMD3100 HIV Study Group. Safety, pharmacokinetics, and antiviral activity of AMD3100, a selective CXCR4 receptor inhibitor, in HIV-1 infection. J Acquir Immune Defic Syndr 2004;37:1253–62.

Molecular and Cellular Endocrinology xxx (2009) xxx–xxx

Contents lists available at ScienceDirect

Molecular and Cellular Endocrinology

journal homepage: www.elsevier.com/locate/mce

Review

Thyroid cancer and inflammation

Valentina Guarino[a], Maria Domenica Castellone[a], Elvira Avilla[a], Rosa Marina Melillo[a,b,*]

[a] Dipartimento di Biologia e Patologia Cellulare e Molecolare/Istituto di Endocrinologia ed Oncologia Sperimentale del CNR "G. Salvatore", Italy
[b] Facoltà di Scienze Biotecnologiche dell'Università di Napoli "Federico II", 80131 Naples, Italy

ARTICLE INFO

Article history:
Received 7 July 2009
Received in revised form 6 October 2009
Accepted 7 October 2009

Keywords:
Thyroid cancer
Inflammatory cell
Chemokine

ABSTRACT

Some cancer types are strongly associated with chronic inflammatory or infectious diseases whereas others are not, but an inflammatory component is present in most human neoplastic lesions. This review focuses on various aspects of thyroid cancer and inflammation. The incidence of thyroid cancer, in particular of well-differentiated papillary thyroid carcinomas (PTCs), is increased in autoimmune thyroid diseases such as Hashimoto's thyroiditis. Thyroid cancer often has an inflammatory cell infiltrate, which includes lymphocytes, macrophages, dendritic cells and mast cells, whose role in thyroid cancer is still not completely understood. However, most experimental evidence suggests these cells exert a protumorigenic function. Moreover, oncoproteins typically expressed in human PTCs, such as RET/PTC, RAS, and BRAF, trigger a proinflammatory programme in thyreocytes. These data suggest that inflammatory molecules are promising targets for thyroid cancer therapy.

Contents

1. Thyroid cancer

Thyroid cancer, although a rare disease, is the most frequent endocrine neoplasia, and its incidence is rapidly increasing. The papillary histotype is the most frequent. Thyroid cancer can derive from both the follicular and the parafollicular component of the thyroid gland. Three malignant lesions may derive from follicular cells: well-differentiated (WDTC), poorly differentiated (PDTC) and anaplastic (ATC) thyroid carcinomas. WDTCs are either papillary (PTC) or follicular (FTC). These two types are characterized by specific histological features, and by the maintenance of some differentiating features (Kondo et al., 2006). WDTCs have a favorable prognosis thanks to the efficacy of combined surgical and radioiodine-based therapy. Nevertheless, 5–10% of WDTCs progress to radioactive iodine refractory-disease. PDTCs and ATCs, which are thought to derive from pre-existing differentiated tumors, do not accumulate radioiodine and respond poorly to medical and surgical treatment (Rosai et al., 1992). Medullary thyroid carcinoma (MTC), which arises from the parafollicular C-cells of the thyroid, is generally treatable by surgery. However, novel chemotherapeutic agents like vandetanib, which target growth factor receptor, are showing promise in the treatment of MTC. This tumor can be inherited in the context of autosomal dominant MEN 2 (multiple endocrine neoplasia type 2) syndromes (MEN2A, MEN2B and familial medullary thyroid carcinoma [FMTC]) (Roman et al., 2009).

Non-overlapping mutations of the RET, TRKA, RAS and BRAF genes are found in about 70% of PTCs. These genes encode activators of the mitogen-activated protein kinase (MAPK) cascade. RET encodes the tyrosine kinase receptor of growth factors belonging to the glial-derived neurotrophic factor (GDNF) family (Manie et al., 2001). RET/PTC rearrangements are thought to be early events in thyroid tumorigenesis since they are very frequent in clinically silent small PTC (Fusco et al., 2002). Similar rearrangements of the high affinity receptor (TRKA) for nerve growth factor (NGF) are also

* Corresponding author at: DBPCM/IEOS, Via S. Pansini, 5, 80131 Naples, Italy. Tel.: +39 0817463603; fax: +39 0817463603.
E-mail address: rosmelil@unina.it (R.M. Melillo).

0303-7207/$ – see front matter © 2009 Elsevier Ireland Ltd. All rights reserved.
doi:10.1016/j.mce.2009.10.003

found, albeit at a low prevalence, in human PTC (Alberti et al., 2003). Activating point-mutations in RAS small GTPases are found mainly in the follicular variant of PTC (PTC-FV) (Zhu et al., 2003). Point-mutations in BRAF are the most common genetic lesion in these tumors (Kimura et al., 2003; Xu et al., 2003; Soares et al., 2003; Cohen et al., 2003). BRAF is a member of the RAF family of serine/threonine kinases, which includes ARAF and RAF1, and it is a component of the RAF–MEK–ERK signaling module.

FTCs are characterized by RAS point-mutations (Nikiforova et al., 2002) or by the PAX8/PPAR rearrangement (Kroll et al., 2000). PDTC and ATC can derive from pre-existing WDTCs. RAS point-mutations and the V600E BRAF mutation are prevalent in PDTC and ATC (Garcia-Rostan et al., 2003; Nikiforova et al., 2003; Soares et al., 2004; Begum et al., 2004). Finally, p53 mutations are often found in ATC (Donghi et al., 1993; Fagin et al., 1993).

MTC can be sporadic or it could be one of the lesions that characterize the autosomal dominant MEN 2 syndromes (MEN2A, MEN2B and FMTC). MEN 2 syndromes are caused by germline point-mutations that convert RET into a dominant oncogene (Santoro et al., 1995). In all MEN2A cases, mutations target extracellular cysteine residues in RET. In more than 80% of cases, MEN2B is caused by the Met918Thr substitution in the kinase domain of the receptor. Roughly 40% of sporadic MTC cases harbor point-mutations in RET (Leboulleux et al., 2004).

2. Chronic inflammation and cancer

Inflammation is a physiological, protective process used by the organism in response to tissue damage. Several chemical signals initiate and sustain the inflammatory response whose aim is to fight pathogens and to repair tissue damage. Several cell types migrate to the sites of tissue damage. This migration is mediated by chemotactic and adhesion proteins, including members of the integrin and selectin family (Coussens and Werb, 2002). The first migrating cells are neutrophils, macrophages and mast cells, all of which secrete reactive oxygen species (ROS), vasoactive molecules, such as histamine and leukotrienes, and cytokines, chemokines and proteases that remodel the extracellular matrix (De Visser et al., 2006). Inflammation is an auto-limiting process; however, abnormal persistence of the stimuli that induced the inflammatory response or the failure of the mechanisms that make it end, result in chronic inflammation (Coussens and Werb, 2002).

A functional relationship between chronic inflammation and cancer was first proposed by Virchow in 1863, and has been sustained by clinical and epidemiological evidence. The most compelling evidence is the association between: (a) intestinal chronic inflammatory diseases (Crohn's disease and ulcerative rectocolitis) and adenocarcinoma of the colon; (b) chronic HBV or HCV hepatitis and liver carcinoma; (c) *Helicobacter pylori*-induced chronic gastritis and gastric carcinoma; (d) asbestosis and mesothelioma; (e) chronic obstructive pulmonary disease (COPD) and lung cancer; and (f) chronic esophagitis and carcinoma of the esophagus (Balkwill and Mantovani, 2001). Moreover, a 40–50% reduction in the incidence of colorectal cancer is associated with the regular use of non-steroidal anti-inflammatory drugs, the COX enzymes that catalyze the synthesis of proinflammatory mediators, such as prostaglandins (Baron and Sandler, 2000; Williams et al., 1999).

Further support for the concept that inflammation can cause cancer comes from the observation that polymorphisms in genes encoding proinflammatory chemokines are associated with an increased risk of some forms of human cancer. For instance, IL1-β polymorphisms are associated with an increased incidence of gastric cancer (Gianfagna et al., 2008). Moreover, gastric-specific expression of this cytokine in transgenic mice can induce gastric inflammation and cancer (Tu et al., 2008).

Various infiltrating cells have been identified in tumors, namely, tumor-associated lymphocytes, tumor-associated macrophages (TAM), immature dendritic cells, mast cells and myeloid-derived suppressor cells. The presence of specific inflammatory-immune cells such as macrophages and mast cells in tumor site has been associated with a poor prognosis of the disease (Fujimoto et al., 2009; Maltby et al., 2009). Pollard and colleagues have shown that transgenic mice prone to breast cancer develop less proliferating and invasive tumors when crossed with mice deficient for CSF1, a macrophage chemotactic factor (Lin et al., 2001). Other cell populations also contribute, via distinct mechanisms, to tumor growth. Indeed, mice deficient in mast cells or CD4+ T cells display a reduction in tumor incidence and progression in models of mice carcinogenesis (Daniel et al., 2003; Soucek et al., 2007). Among the cell populations recruited into tumor sites by cancer cells, a peculiar role is played by bone marrow-derived precursors. These include myeloid-derived suppressor cells that contribute to tumor growth through tumor-induced immune tolerance (Marigo et al., 2008), and bone marrow-derived stem cells, which are thought to be recruited from the bloodstream and to repopulate areas of epithelial destruction. Indeed, these cells constitute all the metaplastic, dysplastic and neoplastic areas in the *Helicobacter*-induced gastric cancer model in mice. Again, IL1-β plays an important role in this process—indeed it seems to be required for both recruitment and activation of bone marrow-derived stem cells (Houghton et al., 2004; Tu et al., 2008).

Cancer cells secrete several cytokines and chemokines, thus sustaining cancer cell growth and recruiting leukocytes into tumor sites. Leukocytes physiologically secrete ROS and reactive nitrogen species to eliminate pathogens. However, these highly reactive metabolites induce the production of peroxynitrite and other mutagenic agents; therefore, they can induce "DNA damage", i.e., mutations in proliferating cells (Coussens and Werb, 2002). Thus, in the case of persistent tissue damage, the O_2 and N highly reactive metabolites secreted by inflammatory cells induce point-mutations, rearrangements and double-strand breaks in the DNA (Colotta et al., 2009). This results in a higher probability of oncogene activation or of tumor suppressor loss of function.

Proinflammatory cytokines produced in tumor sites are pivotal in cancer progression. The production of these cytokines by inflammatory and epithelial cancer cells depends mainly on the NFkB transcription factor. Through conditional deletion of the NFkB upstream activator IKKb, in myeloid and epithelial cells, it has been shown that NFkB plays a major protumorigenic role in an experimental colitis-associated cancer (CAC) model (Greten et al., 2004). Among the cytokines induced by NFkB, IL6 has been identified as one of the most relevant myeloid-derived factors that promote tumorigenesis. Moreover, activation of the IL6 pathway, in particular of the STAT3 transcription factor, which is a downstream mediator of IL6 activity, is necessary for CAC initiation and progression (Grivennikov et al., 2009; Bollrath et al., 2009).

3. Thyroid cancer and autoimmune thyroid diseases

A link between thyroid cancer, in particular the PTC histotype, and autoimmune thyroid diseases (AITD) has long been recognized, although the precise relationship between the two diseases is still debated. This group of diseases includes Hashimoto's thyroiditis and Grave's disease. Hashimoto's thyroiditis (HT) is an autoimmune disorder in which the immune system reacts against a variety of thyroid antigens. The overriding feature of HT is the progressive depletion of thyroid epithelial cells, which are gradually replaced by mononuclear cell infiltration and fibrosis. Multiple immunologic mechanisms may contribute to the death of thyrocytes. Sensitiza-

Please cite this article in press as: Guarino, V., et al., Thyroid cancer and inflammation. Mol. Cell. Endocrinol. (2009), doi:10.1016/j.mce.2009.10.003

tion of autoreactive CD4+ T-helper cells to thyroid antigens appears to be the initiating event. Hashimoto's thyroiditis is characterized by proliferating nodules as well as by cytological alterations and nuclear modifications similar to those of papillary carcinomas (Weetman, 2004).

An epidemiological association has been identified between Hashimoto's thyroiditis and thyroid cancer (Di Pasquale et al., 2001; Wirtschafter et al., 1997; Mechler et al., 2001; Segal et al., 1985; Eisenberg and Hensley, 1989; Ott et al., 1987; Sclafani et al., 1993; Pisanu et al., 2003). The increased incidence of carcinomas in patients with thyroiditis suggests thyroiditis might be a precancerous condition. Most thyroiditis-associated carcinomas are papillary; however, also follicular, anaplastic, medullary and squamous carcinomas have been reported in cases of thyroiditis. Thyroid follicular cells may have chromosomal defects, such as the RET/PTC rearrangement, which is the hallmark of many PTCs. Several authors found RET/PTC rearrangements in non-neoplastic thyroid lesions, such as HT (Wirtschafter et al., 1997; Sheils et al., 2000; Elisei et al., 2001). Additional evidence implicating RET/PTC in the association between thyroiditis and cancer comes from the finding that patients exposed to radiation from the Chernobyl nuclear power plant disaster often develop not only RET/PTC-induced papillary tumors but also autoimmune thyroiditis (Williams, 2002). Accordingly, transgenic mice engineered to express RET/PTC develop papillary carcinomas and chronic thyroiditis (Powell et al., 1998). Finally, Wirtschafter and colleagues detected RET/PTC expression in about 90% of the cases of Hashimoto's thyroiditis they analyzed (Wirtschafter et al., 1997). However, these data partially contrast with other reports. Nikiforova and colleagues detected RET/PTC rearrangements only in PTCs not associated with Hashimoto's disease (Nikiforova et al., 2002). Rhoden et al. detected only a few follicular cells expressing very low levels of RET/PTC in Hashimoto's thyroiditis, which suggests that RET/PTC expression does not necessarily predict the development of PTC in patients with thyroiditis (Rhoden et al., 2006).

Two models can be hypothesized to explain the association between Hashimoto's thyroiditis and the RET/PTC rearrangement. The first suggests that inflammation might facilitate the rearrangement. According to this hypothesis, production of free radicals, cytokine secretion, cellular proliferation and other phenomena correlated with inflammation might predispose to the rearrangement of RET/PTC in follicular cells. In support of this hypothesis, it has been observed that the mutational rate in inflamed tissues is much higher than in normal tissues (Colotta et al., 2009). It is also possible that the inflammatory microenvironment supports thyreocyte survival in stress conditions. It is generally assumed that normal human epithelial cells do not tolerate oncogene expression because excessive growth signals induce DNA replication stress, which, in turn, induces oncogene-mediated senescence or apoptosis (Lowe and Sherr, 2003; Halazonetis et al., 2008; Evan and d'Adda di Fagagna, 2009). Thus, evasion from apoptosis is required for neoplastic transformation and can occur through additional genetic lesions that lead to activation of anti-apoptotic pathways, such as those mediated by phosphatydilinositole 3-kinase. This concept is supported by the finding that the ectopic expression of the RET/PTC oncogene in a continuous rat thyroid cell line (PC Cl3) induces apoptosis (Castellone et al., 2003; Wang et al., 2003). This effect might be due to the strong RET-mediated mitogenic stimuli. It is possible that cytokines and chemokines released by the inflammatory tumoral stroma sustain the survival of those thyroid cells in which RET/PTC rearrangements randomly occur, thereby allowing the selection of clones that acquire additional genetic lesions and thus become resistant to oncogene-induced apoptosis.

It has recently been suggested that tissue stem cells are the targets of malignant transformation. In the setting of chronic inflammation, the pool of resident or bone marrow-derived stem cells is thought to expand (Li et al., 2006). If this applies also to thyroid cancer, AITD-mediated inflammation could cause the expansion of stem cells in which a RET/PTC rearrangement has occurred.

An alternative hypothesis, which does not exclude the previous hypothesis, is that the RET/PTC rearrangement itself, and the consequent activation of the downstream signaling pathways can induce thyroid inflammation. Accordingly, RET/PTC induces the synthesis of many inflammatory proteins in epithelial thyroid cells (Table 1) and a severe inflammatory response is observed in TG-RET/PTC transgenic mice in which RET/PTC expression is confined to the thyroid gland (Powell et al., 2003; Melillo et al., 2005; Puxeddu et al., 2005; Pufnock and Rothstein, 2009). Indeed, RET/PTC transgenic mice develop PTCs and chronic thyroiditis. However, RET/PTC itself is not sufficient to induce complete Hashimoto's thyroiditis in these mice since this disease is characterized not only by lymphocytic infiltration, but also by a humoral autoimmune reaction that results in the production of autoantibodies against thyroid antigens, and by the formation of lymphoid follicles in the thyroid parenchyma. These features are not present in TG-RET/PTC transgenic animals. In conclusion, we favor the hypothesis that AITD creates a protumorigenic microenvironment in which the RET/PTC rearrangement is tolerated. The rearrangement itself then contributes to maintaining the inflammatory reaction.

4. Thyroid cancer and immune-inflammatory infiltrate

There are various reports of immune-inflammatory cell infiltrates in thyroid cancer. Not only are PTCs frequent in the context of Hashimoto's thyroiditis, but these carcinomas are often present with a remarkable lymphocytic infiltrate in the absence of the typical signs of autoimmune thyroiditis, such as autoantibody production and tertiary follicle formation. The prevalence of lymphocytic infiltrate is generally significantly higher in patients with PTC than in patients with benign thyroid lesions (Okayasu, 1997), which indicates that these cells might favor cancer development. However, the presence of chronic lymphocytic thyroiditis in patients with PTC correlates with an improved prognosis (Kebebew et al., 2001). Moreover, thyroid carcinomas with a poor prognosis, such as PDTCs and ATCs, are characterized by a strongly reduced lymphocyte cell infiltrate compared with PTCs, thus suggesting that these cells may play a protective role in thyroid cancer (Ugolini et al., 2007). Macrophages and dendritic cells, mainly characterized by an immature phenotype, have been identified in human PTCs (Scarpino et al., 2000). Again, PDTCs and ATCs are characterized by a greatly reduced dendritic cell infiltrate with respect to PTCs, thus suggesting that these cell types also may play a protective role in thyroid cancer (Ugolini et al., 2007). Tumor-associated macrophages are generally considered protumorigenic (Sica et al., 2008). Ryder and colleagues found that the density of the TAM infiltrate was higher in PDTCs and ATCs than in PTCs and FTCs. Moreover, increased TAM infiltration in PDTCs was found to be positively correlated with capsule invasion, extrathyroidal extension and poor prognosis (Ryder et al., 2008). Taken together, these data support the concept that TAM may favor the malignant progression of thyroid cancer.

We compared the density of tryptase-positive mast cells in 96 PTCs versus normal thyroid tissue from 14 healthy individuals. Mast cell density was higher in PTCs than in control tissue. Mast cell infiltrate correlated with capsule invasion. We also observed that mast cells promoted proliferation, survival and the invasive ability of thyroid cancer cells, thereby contributing to thyroid carcinoma growth and invasiveness (Melillo et al., unpublished observations).

The presence of inflammatory cells has been evaluated in transgenic mice expressing RET/PTC3 in the thyroid gland by

Please cite this article in press as: Guarino, V., et al., Thyroid cancer and inflammation. Mol. Cell. Endocrinol. (2009), doi:10.1016/j.mce.2009.10.003

Table 1
The most relevant inflammatory molecules in thyroid cancer cells. The official symbol and full name, Gene ID, and known function for each molecule are listed. References regarding their role in thyroid cancer are also reported.

Inflammatory molecules	Official symbol	Official full name	Gene ID	Function	References
M-CSF	CSF1	Colony stimulating factor 1 (macrophage)	1435	Cytokine that controls the production, differentiation, and function of macrophages.	Borrello et al. (2005)
G-CSF	CSF3	Colony stimulating factor 3 (granulocyte)	1440	Cytokine that controls the production, differentiation, and function of granulocytes.	Borrello et al. (2005)
GM-CSF	CSF2	Colony stimulating factor 2 (granulocyte–macrophage)	1437	Cytokine that controls the production, differentiation, and function of granulocytes and macrophages.	Russell et al. (2003, 2004), Borrello et al. (2005)
IL1-α	IL1A	Interleukin 1, alpha	3552	Member of the interleukin 1 cytokine family. Pleiotropic cytokine involved in various immune responses, inflammatory processes, and hematopoiesis. It is mainly produced by monocytes and macrophages.	Russell et al. (2003, 2004)
IL1-β	IL1B	Interleukin 1, beta	3553	Member of the interleukin 1 cytokine family. It is produced by activated macrophages as a proprotein, which is proteolytically processed to its active form by caspase 1 (CASP1/ICE). This cytokine is an important mediator of the inflammatory response.	Russell et al. (2003, 2004), Borrello et al. (2005)
IL6	IL6	Interleukin 6 (interferon, beta 2)	3569	Cytokine that functions in inflammation and the maturation of B cells. The protein is primarily produced at sites of acute and chronic inflammation, where it is secreted into the serum and induces a transcriptional inflammatory response.	Russell et al. (2003, 2004), Puxeddu et al. (2005)
IL8/CXCL8	IL8	Interleukin 8	3576	Member of the CXC chemokine family. It is one of the major mediators of the inflammatory response. It is secreted by several cell types, functions as a chemoattractant, and is also a potent angiogenic factor.	Iwahashi et al. (2002), Borrello et al. (2005)
IL4	IL4	Interleukin 4	3565	Pleiotropic cytokine produced by activated T cells. This cytokine is a ligand for interleukin 4 receptor.	Stassi et al. (2003), Todaro et al. (2006)
IL10	IL10	Interleukin 10	3586	Cytokine produced primarily by monocytes and to a lesser extent by lymphocytes. It has pleiotropic effects in immunoregulation and inflammation. It down-regulates the expression of Th1 cytokines, and enhances B cell survival, proliferation, and antibody production.	Stassi et al. (2003), Todaro et al. (2006)
IL24	IL24	Interleukin 24	11009	Member of the IL10 family of cytokines. It can induce apoptosis selectively in various cancer cells.	Shinohara and Rothstein (2004)
VEGFA	VEGFA	Vascular endothelial growth factor A	7422	Member of the PDGF/VEGF growth factor family, acts on endothelial cells and mediates increased vascular permeability, induces angiogenesis, vasculogenesis and endothelial cell growth, promotes cell migration, and inhibits apoptosis.	Belletti et al. (1999)
OPN/IL28/SPP1	SPP1	Secreted phosphoprotein 1	6696	Cytokine secreted by immune and non-immune cells. Involved in cell migration and adhesion, bone metabolism and immune regulation of TH1 cells. Overexpressed in several cancer types.	Castellone et al. (2004a), Borrello et al. (2005)
TNFa	TNF	Tumor necrosis factor (TNF superfamily, member 2)	7124	Proinflammatory cytokine that belongs to the tumor necrosis factor (TNF) superfamily. It is mainly secreted by macrophages and is involved in the regulation of cell proliferation, differentiation, apoptosis, lipid metabolism, and coagulation.	Russell et al. (2003, 2004)
CCL2/mcp-1	CCL2	Chemokine (C–C motif) ligand 2	6347	Small cytokine belonging to the CC chemokine family that displays chemotactic activity for monocytes and basophils but not for neutrophils or eosinophils. Ligand for the CCR2 receptor.	Russell et al. (2003, 2004), Puxeddu et al. (2005), Melillo et al. (2005)
CCL20	CCL20	Chemokine (C–C motif) ligand 20	6364	Small cytokine belonging to the CC chemokine family. It binds to the CCR6 receptor and is strongly chemotactic for lymphocytes and weakly attracts neutrophils. It is implicated in the formation and function of mucosal lymphoid tissues.	Borrello et al. (2005)
CXCL1/GROa	CXCL1	Chemokine (C–X–C motif) ligand 1 (melanoma growth stimulating activity, alpha)	2919	Small cytokine belonging to the CXC chemokine family. It is strongly chemotactic for neutrophils and has been shown to be a major component required for serum-dependent melanoma cell growth. Ligand for the CXCR2 receptor.	Russell et al. (2003, 2004), Melillo et al. (2005)

Please cite this article in press as: Guarino, V., et al., Thyroid cancer and inflammation. Mol. Cell. Endocrinol. (2009), doi:10.1016/j.mce.2009.10.003

Table 1 (*Continued*)

Inflammatory molecules	Official symbol	Official full name	Gene ID	Function	References
CXCL10/IP-10	CXCL10	Chemokine (C–X–C motif) ligand 10	3627	Small cytokine belonging to the CXC chemokine family, ligand for the receptor CXCR3. It has pleiotropic effects, including stimulation of monocytes, natural killer and T-cell migration, and modulation of adhesion molecule expression.	Puxeddu et al. (2005), Melillo et al. (2005)
CXCL12/SDF-1	CXCL12	Chemokine (C–X–C motif) ligand 12 (stromal cell-derived factor 1)	6387	Small cytokine belonging to the CXC chemokine which activate leukocytes and is often induced by proinflammatory stimuli. Ligand for the CXCR4 and the CXCR7 receptors.	Borrello et al. (2005)
CXCR2	IL8RB	Interleukin 8 receptor, beta	3579	Member of the G-protein-coupled receptor family. This protein is a receptor for interleukin 8 (IL8) and for other CXC-chemokines. It mediates neutrophil migration to sites of inflammation and has angiogenic effects.	Melillo et al. (2005)
CXCR3	CXCR3	Chemokine (C–X–C motif) receptor 3	2833	Member of the G-protein-coupled receptor family. It displays selectivity for three chemokines, CXCL10/IP10, Mig and I-TAC. It is prominently expressed in effector/memory T cells, and in T cells present in many types of inflamed tissues.	Melillo et al. (2005)
CXCR4	CXCR4	Chemokine (C–X–C motif) receptor 4	7852	Member of the G-protein-coupled receptor family. CXC chemokine receptor specific for stromal cell-derived factor 1. It acts with the CD4 protein to support HIV entry into cells and is also highly expressed in cancer cells.	Castellone et al. (2004b), Borrello et al. (2005)
CD44	CD44	CD44 molecule (Indian blood group)	960	Cell-surface glycoprotein involved in cell-cell interactions, cell adhesion and migration. It is a receptor for hyaluronic acid (HA), osteopontin, collagens, and matrix metalloproteinases (MMPs). It participates in a wide variety of cellular functions including lymphocyte activation, recirculation and homing, hematopoiesis, and tumor metastasis.	Castellone et al. (2004a)
mPGES1	PTGES	Prostaglandin E synthase	9536	This protein is a glutathione-dependent prostaglandin E synthase. The expression of this gene has been shown to be induced by the proinflammatory cytokine interleukin 1 beta (IL1B).	Puxeddu et al. (2003)
COX2	PTGS2	Prostaglandin-endoperoxide synthase 2 (prostaglandin G/H synthase and cyclooxygenase)	5743	It is the key enzyme in prostaglandin biosynthesis. This gene encodes the inducible isozyme. It is regulated by specific stimulatory events, suggesting that it is responsible for the prostanoid biosynthesis involved in inflammation and mitogenesis.	Puxeddu et al. (2003)

Please cite this article in press as: Guarino, V., et al., Thyroid cancer and inflammation. Mol. Cell. Endocrinol. (2009), doi:10.1016/j.mce.2009.10.003

means of a tissue-specific promoter. In this system, mice develop PTC-like lesions, characterized by a leukocytic infiltrate, mainly constituted by macrophages (Russell et al., 2004). This effect seemed to be RET-specific because a similar oncogene, TRK-T1, which also derives from a rearrangement of a tyrosine kinase receptor with a heterologous gene, did not have the same effect. Interestingly, the tumor incidence and burden in RET/PTC3 mice were influenced by the genetic background of the animals. In fact, tumors were significantly larger in C57BL/6 mice expressing RET/PTC3 than in C3H/HeJ animals. Cytokine expression was much higher in large tumors, suggesting that these molecules play a role in tumor growth. This effect could be due to the different polarization of TCD4+ cells and consequently to the distinct cytokine environment mounted by the C57BL/6 mice with respect to the C3H/HeJ animals. Taken together, these data demonstrate that the RET/PTC3 oncoprotein can induce recruitment of immune cells into tumor sites, and that cytokines produced in a tumor site play an important role in tumor progression.

In another set of experiments, Pufnock and Rothstein investigated whether RET/PTC3 is involved in the recruitment of other immune cell populations into tumor sites (Pufnock and Rothstein, 2009). In that study, RET/PTC3 and its mutant isoform (RET/PTC3 Y1062F), which is defective in the activation of the most relevant RET-mediated signaling pathways, were transduced into a mouse fibrosarcoma cell line. Tumors were induced by injecting RET/PTC3- and RET/PTC3 Y1062F-expressing cells in syngeneic mice. RET/PTC3 tumors were significantly larger than RET/PTC3 mutant tumors. CD4+ and CD8+ T cell infiltrate density was comparable in both tumor groups. However, RET/PTC3, but not RET/PTC3 Y1062F tumors, displayed a remarkable leukocytic infiltrate characterized by CD11b+, Gr1+ myeloid cells, previously described as innate suppressive inflammatory cells (Marigo et al., 2008; Gabrilovich and Nagaraj, 2009). These data suggest that RET/PTC3-positive thyroid cancer, like other cancer types, can induce the recruitment of CD11b+, Gr1+ cells. These cells can mediate tumor escape from the immune response; this phenomenon is dependent on the integrity of the Y1062 residue of RET. Whether other mechanisms of immune evasion also operate in thyroid cancer is unknown. Interestingly, the BRAF–MAPK signaling pathway has been shown to induce the synthesis and secretion of immunosuppressive cytokines in melanomas (Sumimoto et al., 2006). These factors include IL10, VEGF and IL6, which are cytokines that are produced also by thyroid cancer cells (Stassi et al., 2003; Todaro et al., 2006; Russell et al., 2004; Shinohara and Rothstein, 2004; Belletti et al., 1999; Jo et al., 2006; Puxeddu et al., 2005).

5. Oncoprotein signaling in thyroid cancer and inflammation

The activation of RET in PTC derives from a genetic rearrangement between the RET tyrosine-kinase domain and heterologous genes. The consequence of these rearrangements is the constitutive activation of RET due to constitutive dimerization–oligomerization of the oncoprotein induced by the different RET-fused genes. In MEN2A and FMTC, RET activation is achieved by constitutive dimerization of RET through the replacement of an extracellular cysteine and the formation of disulfide bonds (Santoro et al., 2004). Differently, mutations that affect the intracellular domain induce kinase activation in the absence of dimerization, presumably through a modification of the kinase structure. For instance, the MEN2B M918T point-mutation induces a change in substrate specificity with respect to MEN2A mutants, which is reflected in the different capability of MEN2B mutants to phosphorylate endogenous tyrosines and signaling adaptors. These differences can account, at least in part, for the phenotypic differences between the two syndromes. Indeed, although both MEN2A and MEN2B are characterized by the presence of pheochromocytomas and MTCs, MEN2B MTCs occur earlier and are more aggressive. Furthermore, MEN2B patients also present skeletal abnormalities and ganglioneuromas (Hansford and Mulligan, 2000).

Both point-mutations and genetic rearrangements cause constitutive activation of the tyrosine kinase activity of RET in the absence of ligands. Several studies conducted in different laboratories have shown that activation of RET, either by physiological ligands or by oncogenic conversion, results in the phosphorylation of intracellular tyrosine residues that serve as docking sites for the recruitment of signaling adapters. Among the tyrosines phosphorylated after RET activation, Y1062 has been shown to be important for RET-mediated biological activity in thyroid cells. Y1062 is a multi-docking site, being able to bind several PTB-containing adapters, namely, ShcA, FRS2, IRS1, ShcC and dok. Substitution of the Y1062 residue of Ret with a phenylalanine, both in the context of a wild-type and of an oncogenically activated receptor, abrogates Ret-mediated signal transduction and biological activities (Takahashi, 2001). We and others have shown that Ret can activate the MAPK pathway in a Y1062-RAS- and BRAF-dependent manner (Kimura et al., 2003; Melillo et al., 2005).

Several groups demonstrated that RET-induced transcriptional activity depends almost entirely on the integrity of the Y1062 residue and on activation of the RAS/BRAF/MAPK pathway. Russel and colleagues reported that the expression of the RET/PTC3 isoform in a rat thyroid cell line (PC Cl3) induced an increase in NFkB DNA-binding activity and a consequent increase in proinflammatory cytokine secretion (Russell et al., 2003). CXCL1/Groα, CCL2/mcp-1 and GM-CSF were up-regulated upon RET/PTC3 expression, and this increase depended on the integrity of residue 1062 of RET.

GDNF stimulation of the neuroectodermal tumor cell line SK-N-MC, ectopically expressing the human wild-type RET, induced the production of high levels of IL8. This cytokine has also been found in the TT human medullary thyroid carcinoma cell line carrying the RET/MEN2A oncogene and in the TPC1 human PTC cell line (Iwahashi et al., 2002). IL8 is a proinflammatory, mitogenic and proangiogenic chemokine that contributes to several human cancers (Waugh and Wilson, 2008). Russel and colleagues found that RET/PTC3 caused the expression of the proinflammatory proteins IL1-α, IL1-β, IL6 and IL24 in thyroid cancer cells (Russell et al., 2004; Shinohara and Rothstein, 2004). Similar results were obtained by Puxeddu and colleagues, who demonstrated that prostaglandin E2 (PGE2), microsomal prostaglandin E synthase-1 (mPGES1), cyclooxygenase2 (COX2) and several other genes involved in immune response and inflammation were induced by RET/PTC3 in PC Cl3 cells (Puxeddu et al., 2003; Puxeddu et al., 2005).

To study the transcriptional changes associated with thyroid transformation, we used an oligonucleotide-based DNA microarray (Affymetrix) on PC Cl3 cells engineered to stably express wild-type and mutant isoforms of the oncogenic RET/PTC3 protein, or the HRAS (V12) or BRAF(V600E) oncoproteins, respectively. When transfected cells were compared with the parental cells, it was evident that RET/PTC3 induced a complex pattern of gene expression that depended entirely on the integrity of the Y1062 residue. The HRAS (V12) and BRAF(V600E) oncoproteins each modified the expression of several genes, and 50% of these genes were common between the three oncoproteins. Furthermore, by using siRNA and pharmacological inhibitors, we showed that most of these gene changes depended on the ERK pathway (Melillo et al., 2005). Our gene expression profiling studies also revealed the induction of cytokine and chemokines and of their respective receptors in PC RET/PTC3 cells (Fig. 1). Indeed, we found that RET/PTC3 cells expressed high levels of osteopontin (OPN), VEGFA, CCL2, CXCL1 and CXCL10 (Melillo et al., 2005). Interestingly, CD44, CXCR2 and CXCR3, the receptors for OPN, CXCL1 and CXCL10, respectively,

Please cite this article in press as: Guarino, V., et al., Thyroid cancer and inflammation. Mol. Cell. Endocrinol. (2009), doi:10.1016/j.mce.2009.10.003

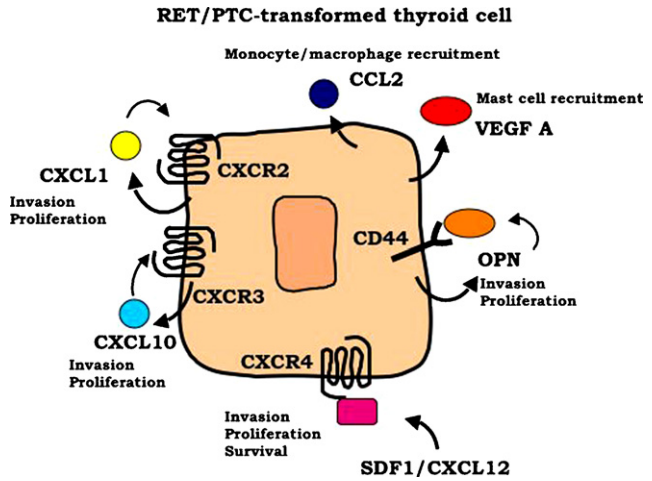

Fig. 1. Cytokines and chemokines secreted by RET/PTC-transformed PC Cl3 rat thyroid cells: main biological effects. Transformation of PC CL3 rat thyroid cells through activation of the RET/PTC–RAS–BRAF–MAPK signaling pathway induces a proinflammatory program that includes cytokines, chemokines and their receptors. Selected mediators and their biological effects are indicated.

were also expressed by transformed cells. We also found the expression of CXCR4, the chemokine receptor for the chemokine CXCL12, in transformed cells with respect to the normal counterparts (Castellone et al., 2004b). These results were confirmed by Borrello and coworkers in human primary thyroid cells transduced with the RET/PTC oncogene (Borrello et al., 2005).

The proinflammatory properties of RET/PTC in the thyroid might have a dual effect: on one hand, molecules such as OPN, CXCL1, CXCL10, CCL2 and GM-CSF can influence the immune response to the tumor by recruiting and functionally regulating immune cells. For instance, transplantation of RET/PTC3-expressing thyreocytes into mice *in vivo* induced intense macrophage infiltrate and neovascularization followed by cell death (Russell et al., 2003). On the other hand, secreted cytokines and chemokines, such as OPN, CXCL1, CXCL10 and IL24, can act as autocrine growth and survival factors for thyroid tumor cells that express the cognate receptors on their plasma membrane (Shinohara and Rothstein, 2004; Castellone et al., 2004a; Melillo et al., 2005). These data are corroborated by studies conducted on human thyroid tumors. Indeed, it has been shown that human thyroid samples express most inflammatory genes (CXCR4, CD44, OPN, CXCL1, CXCL10 and SDF-1) (Castellone et al., 2004a,b; Guarino et al., 2005; De Falco et al., 2007; Melillo et al., 2005; Borrello et al., 2005).

Other studies support the concept that thyroid cancer epithelial cells can produce inflammatory factors, and that these inflammatory factors can sustain the resistance of thyroid cancer cells to various apoptotic stimuli. Stassi and colleagues looked for cytokines involved in the resistance of thyroid cancer cells to chemotherapeutic agents and identified IL4 and IL10. These cytokines are typically secreted by T CD4+ cells polarized toward a T_H2 phenotype. T_H2 cytokines induce humoral immunity and promote thyreocyte survival in AITD by up-regulating levels of anti-apoptotic proteins such as Bcl2 and Bcl-XL (Stassi et al., 2003). Moreover, the authors demonstrated that IL4 and IL10 also induce resistance of thyroid cancer cells to FAS/FASL-mediated apoptosis. This effect is mediated by IL4 and IL10-induction of two anti-apoptotic proteins, namely cFLIP and PED/PEA15 (Todaro et al., 2006).

6. Conclusions

The relationship between inflammation and thyroid cancer is complex and still not completely understood. Like other cancer types, thyroid cancer is influenced by and modulates inflammation. Epidemiological and histological data indicate that thyroid cancer frequently occurs in the context of one of the most common AITDs, Hashimoto's thyroiditis, and that thyroid cancer is frequently infiltrated by inflammatory-immune cells.

The role of these cells is complex, and several studies indicate that, depending on the specific cell population, the effect can be either pro- or anti-tumorigenic. Specifically, the presence of lymphocytes, which belong to the adaptive branch of immunity, is significantly higher in neoplastic than in non-neoplastic lesions. However, lymphocytic infiltration seems to confer protection against cancer progression. On the other hand, the presence of cells belonging to innate immunity, such as macrophages and mast cells, enhances tumor progression and is associated with an unfavorable prognosis. By activating the MAPK cascade, the oncogenes activated in thyroid carcinomas (i.e., RET/PTC, RAS and BRAF) can activate a cell-autonomous proinflammatory transcriptional program that involves mainly cytokines, chemokines and their receptors (Table 1). These molecules exert two main effects in thyroid cancer. First, by acting in an autocrine fashion, they sustain most of the malignant phenotypic features of thyroid cancer cells namely, proliferation, survival and invasiveness. Second, by acting in a paracrine and, possibly, in an endocrine manner, they induce remodeling of the tumoral stroma by recruiting inflammatory, immune, endothelial and bone marrow-derived cells. In this way, cytokines can further enhance tumor progression through the release of mediators from infiltrating cells, by stimulating angiogenesis, and by inducing subversion of the anti-tumoral immune response. Based on these observations, we favor the concept that, at least in the full blown phase, thyroid cancer growth and progression are positively influenced by two major inflammatory components, one dependent on the cells that are present in the cancer stroma, the other dependent on activation, in epithelial cancer cells, of specific oncoprotein-mediated signaling. As a consequence, not only oncoproteins, but also inflammatory molecules are promising targets for novel thyroid cancer therapeutical strategies. In support of this, we have shown that the blockade of CXCR4 chemokine receptor inhibits the growth of ATC cell xenografts in immunodeficient mice (De Falco et al., 2007).

References

Alberti, L., Carniti, C., Miranda, C., Roccato, E., Pierotti, M.A., 2003. RET and NTRK1 proto-oncogenes in human diseases. J. Cell Physiol. 195, 168–186.
Balkwill, F., Mantovani, A., 2001. Inflammation and cancer: back to Virchow? Lancet 357, 539–545.
Baron, J.A., Sandler, R.S., 2000. Nonsteroidal anti-inflammatory drugs and cancer prevention. Ann. Rev. Med. 51, 511–523.
Begum, S., Rosenbaum, E., Henrique, R., Cohen, Y., Sidransky, D., Westra, W.H., 2004. BRAF mutations in anaplastic thyroid carcinoma: implications for tumor origin, diagnosis and treatment. Mod. Pathol. 17, 1359–1363.
Belletti, B., Ferraro, P., Arra, C., Baldassarre, G., Bruni, P., Staibano, S., De Rosa, G., Salvatore, G., Fusco, A., Persico, M.G., Viglietto, G., 1999. Modulation of in vivo growth of thyroid tumor-derived cell lines by sense and antisense vascular endothelial growth factor gene. Oncogene 18, 4860–4869.
Bollrath, J., Phesse, T.J., von Burstin, V.A., Putoczki, T., Bennecke, M., Bateman, T., Nebelsiek, T., Lundgren-May, T., Canli, O., Schwitalla, S., Matthews, V., Schmid, R.M., Kirchner, T., Arkan, M.C., Ernst, M., Greten, F.R., 2009. gp130-mediated Stat3 activation in enterocytes regulates cell survival and cell-cycle progression during colitis-associated tumorigenesis. Cancer Cell 15, 91–102.
Borrello, M.G-, Alberti, L., Fischer, A., Degl'innocenti, D., Ferrario, C., Gariboldi, M., Marchesi, F., Allavena, P., Greco, A., Collini, P., Pilotti, S., Cassinelli, G., Bressan, P., Fugazzola, L., Mantovani, A., Pierotti, M.A., 2005. Induction of a proinflammatory program in normal human thyrocytes by the RET/PTC1 oncogene. Proc. Natl. Acad. Sci. U.S.A. 102, 14825–14830.
Castellone, M.D., Cirafici, A.M., De Vita, G., De Falco, V., Malorni, L., Tallini, G., Fagin, J.A., Fusco, A., Melillo, R.M., Santoro, M., 2003. Ras-mediated apoptosis of PC CL 3 rat thyroid cells induced by RET/PTC oncogenes. Oncogene 22, 246–255.
Castellone, M.D., Celetti, A., Guarino, V., Cirafici, A.M., Basolo, F., Giannini, R., Medico, E., Kruhoffer, M., Orntoft, T.F., Curcio, F., Fusco, A., Melillo, R.M., Santoro, M., 2004a. Autocrine stimulation by osteopontin plays a pivotal role in the expression of the mitogenic and invasive phenotype of RET/PTC-transformed thyroid cells. Oncogene 23, 2188–2196.

Please cite this article in press as: Guarino, V., et al., Thyroid cancer and inflammation. Mol. Cell. Endocrinol. (2009), doi:10.1016/j.mce.2009.10.003

Castellone, M.D., Guarino, V., De Falco, V., Carlomagno, F., Basolo, F., Faviana, P., Kruhoffer, M., Orntoft, T., Russell, J.P., Rothstein, J.L., Fusco, A., Santoro, M., Melillo, R.M., 2004b. Functional expression of the CXCR4 chemokine receptor is induced by RET/PTC oncogenes and is a common event in human papillary thyroid carcinomas. Oncogene 23, 5958–5967.

Cohen, Y., Xing, M., Mambo, E., Guo, Z., Wu, G., Trink, B., Beller, U., Westra, W.H., Ladenson, P.W., Sidransky, D., 2003. BRAF mutation in papillary thyroid carcinoma. J. Natl. Cancer Inst. 95, 625–627.

Colotta, F., Allavena, P., Sica, A., Garlanda, C., Mantovani, A., 2009. Cancer-related inflammation, the seventh hallmark of cancer: links to genetic instability. Carcinogenesis 30, 1073–1081.

Coussens, L.M., Werb, Z., 2002. Inflammation and cancer. Nature 420, 860–867.

Daniel, D., Meyer-Morse, N., Bergsland, E.K., Dehne, K., Coussens, L.M., Hanahan, D., 2003. Immune enhancement of skin carcinogenesis by CD4+ T cells. J. Exp. Med. 197, 1017–1028.

De Falco, V., Guarino, V., Avilla, E., Castellone, M.D., Salerno, P., Salvatore, G., Faviana, P., Basolo, F., Santoro, M., Melillo, R.M., 2007. Biological role and potential therapeutic targeting of the chemokine receptor CXCR4 in undifferentiated thyroid cancer. Cancer Res. 67, 11821–11829.

De Visser, K.E., Eichten, A., Coussens, L.M., 2006. Paradoxical roles of the immune system during cancer development. Nat. Rev. Cancer 6, 24–37.

Di Pasquale, M., Rothstein, J.L., Palazzo, J.P., 2001. Pathologic features of Hashimoto's-associated papillary thyroid carcinoma. Hum. Pathol. 32, 24–30.

Donghi, R., Longoni, A., Pilotti, S., Michieli, P., Della Porta, G., Pierotti, M.A., 1993. Gene p53 mutations are restricted to poorly differentiated and undifferentiated carcinomas of the thyroid gland. J. Clin. Invest. 91, 1753–1760.

Eisenberg, B.L., Hensley, S.D., 1989. Thyroid cancer with coexistent Hashimoto's thyroiditis. Clinical assessment and management. Arch. Surg. 124, 1045–1047.

Elisei, R., Romei, C., Vorontsova, T., Cosci, B., Veremeychik, V., Kuchinskaya, E., Basolo, F., Demidchik, E.P., Miccoli, P., Pinchera, A., Pacini, F., 2001. RET/PTC rearrangements in thyroid nodules: studies in irradiated and not irradiated, malignant and benign thyroid lesions in children and adults. J. Clin. Endocrinol. Metab. 86, 3211–3216.

Evan, G.I., d'Adda di Fagagna, F., 2009. Cellular senescence: hot or what? Curr. Opin. Genet. Dev. 1, 25–31.

Fagin, J.A., Matsuo, K., Karmakar, A., Chen, D.L., Tang, S.H., Koeffler, H.P., 1993. High prevalence of mutations of the p53 gene in poorly differentiated human thyroid carcinomas. J. Clin. Invest. 91, 179–184.

Fujimoto, H., Sangai, T., Ishii, G., Ikehara, A., Nagashima, T., Miyazaki, M., Ochiai, A., 2009. Stromal MCP-1 in mammary tumors induces tumor-associated macrophage infiltration and contributes to tumor progression. Int. J. Cancer 125, 1276–1284.

Fusco, A., Chiappetta, G., Hui, P., Garcia-Rostan, G., Golden, L., Kinder, B.K., Dillon, D.A., Giuliano, A., Cirafici, A.M., Santoro, M., Rosai, J., Tallini, G., 2002. Assessment of RET/PTC oncogene activation and clonality in thyroid nodules with incomplete morphological evidence of papillary carcinoma: a search for the early precursors of papillary cancer. Am. J. Pathol. 160, 2157–2167.

Gabrilovich, D.I., Nagaraj, S., 2009. Myeloid-derived suppressor cells as regulators of the immune system. Nat. Rev. Immunol. 9, 162–174.

Garcia-Rostan, G., Zhao, H., Camp, R.L., Pollan, M., Herrero, A., Pardo, J., Wu, R., Carcangiu, M.L., Costa, J., Tallini, G., 2003. *ras* Mutations Are Associated With Aggressive Tumor Phenotypes and Poor Prognosis in Thyroid Cancer. J. Clin. Oncol 21, 3226–3235.

Gianfagna, F., De Feo, E., van Duijn, C.M., Ricciardi, G., Boccia, S., 2008. A systematic review of meta-analyses on gene polymorphisms and gastric cancer risk. Curr. Genomics 9, 361–374.

Greten, F.R., Eckmann, L., Greten, T.F., Park, J.M., Li, Z.W., Egan, L.J., Kagnoff, M.F., Karin, M., 2004. IKKbeta links inflammation and tumorigenesis in a mouse model of colitis-associated cancer. Cell 118, 285–296.

Grivennikov, S., Karin, E., Terzic, J., Mucida, D., Yu, G.Y., Vallabhapurapu, S., Scheller, J., Rose-John, S., Cheroutre, H., Eckmann, L., Karin, M., 2009. IL-6 and Stat3 are required for survival of intestinal epithelial cells and development of colitis-associated cancer. Cancer Cell 15, 103–113.

Guarino, V., Faviana, P., Salvatore, G., Castellone, M.D., Cirafici, A.M., De Falco, V., Celetti, A., Giannini, R., Basolo, F., Melillo, R.M., Santoro, M., 2005. Osteopontin is overexpressed in human papillary thyroid carcinomas and enhances thyroid carcinoma cell invasiveness. J. Clin. Endocrinol. Metab. 90, 5270–5278.

Halazonetis, T.D., Gorgoulis, V.G., Bartek, J., 2008. An oncogene-induced DNA damage model for cancer development. Science 319, 1352–1355.

Hansford, J.R., Mulligan, L.M., 2000. Multiple endocrine neoplasia type 2 and RET: from neoplasia to neurogenesis. J. Med. Genet. 37, 817–827.

Houghton, J., Stoicov, C., Nomura, S., Rogers, A.B., Carlson, J., Li, H., Cai, X., Fox, J.G., Goldenring, J.R., Wang, T.C., 2004. Gastric cancer originating from bone marrow-derived cells. Science 306, 1568–1571.

Iwahashi, N., Murakami, H., Nimura, Y., Takahashi, M., 2002. Activation of RET tyrosine kinase regulates interleukin-8 production by multiple signaling pathways. Biochem. Biophys. Res. Commun. 294, 642–649.

Jo, Y.S., Li, S., Song, J.H., Kwon, K.H., Lee, J.C., Rha, S.Y., Lee, H.J., Sul, J.Y., Kweon, G.R., Ro, H.K., Kim, J.M., Shong, M., 2006. Influence of the BRAF V600E mutation on expression of vascular endothelial growth factor in papillary thyroid cancer. J. Clin. Endocrinol. Metab. 91, 3667–3670.

Kebebew, E., Treseler, P.A., Ituarte, P.H., Clark, O.H., 2001. Coexisting chronic lymphocytic thyroiditis and papillary thyroid cancer revisited. World J. Surg. 25, 632–637.

Kimura, E.T., Nikiforova, M.N., Zhu, Z., Knauf, J.A., Nikiforov, Y.E., Fagin, J.A., 2003. High prevalence of BRAF mutations in thyroid cancer: genetic evidence for constitutive activation of the RET/PTC–RAS–BRAF signaling pathway in papillary thyroid carcinoma. Cancer Res. 63, 1454–1457.

Kondo, T., Ezzat, S., Asa, S.L., 2006. Pathogenetic mechanisms in thyroid follicular-cell neoplasia. Nat. Rev. Cancer 6, 292–306.

Kroll, T.G., Sarraf, P., Pecciarini, L., Chen, C.J., Mueller, E., Spiegelman, B.M., Fletcher, J.A., 2000. PAX8-PPARgamma1 fusion oncogene in human thyroid carcinoma. Science 289, 1357–1360.

Leboulleux, S., Baudin, E., Travagli, J.P., Schlumberger, M., 2004. Medullary thyroid carcinoma. Clin. Endocrinol. (Oxf.) 61, 299–310.

Li, H.C., Stoicov, C., Rogers, A.B., Houghton, J., 2006. Stem cells and cancer: evidence for bone marrow stem cells in epithelial cancers. World J. Gastroenterol. 12, 363–371.

Lin, E.Y., Nguyen, A.V., Russell, R.G., Pollard, J.W., 2001. Colony-stimulating factor 1 promotes progression of mammary tumors to malignancy. J. Exp. Med. 193, 727–740.

Lowe, S.W., Sherr, C.J., 2003. Tumor suppression by Ink4a-Arf: progress and puzzles. Curr. Opin. Genet. Dev. 13, 77–83.

Maltby, S., Khazaie, K., McNagny, K.M., 2009. Mast cells in tumor growth: angiogenesis, tissue remodelling and immune-modulation. Biochim. Biophys. Acta 1796, 19–26.

Manie, S., Santoro, M., Fusco, A., Billaud, M., 2001. The RET receptor: function in development and dysfunction in congenital malformation. Trends Genet. 17, 580–589.

Marigo, I., Dolcetti, L., Serafini, P., Zanovello, P., Bronte, V., 2008. Tumor-induced tolerance and immune suppression by myeloid derived suppressor cells. Immunol. Rev. 222, 162–179.

Mechler, C., Bounacer, A., Suarez, H., Saint Frison, M., Magois, C., Aillet, G., Gaulier, A., 2001. Papillary thyroid carcinoma: 6 cases from 2 families with associated lymphocytic thyroiditis harbouring RET/PTC rearrangements. Br. J. Cancer 85, 1831–1837.

Melillo, R.M., Castellone, M.D., Guarino, V., De Falco, V., Cirafici, A.M., Salvatore, G., Caiazzo, F., Basolo, F., Giannini, R., Kruhoffer, M., Orntoft, T., Fusco, A., Santoro, M., 2005. The RET/PTC–RAS–BRAF linear signalling cascade mediates the motile and mitogenic phenotype of thyroid cancer cells. J. Clin. Invest. 115, 1068–1081.

Nikiforova, M.N., Caudill, C.M., Biddinger, P., Nikiforov, Y.E., 2002. Prevalence of RET/PTC rearrangements in Hashimoto's thyroiditis and papillary thyroid carcinomas. Int. J. Surg. Pathol. 10, 15–22.

Nikiforova, M.N., Lynch, R.A., Biddinger, P.W., Alexander, E.K., Dorn II, G.W., Tallini, G., Kroll, T.G., Nikiforov, Y.E., 2003. RAS point mutations and PAX8-PPAR gamma rearrangement in thyroid tumors: evidence for distinct molecular pathways in thyroid follicular carcinoma. J. Clin. Endocrinol. Metab. 88, 2318–2326.

Okayasu, I., 1997. The relationship of lymphocytic thyroiditis to the development of thyroid carcinoma. Endocr. Pathol. 8, 225–230.

Ott, R.A., McCall, A.R., Jarosz, H., Armin, A., Lawrence, A.M., Paloyan, E., 1987. The incidence of thyroid carcinoma in Hashimoto's thyroiditis. Am. Surg. 53, 442–445.

Pisanu, A., Piu, S., Cois, A., Uccheddu, A., 2003. Coexisting Hashimoto's thyroiditis with differentiated thyroid cancer and benign thyroid disease: indications for thyroidectomy. Chir. Ital. 55, 365–372.

Powell Jr., D.J., Russell, J., Nibu, K., Li, G., Rhee, E., Liao, M., Goldstein, M., Keane, W.M., Santoro, M., Fusco, A., Rothstein, J.L., 1998. The RET/PTC3 oncogene: metastatic solid-type papillary carcinomas in murine thyroids. Cancer Res. 58, 5523–5528.

Powell Jr, D.J., Eisenlohr, L.C., Rothstein, J.L., 2003. A thyroid tumor-specific antigen formed by the fusion of two self proteins. J. Immunol. 170, 861–869.

Pufnock, J.S., Rothstein, J.L., 2009. Oncoprotein signaling mediates tumor-specific inflammation and enhances tumor progression. J. Immunol. 182, 5498–5506.

Puxeddu, E., Mitsutake, N., Knauf, J.A., Moretti, S., Kim, H.W., Seta, K.A., Brockman, D., Myatt, L., Millhorn, D.E., Fagin, J.A., 2003. Microsomal prostaglandin E2 synthase-1 is induced by conditional expression of RET/PTC in thyroid PCCL3 cells through the activation of the MEK–ERK pathway. J. Biol. Chem. 278, 52131–52138.

Puxeddu, E., Knauf, J.A., Sartor, M.A., Mitsutake, N., Smith, E.P., Medvedovic, M., Tomlinson, C.R., Moretti, S., Fagin, J.A., 2005. RET/PTC-induced gene expression in thyroid PCCL3 cells reveals early activation of genes involved in regulation of the immune response. Endocr. Relat. Cancer 12, 319–334.

Rosai, J., Carcangiu, M.L., DeLellis, R.A., 1992. Atlas of Tumor Pathology—Tumors of the Thyroid Gland. 3rd series. Armed Force Institute of Pathology, Washington.

Rhoden, K.J., Unger, K., Salvatore, G., Yilmaz, Y., Vovk, V., Chiappetta, G., Qumsiyeh, M.B., Rothstein, J.L., Fusco, A., Santoro, M., Zitzelsberger, H., Tallini, G., 2006. RET/papillary thyroid cancer rearrangement in nonneoplastic thyrocytes: follicular cells of Hashimoto's thyroiditis share low-level recombination events with a subset of papillary carcinoma. J. Clin. Endocrinol. Metab. 91, 2414–2423.

Roman, S., Mehta, P., Sosa, J.A., 2009. Medullary thyroid cancer: early detection and novel treatments. Curr. Opin. Oncol. 21, 5–10.

Russell, J.P., Shinohara, S., Melillo, R.M., Castellone, M.D., Santoro, M., Rothstein, J.L., 2003. Tyrosine kinase oncoprotein, RET/PTC3, induces the secretion of myeloid growth and chemotactic factors. Oncogene 22, 4569–4577.

Russell, J.P., Engiles, J.B., Rothstein, J.L., 2004. Proinflammatory mediators and genetic background in oncogene mediated tumor progression. J. Immunol. 172, 4059–4067.

Ryder, M., Ghossein, R.A., Ricarte-Filho, J.C., Knauf, J.A., Fagin, J.A., 2008. Increased density of tumor-associated macrophages is associated with decreased survival in advanced thyroid cancer. Endocr. Relat. Cancer 15, 1069–1074.

Santoro, M., Carlomagno, F., Romano, A., Bottaro, D.P., Dathan, N.A., Grieco, M., Fusco, A., Vecchio, G., Matoskova, B., Kraus, M.H., et al., 1995. RET/PTC activation in human thyroid carcinomas. Science 267, 381–383.

Please cite this article in press as: Guarino, V., et al., Thyroid cancer and inflammation. Mol. Cell. Endocrinol. (2009), doi:10.1016/j.mce.2009.10.003

Santoro, M., Carlomagno, F., Melillo, R.M., Fusco, A., 2004. Dysfunction of the RET receptor in human cancer. Cell. Mol. Life Sci. 61, 2954–2964.
Scarpino, S., Stoppacciaro, A., Ballerini, F., Marchesi, M., Prat, M., Stella, M.C., Sozzani, S., Allavena, P., Mantovani, A., Ruco, L.P., 2000. Papillary carcinoma of the thyroid: hepatocyte growth factor (HGF) stimulates tumor cells to release chemokines active in recruiting dendritic cells. Am. J. Pathol. 156, 831–837.
Sheils, O.M., O'eary, J.J., Uhlmann, V., Lättich, K., Sweeney, E.C., 2000. ret/PTC-1 activation in Hashimoto thyroiditis. Int. J. Surg. Pathol. 8, 185–189.
Sclafani, A.P., Valdes, M., Cho, H., 1993. Hashimoto's thyroiditis and carcinoma of the thyroid: optimal management. Laryngoscope 103, 845–849.
Segal, K., Ben-Bassat, M., Avraham, A., Har-El, G., Sidi, J., 1985. Hashimoto's thyroiditis and carcinoma of the thyroid gland. Int. Surg. 70, 205–209.
Shinohara, S., Rothstein, J.L., 2004. Interleukin 24 is induced by the RET/PTC3 oncoprotein and is an autocrine growth factor for epithelial cells. Oncogene 23, 7571–7579.
Sica, A., Allavena, P., Mantovani, A., 2008. Cancer related inflammation: the macrophage connection. Cancer Lett. 267, 204–215.
Soares, P., Trovisco, V., Rocha, A.S., Lima, J., Castro, P., Preto, A., Maximo, V., Botelho, T., Seruca, R., Sobrinho-Simoes, M., 2003. BRAF mutations and RET/PTC rearrangements are alternative events in the etiopathogenesis of PTC. Oncogene 22, 4578–4580.
Soares, P., Trovisco, V., Rocha, A.S., Feijão, T., Rebocho, A.P., Fonseca, E., Vieira de Castro, I., Cameselle-Teijeiro, J., Cardoso-Oliveira, M., Sobrinho-Simões, M., 2004. BRAF mutations typical of papillary thyroid carcinoma are more frequently detected in undifferentiated than in insular and insular-like poorly differentiated carcinomas. Virchows Arch. 444, 572–576.
Soucek, L., Lawlor, E.R., Soto, D., Shchors, K., Swigart, L.B., Evan, G.I., 2007. Mast cells are required for angiogenesis and macroscopic expansion of Myc-induced pancreatic islet tumors. Nat. Med. 13, 1211–1218.
Stassi, G., Todaro, M., Zerilli, M., Ricci-Vitiani, L., Di Liberto, D., Patti, M., Florena, A., Di Gaudio, F., Di Gesù, G., De Maria, R., 2003. Thyroid cancer resistance to chemotherapeutic drugs via autocrine production of interleukin-4 and interleukin-10. Cancer Res. 63, 6784–6790.
Sumimoto, H., Imabayashi, F., Iwata, T., Kawakami, Y., 2006. The BRAF–MAPK signaling pathway is essential for cancer-immune evasion in human melanoma cells. J. Exp. Med. 203, 1651–1656.
Takahashi, M., 2001. The GDNF/RET signaling pathway and human diseases. Cytokine Growth Factor Rev. 12, 361–373.
Todaro, M., Zerilli, M., Ricci-Vitiani, L., Bini, M., Perez Alea, M., Maria Florena, A., Miceli, L., Condorelli, G., Bonventre, S., Di Gesù, G., De Maria, R., Stassi, G., 2006. Autocrine production of interleukin-4 and interleukin-10 is required for survival and growth of thyroid cancer cells. Cancer Res. 66, 1491–1499.
Tu, S., Bhagat, G., Cui, G., Takaishi, S., Kurt-Jones, E.A., Rickman, B., Betz, K.S., Penz-Oesterreicher, M., Bjorkdahl, O., Fox, J.G., Wang, T.C., 2008. Overexpression of interleukin-1beta induces gastric inflammation and cancer and mobilizes myeloid-derived suppressor cells in mice. Cancer Cell 14, 408–419.
Ugolini, C., Basolo, F., Proietti, A., Vitti, P., Elisei, R., Miccoli, P., Toniolo, A., 2007. Lymphocyte and immature dendritic cell infiltrates in differentiated, poorly differentiated, and undifferentiated thyroid carcinoma. Thyroid 17, 389–393.
Xu, X., Quiros, R.M., Gattuso, P., Ain, K.B., Prinz, R.A., 2003. High prevalence of BRAF gene mutation in papillary thyroid carcinomas and thyroid tumor cell lines. Cancer Res. 63, 4561–4567.
Wang, J., Knauf, J.A., Basu, S., Puxeddu, E., Kuroda, H., Santoro, M., Fusco, A., Fagin, J.A., 2003. Conditional expression of RET/PTC induces a weak oncogenic drive in thyroid PCCL3 cells and inhibits thyrotropin action at multiple levels. Mol. Endocrinol. 17, 1425–1436.
Waugh, D.J., Wilson, C., 2008. The interleukin-8 pathway in cancer. Clin. Cancer Res. 14, 6735–6741.
Weetman, A.P., 2004. Cellular immune responses in autoimmune thyroid disease. Clin. Endocrinol. 61, 405–413.
Williams, C.S., Mann, M., DuBois, R.N., 1999. The role of cyclooxygenases in inflammation, cancer, and development. Oncogene 18, 7908–7916.
Williams, D., 2002. Cancer after nuclear fallout: lessons from the Chernobyl accident. Nat. Rev. Cancer 2, 543–549.
Wirtschafter, A., Schmidt, R., Rosen, D., Kundu, N., Santoro, M., Fusco, A., Multhaupt, H., Atkins, J.P., Rosen, M.R., Keane, W.M., Rothstein, J.L., 1997. Expression of the RET/PTC fusion gene as a marker for papillary carcinoma in Hashimoto's thyroiditis. Laryngoscope 107, 95–100.
Zhu, Z., Gandhi, M., Nikiforova, M.N., Fischer, A.H., Nikiforov, Y.E., 2003. Molecular profile and clinical-pathologic features of the follicular variant of papillary thyroid carcinoma. An unusually high prevalence of ras mutations. Am. J. Clin. Pathol. 120, 71–77.

Please cite this article in press as: Guarino, V., et al., Thyroid cancer and inflammation. Mol. Cell. Endocrinol. (2009), doi:10.1016/j.mce.2009.10.003

Mast cells play a protumorigenic role in human thyroid cancer

Running title: the role of mast cells in thyroid cancer

Rosa Marina Melillo[1,2], Valentina Guarino[1], Elvira Avilla[1], Maria Rosaria Galdiero[3], Federica Liotti[1], Nella Prevete[3], Francesca Wanda Rossi[3], Fulvio Basolo[4], Clara Ugolini[4], Amato de Paulis[3], Massimo Santoro[1] and Gianni Marone[3]

[1] *Dipartimento di Biologia e Patologia Cellulare e Molecolare/Istituto di Endocrinologia ed Oncologia Sperimentale del CNR,* [2] *Facoltà di Scienze Biotecnologiche*[3], *Divisione di Immunologia Clinica ed Allergologia/Centro Interdipartimentale di Ricerca in Scienze Immunologiche di Base e Cliniche (CISI), Università di Napoli "Federico II", Naples, Italy;*

[4] *Dipartimento di Chirurgia, Pisa, Italy.*

Grant Support: the *Associazione Italiana per la Ricerca sul Cancro* (AIRC), the *Istituto Superiore di Oncologia* (ISO), the Project "*Applicazioni Biotecnologiche dalle molecole all'uomo*" (MoMa), the E.C. Contract 03695 (GenRisk-T), the Project "*Sviluppo di nuovi farmaci capaci alterare il microambiente tumorale e ripristinare la risposta immune anti-tumorale*" (ACC), and the Project "*Molecular diagnostic and prognostic markers of thyroid neoplasis*" RF-CAM-353005 of the Health Ministry. VG was a fellow of the *Fondazione Italiana per la Ricerca sul Cancro* (FIRC).

Address correspondence and offprint requests to: Rosa Marina Melillo, DBPCM/IEOS, Via S. Pansini, 5, 80131, Naples, Italy. Phone: 39-0817463603; Fax: 39-0817463603; E-mail: rosmelil@unina.it

Abstract

Mast cells function as effector cells during inflammatory and immune responses. Mast cell infiltrate is increased in several human tumors. We compared the density of tryptase-positive mast cells in 96 papillary thyroid carcinomas (PTCs) versus normal thyroid tissue from 14 healthy individuals. Mast cell density was higher in 95% of PTCs (n=91) than in control tissue. Mast cell infiltrate correlated with capsule invasion (p= 0.0005). Conditioned media from thyroid cancer cells stimulated histamine release and cytokine synthesis in human mast cells and induced mast cell chemoattraction *in vitro*. The latter effect required vascular endothelial growth factor A produced by cancer cells. Conditioned media from two human mast cell lines (LAD2 and HMC-1), and from primary human lung mast cells induced thyroid cancer cell Matrigel invasion, survival and DNA synthesis *in vitro*. The latter effect was mainly mediated by three mast cell-derived mediators: histamine, and chemokines CXCL1/GROα and CXCL10/IP10. Co-injection of LAD2 and HMC-1 cells accelerated the xenograft growth of human thyroid cancer cells (8505-C) in athymic mice. This effect was mediated by increased vascularization and cancer cell proliferation. In conclusion, mast cells promote proliferation, survival and invasive ability of thyroid cancer cells, thereby contributing to thyroid carcinoma growth and invasiveness.

Key words: chemokine, mast cell, thyroid cancer.

Introduction

Inflammation was first linked to cancer in the nineteenth century consequent to observations that tumors often arose at sites of chronic inflammation and that inflammatory cells were present around tumors. Several chronic inflammatory diseases predispose to cancer. Cytokines, secreted by stromal cells can exacerbate the malignant phenotype of cancer cells. These, by producing chemoattractant molecules, recruit inflammatory cells into tumor sites, influencing them in a way that ultimately promotes cancer progression (**Coussens and Werb, 2002; Balkwill, 2004; Mantovani et al., 2008**).

There are four types of thyroid carcinomas: differentiated papillary (PTCs) and follicular carcinomas, poorly differentiated carcinomas and rapidly growing undifferentiated carcinomas. PTC is the most common thyroid malignancy and it is usually associated with a good therapeutic response and prognosis. However, 10% of PTC patients develop recurrences and distant metastases. At somatic level, PTC is associated with four genetic lesions, namely, chromosomal aberrations affecting the RET or TRKA tyrosine kinase receptors and point-mutations in the RAS or BRAF genes (**Kondo et al., 2006**).

Inflammatory infiltrates have been found in human thyroid tumors. An association between PTC and lymphocytic thyroiditis has been reported in various studies starting from the 1950s (**Di Pasquale et al., 2001; Rhoden et al., 2006**). Furthermore, macrophages and immature dendritic cells accumulate in PTCs, both in tumoral stroma and at the invasive front (**Scarpino et al., 2000**).

Mast cells are are bone marrow-derived immune cells widely distributed throughout vascularized tissues, and at interfaces with the external environment (**Marone et al.., 2005; Kaleshnikoff and Galli, 2008**).-Mast cells are present in several tumors where they influence many aspects of tumor biology (**Cousens et al., 1999; Nakayama et al., 2004; Soucek et al, 2007; Huang et al., 2008; Yang et al., 2008)** such as angiogenesis (**Detoraki et al., 2009)** and tumor invasion of the extracellular matrix by releasing cytokines and proteases (**Coussens et al., 1999**).

The role of mast cells in tumor growth is supported by the observation that carcinoma formation and expansion is greatly reduced in mast cell-deficient $Kit^{W\text{-}sh}$ mutant mice (**Cousens et al., 1999; Soucek et al, 2007;)**.

In this study, we investigated the possibility that mast cells and their mediators play a role in human thyroid cancer. We found that human thyroid carcinomas feature a remarkable mast cell infiltrate whose intensity correlates with the invasive phenotype and bilaterality. Using *in vitro* and *in vivo* assays, we show that thyroid cancer cells attract mast cells through the release of VEGF-A. Thyroid cancer cells stimulate histamine release and cytokine synthesis in human mast cells. Mast cell-released mediators enhanced the proliferation, survival and invasive behavior of thyroid cancer cells *in vitro*. Moreover, mast cells promote the growth of thyroid carcinoma xenografts in nude mice. Our data indicate that mast cell-derived chemokines and histamine are the major mediators of the growth-inducing effect of mast cells on thyroid cancer cells.

Materials / subjects and Methods

Tissue samples and immunohistochemistry

Retrospectively-collected archival thyroid tissue samples from 96 patients affected by papillary thyroid carcinomas (PTC) were retrieved from the files of the Pathology Department of the University of Pisa upon informed consent. Normal thyroid tissue samples, derived from enlarged neck dissection for tracheal or laryngeal carcinomas, were also retrieved from the files of the same Department. We used an anti-human tryptase antibody (DAKO, Glostrup, Denmark) for mast cell staining. Tryptase expression was counted in 10 high power fields and scored as follows: 0= absence of positive cells; + = 1-20 cells; ++ = 21-50 cells; +++ = > 50 cells. Anti-ki-67 (Santa Cruz Biotechnology, Inc., Santa Cruz, CA, USA) and anti-CD34 (Novocastra Lab., Ltd Newcastle, UK) antibodies were used to evaluate cell proliferation and vessel density in xenografts.

Cell lines

Human primary cultures of normal thyroid cells were obtained and maintained according to F. Curcio (**Curcio et al., 1994**). Human thyroid cancer cell lines TPC1, 8505-C and NIM have been described and were maintained as previously described (**Visconti et al., 1997; Salvatore et al., 2006**). HMC-1 and LAD2 mast cell lines were generous gifts of J.H. Butterfield and A.S. Kirshenbaum, respectively. These cells were grown as previously described (**Butterfield et al., 1998; Kirshenbaum et al., 2003**). Jurkat cells were obtained from ATCC and cultured as described (**Schneider et al., 1977**).

RNA extraction and reverse transcription polymerase chain reaction

Total RNA was isolated by the RNeasy Kit (Qiagen, Crawley, West Sussex, UK) and subjected to on-column DNase digestion with the RNase-free DNase set (Qiagen). Primers were designed with a software available at http://www-genome.wi.mit.edu/cgi-bin/primer/primer3_www.cgi and synthesized by MWG Biotech (Ebersberg, Germany). Quantitative (real-time) reverse transcription

polymerase chain reactions (qRT-PCR) were performed as previously described (**Melillo et al., 2005**). Quantitative RT-PCR for CXCL1 and CXCL10 was performed by using the pre-developed TaqMan assay reagent kit ("Assay on demand" from Applied Biosystems).

ELISA assay

Mast cells (70% confluent) were serum-deprived for 12 h and then treated with thyroid carcinoma cell conditioned medium (CM). Cells were incubated for further 12 h in serum-free media. CXCL1 levels in culture supernatants were measured using a quantitative immunoassay ELISA kit (QuantiKine colorimetric sandwich assay, ELISA, R&D Systems Europe, Ltd, Abingdon, UK). Triplicate samples were analyzed at 490 nM with an ELISA reader and results were normalized for protein content (Model 550 microplate reader, Bio-Rad).

Cell motility

In vitro cell chemotaxis and invasiveness through Matrigel was assayed using transwell cell culture chambers as described elsewhere (**Castellone et al., 2004)**. Briefly, $1X10^5$ cells were added to the upper chamber of a pre-hydrated polycarbonate membrane filter of 8 μM pore size (Costar, Cambridge, MA) coated with fibronectin (Millipore Corporate, Billerica, MA) or Matrigel (Collaborative Research Inc., Bedford, MA). The lower chamber was filled with thyroid carcinoma or mast cell CM. When required, thyroid carcinoma cell CM was pretreated with VEGF-A blocking antibodies (1 μg/ml, Santa Cruz Clone C-1; Clone 147; Clone A-20). Plates were incubated at 37°C in a humidified incubator in 5% CO_2 and 95% air for 24 h. Non-migrating cells on the upper side of the filter were wiped off and migrating cells on the reverse side of the filter were stained with 0.1% crystal violet in 20% methanol for 15 min. The stained cells were lysed in 10% acetic acid. Triplicate samples were analyzed at 570 nM with an ELISA reader (Model 550 microplate reader, Bio-Rad). The percentage of migrated cells was calculated with respect to total cell number.

S-phase entry

S-phase entry was evaluated by BrdU incorporation and indirect immunofluorescence (5-bromo-2'-deoxy-uridine Labeling and Detection Kit I, Roche Diagnostics, Indianapolis, IN). Cells were grown on coverslips, and serum deprived for 12 h. When indicated, thyroid carcinoma cells were treated with mast cell CM, PBL CM, Jurkat CM, CXCL1, CXCL10 (PeproTech, Inc. Rocky Hill, NJ) or histamine (Sigma-Aldrich, St Louis, MO for 48 h. For immunodepletion experiments, HMC-1 CM was treated with 1 μg/ml CXCL1 (Clone 20326, R&D) or CXCL10 blocking antibodies (Clone 33036, R&D Systems, Minneapolis, MN). BrdU-positive cells were revealed with FITC-conjugated secondary antibodies (Jackson Immuno Research Laboratories, Inc., Philadelphia, PA). Cell nuclei were identified by Hoechst 33258 staining (final concentration, 1ug/ml; Sigma-Aldrich). Fluorescence was visualized with a Zeiss 140 epifluorescent microscope.

TUNEL assay

For terminal desoxynucleotidyl transferase-mediated desoxyuridine triphosphate nick end-labeling (TUNEL), an equal number (5×10^3) of thyroid carcinoma cells was seeded onto single-well Costar glass slides. Cells were serum-deprived for 48 h or treated with HMC-1 or LAD2 CM, fixed in 4% (w/v) paraformaldehyde and permeabilized by the addition of 0.1% Triton X-100/0.1% sodium citrate. Slides were subjected to the TUNEL reaction (Roche). All coverslips were counterstained in PBS containing Hoechst 33258. The fluorescent signal was visualized with an epifluorescent microscope (Axiovert 2, Zeiss) (equipped with a 100X objective) interfaced with the image analyzer software KS300 (Zeiss).

Xenografts in nude mice

Three groups of 10 mice (4-week-old male BALB/c nu/nu mice, Jackson Laboratories, Bar Harbor, ME) were inoculated subcutaneously into the right dorsal portion with 8505-C cells (10×10^6/mouse), HMC-1 (1×10^6/mouse), or a mixture of both. Tumor diameters were measured

at regular intervals with a caliper. Tumor volumes (V) were calculated with the formula: V= A x $B^2/2$ (A=axial diameter; B= rotational diameter). Mice were housed in barrier facilities that provided 12-h light-dark cycles and received food and water ad libitum. This study was conducted in accordance with Italian regulations for experimentation on animals. All manipulations were performed while mice were under isoflurane gas anesthesia. No mouse showed signs of wasting or other signs of toxicity.

Isolation and purification of human lung mast cells

Macroscopically normal lung parenchyma was dissected free from pleura, bronchi, and blood vessels and minced into a single-cell suspension (**de Paulis et al., 2006**). Lung mast cells were purified by countercurrent elutriation (J2/21; Beckman) and by discontinuous Percoll density gradient and further purified by using an antibody anti-CD117 conjugated to magnetic beads (MACS system; Miltenyi Biotec, Bergisch Gladbach, Germany). The final preparations contained > 95% viable cells, assessed by the Trypan blue exclusion method, and purity was > 98% mast cells.

Histamine release

LAD2 cells were grown in complete medium, and serum-deprived for 1 h in DMEM without phenol red. LAD2 cells ($1x10^4$ mast cell/tube) were suspended in DMEM, placed in 12x75 mm polyethylene tubes and warmed at 37^0 C; each prewarmed releasing stimulus (TPC1 CM, 8505-C CM, or the Ca^{++} ionophore A23187, 1µg/ml) was added, and incubation was continued at 37^0 C for 1 h. The reactions were stopped by centrifugation (1000 x *g*, 22^0 C, 2 min), and the cell free supernatants were assayed for histamine content by an histamine ELISA kit (IBL Hamburg, Germany).

Purification of peripheral blood leukocytes

Human peripheral blood leukocytes (PBL) were purified from human healthy donors. Heparinized blood was centrifuged (300 × *g* for 30 min) in a gradient of ficoll-hypaque with a density of 1114. Peripheral blood leukocytes were suspended in RPMI 1640 plus 10% FCS and gentamycin (100 μg/ml), and were washed three times in PBS. Cell viability (higher than 98%) was measured in all the samples by using the Trypan blue exclusion test. Lymphocytes were identified as 91–95% of the PBLs obtained.

Statistical Analysis

To compare 8505-C versus 8505-C /HMC1 xenograft growth nude mice, we used the unpaired Student's *t* test (normal distributions and equal variances). The clinico-pathological data and their correlation with mast cell infiltrate density were statistically evaluated with a two-tailed Student's t test; the chi^2 test was used to establish the statistical significance of the distributions. Statistical analysis was done with the GraphPad Instat software, v.3.0b. Differences were statistically significant at $P < .05$.

Results

Mast cell density is increased in human thyroid cancer and correlates with capsule invasion.

Samples from normal and pathological thyroid tissues were evaluated by immunohistochemistry for mast cell infiltrate. We evaluated the density of tryptase-positive cells in PTCs (n=96) and in thyroid tissues from healthy individuals (n=14) whose average age and gender were comparable to PTC samples (**Table 1**). Mast cells were counted in each sample and cases were classified depending on mast cell number, as indicated in the Methods section. Mast cell infiltrate was present both within the tumors and at the invasive front but was virtually absent from normal tissues (**Fig. 1A**): of the 14 healthy thyroid samples, 13 were negative for mast cells, and the remaining one was weakly (+) positive for tryptase. Instead, mast cell density was increased, to various degrees, in 95% of PTCs (n=91) (**Fig. 1A**). Thus, the presence of mast cell infiltrate distinguished normal tissues from carcinomas (P=0.0001). A representative example of cell staining with tryptase antibody is shown in **figure 1B**. An isotype-matched non related antibody gave negative results for both normal and pathological samples (not shown).

We then looked for correlations between clinico-pathological features (**Table 1**), angiogenesis and mast cell infiltrate. To this aim, PTCs were divided into two groups, those with intense (+++, ++) tryptase staining, which represented 65% (63/96) of the samples, and those with weak tryptase staining, which represented 35% (33/96) of the samples. The group of PTCs with intense tryptase staining tended to be more invasive, i.e., capsule invasion was more frequent (P = 0.0005, **Table 2**), as was bilateral disease ($P < 0.05$). Tryptase staining did not correlate with gender, age, PTC histological variant, tumor size, lymph node metastasis, multifocality or the degree of angiogenesis (**data not shown**). These results indicate that mast cells are present in PTCs, but not in normal thyroid tissues, and that their presence and intensity positively correlates with capsule invasion and bilateral occurrence.

Recruitment of mast cells by human thyroid carcinoma cells: a role for VEGF-A

To evaluate whether the increased number of mast cells in a tumor site could be due to mast cell recruitment by thyroid carcinoma cells, we performed *in vitro* chemotaxis assays. For these experiments, we used two human mast cells lines, HMC-1 and LAD2, derived, respectively, from a patient with mast cell leukemia and a patient with mastocytosis (**Butterfield et al., 1998; Kirshenbaum et al., 2003**). We tested the ability of conditioned culture media (CM) from the thyroid carcinoma cell lines TPC1, NIM and 8505-C to induce migration of mast cells through a fibronectin matrix. **Figure 2A** shows that CM from each of the three thyroid carcinoma cell lines induced migration of both LAD2 and HMC-1 cells; non-conditioned CM was used as a negative control. CM from normal thyroid primary cultures did not induce mast cell migration (not shown). These data indicate that soluble factors secreted by thyroid cancer cells were responsible for the chemoattractant effect exerted on mast cells.

A likely candidate for the chemoattractant effect is vascular endothelial growth factor-A (VEGF-A), since we and others demonstrated that thyroid carcinoma cells produce VEGF-A (**Viglietto et al., 1995; de la Torre et al., 2006**) and human mast cells and basophils express the VEGF-A receptors VEGFR-1 and -2 (**Detoraki et al., 2009; de Paulis et al., 2006**). As shown in **Fig. 2B**, thyroid carcinoma, but not normal cells produced high levels of VEGF-A. We then blocked the activity of this cytokine in conditioned medium from TPC1 cells with three different neutralizing VEGF-A antibodies and found that mast cell chemotaxis was significantly impaired **(Fig. 2C**). These data indicate that human thyroid cancer cells secrete VEGF-A, and that this cytokine acts as chemoattractant for mast cells.

Human thyroid carcinoma cells induce mast cell activation

Human mast cells release a large array of mediators (**Kaleshnikoff and Galli, 2008)** among which is histamine, rapidly released upon mast cell activation. We stimulated LAD2 cells with thyroid carcinoma cell CM, and evaluated histamine release by ELISA assay. **Figure 3** shows that both TPC1 and 8505-C CM concentration-dependently stimulated histamine release from LAD2,

being TPC-1 CM almost as powerful than the Ca^{++} ionophore A23187. Histamine concentrations in 8505-C CM and TPC1 CM were undetectable (data not shown). Similar results were obtained when HMC-1 or primary mast cells purified from human lung (HLMC) were activated by both TPC1 CM and 8505-C CM (**Supp. Fig. 1 and data not shown**).

We verifyed whether thyroid carcinoma cell CM could induce also a transcriptional response in mast cells. After 24 hours of incubation with thyroid carcinoma cell CM, HMC-1 cell RNAs were extracted and subjected to quantitative RT-PCR. **Figure 4A** shows that treatment of mast cells with thyroid carcinoma cell CM significantly up-regulated the mRNA of cytokines (IL-6, GM-CSF, TNF-α) and of chemokines (CXCL1/Groα and CXCL10/IP10). As shown in **Figure 4B**, CXCL1 was abundantly secreted by HMC-1 and LAD2 cells stimulated with thyroid carcinoma cell CM. These data indicate that thyroid cancer cells produce soluble mediators that activate mast cells.

Mast cell-derived mediators induce proliferation, survival and invasive ability of thyroid carcinoma cells

We measured BrdU incorporation, as an indication of DNA synthesis, after 48 h of treatment of thyroid carcinoma cells (TPC1 and 8505-C) with HMC-1 and LAD2 CM. **Figure 5A** shows that HMC-1 and LAD2 CM increased BrdU incorporation by 2.5 fold in thyroid carcinoma cells compared with the non-conditioned medium. P5 normal thyroid primary cultures were not affected by treatment with HMC-1 and LAD2 CM.

HMC-1 and LAD2 are neoplastic mast cell lines. Therefore, to exclude the possibility that the observed pro-proliferative effect was due to the neoplastic phenotype of the mast cell lines, we did the same experiment with HLMC. In the presence of HLMC CM, there was an increase in BrdU incorporation of TPC1 and 8505-C cells comparable to that induced by HMC-1 and LAD2 (**Fig. 5B**). To ascertain that this effect was specific of mast cells, and not a common feature of human bone marrow-derived cells, we used peripheral blood lymphocytes (PBL) from different donors and the Jurkat cell line, which is derived from a human T-cell leukemia. Conditioned media of PBL and

Jurkat were significantly less efficient in inducing proliferation of TPC1 and did not induce any proliferation of 8505-C cells. Indeed, BrdU incorporation was increased 3 fold in the presence of HLMC CM, and 1.8 fold in the presence of PBL or Jurkat CM (**Fig. 5B)**. We then evaluated whether mast cell CM inhibited apoptosis of thyroid carcinoma cells. To this aim, TPC1 and 8505-C cells were serum-deprived for 48 h, a condition that induces apoptosis. Apoptosis was evaluated with TUNEL assays. **Figure 5C** shows that both HMC-1 and LAD2 CM strongly reduced the levels of serum starvation-induced apoptosis. Thus, soluble factor(s) secreted by mast cells are able to stimulate S-phase entry and inhibit apoptosis of thyroid carcinoma cells.

We evaluated whether mast cells could directly influence the invasive behavior of thyroid carcinoma cells through Matrigel chemoinvasion assays. Thyroid carcinoma cells were seeded on the top chamber of transwells, and their ability to invade a reconstituted extracellular matrix (Matrigel) toward mast cell CM was evaluated. As shown in **Figure 6**, mast cell CM, but not non-conditioned media induced thyroid carcinoma cell migration in Matrigel.

Mast cell-derived mediators involved in thyroid cancer cell proliferation

We next asked whether histamine could mediate mast cell-induced proliferation of thyroid carcinoma cells. We first verified the expression of the four principal histamine receptors (H_1, H_2, H_3, H_4) on thyroid carcinoma and normal thyroid cells using qRT-PCR. H_1 and H_2 receptors were markedly upregulated in four thyroid carcinoma cell lines. Normal thyroid cells were negative for each of the histamine receptors (**Supp. Fig.2 A**). Histamine H_3 and H_4 receptors were not detected in either normal or cancer thyroid cell lines (data not shown). We also confirmed, by western blot, that H_1 and H_2 receptors were expressed in thyroid carcinoma, but not in normal thyroid cells **(Supp Fig. 2B)**. Then, we evaluated the ability of histamine to enhance the S-phase entry rate of thyroid carcinoma cells lines by performing BrdU assays using TPC1 and 8505-C cells. Consistent with the finding that thyroid carcinoma cells express H_1 and H_2 receptors, histamine (10^{-7} to 10^{-4} M) concentration-dependently enhanced S-phase entry in these cells. Moreover, the specific inhibitors

of receptors H_1 (loratadine) and H_2 (cimetidine) blocked this effect (**supp. Fig. 3**). Histamine (10^{-5} M) induced an increase of S-phase entry (**Fig. 7A**).

Because histamine could not account for the total DNA synthesis-stimulating activity of mast cell CM, we hypothesized that other mediators might be involved. We previously demonstrated that two chemokines, CXCL1/GROα and CXCL10/IP10, were important mediators of PTC cell proliferation and invasive ability (**Melillo et al., 2005**). Moreover, in the present study, thyroid carcinoma CM induced up-regulation of the expression and secretion of these chemokines in HMC-1 and LAD2 cells (**Fig. 4**). Consequently, we evaluated whether CXCL1 and CXCL10 could be involved in the proliferative effect caused by mast cell CM, and found that both chemokines induced BrdU incorporation of TPC1 and 8505-C cells with a higher efficiency than histamine (**Fig. 7A**). Moreover, histamine enhanced CXCL1- and CXCXL10-induced proliferation. When all three mediators were added to the medium together, there was a 5-fold increase in BrdU incorporation (**Fig. 7A**). To verify these results, we used CXCL1- and CXL10 neutralizing antibodies to immunodeplete mast cell CM of the two ligands. Chemokine immunodepletion was confirmed by ELISA assay (not shown). The removal of each chemokine from mast cell CM caused the proliferation rate of TPC1 cells to return to basal level. The addition of the recombinant chemokines to the immunodepleted mast cell CM rescued the proliferation effect of the complete medium (**Fig. 7B**). These data suggest that CXCL1 and CXCL10 are the major mediators of the mast cell CM-induced proliferation of thyroid carcinoma cells identified in this study.

Mast cells enhance the xenograft growth of human thyroid cancer cells in athymic nu/nu mice

To verify if mast cells can tumor growth, we performed thyroid carcinoma cell xenografts in nude mice. Mice were randomly divided into three groups of 10 mice each and the cells were injected subcutaneously. The first group was injected with $10x10^6$ 8505-C thyroid carcinoma cells, the second with $1x10^6$ HMC-1 cells, and the third was co-injected with $10x10^6$ 8505-C cells and $1x10^6$ HMC-1 cells. As shown in **Figure 8A**, HMC-1 cells alone did not induce tumor formation. In

contrast, 8505-C cell xenografts formed tumors with high efficiency. These tumors appeared 4 weeks after injection and progressively increased up to 6 weeks. When 8505-C were co-injected with HMC-1 cells, tumors occurred earlier and the final tumor volume was consistently higher than those of 8505-C tumors ($P< 0.001$). Similar results were obtained with LAD2 cells (data not shown).

End-stage tumors excised from the animals at 6 weeks postinoculation were immunostained for tryptase, CD34 and ki67, markers for mast cells, endothelial cells and cycling cells, respectively. Immunostaining for tryptase (**Fig. 8B**) revealed HMC-1 cells in mixed xenografts. Evaluation of at least 10 high magnification microscopic fields, showed that tryptase-positive cells represented 10-20% of all cells. These data indicate that mast cells survive and proliferate in the presence of thyroid carcinoma cells. Immunostaining for ki67 (**Fig. 8B**) showed that mixed xenografts had a higher proliferative index than tumors induced by 8505-C cells alone. In the latter, 38% of cells were ki67+ versus 68% in mixed xenografts (**Fig. 8C**). Thus, the presence of mast cells enhanced the proliferation of 8505-C cells. We also evaluated vessel number and diameter in tumor tissues using the CD34 antibody. This analysis revealed a significant enhancement of vascularization in 8505-C/HMC-1 tumors compared to 8505-C tumors (**Fig. 8B**). Thus, mast cells enhanced tumor formation by increasing 8505-C proliferation. This proliferation might be a consequence of increased vessel density.

Discussion

Mast cells are present in several tumors**,** where they can mediate pro- or anti-tumorigenic activities by modulating tumor angiogenesis and invasiveness (**Theoharides and Conti, 2004; Welsh et al., 2005).** Chronic inflammatory reactions occur in human PTCs and in genetically modified mice models predisposed to develop thyroid carcinomas (**Rhoden et al., 2006; Pufnock and Rothstein, 2009**), and an inflammatory transcriptional response can be induced in normal thyroid epithelial cells upon the ectopic expression of PTC oncogenes. This inflammatory response involves chemokines and cytokines, including VEGF-A (**Borrello et al., 2008).** VEGF-A was identified also in human thyroid cancer samples, where it correlated with tumor aggressiveness (**Klein et al., 2001; Jo et al., 2006**), and it has been linked to activation of BRAF-ERK signaling also in melanomas (**Sumimoto et al., 2006**). Interestingly, VEGF-A induces human mast cell chemotaxis by activating VEGFR1 and VEGFR2 (**Detoraki et al., 2009**). We found that mast cell density is much greater in human thyroid cancer tissue than in normal thyroid tissue. This observation may be due to: 1) recruitment of mast cell precursors or 2) increased proliferation/survival of resident mast cells. We show that thyroid carcinoma cells are a potent chemoattractant for mast cells. This effect required thyroid carcinoma cell-derived VEGF-A because it was inhibited by an anti-VEGF-A antibody. *In vivo* experiments showed that HMC-1 and HMC-1 cells inoculated in immunodeficient mice do not form tumors. Interestingly, when the two cell lines were co-injected, mast cells survived and proliferated, as shown by the immunohistochemical analysis of mixed xenografts. This finding indicates that thyroid cancer cells provide mast cells with a favorable environment that ultimately promotes their survival and growth. Consequently, the greater cell density in human thyroid cancer tissue could be due to both recruitment of mast cell precursors and increased proliferation/survival of resident mast cells.

We also show that thyroid carcinoma cell CM induces mast cell activation (i.e., histamine release and cytokine synthesis). Human mast cells can be activated by immunologic and non-immunologic stimuli through distinct signaling pathways (**Gilfillian and Tzaczyc, 2006**). How

mast cells are activated in our model system is not known, and will be the object of future investigation.

We previously showed that thyroid carcinoma cells express CXCR2 and CXCR3, and their ligands, CXCL1 and CXCL10. These autocrinously produced chemokines sustain PTC cell proliferation and invasion (**Melillo et al., 2005**). In the same study, the addition of exogenous CXCL1 and CXCL10 to PTC cells further enhanced their proliferation and matrigel invasion, which suggests that the CXCR2 and CXCR3 receptors on PTC cells remain available for exogenous ligand binding**.** The results of the present study suggest that the mast cell-derived chemokines CXCL1 and CXCL10 are probably the mediators responsible for the mast cell CM-induced growth-inducing effect on thyroid carcinoma cells. These findings support the hypothesis that mast cell-derived CXCL1 and CXCL10 might be one of the sources of exogenous chemokines at tumor sites.

Here we report that histamine, one of the mast cell preformed mediators, contributes to the growth inducing activity of mast cell CM on thyroid carcinoma cells. Although the role of histamine in cancer growth is still controversial, several studies identified H_1 and/or H_2 receptor expression in cancer cells and showed that histamine functions as a growth factor (**Rivera et al., 2000**). In our system, histamine exerts an autonomous effect on cell growth and potentiates chemokine-induced cell proliferation. This effect appears to be mediated by the H1 and H2 receptors expressed by thyroid carcinoma cells, since specific inhibitors of H_1 and H_2 reverted His-induced BrdU incorporation. Both CXC and histamine receptors are G-protein-linked receptors (**Tan et al., 2006; Raman et al., 2007; Parsons and Ganellin, 2007**). Whether these receptors display typical coupling to signal transducers and how the different signaling pathways associated with these receptors integrate and induce cell proliferation will be the object of further investigation.

Besides arguing for a role of mast cells in thyroid carcinoma growth and invasiveness, our data also raise several questions. First and foremost, are mast cells an absolute requirement for thyroid carcinoma formation or are they only necessary for tumor progression? We plan to conduct

experiments involving pharmacological depletion of mast cells and mice with genetically defective mast cell development to clarify this issue.

Acknowledgements

We would like to dedicate this paper to the memory of Professor Gaetano Salvatore, who continues to inspire our work. We are indebted to A.S. Kirshenbaum and J.H. Butterfield for the LAD2 and HMC-1 cell lines, respectively. We are also grateful to F. Curcio for the P5 primary thyroid culture. We thank Jean Ann Gilder for text editing.

Conflict of interest

None of the authors of the manuscript have conflicts of interest

References

Balkwill F. (2004). Cancer and the chemokine network. *Nat Rev Cancer* **4:** 540-550

Borrello MG, Degl'innocenti D, Pierotti M.A. (2008). Inflammation and cancer: The oncogene-driven connection. *Cancer Lett.* **67**:262-70

Butterfield JH, Weiler D, Dewald G, Gleich GJ. (1988). Establishment of an immature mast cell line from a patient with mast cell leukaemia. *Leuk Res* **12**: 345

Castellone MD, Guarino V, De Falco V, Carlomagno F, Basolo, F, Faviana P et al. (2004). Functional expression of the CXCR4 chemokine receptor is induced by RET/PTC oncogenes and is a common event in human papillary thyroid carcinomas. *Oncogene* **23**: 5958-67.

Coussens LM, Raymond WW, Bergers G, Laig-Webster M, Behrendysen O, Werb Z et al. (1999). Inflammatory mast cells up-regulate angiogenesis during squamous epithelial carcinogenesis. *Genes Dev* **13**: 1382-1397

Coussens LM, Werb Z. (2002). Inflammation and cancer. *Nature* **420**: 860-867

Curcio F, Ambesi-Impiombato FS, Perrella G, Coon HG. (1994). Long-term culture and functional characterization of follicular cells from adult normal human thyroids. *Proc Natl Acad Sci U S A* **91**: 9004-8.

de la Torre NG, Buley I, Wass JA, Turner HE. (2006). Angiogenesis and lymphangiogenesis in thyroid proliferative lesions: relationship to type and tumour behaviour. *Endocr Relat Cancer*. **13**:931-44.

de Paulis , Prevete N, Fiorentino I, Rossi FW, Staibano S, Montuori N et al. (2006). Expression and functions of the vascular endothelial growth factors and their receptors in human basophils. *J Immunol* **177**: 7322-7331

Detoraki A, Staiano RI, Granata F, Giannattasio G, Prevete N, de Paulis A et al. (2009). Vascular endothelial growth factors synthesized by human lung mast cells exert angiogenic and proinflammatory effects. *J Allergy Clin Immunol* **123**: 1142-9

Di Pasquale M, Rothstein JL, Palazzo JP. (2001). Pathologic features of Hashimoto's-associated papillary thyroid carcinoma. *Hum Pathol* **32**: 24-30

Gilfillan AM and Tzaczyk C. (2006). Integrated signalling pathways for mast-cell activation. *Nat Rev Immunol* **6**: 218-30.

Huang B, Lei Z, Zhang GM, Li D, Song C, Li B et al. (2008). SCF-mediated mast cell infiltration and activation exacerbate the inflammation and immunosuppression in tumor microenvironment. *Blood* **112**:1269-79.

Jebreel A, England J, Bedford K, Murphy J, Karsai L, Atkin S. (2007). Vascular endothelial growth factor (VEGF), VEGF receptors expression and microvascular density in benign and malignant thyroid diseases. *Int J Exp Pathol* **88**:271-7.

Jo YS, Li S, Song JH, Kwon KH, Lee JC, Rha SY et al. (2006). Influence of the BRAF V600E mutation on expression of vascular endothelial growth factor in papillary thyroid cancer. *J Clin Endocrinol Metab* **91**: 3667-70.

Kalesnikoff J, Galli SJ. (2008). New developments in mast cell biology. *Nat Immunol* **9**:1215-23.

Kirshenbaum AS, Aki C, Wu Y, Rottem M, Goff JP, Beaven MA et al. (2003). Characterization of novel stem cell factor responsive human mast cell lines LAD1 and 2 established from a patient with mast cell sarcoma/leukaemia; activation following aggregation of FcεRI or FcγRI. *Leuk Res* **27**: 677-82

Klein M, Vignaud JM, Hennequin V, Toussaint B, Bresler L, Plénat et al. (2001). Increased expression of the vascular endothelial growth factor is a pejorative prognosis marker in papillary thyroid carcinoma. *J Clin Endocrinol Metab* **86**: 656-8.

Kondo T, Ezzat S, Asa SL. (2006). Pathogenetic mechanisms in thyroid follicular-cell neoplasia. *Nat Rev Cancer* **6**: 292-306. R

Mantovani A., Allavena P., Sica A., Balkwill F. (2008). Cancer-related inflammation. *Nature* **454**:436-44.

Marone G, Triggiani M, Genovese A, Paulis AD. (2005). Role of human mast cells and basophils in bronchial asthma. *Adv Immunol*. **88**: 97-160.

Melillo RM, Castellone MD, Guarino V, De Falco V, Cirafici AM, Salvatore G et al. (2005). The RET/PTC-RAS-BRAF linear signalling cascade mediates the motile and mitogenic phenotype of thyroid cancer cells. *J Clin Invest* **115**: 1068-1081

Nakayama T, Yao L, Tosato G. (2004). Mast cell-derived angiopoietin-1 plays a critical role in the growth of plasma cell tumors. *J Clin Invest* **114**: 1317-25.

Parsons ME, Ganellin CR. (2006). Histamine and its receptors. *Br J Pharmacol* **147** Suppl 1:

Pufnock JS, Rothstein JL. (2009). Oncoprotein signaling mediates tumor-specific inflammation and enhances tumor progression. *J Immunol* **182**:5498-506.

Raman D, Baugher PJ, Thu YM, Richmond A. (2007). Role of chemokines in tumor growth. *Cancer Lett* **256**: 137-65.

Rhoden KJ, Unger K, Salvatore G, Yilmaz Y, Vovk V, Chiappetta G et al. (2006). RET/papillary thyroid cancer rearrangement in nonneoplastic thyrocytes: follicular cells of Hashimoto's thyroiditis share low-level recombination events with a subset of papillary carcinoma. *J Clin Endocrinol Metab* **91**:2414-23.

Rivera ES, Cricco GP, Engel NI, Fitzsimons CP, Martín GA, Bergoc RM. (2000). Histamine as an autocrine growth factor: an unusual role for a widespread mediator. *Semin Cancer Biol*. **10**: 15-23.

Salvatore G, De Falco V, Salerno P, Nappi TC, Pepe S, Troncone G et al. (2006). BRAF is a therapeutic target in aggressive thyroid carcinoma. *Clin Cancer Res* **12**: 1623-9.

Scarpino S, Stoppacciaro A, Ballerini F, Marchesi M, Prat M, Stella MC et al. (2000). Papillary carcinoma of the thyroid: hepatocyte growth factor (HGF) stimulates tumor cells to release chemokines active in recruiting dendritic cells. *Am J Pathol*. **156**:831-7.

Schneider U, Schwenk HU, Bornkamm G. (1977). Characterization of EBV-genome negative "null" and "T" cell lines derived from children with acute lymphoblastic leukemia and leukemic transformed non-Hodgkin lymphoma. *Int J Cancer* **19**: 621-6.

Soucek L, Lawlor ER, Soto D, Shchors K, Swigart LB, Evan GI. (2007). Mast cells are required for angiogenesis and macroscopic expansion of Myc-induced pancreatic islet tumors. *Nat Med.* **13**:1211-8.

Sumimoto H, Imabayashi F, Iwata T, Kawakami Y. (2006). The BRAF-MAPK signaling pathway is essential for cancer-immune evasion in human melanoma cells. *J Exp Med* **203**:1651-6.

Tan W, Martin D, Gutkind JS. (2006). The Galpha13-Rho signaling axis is required for SDF-1-induced migration through CXCR4. *J Biol Chem* **281**: 39542-9.

Theoharides TC, Conti P. (2004). Mast cells: the Jekyll and Hyde of tumor growth. *Trends Immunol*. **25**: 235-41.

Viglietto G, Maglione D, Rimbaldi M, Cerutti J, Romano A, Trapasso F et al. 1995. Upregulation of vascular endothelial growth factor (VEGF) and downregulation of placental growth factor (PlGF) associated with malignancy in human thyroid tumors and cell lines. *Oncogene* **11**: 1569-1579

Visconti R, Cerutti J, Battista S, Fedele M, Trapasso F, Zeki et al. 1997. Expression of the neoplastic phenotype by human thyroid carcinoma cell lines requires NFkappaB p65 protein expression. *Oncogene* **15**: 1987-94.

Yang FC, Ingram DA, Chen S, Zhu Y, Yuan J, Li X et al. (2008). Nf1-dependent tumors require a microenvironment containing Nf1+/-- and c-kit-dependent bone marrow. *Cell* **135**:437-48.

Welsh TJ, Green RH, Richardson D, Waller DA, O'Byrne KJ, Bradding P. (2005). Macrophage and mast-cell invasion of tumor cell islets confers a marked survival advantage in non-small-cell lung cancer. *J Clin Oncol*. **23**:8959-67.

Figure legends

Figure 1

Immunohistochemical analysis of tryptase in human papillary thyroid carcinoma (PTC).

A. Distribution of tryptase positivity in human normal thyroid tissue (NT) and in PTC. 98% of NT samples scored negative for tryptase-positive cells. 95% of the PTC samples displayed strong immunoreactivity to tryptase. Tryptase expression was scored as follows: 0= absence of positive cells; += 1-20 cells/10 fields 40x; ++= 21-50 cells/10 fields 40x; +++= > 50 cells/10 fields 40x.

B. Normal thyroid tissues (1, 4) were negative for tryptase staining. The degree of tryptase-positive cell staining differed among PTC samples (see samples, 2, 3, 5, 6). No signal was detected after incubation of samples with isotype-matched antibodies (not shown).

Figure 2

Migration of LAD2 and HMC-1 cells in response to thyroid cancer cell line-conditioned media (CM).

A. Mast cells were plated on the top of a transwell chamber pre-coated with fibronectin and incubated with thyroid carcinoma cell CM (TPC1, 8505-C, NIM CM) or non conditioned medium (-). Migrated cells were fixed and stained with crystal violet, and the percentage of migration was evaluated with an ELISA reader, and calculated with respect to total cell number ($1x10^5$). Top, representative micrographs. Bottom, average results of three independent assays

B. VEGF-A expression in human thyroid cell lines was evaluated by ELISA. The TPC1, NIM and 8505-C cell lines released high levels of VEGF-A with respect to the normal primary thyroid P5 cells, as assessed in triplicate determinations (± S.D.)

C. Matrigel invasion of mast cells in response to TPC1 CM was performed in the presence and absence of three distinct anti-VEGF-A blocking antibodies. Each antibody, and the mix of them, inhibited mast cell migration. Top, representative micrographs. Bottom, average results of three independent assays.

Figure 3

Histamine release of human mast cells in response to thyroid carcinoma cell CM.

LAD2 cells were incubated 1 h at 37^0 C with the indicated dilutions of 8505-C CM, TPC1 CM, or with the Ca^{++} ionophore A23187 (1μg/ml). The release of histamine in the supernatants of LAD2 cells was evaluated by ELISA. Both 8505-C CM and TPC1 CM stimulated histamine release of LAD2 cells. Dilutions (> 1: 25) of both thyroid cancer cell CM abrogated this effect. Histamine release was not detected in the presence of non conditioned medium.

Figure 4

Activation of HMC-1 in response to thyroid carcinoma cell CM.

A. Quantitative RT-PCR was used to evaluate the mRNA levels of cytokines and chemokines of HMC-1 cells in response to the indicated thyroid carcinoma cell line CM. Non-conditioned medium (-) was used as a control. Beta- actin mRNA detection was used for normalization. For each target (x-axis), the expression level values are calculated relative to the expression level in unstimulated HMC-1 cells, arbitrarily considered equal to 1. Experiments were performed in triplicate, and the average value of the results ± S.D. was plotted.

B. CXCL1 expression in human mast cell lines was evaluated by ELISA. Both HMC-1 and LAD2 mast cell lines released high levels of CXCL1 in response to the indicated thyroid carcinoma cell line CM , as assessed in triplicate determinations (± S.D.) of CXCL1. Normal thyroid cell (NT) conditioned medium was used as negative control.

Figure 5

Mast cells stimulate proliferation and survival of thyroid carcinoma cell lines.

A. The indicated thyroid carcinoma cell lines were serum-deprived for 12 h and stimulated with mast cell conditioned culture medium (CM) or with non conditioned medium for 48 h. BrdU was added two hours before the reaction was stopped, and cells were processed for immunofluorescence. Mast cell CM stimulated S-phase entry of thyroid carcinoma cell lines, but not of the P5 normal primary thyroid cultures. The results are expressed as BrdU incorporation relative fold change with respect to unstimulated TPC1 cells, which were arbitrarily considered equal to 1. The average results and the standard deviations of three independent experiments in which at least 400 cells were counted are reported.

B. TPC1 and 8505-C cells were serum-deprived and then stimulated with CM from human primary lung mast cells (HLMC), peripheral blood lymphocytes (PBL), and Jurkat T-cell leukemia cell line. Mast cell CM, but not CM from the other cultures, induced BrdU incorporation of thyroid cancer cells. The results are expressed as BrdU incorporation relative fold change with respect to unstimulated cells, which were arbitrarily considered equal to 1. The average results and S.D. of three independent experiments in which at least 400 cells were counted is reported.

C. The indicated thyroid carcinoma cell lines were serum-deprived for 48 h in the presence of mast cell CM or non conditioned medium. The percentage of apoptotic cells was evaluated with the TUNEL reaction. Mast cell CM, but not non conditioned medium, induced survival of TPC1 and 8505-C cells in condition of serum starvation. The results are expressed as apoptosis relative fold change with respect to unstimulated cells, which were arbitrarily considered equal to 1. The average results and S.D. of three independent experiments is reported.

Figure 6

Mast cells stimulate the invasiveness of thyroid carcinoma cells.

The indicated thyroid carcinoma cell lines cells were seeded in the upper chamber of Matrigel-coated 8 μM pore transwells and allowed to migrate for 24 h towards HMC-1 CM or non conditioned medium. Top, a representative assay. Bottom, average results of three independent assays. SD is also shown.

Figure 7

The chemokines CXCL1 and CXCL10 and histamine mediate the proliferative effect of mast cell CM on thyroid carcinoma cell lines.

A. BrdU-incorporation was measured to evaluate S-phase entry of TPC1 and 8505-C cells upon treatment with CXCL1 (60 pg/ml), CXCL10 (60 pg/ml), histamine (10^{-5} M) or the indicated combinations of these factors. As shown, histamine potentiated the effect of each chemokine. BrdU incorporation was highest when the three molecules were added together. The results are expressed as the relative fold change of BrdU incorporation with respect to unstimulated cells, which were arbitrarily considered equal to 1. Average results of three independent experiments ± S.D are shown.

B. Neutralizing antibodies to CXCL1 and CXCL10 were used to deplete mast cell CM from chemokines. Immunodepletion was confirmed by ELISA assay (not shown). Chemokine-immunodepletion abrogated the proliferative effect of mast cell CM on TPC1 cells, whereas mock immunodepletion did not. The add back of excess chemokine to immunodepleted media restored the effect of mast cell CM on TPC1 cells proliferation. The results are expressed as relative fold change of BrdU incorporation with respect to unstimulated TPC1 cells, which were arbitrarily considered equal to 1. The average results of three independent experiments ± S.D is shown.

Figure 8

Enhancement of 8505-C xenografts growth in nude mice in the presence of mast cells

A. Xenograft growth of 8505-C thyroid cancer cells in the presence and in the absence of the HMC-1 mast cell line was monitored by measuring tumor size weekly. The addition of HMC-1 to 8505-C cells caused a marked increase in tumor volume. HMC-1 alone cells did not form tumors.

B. The expression of tryptase, ki67 and CD34 in xenografts was evaluated by immunohistochemistry. Tryptase positivity indicated that mast cells survived in mixed xenografts. Ki67- and CD34-positive cells were more abundant in mixed than in 8505-C xenografts.

C. Ki-67-positive cells were counted in 10 high magnification (40x) microscopic fields. The percentage of Ki67-positive cells was determined in 8505-C and 8505-C/HMC-1 xenografts.

Table 1. Clinico-pathological features of normal and papillary thyroid carcinoma (PTC) patients

Normal patients

FEATURES		**Total (%)**
no. subjects		14 (100)
Gender		
male		4 (29)
female		10 (71)
Age		
<45y		6 (43)
>/=45y		8 (57)

PTC patients

FEATURES		**Total (%)**
no. subjects		96 (100)
Gender		
male		21 (22)
female		75 (78)
Age		
<45y		51 (53)
>/=45y		45 (47)
Histotype		
PTC-CV		44 (46)
PTC-FV		41 (42)
PTC-TCV		10 (11)
PTC-WLV		1 (1)
Capsule invasion		
yes		58 (61)
no		38 (39)
Lymph-node metastasis		
yes		23 (25)
no		73 (75)
Multifocality		
yes		28 (30)
no		68 (70)
Bilateral occurrence		
yes		20 (21)
no		76 (79)

Table 2: Correlations between tryptase score and clinical features of papillary thyroid carcinomas

Tryptase score	Clinical features		*P* value*
	Capsule invasion -	**Capsule invasion +**	
Intense tryptase staining	45% (17/38)	77% (46/58)	**0.0005**
Weak tryptase staining	55% (21/38)	23% (12/58)	

	Bilateral occurrence -	**Bilateral occurrence+**	
Intense tryptase staining	60% (46/76)	85% (17/20)	**0.0403**
Weak tryptase staining	40% (30/76)	15% (3/20)	

* The chi^2 test was used to establish the statistical significance of distributions. Mast cell infiltrate correlated with capsule invasion and bilateral occurrence.

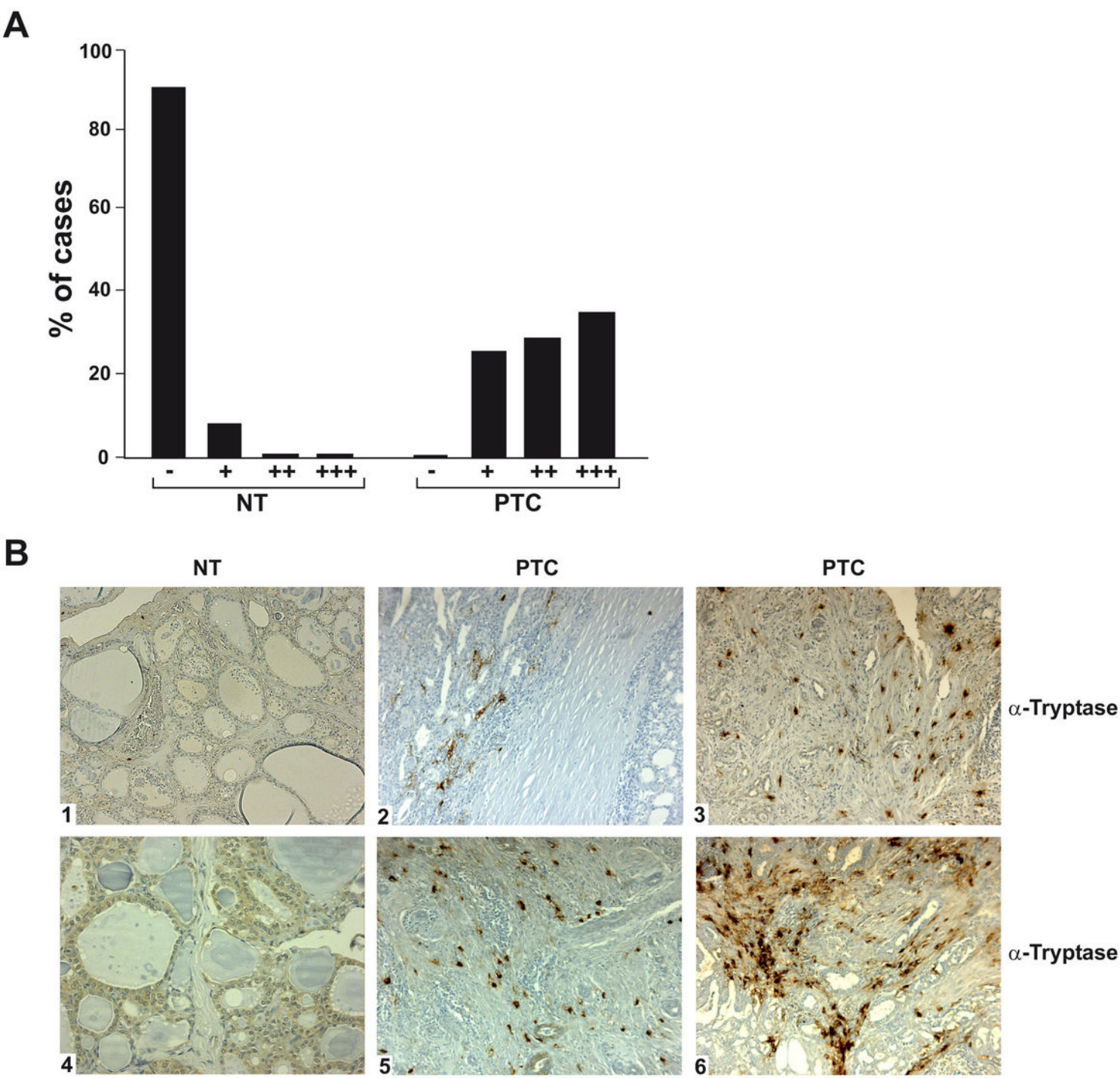
A
100
80
60
40
20
0
% of cases
-
+
++
+++
NT
-
+
++
+++
PTC
B
NT
PTC
PTC
α-Tryptase
α-Tryptase
1
2
3
4
5
6

Figure 1

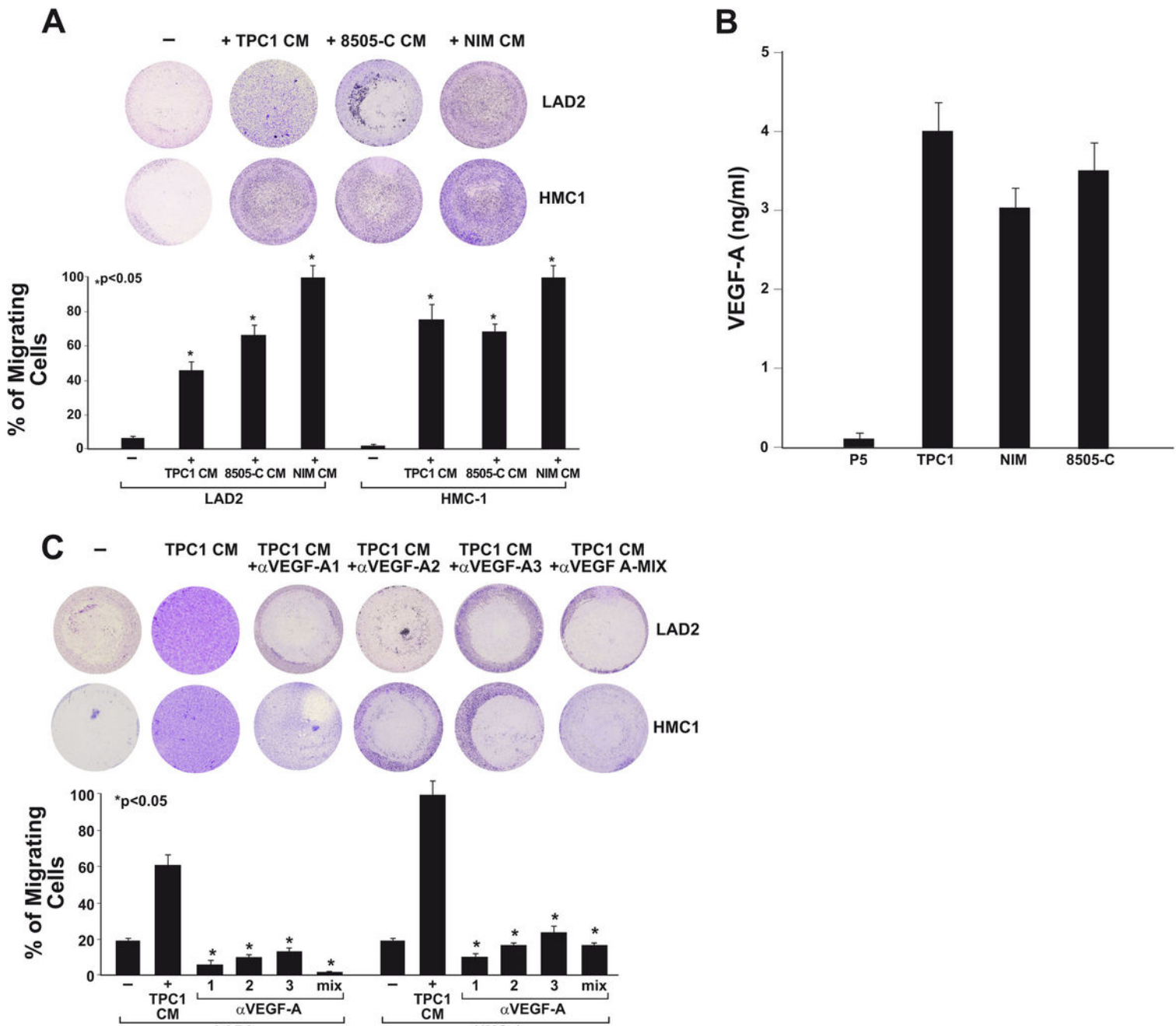
A
–
+ TPC1 CM
+ 8505-C CM
+ NIM CM
LAD2
HMC1
% of Migrating Cells
*p<0.05
100
80
60
40
20
0
– + TPC1 CM + 8505-C CM + NIM CM
LAD2
HMC-1
B
VEGF-A (ng/ml)
5
4
3
2
1
0
P5
TPC1
NIM
8505-C
C
–
TPC1 CM
TPC1 CM +αVEGF-A1
TPC1 CM +αVEGF-A2
TPC1 CM +αVEGF-A3
TPC1 CM +αVEGF A-MIX
LAD2
HMC1
% of Migrating Cells
*p<0.05
100
80
60
40
20
0
– + 1 2 3 mix
TPC1 CM
αVEGF-A
LAD2
HMC-1

Figure 2

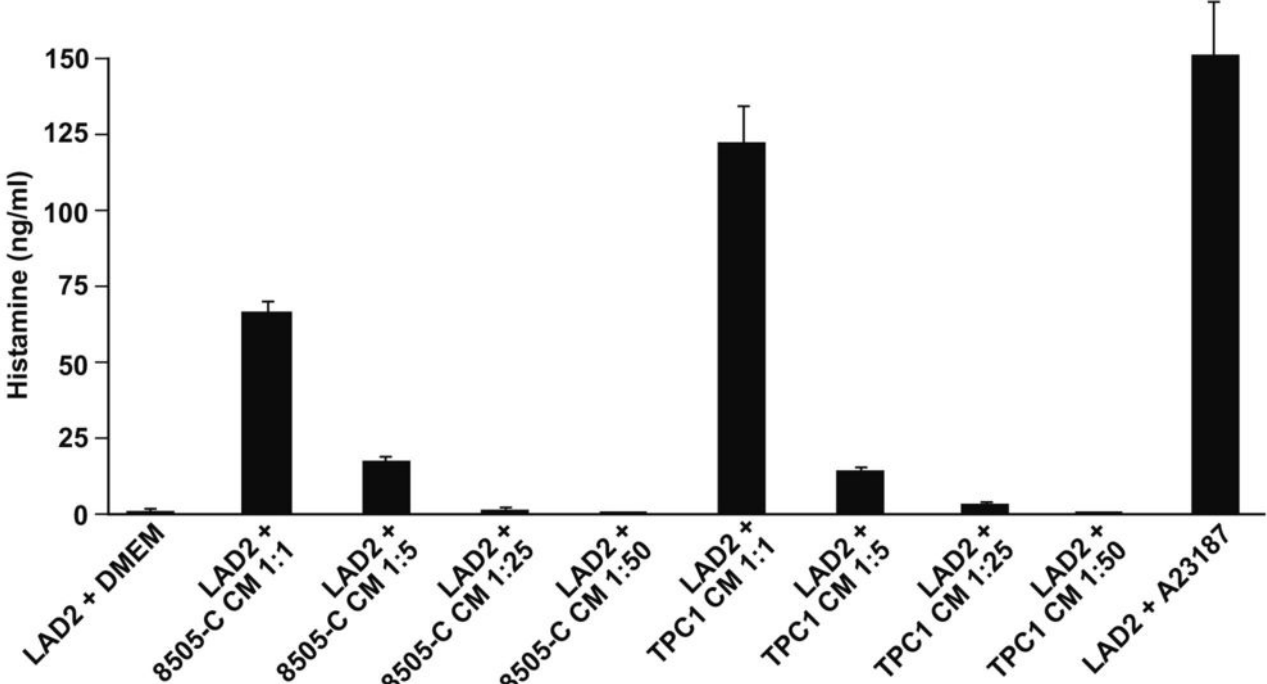
Histamine (ng/ml)
150
125
100
75
50
25
0
LAD2 + DMEM
LAD2 + 8505-C CM 1:1
LAD2 + 8505-C CM 1:5
LAD2 + 8505-C CM 1:25
LAD2 + 8505-C CM 1:50
LAD2 + TPC1 CM 1:1
LAD2 + TPC1 CM 1:5
LAD2 + TPC1 CM 1:25
LAD2 + TPC1 CM 1:50
LAD2 + A23187

Figure 3

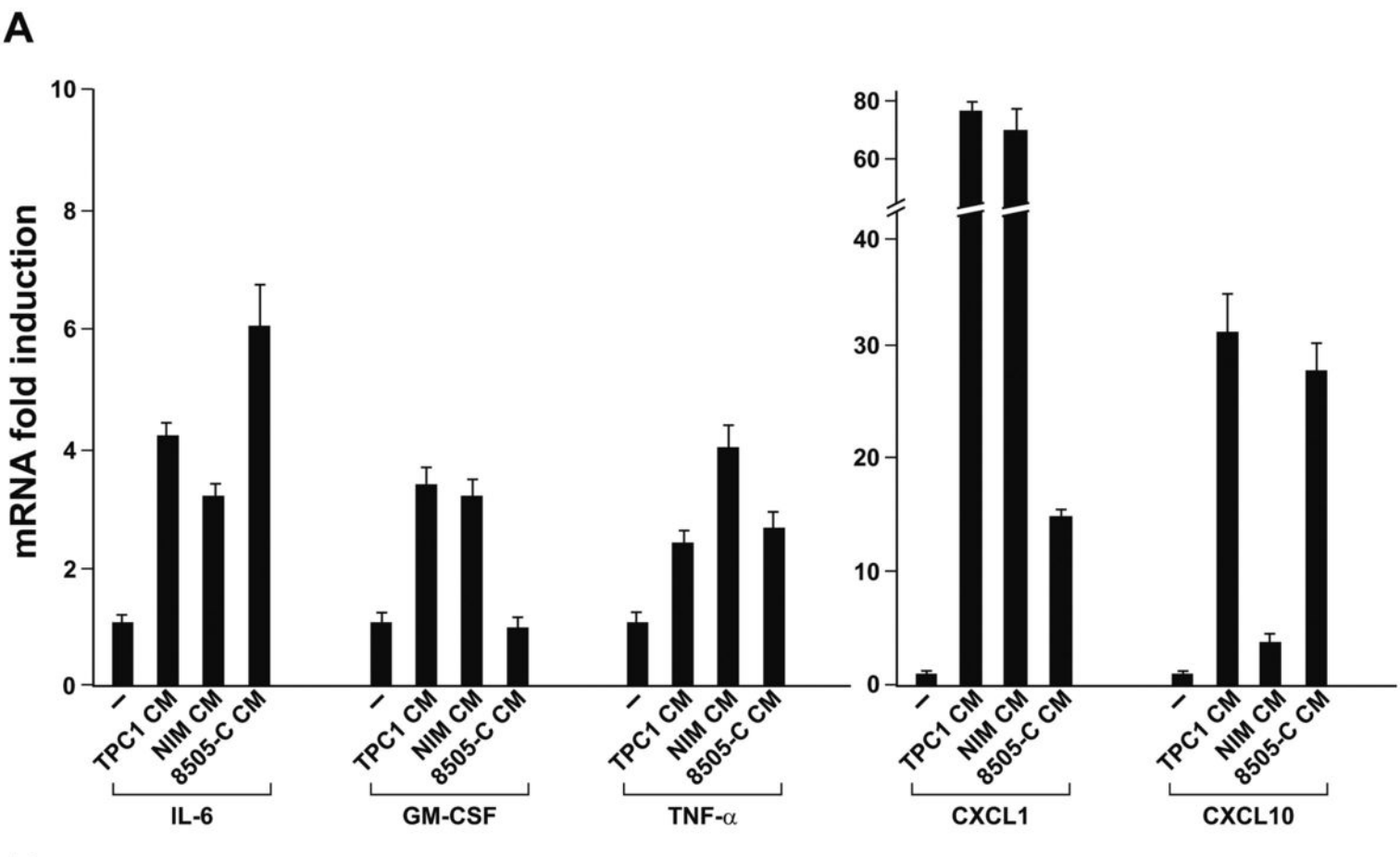
A
mRNA fold induction
10
8
6
4
2
0
80
60
40
30
20
10
0
–
TPC1 CM
NIM CM
8505-C CM
IL-6
GM-CSF
TNF-α
CXCL1
CXCL10

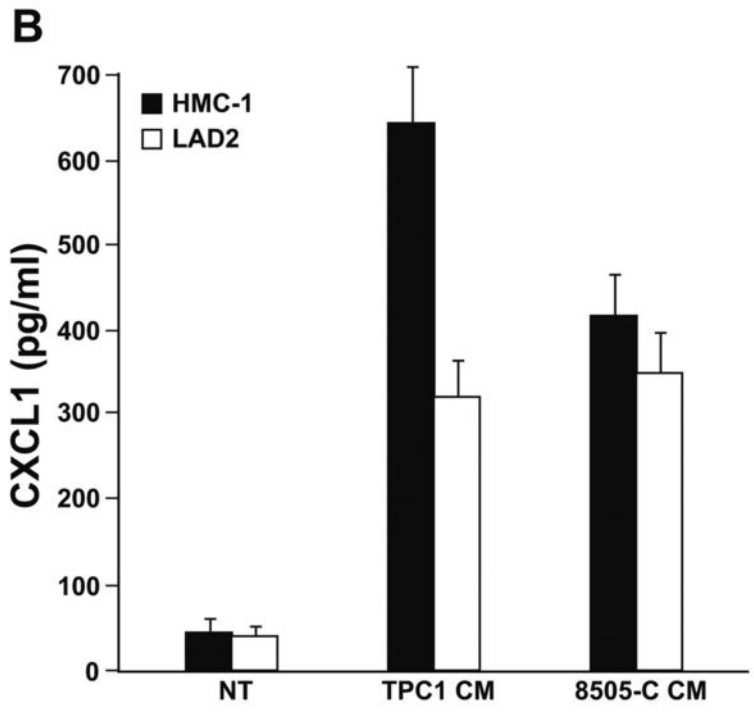
B
CXCL1 (pg/ml)
700
600
500
400
300
200
100
0
HMC-1
LAD2
NT
TPC1 CM
8505-C CM

Figure 4

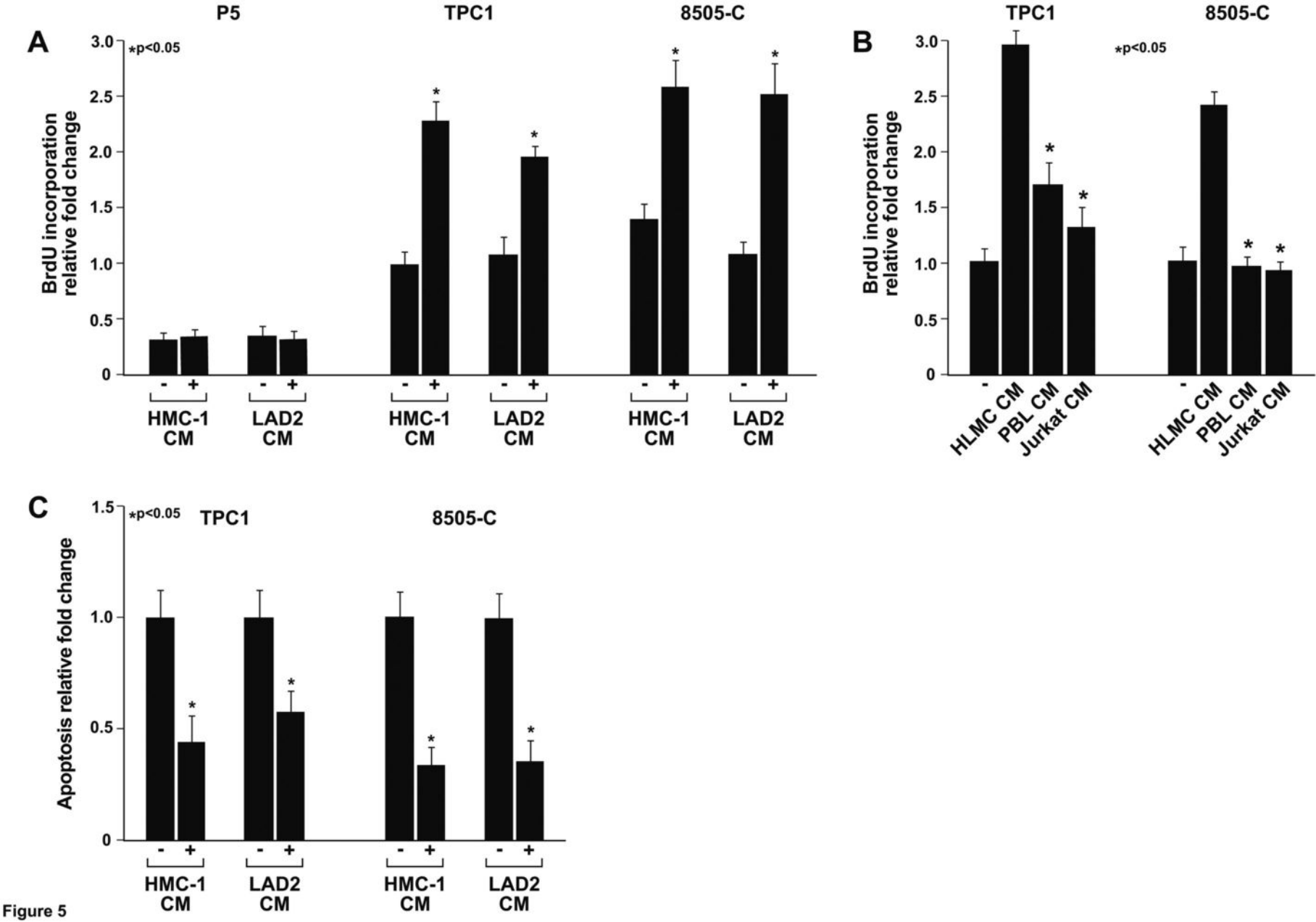
A
P5
TPC1
8505-C
*p<0.05
BrdU incorporation relative fold change
3.0
2.5
2.0
1.5
1.0
0.5
0
- +
HMC-1 CM
LAD2 CM
B
TPC1
8505-C
*p<0.05
BrdU incorporation relative fold change
-
HLMC CM
PBL CM
Jurkat CM
C
*p<0.05
TPC1
8505-C
Apoptosis relative fold change
1.5
1.0
0.5
0
HMC-1 CM
LAD2 CM

Figure 5

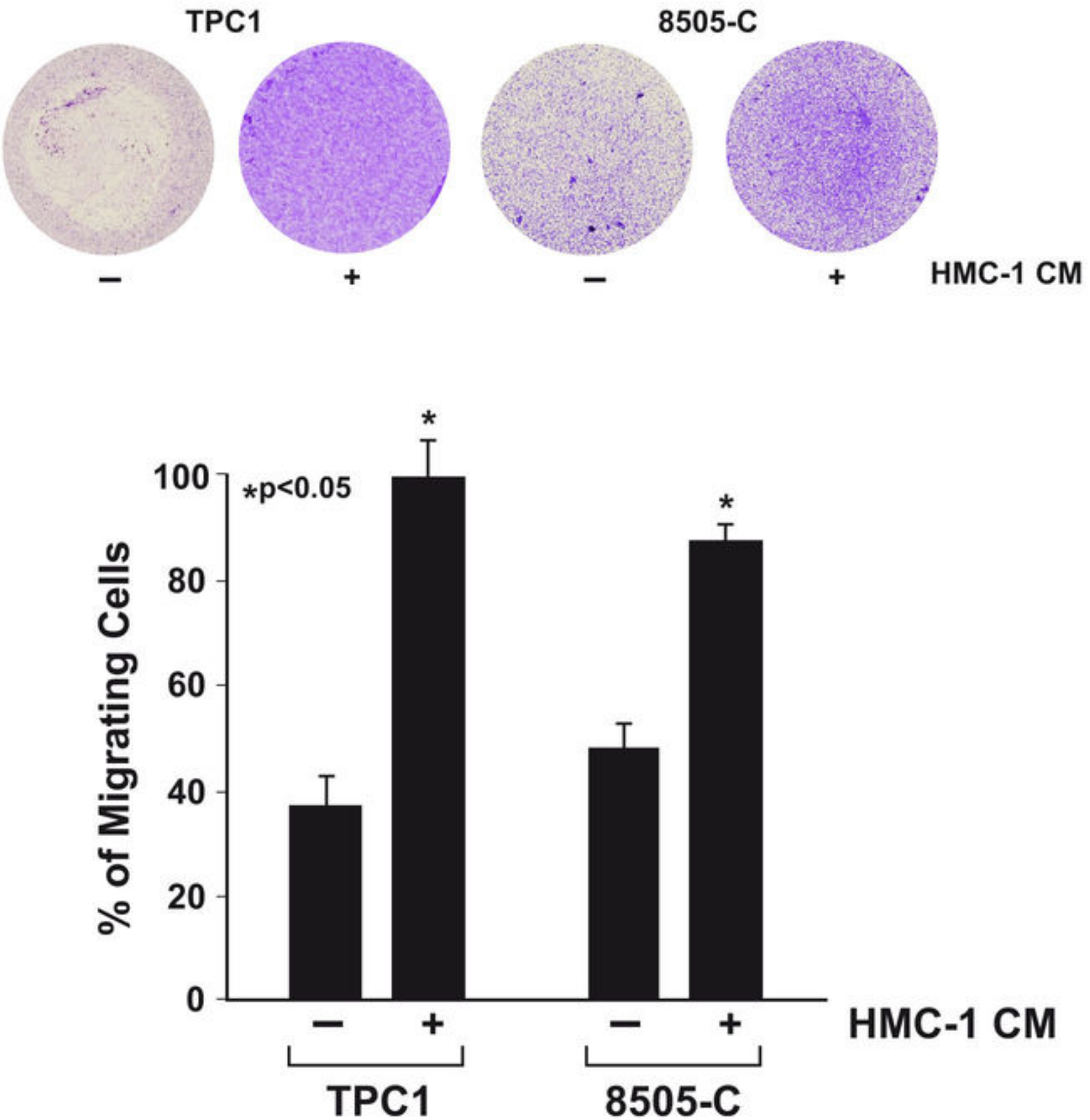
TPC1
8505-C
–
+
–
+
HMC-1 CM
*
*
*p<0.05
100
80
60
40
20
0
% of Migrating Cells
–
+
–
+
HMC-1 CM
TPC1
8505-C

Figure 6

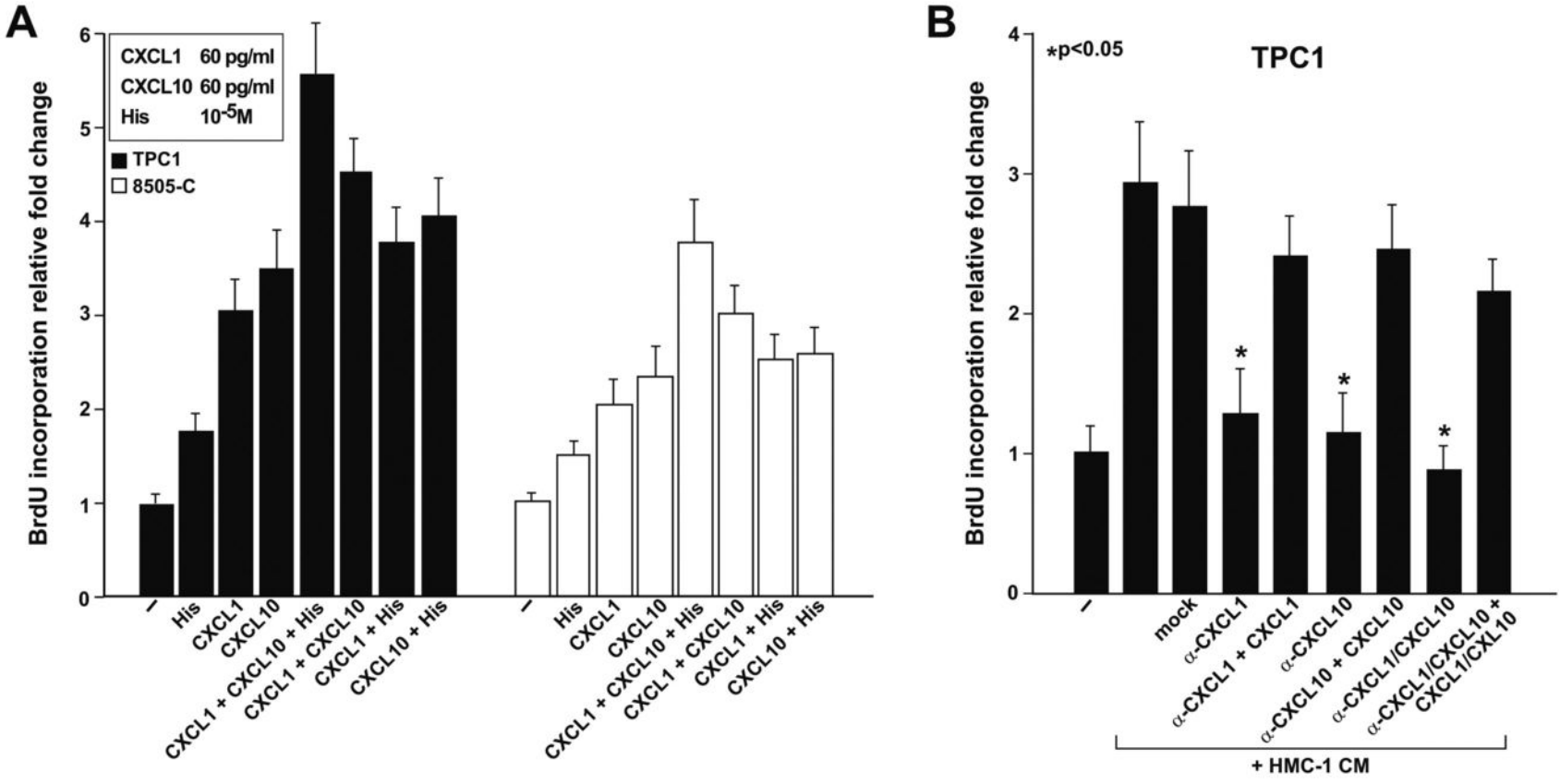
A
CXCL1 60 pg/ml
CXCL10 60 pg/ml
His 10-5M
TPC1
8505-C
BrdU incorporation relative fold change
0
1
2
3
4
5
6
–
His
CXCL1
CXCL10
CXCL1 + CXCL10 + His
CXCL1 + CXCL10
CXCL1 + His
CXCL10 + His
B
*p<0.05
TPC1
BrdU incorporation relative fold change
0
1
2
3
4
–
mock
α-CXCL1
α-CXCL1 + CXCL1
α-CXCL10
α-CXCL10 + CXCL10
α-CXCL1/CXCL10
α-CXCL1/CXCL10 + CXCL1/CXL10
+ HMC-1 CM

Figure 7

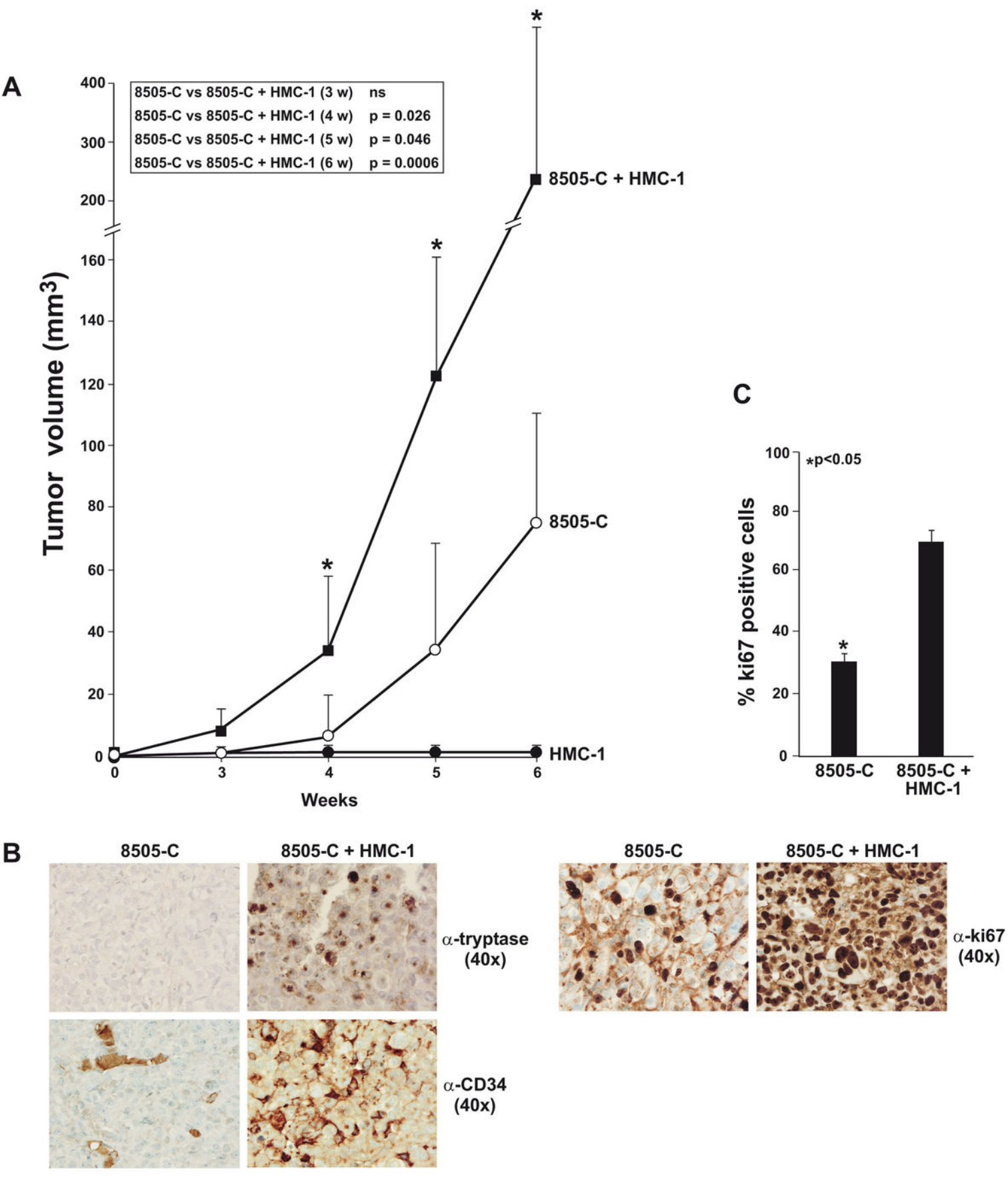
A
8505-C vs 8505-C + HMC-1 (3 w) ns
8505-C vs 8505-C + HMC-1 (4 w) p = 0.026
8505-C vs 8505-C + HMC-1 (5 w) p = 0.046
8505-C vs 8505-C + HMC-1 (6 w) p = 0.0006
Tumor volume (mm3)
Weeks
8505-C + HMC-1
8505-C
HMC-1
C
*p<0.05
% ki67 positive cells
8505-C
8505-C + HMC-1
B
8505-C
8505-C + HMC-1
α-tryptase (40x)
α-CD34 (40x)
8505-C
8505-C + HMC-1
α-ki67 (40x)

Figure 8

Activation of TYRO3/AXL tyrosine kinase receptors in thyroid cancer

Elvira Avilla[1], Valentina Guarino[1], Carla Visciano[1], Federica Liotti[1], Maria Svelto[1,2], Gnanaprakasam Krishnamoorty[1], Renato Franco[2], Rosa Marina Melillo[1]

[1]*Dipartimento di Biologia e Patologia Cellulare e Molecolare/Istituto di Endocrinologia ed Oncologia Sperimentale del CNR "G. Salvatore"*; [2]*Struttura Complessa di Anatomia Patologica, Istituto Nazionale Tumori, Fondazione G. Pascale, Naples, Italy.*

Address correspondence and offprint requests to: Rosa Marina Melillo, DBPCM/IEOS, Via S. Pansini, 5, 80131, Naples, Italy. Phone: 39-0817463603; Fax: 39-0817463603; E-mail: rosmelil@unina.it

ABSTRACT

To search for CXCR4/SDF-1α transcriptional targets in thyroid cancer, we analyzed global gene expression profiles of CXCR4-expressing human papillary thyroid carcinoma cells (TPC-1) treated or not with SDF-1α. We identified two tyrosine-kinase receptors: TYRO3 and AXL: these proteins belong to the TAM family of receptors (TYRO3, AXL and MER), can be activated by two ligands, GAS6 and Protein S, are involved in the regulation of the immune response, and are overexpressed in some epithelial cancers. We found that TPC-1 cells constitutively express TYRO3 and AXL, but SDF-1 stimulation increased their protein level and tyrosine phosphorylation. We found that most of the available thyroid cancer cell lines express both the receptors, albeit to different extent, and AXL was always much more abundant than TYRO3. In most cell lines, the two receptors display high levels of tyrosine-phosphorylation, due to constitutive expression of GAS6. An exception to this rule was the TPC-1 cell line, in which AXL was highly phosphorylated despite the fact that GAS6 is absent. AXL and its ligand GAS6 are also overexpressed in human thyroid carcinoma samples with respect to normal thyroid, as assessed by IHC. The inhibition of TYRO3 and AXL by blocking reagents or RNA interference targeting each receptor or the ligand decreased cell proliferation and resistance to apoptotic stimuli in different thryoid cancer cell lines. In cell lines that expressed both receptors and ligand, the simultaneous blockade of these molecules dramatically affected cell viability. Accordingly, we show that the stimulation of GAS6-negative TPC-1 cells with GAS6 increased their proliferation and survival. Moreover, we found that stable silencing of Axl reduces thyroid cancer cells invasiveness and inhibits experimental tumor growth in nude mice.. These results show that TYRO3/AXL-GAS6 axis sustain proliferation and survival of thyroid cancer cells. For these reasons, targeting the Axl-Tyro3/Gas6 axis might be exploited as a novel therapy for thyroid cancer.

INTRODUCTION

Thyroid cancer is the most common endocrine malignancy, and its incidence is increasind worldwide. Thyroid cancer hystotypes include well-differentiated lesions, such as papillary and follicular thyroid carcinoma (PTC and ATC), poorly differentiated thyroid carcinoma (PDTC) and anaplastic thyroid carcinoma (ATC). WDTC represents more than 90% of all thyroid cancers, while ATC accounts for approximately 2-5% of them (**De Lellis et al., 2004**; **Slough et al., 2006**; **Sherman et al., 2003**; **Rosai et al., 2004**). While WDTC can be cured in approximately in 90% of the cases, patients which present with PDC or ATC have a poor prognosis. Genetic rearrangements of the RET and TRKA tyrosine kinase receptors, point mutations of the BRAF serine-threonine kinase or, less frequently, mutations of the RAS family of small G-proteins, are associated with PTC. Human FTC features rearrangements of the nuclear receptor PPARγ or RAS point mutations (**Kondo et al., 2006**; **Nikiforova et al., 2004**). Some specific genetic alterations, such as RAS or BRAF point mutations, are detected at low frequency in ATC, suggesting that some ATC may arise from a preexisting WDTC, while others may arise *de novo* (**Nikiforova et al., 2004**; **Garcia-Rostan et al, 2005**). ATC also displays inactivating point mutations of the p53 tumor suppressor and activating point mutations of the of β-catenin or of the p110 PI3-Kinase (**Garcia-Rostan et al, 2005**; **Garcia-Rostan et al, 1999**).

Thyroid cancer also features overexpression of specific chemokine and their receptors. Among the different receptor-ligand couples, the CXCR4-SDF-1 axis has been shown to have an important role in promoting cell growth, invasiveness and survival in thyroid cancer cell cultures (**Melillo et al., 2005**; **Castellone et al., 2004**). Importantly, it has been shown that AMD3100, a small molecular inhibitor of CXCR4, inhibits the growth of xenografts of ATC in immunodeficient mice, suggesting that this receptor and its ligand(s) are required for tumor growth *in vivo*. These data prompted us to investigate the molecular mechanisms of the biological effects of CXCR4/SDF-1α in thyroid cancer cells. To this aim, we performed global gene expression profiling of the TPC-1 cell line, derived from a human PTC, and identified, as CXCR4 transcriptional targets, the TYRO3 and AXL receptor tyrosine kinases. These receptors belong to a small Protein Tyrosine Kinase (PTK) subfamily, that includes three members, Tyro3, Axl and Mer, from which this family was named TAM. These receptors are frequently co-expressed in vascular, reproductive, nervous and immune system in adults, and their expression is not indispensable for life, since knockout of each receptor produces viable and fertile mice. Interestingly, when all the three receptors are deleted, several phenotypes arise few weeks after birth. Indeed, TAM-deficient mice are unfertile, display retinal degeneration, and develop a systemic autoimmune disease. Tyro3 (also named Tif/Sky/Dtk/Rse) was first cloned from a human myelogenous leukemia cell line. Its expression is widely distributed, but it appears to be higher in the CNS. Axl (alternatively named Ufo/Ark) was

originally identified in patients with chronic mielogenous leukemia; it is overexpressed in several cancer types and its levels correlate with cancer progression in some epithelial neoplasia. Human Mer (alternatively named Eyk) was firstly identified as the homologue of the avian retroviral *v-eyk* oncogene. It displays tissue specific expression and has a role in the phagocytosis of apoptotic cells by macrophages and in the homeostasis of the retina and of the immune system. The three receptors share a common structure, being composed by an extracellular domain which contains two consecutive Ig-like and two FNII repeats, and a tyrosine kinase intracellular domain. The physiological ligands for TAM receptors are two homologous vitamin K-dependent proteins, namely Gas6 and protein S. Gas6 (Growth-Arrest-Specific gene 6) was identified as a gene up-regulated in NIH3T3 fibroblasts upon serum deprivation. Gas6 can bind, with distinct affinities, the three receptors. Protein S has been identified as a negative regulator of the blood coagulation process, and has a role in the engulfment of apoptotic bodies by phagocytic cells. It has been shown that Protein S can act as an agonist for Tyro3 and Mer, while there are no data available sustaining Axl/Protein S interaction; moreover, it is not clear whether ligands can bind as heterodimers and how receptor homo-heterodimers eventually respond to different combinations of ligands. These two proteins display 43% aminoacid identity and share a common structure, characterized by an N-terminal domain rich in γ-carboxyglutamic acid residues, a loop region, four Epidermal Growth Factor (EGF)-like repeats, and a C-terminal globular sex hormone binding globulin (SHGB)-like domain. This last region is both necessary and sufficient for receptor activation and biological activity. TAM receptors are endowed with transforming ability and also play an important role in cancer development and progression. In particular, Axl overexpression has been reported in several types of human cancer, including myeloid leukemias, malignant gliomas, breast, colon, oesopageal and lung carcinomas. Relatively few data are available involving the expression of Tyro3 in cancer: it has been detected in myeloid leukemias, multiple myelomas and in human lung carcinoma cells. Gas6 is frequently co-expressed with Axl or Tyro3 in cancer cells; in some cancer types its expression levels correlate with a poor prognosis (**Hutterer M et al., 2008**).

Having identified Axl and Tyro3 as CXCR4 transcriptional targets in thyroid cancer, we aimed to study their involvement in these tumors. In this report, we show that SDF-1 treatment of PTC cells induces Axl/Tyro3 up-regulation and tyrosine-phosphorylation. Human PTC and ATC, but not normal thyroid cells consitutively express Axl, Tyro3 and their ligand Gas6. By using IHC, we show that human PTC and ATC, but not normal thyroid samples score positive for both Axl and Gas6 expression.We show that Axl, Tyro3 and Gas6 have a critical role in mediating thyroid cancer cell proliferation and resistance to apoptosis. Moreover, we show that stable silencing of AXL in an ATC cell line strongly affects tumor growth in immunodeficient mice. These data provide evidences that targeting the

Axl/Tyro3/Gas6 axis might be exploited as a novel anticancer therapy for human thyroid cancer.

MATERIALS AND METHODS

Cell cultures

Human primary cultures of normal thyroid and ATC cells were obtained from F. Curcio (Dipartimento di Patologia e Medicina Sperimentale e Clinica, University of Udine, Udine, Italy;) P5, P5-2N, P5-3N, P5-4N (hereafter "NT") and U-HTH83/U-HTH7, and cultured as described previously (Salvatore et al., 2006). Human thyroid papillary cancer cell lines TPC1 , BcPAP and NIM have been described previously (Carlomagno et al., 2003; Inokuchi et al., 1995). TPC1 cells harbor a RET/PTC1 rearrangement; BcPAP cells harbor a BRAF(V600E)mutation in homozygosis; NIM cells harbor a BRAF(V600E)mutation in heterozygosis. Primary cultures of ATC were also a kind gift of H. Zitzelsberger (Institute of Molecular Radiobiology, GSF-National Research Center for Environment and Health GmbH, Neuherberg, Germany). The anaplastic cells FB1 cells harbor a BRAF(V600E) mutation in heterozygosis; 8505C and FRO harbor a BRAF(V600E) mutation in homozygosis (**Salvatore et al., 2006**); CAL62 cells express wild-type BRAF but mutant NRAS allele (Q61K); U-HTH83 cells express wild-tipe BRAF but mutant HRAS allele (Q61R) ; C643 cells express wild-type BRAF but mutant HRAS allele (G13R); SW1736 cells harbor a BRAF(V600E); U-HTH7 cells express wild-type BRAF but mutant NRAS allele (Q61R); OCUT-1 cells harbor a BRAF(V600E) mutation in heterozygosis; ACT-1 cells express a wild-type BRAF but mutant NRAS (Q61K). (**Guida et al., 2005**). Continuous cell lines were maintained in DMEM supplemented with 10% fetal bovine serum, 1% penicillin-streptomycin, and 1% glutamine. PC Cl 3 (hereafter "PC") is a differentiated thyroid follicular cell line derived from 18-month-old Fischer rats. PC cells were cultured in Coon's modified Ham F12 medium supplemented with 5% calf serum and a mixture of 6 hormones (6H), including thyrotropin (TSH, 10 mU/ml), hydrocortisone (10 nM), insulin (10 μg/ml), apo-transferrin (5 μg/ml), somatostatin (10 ng/ml) and glycyl-histidyl-lysine (10 ng/ml) (Sigma Chemical Co., St. Louis, MO) (**Fusco et al 1987**).

Tissue samples and immunoistochemistry

Retrospectively-collected archival frozen thyroid tissue samples from 26 patients affected by thyroid carcinomas (8 PTCs, 10 FTCs and 8 PDCs/ATCs) were retrieved from the files of the Struttura Complessa di Anatomia Patologica, Istituto Nazionale Tumori, Fondazione G. Pascale, of Naples, upon informed consent. Special care was taken to select cases whose corresponding histological samples were available for matched analysis. Sections (4-8 μM thick) of paraffin-embedded samples were stained with hematoxylin and eosin for histological examination to ensure that the samples fulfilled the diagnostic criteria required for the identification of PTC, FTC, PDC/ATC. Normal thyroid tissue samples were also retrieved from the files of the Struttura Complessa di

Anatomia Patologica, Istituto Nazionale Tumori, Fondazione G. Pascale, of Naples. We used an anti-AXL (R&D Systems) and anti-GAS6 antibodies for the staining(R&D Systems).

RNA extraction and reverse transcription polymerase chain reaction

Total RNA was isolated by the RNeasy Kit (Qiagen, Crawley, West Sussex, UK) and subjected to on-column DNase digestion with the RNase-free DNase set (Qiagen) according to the manufacturer's instructions. Where indicated, cells were stimulated with SDF-1α (100ng/ml) (CXCR4 ligand) (Peprotech, Princeton Business Park, Rocky Hill, NJ) for 3h-6h-12h-24h-48h and treated with AMD3100 (1μg/μl) (CXCR4 antagonist) and harvested 24h after treatment. The quality of RNA was verified by electrophoresis through 1% agarose gel and visualized with ethidium bromide. Random-primed first strand cDNA was synthesized in a 50 μl reaction volume starting from 2 μg RNA by using the GeneAmp RNA PCR Core Kit (Applied Biosystems, Warrington, UK). Primers were designed by using softwareavailable at http://www-genome.wi.mit.edu/cgi-bin/primer/primer3_www.cgi and synthesized by the MWG Biotech (Ebersberg, Germany). To exclude DNA contamination, each PCR reaction was also performed on untranscribed RNA. Quantitative (real-time) reverse transcription polymerase chain reactions (QRT- PCR) were performed by using the SYBR Green PCR Master mix (Applied Biosystems) in the iCycler apparatus (Bio-Rad, Munich, Germany). Amplification reactions (25μl final reaction volume) contained 200 nM of each primer, 3 mM MgCl2, 300 μM dNTPs, 1x SYBR Green PCR buffer, 0.1U/μl AmpliTaq Gold DNA Polymerase, 0.01U/μl Amp Erase, RNase-free water, and 2 μl cDNA samples. Thermal cycling conditions were optimized for each primer pair and are available upon request. To verify the absence of nonspecific products, 80 cycles of melting curve (55°C for 10 sec) were performed. In all cases, the melting curve confirmed that a single product was generated. Amplification was monitored by measuring the increase in fluorescence caused by the SYBR-Green binding to double-stranded DNA. Fluorescent threshold values were measured in triplicate and fold changes were calculated by the formula: 2-(sample 1 ΔCt - sample 2 ΔCt), where Δ*Ct* is the difference between the amplification fluorescent thresholds of the mRNA of interest and the ß actin mRNA.

RNA interference

*SMART*pool (custom-synthesized siRNA) system by Dharmacon was used for AXL, TYRO3 and GAS6 silencing. Cells were grown under standard conditions. The day before transfection, cells were plated in six-well dishes at the density of 3 x 10^5. As transfection reagent, Dharma*FECT* was used. Transfection was performed by using 100nM of *SMART*pool and 6 μl of

Dharma*FECT* (Dharmacon). Cells were harvested at 24 and 48 h after transfection and analyzed for protein expression and biological activity.

Generation of stable shRNA-expressing cell lines

We obtained 5 lentiviral constructs (pLKO.1*puro*) containing custom synthesized, 21-mer short hairpin RNA (shRNA) directed to various coding region of AXL cDNA and with puromycin resistance locus (Mission shRNA, pLKO.1 *puro*) from Sigma-Aldrich, Inc. (**Stewart et al., 2003**). We transfected 8505-C the plasmid shAxl pool or a pool of non-targeting vectors (control, shCTR) by electroporation. Stable transfectants were clonally selected in medium with 500ng/ml puromycin for 15 days, and cell colonies were screened for Axl silencing by Western blot analysis.

Protein studies

Protein extractions and immunoblotting experiments were performed according to standard procedures. Briefly, cells were harvested in lysis buffer (50 mM HEPES, pH7.5, 150 mM NaCl, 10% glycerol, 1% Triton X-100, 1 mM EGTA, 1.5 mM MgCl2, 10 mM NaF, 10 mM sodium pyrophosphate, 1 mM Na3VO4, 10 μg of aprotinin/ml, 10 μg of leupeptin/ml) and clarified by centrifugation at 10,000 x g for 30 min. Protein concentration was estimated with a modified Bradford assay (Bio-Rad, Munich, Germany). Immune complexes were detected with the enhanced chemiluminescence kit (ECL, Amersham). Signal intensity was analyzed at the Phosphorimager (Typhoon 8600, Amersham Pharmacia Biotech) interfaced with the ImageQuant software. Anti-AXL for Western Blot and immunoprecipitation analysis was from Santa Cruz Biotechnology, Inc. (Santa Cruz, CA); anti-phosphorilated AXL, specific for the active AXL phosphorilated at tyrosine 790, was from R&D Systems; anti-GAS6 for Western Blot was from R&D Systems.. Anti-TYRO3 for Western Blot and immunoprecipitation was from Novus Biologicals. Anti-AKT and antiphosphoAKT, specific for the active AKT phosphorylated at serine 473, were from Cell Signaling (Beverly, MA). Anti-phosphorylated p44/42 MAPK, specific for the active MAPK phosphorilated at threonin 202 and 204, and anti-p44/42 MAPK were from Cell Signaling (Beverly, MA) . Monoclonal anti-αtubulin was from Sigma Chemical Co. Secondary anti-mouse and anti-rabbit antibodies coupled to horseradish peroxidase were from Bio-Rad; secondary antibody donkey anti-goat coupled to horseradish peroxidase was from Santa Cruz Biotechnology, Inc. (Santa Cruz, CA). Anti-phosphotyrosine antibodies were from Upstate Biotechnology Inc., (Lake Placid, NY, USA).

ELISA assay

Thyroid cells plated in 6-well dishes were allowed to grow to 70% confluency and then serum-deprived for 24h. Culture media were cleared by centrifugation at 2,000 RPM at 4°C to remove detached cells and debris. Gas6 levels in culture supernatants were measured using a quantitative immunoassay ELISA kit (QuantiKine colorimetric Sandwich assay ELISA, R&D Systems, UK), following the manufacturer's instructions. Triplicated samples were analyzed at 490 nM with an ELISA reader (Model 550 microplate reader, Bio-Rad). ELISA results were validated on cell lysates by Western Blotting analysis by using an anti-GAS6 antibody (R&D Systems).

Matrigel invasion

In vitro invasiveness through Matrigel was assayed using transwell cell culture chambers according to described procedures. Briefly, confluent cell monolayers were harvested with trypsin/EDTA and centrifuged at 800x*g* for 10 min. The cell suspension ($1x10^5$ cells/well) was added to the upper chamber of a pre-hydrated polycarbonate membrane filter of 8 μM pore size (Costar, Cambridge, MA, USA) coated with 35 μg Matrigel (Collaborative Research Inc., Bedford, MA, USA). The lower chamber was filled with complete medium or 2.5% FCS (as indicated). After having plated stably-AXL-silenced cells on matrigel, cells were then incubated at 37°C in a humidified incubator in 5% CO2 and 95% air for 24h and 48h. Nonmigrating cells on the upper side of the filter and Matrigel were wiped off and migrating cells on the reverse side of the filter were stained with 0.1% crystal violet in 20% methanol for 15 min, and photographed. The stained cells were lysed in 10% acetic acid. Triplicated samples were analyzed at 570 nM with an ELISA reader (Model 550 microplate reader, Bio-Rad). The results were expressed as percentage of migrating cells with respect to the sh-ctr silenced ones.

Cell proliferation

S-phase entry was evaluated by BrdU incorporation and indirect immunofluorescence. Cells were grown on coverslips and, when indicated, after 12h of starvation, cells were treated with recombinant human GAS6 (200ng/ml) for 24h or with a blocking chimaeric protein (Dtk/FC) which contains the extracellular domain of Tyro3 fused to the FC portion of the IgG (R&D Systems) (2μg/ml) for 24h. Moreover, where indicated, cells have been silenced with siRNA (Dharmacon, CO); after 24h of silencing, cells have been serum-deprivated for 12h and then treated with recombinant human GAS6 (200ng/ml) for 24h. In both cases, BrdU was added at a concentration of 10 μM for the last 2h before the reaction was stopped.. Subsequently, cells were fixed in 3% paraformaldehyde and permeabilized with 0.2% Triton X-100. BrdU-positive cells were revealed with Texas-Red-conjugated secondary

antibodies, respectively (Jackson Immuno Research Laboratories, Inc. Philadelphia, PA). Cell nuclei were identified by Hoechst staining. Fluorescence was visualized with a Zeiss 140 epifluorescent microscope.

For growth curves, cells were plated at a density of 0.5 x 10^5 with complete medium or in low serum conditions (2.5%) (as shown) and counted at the indicated time-points.

TUNEL assay

For terminal desoxynucleotidyl transferase-mediated desoxyuridine triphosphate nick end-labeling (TUNEL), an equal number (5 x 10^3) of thyroid carcinoma cells from the different lines was seeded onto single-well Costar glass slides. Cells were treated with a proapoptotic substance DEM (DiEthylMaleate) at the concentration of 0.6 mM for 12h; then, where indicated, cells were treated with recombinant human GAS6 (200ng/ml) for 24 h or with the blocking chimaeric protein (Dtk/FC). Moreover, where indicated, cells have been silenced with siRNA (Dharmacon, CO); after 24h of silencing, cells have been serum-deprivated for 12h and then treated with recombinant human GAS6 (200ng/ml) for 24h. Cells were fixed in 4% (w/v) paraformaldehyde and permeabilized by the addition of 0.1% Triton X-100/0.1% sodium citrate. Slides were rinsed twice with PBS, air-dried and subjected to the TUNEL reaction (Roche). All coverslips were counterstained in PBS containing Hoechst 33258, rinsed in water and mounted in Moviol on glass slides. The fluorescent signal was visualized with an epifluorescent microscope (Axiovert 2, Zeiss) (equipped with a 100X objective) interfaced with the image analyzer software KS300 (Zeiss).

Xenografts in nude mice

Mice were housed in barrier facilities and 12-hour light-dark cycles and received food and water ad libitum at the Dipartimento di Biologia e Patologia Cellulare e Molecolare (University of Naples "Federico II", Naples, Italy). This study was conducted in accordance with Italian regulations for experimentation on animals. All manipulations were performed while mice were under isoflurane gas anesthesia. No mouse showed signs of wasting or other signs of toxicity. BHT101 cells (5 x 10^6 per mouse) were inoculated s.c. into the right dorsal portion of 4-week-old male BALB/c nu/nu mice (The Jackson Laboratory). When tumors measured 40 mm3, mice were randomized to receive AMD3100 (n = 10; 1.25 mg/kg/twice daily) or vehicle alone (n = 10; PBS) by i.p. injection for 5 consecutive days per week for 3 to 4 weeks. Moreover, three groups of mice (4-week-old male BALB/c nu/nu mice, Jackson Laboratories, Bar Harbor, ME) were inoculated subcutaneously into the right dorsal portion with 8505-C shCTR cells (10x10^6/mouse), 8505-C shAXL CL1(1x10^6/mouse), 8505-C shAXL CL2 (1x10^6/mouse). Tumor diameters were measured at regular intervals with a caliper. Tumor volumes

(V) were calculated with the formula: V= A x B2/2 (A=axial diameter; B= rotational diameter). Tumors were excised and fixed overnight in neutral buffered formalin and processed by routine methods.

Statitical analysis

To compare 8505-CshCTR versus 8505-CshAXL xenograft growth nude mice, we used the unpaired Student's *t* test (normal distributions and equal variances). The clinico-pathological data were statistically evaluated with a two-tailed Student's t test; the chi2 test was used to establish the statistical significance of the distributions. Statistical analysis was done with the GraphPad Instat software, v.3.0b. Differences were statistically significant at $P < 0.05$.

RESULTS

The Tyro3 and Axl receptors are transcriptional targets of the CXCR4/SDF-1α axis and are overexpressed in thyroid cancer cells

To better understand the biological role of the SDF-1α chemokine and of its receptor CXCR4 in thyroid cancer, we performed global gene expression profiling of human TPC-1 cells, derived from a human PTC. By using an oligonucleotide-based array, representing the entire human genome, we found high expression levels for Tyro3 and Axl in SDF-1α–treated cells. Tyro3 and Axl mRNA levels were evaluated by Real-time RT-PCR (data not shown) and the corresponding proteins were assessed by using western blot analysis. As shown in **fig.1A,** Tyro3 basal levels were much lower than those of Axl in TPC1 cells, but SDF-1α treatment increased both Axl and Tyro3 protein levels in time-course experiments. Interestingly, tyrosine-phosphorylation of the two receptors also increased upon SDF-1α treatment.

We then looked at Tyro3 and Axl levels by western blot analysis in a panel of thyroid cancer cell lines and in primary cultures of thyroid normal cells. As shown in **Fig. 1B**, Tyro3 and Axl protein levels were not elevated in normal thyroid cells, while most of the cancer cell lines featured high levels of the two receptors, being overall Axl consistently more expressed than Tyro3. This was also confirmed by RT-PCR experiments (data not shown). We also evaluated the expression of both the receptors in a rat thyroid cell line (PC Cl3) and in PC Cl3-derived cell lines transduced with different oncogenes. While we could not detect endogenous Tyro3, we were able to show that two RET/PTC isoforms, RET/PTC1 and RET/PTC3, the cooperation between E1A and RAF, and the v-mos oncogenes were able to induce Axl overexpression in these cells. Since it has been reported that TAM receptors are activated in different cancer hystotypes (**Craven et al.,1995; Nemoto et al., 1997; Ito 2002; Zantek et al., 2001; Shieh et al., 2005; Gustafsson et al., 2009**) , we evaluated the levels of phosphorylation of both Tyro3 and Axl in our cell lines by means of immunoprecipitation followed by western blot analysis with anti-phosphotyrosine antibodies. As shown in **fig. 1C**, we then analyzed Axl tyrosine-phosphorylation and found that all the cell lines tested displayed Axl activation, being phosphorylation levels higher in Cal62, SW1736, 8505-C and Nim with respect to OCUT-1 and ACT1. The TPC1 cell line, derived from a human PTC featuring a spontaneous RET/PTC1 rearrangement, showed the highest levels of phospho-Axl relative to total Axl. We also evaluated the activation of Axl by using an anti-phospho-Axl antibody, which specifically recognizes Tyr 779 (Y779), a residue of the carboxy-terminal tail that is phosphorylated upon Axl stimulation, as previously reported. As shown in Fig 1C, CAL62, NIM and TPC1 cell lines diplayed the highest Y779 phosphorylation levels. Axl-expressing PC Cl3 rat cell lines PC PTC3, PC663 and PC E1A RAF were tested for Axl activation. As shown in **fig. 1C**, Axl

phosphorylation was detected in all the three cell lines, with PC PTC3 displaying the highest levels. Since it has been reported that Axl activation in tumor cells is due to autocrine or paracrine loops, we asked whether thyroid cancer cell lines expressed one of the Axl/Tyro3 ligands. RT-PCR experiments suggested that Gas6, but not ProteinS, was expressed by our cells (not shown). To confirm this finding, we evaluated Gas6 levels by using both ELISA immunoassay and western blot analysis. As shown in **Fig. 2A**, 8505-C, NIM, CAL62 and SW1736 secreted detectable levels of Gas6 in the culture medium. When we screened the cell lines for Gas6 expression by WB analysis, we found that all the cell lines produced Gas6, with the exception of TPC1 (**Fig 2B**). Based upon these data, we identified cell lines, such as CAL62and SW1736, that produce different levels of Gas6, which is inefficiently released in the culture medium; cell lines, such as NIM and 8505-C, that produce and secrete high levels of Gas6; cell lines, such as TPC1, that did not produce detectable levels of Gas6, but, despite this, display high levels of Axl phosphorylation. These data indicate that thyroid cancer cells widely express Axl and Tyro3 receptors, being Tyro3 expressed at lower levels than Axl. In most cell lines Axl and Tyro3 are activated, as demonstrated by the high levels of phosphotyrosine content of the receptors. Receptor activation is probably be due to an autocrine effect, since all the cell lines, with the exception of the TPC1, express variable amount of the ligand, Gas6.

Human thyroid cancer specimens express Axl and its ligand Gas6

We analysed human thyroid cancer specimens for Axl expression. To this aim, we collected 26 thyroid carcinoma samples (8 PTCs, 10 FTCs and 8 PDC/ATCs) (**Table 1**) and analysed them by using immunohistochemical staining with a specific anti-human Axl antibody. Of all the carcinoma analised, 73% (19/26) scored positive for Axl expression. These data are summarized in Table 1. Axl positivity was observed mainly in tumoral cells (Fig. 3A). Most of the samples display membrane positivity, but a small number of specimens were characterized by cytosolic staining. When Axl was cytosolic, it was found into perinuclear vescicles probably representing the Golgi apparatus. This pattern is typical of overexpressed transmembrane proteins. Tumoral stroma and non tumoral adjacent tissues were negative for Axl staining, with the exception of red blood cells, that were strongly recognized by anti-Axl antibody. This observation confirms previous findings indicating that this receptor is indeed physiologically expressed in eritrocytes (**Tang et al., 2009**). To assess whether thyroid carcinomas feature autocrine/paracrine loops involving Axl and its ligand, we also assessed Gas6 expression by IHC in the same sample set. As shown in fig. 3B, most of the analysed specimens scored positive for Gas6 expression. Gas6 staining was cytosolic and was mainly found in carcinoma cells; some samples also displayed stromal positivity, suggesting that ligand can also be provided by

other cells of the tumor microenvironment. Table 1 summarizes the expression data of Axl and Gas6 in thyroid carcinoma samples.

Axl/Tyro3-Gas6 axis blockade inhibits thyroid cancer cell proliferation and survival

To investigate whether the Axl/Gas6 loop has a role in thyroid cancer biology, we selected two PTC cell lines, TPC-1 and NIM. As shown above, TPC1 cells express high levels of activated Axl in the absence of ligand. We analyzed the levels of DNA synthesis by BrdU incorporation assays in basal conditions (serum deprivation) and in the presence of Gas6. As shown in **Fig. 3A**, 10% of TPC1 incorporated BrdU in conditions of serum starvation. When Gas6 was added, BrdU incorporation increased to 20%. Consistently, a chimaeric protein (Dtk/FC)which contains the extracellular domain of Tyro3 fused to the FC portion of the IgG, that is able to suppress Gas6-mediated effects by sequestering this ligand, does not modify the rate of BrdU-positive cells grown in basal conditions, but inhibits the effects of Gas6 treatment. To further evaluate the role of Axl in TPC1 cell proliferation, we used RNA interference. Axl silencing was verified by western blot analysis (**Fig 4C**). As shown in Fig. **4A**, when Axl was silenced, there was only a modest reduction of BrdU incorporation in basal conditions. This reduction was more dramatic in the presence of Gas6: BrdU-positive cell rate dropped from 27% to 8%. Gas6 silencing did not modify TPC1 growth rate, consistent with the observation that Gas6 is not produced by TPC1 cells (not shown). To evaluate whether Axl blockade influences TPC1 survival, we first treated these cells with a proapoptotic substance, Diethylmaleate (DEM), for 24h, and performed TUNEL assays (**Fig. 4B**). In this condition, 48% of TUNEL-positive cells were obtained; Gas6 addition dramatically decreased this percentage. The blockade of exogenous Gas6 with DtkFC almost completely reverted this effect. Accordingly, DtkFC did not modify the percentage of apoptotic cells when used in the absence of Gas6. We also performed apoptosis assays in the presence of Axl- or Gas6-targeting small interfering RNAs. In this case, apoptosis was induced by 24 h serum deprivation. In this condition, 10% of apoptotic cells were observed. This percentage decreased to 5% when Gas6 was added. Axl silencing dramatically increased the rate of apoptotic cells to 30%. Interestingly, when Gas6 was added to Axl-silenced cells, the pro-apoptotic effects of Axl silencing were significantly inhibited (**Fig. 4B**). This effect is not likely to be due to incomplete Axl silencing, since western blot analysis of silenced cells showed a complete disappearance of the protein. A possible explanation is that the other receptor, Tyro3, can substitute Axl function. Again, Gas6 silencing did not modify the apoptosis rate both in the presence and in the absence of Gas6 (not shown). Since the additon of Gas6 partially recovered the effects of Axl blockade in this cell line, we evaluated whether Tyro3 also has a role in thyroid cancer cell proliferation and survival.

To this aim, Tyro3 was knocked down in TPC1 cells through RNA interference, and DNA synthesis and apoptosis were evaluated. As shown in figure **4A and B**, Tyro3 silencing affected both BrdU incorporation and apoptosis. Silencing of both Tyro3 and Axl receptors increased the effect of the single knockouts; finally, Gas6 treatment did not modify the effect of the double knockouts. Similar experiments were performed by using the NIM cell line. As shown above, these cell express both Axl and Gas6. Exogenous addition of this ligand did not significantly modify BrdU incorporation and apoptosis rate of NIM cells. Instead, the blockade of both endogenous Axl and Gas6 by using DtkFC or RNAi inhibited NIM DNA synthesis (**fig.5A**), and exogenous Gas6 addition reverted these effects. Similar results were obtained when apoptosis was evaluated. DEM treatment induced 40% of apoptotic cells, and the blockade of Gas6 with DtkFC increased to 62% the percentage apoptotic cells. When cells were serum deprived, we observed 10% of apoptotic cells. This percentage was only slightly modified by Gas6 treatment. Axl or Gas6 silencing strongly enhanced NIM apoptotic rate, and these effects were again reverted by exogenous Gas6 (**fig. 5B**). Tyro3 silencing also affected NIM proliferation and survival, and Tyro3/Axl silencing was as effective as Gas6. Again, Gas6 treatment did not modify the effect of the double knockouts. Gas6, Tyro3 and Axl knockdown was verified by western blot analysis (**fig. 5C**). We also used siRNA-mediated silencing to verify whether Axl Knockdown could impair proliferation and survival of human ATC cell lines. To this aim, we used 8505-C and Cal62 cells. As shown in **figure 6A and B**, Gas6 stimulated cell proliferation and inhibited apoptosis of 8505-C. Consistently, Axl silencing slightly inhibited BrdU incorporation and enhanced apoptosis of these cells.

Effects of stable silencing of Axl in 8505-C ATC cells

To confirm that Axl silencing effectively inhibited the viability of thyroid cancer cells, we stably transfected 8505-C with a pool of vectors expressing five different shRNAs directed to Axl or expressing control non-targeting shRNAs. After antibiotic selection, cell clones were isolated and screened by western blot analysis for Axl expression: as shown in **fig. 7A**, we identified several clones in which Axl expression was completely knocked down. Six Axl-knockout (shAxl Cl 1-6) and two control clones (shCTR Cl 1-2) were selected for further analyses. We first verified whether Axl knockdown could impair cell growth both in optimal (10% FCS) or in low serum (2,5% FCS) conditions by performing growth curves. As shown in **Fig. 7B**, shRNA-mediated Axl silencing showed mild effects on cell proliferation in complete culture medium, while it was significantly more effective in low serum conditions. To assess whether reduced cell growth was due to decreased DNA synthesis or increased cell death, cells were serum starved for 12h and we evaluated the percentage of BrdU- and TUNEL-positive cells. As shown in

figure 7C, all shAxl clones displayed a significant reduction of BrdU incorporation and a significant increase in apoptosis when compared to control clones. Moreover, we asked whether stable AXL silencing on ATC cell lines could impair cell invasiveness through Matrigel. Invasive ability of cells was verified both in optimal (10%FCS) or in low-serum (2,5%FCS) conditions. As indicated in **Fig. 8**, shAXL clones showed a clear decrease of invasive ability with respect to shCTR, but only in low-serum conditions (**Fig. 8**).

Axl silencing inhibits experimental tumor growth

Next, we evaluated the role of Axl in tumor growth by using xenografts of ATC cells into (*nu/nu)* immunodeficient mice. To this aim, we choose 8585-C as a model cell line because it expresses Axl and it is able to efficiently form tumors when injected into nude mice. To study the role of Axl in tumor growth, we injected animals with parental, shCTR-transfected (shCTR Cl1), and shAxl- expressing (shAxl ClX and ClY) 8505-C cell lines, and compared their growth rate. Parental cells formed tumors with the same efficiency as shCTR-transfected cells did (not shown). As shown in **fig. 9**, the tumorigenicity of 8505-C shAxl Cl4 and Cl6 was dramatically reduced when compared with 8505-C shCTR control cells. when compared with 8505-C shCTR cells. At three weeks, shCTR tumor median volume was 34 mm^3, while shAXL was < 10 mm^3. At four, five and six weeks, shCTR tumors continued to grow, reaching a median volume of ~150 $mm^{3.}$ shAXL tumors did not grow or regressed. At the end of the experiment, no shAXL tumors were available. This precluded histological analysis.

DISCUSSION

Thyroid cancer is the most frequent endocrine neoplasia, and its incidence is rapidly increasing. We previously found that normal rat thyroid cells, transduced with Papillary Thyroid Cancer (PTC)-related oncogenes, display an inflammatory signature, that includes cytokines, chemokines and their receptors (**Melillo et al., 2005**). One of the chemokine receptor we identified, CXCR4, is frequently up-regulated in thyroid cancer. SDF-1, a CXCR4 ligand, induces proliferation, survival and invasive ability of PTC cells, and a CXCR4 blocking compound, AMD 3100, inhibits thyroid cancer growth (**Castellone et al., 2004**; **De Falco et al., 2007**). To better understand the molecular basis of SDF-1 activity in thyroid cancer cells, we performed global genome expression profiling analysis on CXCR4-expressing human PTC cells upon SDF-1 stimulation, and we identified two tyrosine-kinase receptors, TYRO3 and AXL, as transcriptional targets of this chemokine.

TYRO3 and AXL belong to the subfamily of receptor tyrosine kinases (RTKs) that also includes Mer (from which the family name: TAM) (**Lai and Lemke, 1991**; **O'Bryan et al., 1991**). The ligands for TAM receptors are Gas6 (Growth Arrest-Specific 6) and protein S, two vitamin K-dependent proteins that exhibit 43% amino-acid sequence identity and share similar domain structures (**Stitt et al., 1995**; **Varnum et al., 1995**). TAM activation and signaling has been implicated in multiple cellular responses including cell survival, proliferation, migration and adhesion (**Hafizi and Dahlback, 2006**). TAM receptor signaling has been shown to regulate vascular smooth muscle homeostasis (**Korshunov et al., 2006, 2007**), platelet function, thrombus stabilization (**Angelillo-Scherrer et al., 2001**; **Gould et al., 2005**) and erythropoiesis (**Angelillo-Scherrer et al., 2008**). TAM receptors are also implicated in the control of oligodendrocyte cell survival (**Shankar et al., 2006**) and in the regulation of osteoclast function (**Katagiri et al., 2001**). Recent studies in knockout mice have revealed that TAM receptors play pivotal roles in innate immunity (**Lemke and Rothlin, 2008**). TAM receptors inhibit inflammation in macrophages and dendritic cells (**Sharif et al., 2006**; **Rothlin et al., 2007**), promote the phagocytosis of apoptotic cells (**Lu et al., 1999**; **Prasad et al., 2006**) and stimulate the differentiation of Natural Killer cells (**Caraux et al., 2006**). In many of these instances, the primary downstream TAM signaling pathway appears to be PI3K/AKT pathway (**Angelillo- Scherrer et al., 2001**; **Keating et al., 2006**; **Shankar et al., 2006**); however, the Janus kinase-STAT pathway is essential for TAM-mediated immune responses (**Rothlin et al., 2007**). In addition, cooperative interaction between TAM receptors and cytokine receptor signaling network is required for many TAM-regulated biological functions (**Budagian et al., 2005b**; **Rothlin et al., 2007**).

Several reports underlined the importance of TAMs receptor in cancer. In particular, AXL was first identified in patients with chronic myelogenous leukemia and, if overexpressed in non-transformed cells, it induces neoplastic

conversion (**Janssen et al., 1991**; **O'Bryan et al., 1991**). AXL overexpression has been reported in a variety of human cancers (**Craven et al., 1995**; **Ito et al., 1999**; **Berclaz et al., 2001**; **Sun et al., 2004**; **Shieh et al., 2005**), and is associated with invasiveness and metastasis in lung (**Shieh et al., 2005**), prostate (**Sainaghi et al., 2005**), breast (**Meric et al., 2002**), and gastric cancers (**Wu et al., 2002**) as well as in renal cell carcinoma (**Chung et al., 2003**; **Gustafsson et al., 2009**) and glioblastoma (**Hutterer et al., 2008**). A recent study showed that AXL overexpression, through a 'tyrosine kinase switch', leads to resistance to the samll TK inhibitor Imatinib in gastrointestinal stromal tumors (**Mahadevan et al., 2007**). AXL expression is induced by chemotherapeutic drugs and it confers drug resistance in acute myeloid leukemia (**Hong et al., 2008**). These evidences suggest that AXL may be involved in the regulation of multiple aspects of tumorigenesis. For these reasons, we decided to investigate the biological role of TYRO and AXL receptors in human thyroid carcinomas.

In this study, we found that TYRO3 and AXL expression can be induced by SDF-1-α. Axl and Tyro3 were expressed in human thyroid cancer cells and in rat thyroid cells neoplastically transformed by several oncogenes, but not in normal thyroid cells. AXL was also constitutively phosphorylated in most of these cells. This was due to the constitutive presence of the ligand Gas6; the only exception to this rule was represented by the TPC1 cell line, in which AXL was highly phosphorylated although ligands are absent. In this case, some other mechanisms, still not understood, may be active to keep the receptor in a constitutively active status. We showed AXL expression in a set of human thyroid carcinoma samples (8 PTCs, 10 FTCs and 8 PDC/ATCs), but not in normal thyroid specimens, by immunohystochemistry. Interestingly, we found that 73% of evaluated samples displayed strong AXL positivity which was confined to tumoral cells. Moreover, most of the analysed specimens scored positive for Gas6 expression; Gas6 staining was cytosolic and mainly found in carcinoma cells, thus suggesting the existence of an autocrine loop.

In cell lines that expressed both receptors and ligand, the inhibition of TYRO3, AXL or Gas6 reduced cell proliferation and increased apoptotic rate. When either Tyro3 or Axl were silenced, Gas6 could partially recover proliferation and antiapoptotic activity, indicating that both the receptors are involved in Gas6-mediated biological activities. Instead, when both the receptors were inhibited, Gas6 had no effect on cell proliferation and survival. Accordingly, we show that the stimulation of GAS6-negative TPC-1 cells with exogenous GAS6 increased their proliferation and survival. These data, taken together, indicate that the two tyrosine-kinase receptors are able to modulate two of the main features of malignant cells, proliferation and resistance to apoptotic stimuli.

AXL expression is associated with invasiveness and metastasis in various cancers including breast (**Meric et al., 2002**; **Zhang et al., 2008**), lung (**Shieh et al., 2005**) and gastric (**Sainaghi et al., 2005**) cancers, as well as in glioblastoma (**Hutterer et al., 2008**). The involvement of AXL in promoting

cancer cell migration and invasion has been demonstrated *in vitro* (**Vajkoczy et al., 2006; Tai et al., 2008**; **Zhang et al., 2008**). In breast cancer models, ectopic expression of AXL was sufficient to confer a highly invasive phenotype to weakly invasive MCF7 cells. Consistently, inhibition of AXL signaling by shRNA knockdown or an anti-AXL antibody decreased mobility and invasiveness of highly invasive breast cancer cells (**Zhang et al., 2008**). We also found that stable silencing of AXL in 8505-C ATC cells (8508-C shAXL) drammatically reduced thyroid cancer cell viability; we also observed that stable-AXL-silenced clones displayed a reduction of their invasive ability. Taken together these studies established a critical role of AXL in promoting cell migration and invasion. When we injected immunodeficient mice with 8505-C shAXL clones, we observed a complete inhibition of tumor formation *in vivo*. Our data confirm previous studies showing that AXL expression is involved in tumor growth of glioblastoma (**Vajkoczy et al., 2006**) and breast cancer models (**Holland et al., 2005**). It has been shown that activated AXL can interact with the p85α and p85β subunits of phosphatidylinositol 3-kinase (**Braunger et al., 1997)** and this mediates the strong the antiapoptotic effect mediated by the receptor. Furthermore, AXL can induce angiogenesis, as confirmed by the observation that AXL and GAS6 are co-expressed in tumor associated vascular cells in gliomas (**Hutterer et al., 2008**) and that AXL knockdown is additive with anti-VGEF to inhibit endothelial tube formation (**Li et al., 2009**). Whether this is also the case for thyroid cancer is still unknown. Unfortunaltely, the complete suppression of tumor growth of 8505-C shAXL cells precluded further analysis of excised tumors. However, preliminary observations obtained by us indicate that Gas6 is a strong stimulator of the PI3-K/Akt pathway in thyroid cancer cells and that the blockade of Axl/Tyro3-Gas6 axis inhibits Akt phosphorylation. These data indicate that Axl blockade could impair tumor growth, at lea st in part, by inhibiting of the PI-3K pathway.

In conclusion, our data strongly suggest that AXL/TYRO3-Gas6 axis can be considered as a novel potential target of thyroid anticancer therapy. Several compounds have been identifyed (small inhibitors and monoclonal antibodies) that could block AXL signaling by acting at different levels (**Li et al., 2009**). Our data indicate that these compound should be exploited to treat thyroid cancer.

REFERENCES

Angelillo-ScherrerA, de Frutos P, Aparicio C, et al. Deficiency or inhibition of Gas6 causes platelet dysfunction and protects mice against thrombosis. Nat Med 2001;7:215-21.

Berclaz G, Altermatt HJ, Rohrbach V, Kieffer I, Dreher E, Andres AC. Estrogen dependent expression of the receptor tyrosine kinase axl in normal and malignant human breast. Ann Oncol 2001;12:819-24.

Braunger J, Schleithoff L, Schulz AS, et al. Intracellular signalling of the Ufo/Axl receptor tyrosine kinase is mediated mainly by a multisubstrate docking-site. Oncogene 1997;14:2619–31.

BudagianV, Bulanova E, Orinska Z, et al. SolubleAxl is generated by ADAM10-dependent cleavage and associates with Gas6 in mouse serum. Mol Cell Biol 2005;25:9324-39.

Caraux A, Lu Q, Fernandez N, Riou S, Di Santo JP, Raulet DH et al. (2006). Natural killer cell differentiation driven by Tyro3 receptor tyrosine kinases. Nat Immunol 7: 747–754.

Castellone MD, Guarino V, De Falco V, Carlomagno F, Basolo F, Faviana P, Kruhoffer M, Orntoft T, Russell JP, Rothstein JL, Fusco A, Santoro M, Melillo RM. Functional expression of the CXCR4 chemokine receptor is induced by RET/PTC oncogenes and is a common event in human papillary thyroid carcinomas. Oncogene 2004; Aug 5; 23(35):5958-67.

Chung BI, Malkowicz SB, NguyenTB, Libertino JA, McGarvey TW. Expression of the proto-oncogene Axl in renal cell carcinoma. DNA Cell Biol 2003;22:533-40.

Craven RJ, Xu LH, Weiner TM, et al. Receptor tyrosine kinases expressed in metastatic colon cancer. Int J Cancer 1995;60:791–7.

Crosier PS, Hall LR, Vitas MR, Lewis PM, Crosier KE. Identification of a novel receptor tyrosine kinase expressed in acute myeloid leukaemic blasts. Leukemia Lymphoma 1995;18:443–9.

De Falco V, Guarino V, Avilla E, Castellone MD, Salerno P, Salvatore G, Faviana P, Basolo F, Santoro M, Melillo RM. Biological role and potential therapeutic targeting of the chemokine receptor CXCR4 in undifferentiated thyroid cancer. *Cancer Res. 2007 Dec 15;67(24):11821-9.*

De Lellis RA, Williams ED. Thyroid and parathyroid tumors. In: De Lellis RA, Lloyd RV, Heitz PU, Eng C, editors. World Health Organization classification of tumors: tumors of the endocrine organs. Lyons (France): IARC Press; 2004. p. 51–6.

Fusco A, Berlingieri MT, Di Fiore PP, Portella G, Grieco M, Vecchio G. Oneand two-step transformations of rat thyroid epithelial cells by retroviral oncogenes. Mol Cell Biol. 1987 Sep;7(9):3365-70.

Garcia-Rostan G, Costa AM, Pereira-Castro I, et al. Mutation of the PIK3CA gene in anaplastic thyroid cancer. Cancer Res 2005;65:10199–207.

Garcia-Rostan G, Tallini G, Herrero A, D'Aquila TG, Carcangiu ML, Rimm DL. Frequent mutation and nuclear localization of h-catenin in anaplastic thyroid carcinoma. Cancer Res 1999;59:1811–5.

Gould WR, Baxi SM, Schroeder R, Peng YW, Leadley RJ, Peterson JT et al. (2005). Gas6 receptors Axl, Sky and Mer enhance platelet activation and regulate thrombotic responses. J Thromb Haemost 3:733–741.

Guida T, Salvatore G, Faviana P, Giannini R, Garcia-rostan, Provitera L, Basolo F, Fusco A, Carlomagno F, Santoro M. Mitogenic effects of the up-regulation of minichromosome maintenance proteins in anaplastin thyroid carcinoma. 2005. *The J Clin Endoc. Metab.* 90:4703-4709.

Gustafsson A, Bostrom AK, Ljungberg B, Axelson H, Dehlback B. Gas6 and the receptor tyrosine kinase AXL in clear cell renal cell carcinoma. *PLOS One* 2009. Oct 30;4(10):e7575.

Hafizi S, Dahlback B. Gas6 and protein S.Vitamin Kdependent ligands for theAxl receptor tyrosine kinase subfamily. FEBS J 2006;273:5231-44.

Holland SJ,PowellMJ, Franci C, et al.Multiple roles for the receptor tyrosine kinase axl in tumor formation. Cancer Res 2005;65:9294-303.

Hong CC, Lay JD, Huang JS, Cheng AL, Tang JL, Lin MT et al. (2008). Receptor tyrosine kinase AXL is induced by chemotherapy drugs and overexpression of AXL confers drug resistance in acute myeloid leukemia. Cancer Lett 268: 314–324.

Hutterer M, Knyazev P, Abate A, et al. Axl and growth arrest-specific gene 6 are frequently overexpressed in human gliomas and predict poor prognosis in patients with glioblastoma multiforme. Clin Cancer Res 2008;14:130- 8.

ItoT, Ito M, Naito S, et al. Expression of the Axl receptor tyrosine kinase in human thyroid carcinoma.Thyroid 1999;9:563-7.

Ito M, NakashimaM, Nakayama T, et al. Expression of receptor-type tyrosine kinase, Axl, and its ligand, Gas6, in pediatric thyroid carcinomas around chernobyl. Thyroid 2002;12:971–5.

Janssen JW, Schulz AS, Steenvoorden AC, et al. A novel putative tyrosine kinase receptor with oncogenic potential. Oncogene 1991;6:2113-20.

Katagiri M, Hakeda Y, Chikazu D, Ogasawara T, Takato T, Kumegawa M et al. (2001). Mechanism of stimulation of osteoclastic bone resorption through Gas6/Tyro 3, a receptor tyrosine kinase signaling, in mouse osteoclasts. J Biol Chem 276: 7376–7382.

Keating AK, Salzberg DB, Sather S, Liang X, Nickoloff S, Anwar A et al. (2006). Lymphoblastic leukemia/lymphoma in mice overexpressing the Mer (MerTK) receptor tyrosine kinase. Oncogene 25:6092–6100.

Kondo T, Ezzat S, Asa SL. Pathogenetic mechanisms in thyroid follicular-cell neoplasia. Nat RevCanc er 2006;6:292–306.

Korshunov VA, Mohan AM, Georger MA, Berk BC. (2006). Axl, a receptor tyrosine kinase, mediates flow-induced vascular remodeling. Circ Res 98: 1446–1452.

Lai C, Lemke G. (1991). An extended family of protein-tyrosine kinase genes differentially expressed in the vertebrate nervous system. Neuron 6: 691–704.

Lemke and Rothlin. *Nature* 2008;(8):327-336 (Review).

Li Y, Ye X, Tan C, Hongo J-A, Zha J, Liu J, Kallop D, Ludlam MJC and Pei L. Axl as a potential therapeutic target in cancer: role of Axl in tumor growth, metastasis and angiogenesis. (2009) Oncogene 28(39):3442-55.

Lu, Q. *et al.* Tyro‑3 family receptors are essential regulators of mammalian spermatogenesis. *Nature* 398, 723–728 (1999).

Mahadevan D, Cooke L, Riley C, Swart R, Simons B, Della Croce K et al. (2007). A novel tyrosine kinase switch is a mechanism of imatinib resistance in gastrointestinal stromal tumors. Oncogene 26:3909–3919.

Melillo R.M, Castellone, M.D, Guarino, V, De Falco V, Cirafici AM, Salvatore G, Chiazzo F, Basolo F, Giannini R, Kruhoffer M, Orntoft T, Fusco A. and Santoro M. The RET/PTC-RAS-BRAF linear signalling cascade mediates the motile and mitogenic phenotype of thyroid cancer cells. J Clin Invest 2005; 115: 1068-108.

Meric F, Lee WP, Sahin A, Zhang H, Kung HJ, Hung MC. (2002). Expression profile of tyrosine kinases in breast cancer. Clin Cancer Res 8: 361–367.

Nemoto T, Ohashi K, Akashi T, Johnson JD, Hirokawa K. Overexpression of protein tyrosine kinases in human oesophageal cancer. Pathobiology 1997;65:195–203.

Nikiforova YE. Genetic alterations involved in the transition from well-differentiated to poorly differentiated and anaplastic thyroid carcinomas. Endocr Pathol 2004;15:319–27.

O'Bryan, J. P. *et al. axl*, a transforming gene isolated from primary human myeloid leukemia cells, encodes a novel receptor tyrosine kinase. *Mol. Cell. Biol.* 11, 5016–5031 (1991).

Prasad D, Rothlin CV, Burrola P, Burstyn-Cohen T, Lu Q, Garcia de Frutos P et al. (2006). TAM receptor function in the retinal pigment epithelium. Mol Cell Neurosci 33: 96–108.

Rosai J. Poorly differentiated thyroid carcinoma: introduction to the issue, its landmarks, and clinical impact. Endocr Pathol 2004;15:293–6.

Rothlin CV, Ghosh S, Zuniga EI, Oldstone MB, Lemke G. (2007). TAM receptors are pleiotropic inhibitors of the innate immune response. Cell 131: 1124–1136.

Sainaghi PP, Castello L, Bergamasco L, Galletti M, Bellosta P, Avanzi GC. (2005). Gas6 induces proliferation in prostate carcinoma cell lines expressing the Axl receptor. J Cell Physiol 204: 36–44.

Salvatore G, De Falco V, Salerno P, et al. BRAF is a therapeutic target in aggressive thyroid carcinoma. Clin Cancer Res 2006;12:1623–9.

Shankar SL, O'Guin K, Kim M, Varnum B, Lemke G, Brosnan CF et al. (2006). Gas6/Axl signaling activates the phosphatidylinositol 3-kinase/Akt1 survival pathway to protect oligodendrocytes from tumor necrosis factor alpha-induced apoptosis. J Neurosci 26: 5638–5648.

Sharif MN, Sosic D, Rothlin CV, Kelly E, Lemke G, Olson EN et al. (2006). Twist mediates suppression of inflammation by type I IFNs and Axl. J Exp Med 203: 1891–1901.

Sherman SI. Thyroid carcinoma. Lancet 2003;361501–11.

Shieh YS, Lai CY, Kao YR, et al. Expression of axl in lung adenocarcinoma and correlation with tumour progression. Neoplasia 2005;7:1058–64.

Slough CM, Randolph GW. Workup of well-differentiated thyroid carcinoma. Cancer Control 2006;13:99–105.

Stewart, S.A., et al., Lentivirus-delivered stable gene silencing by RNAi in primary cells. RNA, 9, 493-501 (2003).

Stitt, T. N. *et al.* The anticoagulation factor protein S and its relative, Gas6, are ligands for the Tyro 3/Axl family of receptor tyrosine kinases. *Cell* 80, 661–670 (1995).

SunW, FujimotoJ,TamayaT. Coexpression of Gas6/ Axl in human ovarian cancers. Oncology 2004;66:450-7.

Tai KY, Shieh YS, Lee CS, Shiah SG, Wu CW. (2008). Axl promotes cell invasion by inducing MMP-9 activity through activation of NF-kappaB and Brg-1. Oncogene 27: 4044–4055.

Tang H, Chen S, Wang H, Wu H, Lu Q, Han D. *Haematoliga* 2009 Mar;94(3):326-334.

Vajkoczy P, Knyazev P, Kunkel A, et al. Dominantnegative inhibition of the Axl receptor tyrosine kinase suppresses brain tumor cell growth and invasion and prolongs survival. Proc Natl Acad Sci U S A 2006;103:5799-804.

Varnum BC, Young C, Elliott G, et al. Axl receptor tyrosine kinase stimulated by the vitamin K-dependent protein encoded by growth-arrest-specific gene 6. Nature 1995;373:623-6.

Wu CW, Li AF, Chi CW, Lai CH, Huang CL, Lo SS et al. (2002). Clinical significance of AXL kinase family in gastric cancer. Anticancer Res 22: 1071–1078.

Zantek ND, Walker-Daniels J, Stewart J, et al. MCF-10A-NeoST: a new cell system for studying cell-ECM and cell–cell interactions in breast cancer. Clin Cancer Res 2001;7:3640–8.

Zhang YX, Knyazev PG, Cheburkin YV, Sharma K, Knyazev YP, Orfi L et al. (2008). AXL is a potential target for therapeutic intervention in breast cancer progression. Cancer Res 68: 1905–1915.

FIGURE LEGENDS

FIGURE 1
Expression levels analysis of AXL and TYRO3 receptors in human cancer thyroid cells.

- **A)** Analysis of Tyro3 and Axl protein levels by western blot analysis on TPC1 cells stimulated with SDF-1α at different time-points.
- **B)** Evaluation of TYRO3 and AXL protein levels by western blot in a panel of thyroid cancer cell lines and in primary cultures of thyroid normal cells (NT). Equal amounts of proteins (50 μg) were immunoblotted with anti-TYRO3 and anti-AXL polyclonal antibodies. Anti-αtubulin monoclonal antibody was used as a control for equal loading.
- **C)** Analysis of AXL tyrosine-phosphorylation by immunoprecipitation followed by anti-phosphotyrosine and phospho-AXL western blot in a panel of human PTCs and ATCs cell lines and in a rat thyroid cell line (PC Cl3)-derived cell lines transduced with different oncogenes. AXL-phosphorilation levels were evaluated with an anti-AXL antibody by western blot with respect to the total AXL protein levels.

FIGURE 2
Analysis of AXL/TYRO3 ligand, Gas6

- **A)** Evaluation of Gas6 levels by using ELISA immunoassay.
- **B)** Western blot analysis with specific anti-Gas6 antibody. Anti-αtubulin monoclonal antibody was used as a control for equal protein loading.

FIGURE 3
Immunohistochemistry on human thyroid cancer specimens
26 thyroid carcinoma samples (8 PTCs, 10 FTCs and 8 PDC/ATCs) were analysed by using immunohistochemical staining with a specific anti-human AXL antibody. AXL positivity was observed mainly in tumoral cells. Gas6 staining was cytosolic and was mainly found in carcinoma cells but also a stromal positivity was displayed.

FIGURE 4
Axl/Tyro3-Gas6 axis blockade inhibits TPC1 cell proliferation and survival

- **A)** TPC1 cells were serum-deprived for 12h and, where indicated, treated with GAS6 (200ng/ml) and/or the blocking chimaeric protein Dtk/FC for 24h (left panel). As shown in the right panel, TPC1 were silenced for AXL or TYRO3 receptors; after 24h of silencing, cells were serum-deprived for 12h and then treated or not with GAS6 for 24h. Gas6 stimulated BrdU incorporation of TPC1

cells and this effect was blocked by the Dtk/FC protein. Consistently, AXL and TYRO3 silencing inhibited TPC1 BrdU incorporation. BrdU was added two hours before the reaction was stopped, and cells were processed for immunofluorescence. The results are expressed as percentage of BrdU incorporation with respect to untreated and sictr-silenced TPC1 cells, respectively. The average results and the standard deviations of three independent experiments in which at least 400 cells were counted are reported.

B) The indicated cell line was treated with a proapoptotic sunstance DEM (DiEthylMaleate) for 12h and then with GAS6 and/or Dtk/FC for 24h; in these conditions, Gas6 decreased the percentage of TPC1 apoptotic cells and Dtk/FC reverted this effect (left panel). Accordingly, when TPC1 were serum-deprived and AXL, TYRO3 or both were silenced, the percentage of apoptotic cells increased (right panel). The percentage of apoptotic cells was evaluated with the TUNEL reaction. The results are expressed as percentage of apoptotic cells. The average results and S.D. of three independent experiments in which at least 400 cells were counted is reported.

C) Western blot analysis to verify AXL-TYRO3 silencing with anti-AXL and anti-TYRO3 antibodies. Anti-tubulin monoclonal antibody was used as a control for equal protein loading.

FIGURE 5

Axl/Tyro3-Gas6 axis blockade inhibits NIM cell proliferation and survival.

A) NIM cell lines were serum-deprived and then treated with GAS6 and Dkt/FC as indicated in left panel. BrdU incorporation was evaluated in presence or absence of human recombinant GAS6. Dtk/FC inhibited DNA synthesis of NIM cells but exogenous Gas6 didn't modify the percentage of BrdU incorporation (left panel). Moreover, as shown in the right panel, NIM were silenced for AXL, TYRO3 and GAS6; AXL-, TYRO3- and much more evident Gas6-silencing strongly affected NIM BrdU incorporation. BrdU was added two hours before the reaction was stopped, and cells were processed for immunofluorescence. The results are expressed as percentage of BrdU incorporation with respect to untreated and sictr-silenced NIM cells,respectively. The average results and the standard deviations of three independent experiments in which at least 400 cells were counted are reported.

B) NIM cell line was treated with the proapoptotic sunstance DEM (DiEthylMaleate) and then with GAS6 and Dtk/FC (left panel). Gas6, as expected, did not modify NIM apoptotic rate while the Dtk/FC protein increased the percentage of apoptotic cells and the addition of exogenous Gas6 reverted this effect. NIM cells were serum deprived after AXL, TYRO3(individually or both) and Gas6 silencing. In these conditions,the prencentage of apoptotic cells

increased and exogenous Gas6 reverted this effect (right panel). The percentage of apoptotic cells was evaluated with the TUNEL reaction. The results are expressed as percentage of apoptotic cells. The average results and S.D. of three independent experiments in which at least 400 cells were counted is reported.

C) Western blot analysis to verify Axl- Tyro3-GAS6 silencing with anti-AXL, anti-TYRO3 and anti-GAS6 antibodies. Anti-tubulin monoclonal antibody was used as a control for equal protein loading.

FIGURE 6

Axl/Tyro3-Gas6 axis blockade also inhibits ATC cell proliferation and survival.

A) 8505-C were silenced for AXL receptor and BrdU incorporation was evaluated. Gas6 stimulated 8505C BrdU incorporation while siAXL inhibeted. Gas6 reverted this effect. BrdU was added two hours before the reaction was stopped, and cells were processed for immunofluorescence. The results are expressed as percentage of BrdU incorporation with respect to sictr-silenced. 8505-C cells. The average results and the standard deviations of three independent experiments in which at least 400 cells were counted are reported.

B) 8505C cell line was subjected to AXL silencing and serum-deprivation. AXL silencing increased the percentage of apoptotic cells and Gas6 reverted this effect. The percentage of apoptotic cells was evaluated with the TUNEL reaction. The results are expressed as percentage of apoptotic cells. The average results and S.D. of three independent experiments in which at least 400 cells were counted is reported.

C) Western blot analysis to verify Axl silencing with an anti-AXL antibody. Anti-αtubulin monoclonal antibody was used as a control for equal protein loading.

FIGURE 7

Biological effects of stable silencing of Axl in 8505-C ATC cells.

A) Screening of cell clones (8505-C shAXL) by Western blot analysis with an anti-AXL antibody. Anti-tubulin monoclonal antibody was used as a control for equal protein loading.

B) Growth curves on screened 8505-C clones. Cells were plated at a density of 0.5×10^5 in complete (10% FCS) (left panel) or in low serum conditions (2.5% FCS) (right panel), harvested and counted at the indicated time-points. The average results of at least three independent determinations were reported.

C) BrdU-incorporation was measured to evaluate S-phase entry of stably silenced clones. AXL silencing decreased the percentage of BrdU-positive cells. Cells were grown on coverslips, and kept in serum-

deprivation conditions for 12h. BrdU was added two hours before the reaction was stopped, and cells were processed for immunofluorescence. The average results and the S.D. of three independent experiments in which at least 400 cells were counted are reported.

D) TUNEL reaction was performed on cell clones to evaluated the proapoptotic effect of AXL stable silencing. Cells were serum-deprived for 12h and then processed for TUNEL assay. AXL silencing increased the percentage of apoptotic cells. The results are expressed as percentage of apoptotic cells. The average results and S.D. of three independent experiments in which at least 400 cells were counted is reported.

FIGURE 8
Matrigel invasion on 8505-C shAXL

A) Cells were added to the upper chamber of a pre-hydrated polycarbonate membrane filter of 8 μM pore size coated with 35 μg Matrigel. The lower chamber was filled with complete medium or 2.5% FCS (as indicated). Triplicated samples were analyzed at 570 nM with an ELISA reader (Model 550 microplate reader, Bio-Rad). The results were expressed as percentage of migrating cells with respect to the unsilenced ones.

B) Densitometric analysis of Matrigel invasion assay was reported. AXL silencing inhibited Matrigel invasion in low-serum conditions.

FIGURE 9
Tumorigenicity of 8505-C shAxl in ATC cell xenografts.
Three groups of mice (4-week-old male BALB/c nu/nu mice) were inoculated subcutaneously into the right dorsal portion with 8505-C shCTR cells ($10x10^6$/mouse), 8505-C shAXL CL1($1x10^6$/mouse), 8505-C shAXL CL2($1x10^6$/mouse), respectively Tumor diameters were measured at regular intervals with a caliper. Tumor volumes (V) were calculated with the formula: V= A x B2/2 (A=axial diameter; B= rotational diameter). 8505C tumor growth was strongly impaired in shAXL clones with respect to shCTR. Unpaired Student's T test (normal distributions and equal variances) was applied. All P values were two sided,and differences were statistically significant at $P < 0.05$.

TABLE 1
Percentage of AXL and GAS6 positivity in the panel of human thyroid cancer specimens analysed by immunohistochemistry.

FIGURE 1

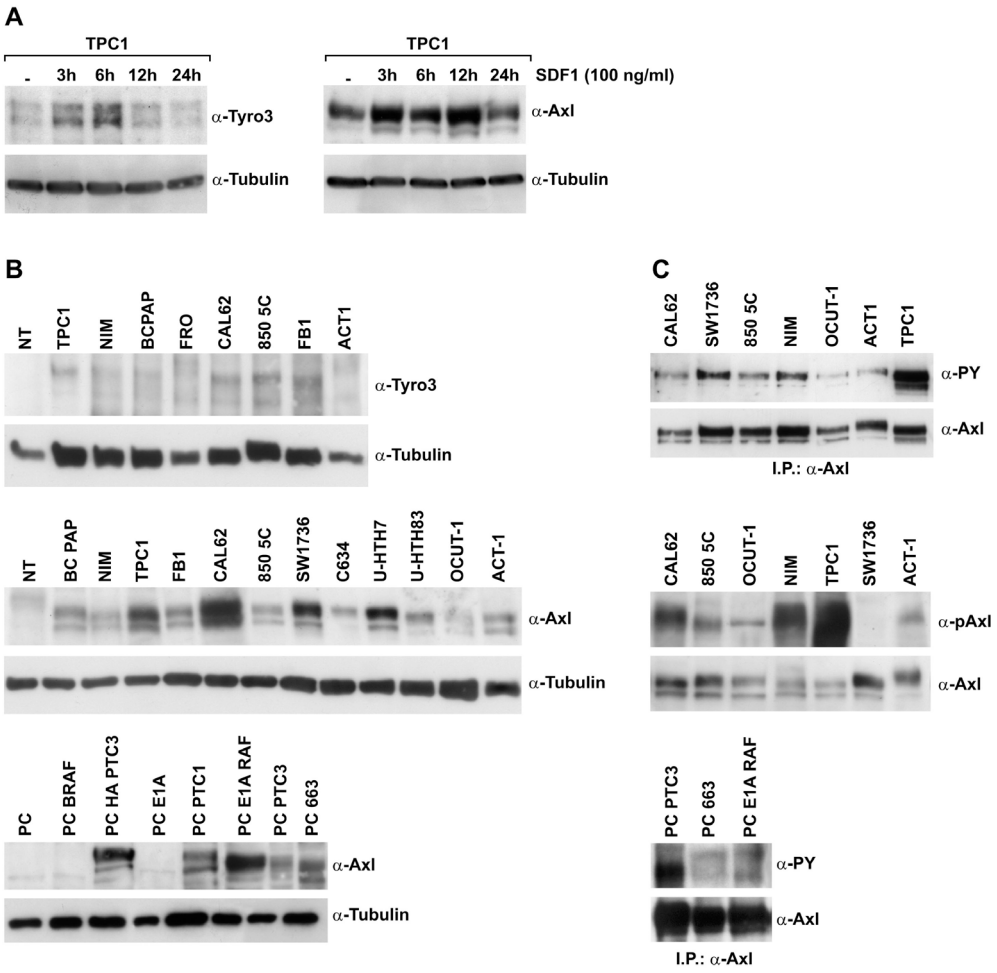
A
TPC1
- 3h 6h 12h 24h
α-Tyro3
α-Tubulin
TPC1
- 3h 6h 12h 24h SDF1 (100 ng/ml)
α-Axl
α-Tubulin
B
NT TPC1 NIM BCPAP FRO CAL62 850 5C FB1 ACT1
α-Tyro3
α-Tubulin
NT BC PAP NIM TPC1 FB1 CAL62 850 5C SW1736 C634 U-HTH7 U-HTH83 OCUT-1 ACT-1
α-Axl
α-Tubulin
PC PC BRAF PC HA PTC3 PC E1A PC PTC1 PC E1A RAF PC PTC3 PC 663
α-Axl
α-Tubulin
C
CAL62 SW1736 850 5C NIM OCUT-1 ACT1 TPC1
α-PY
α-Axl
I.P.: α-Axl
CAL62 850 5C OCUT-1 NIM TPC1 SW1736 ACT-1
α-pAxl
α-Axl
PC PTC3 PC 663 PC E1A RAF
α-PY
α-Axl
I.P.: α-Axl

FIGURE 2

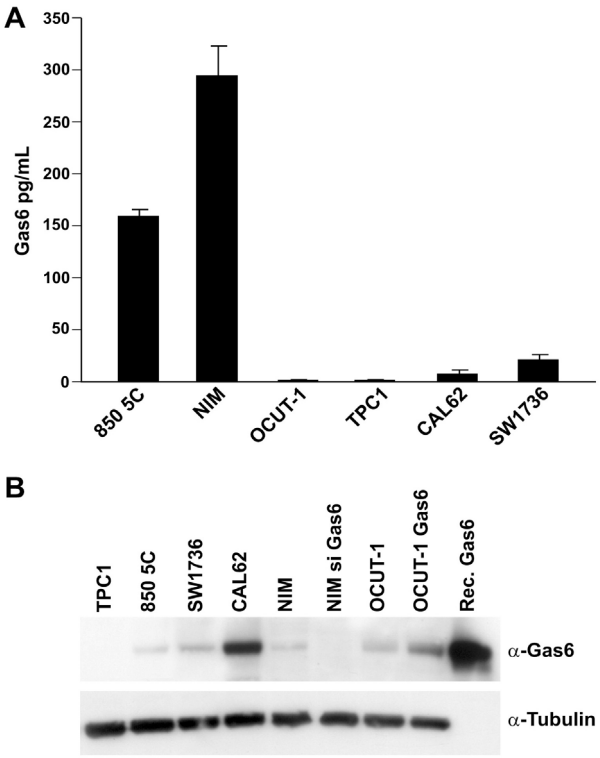
A
Gas6 pg/mL
350
300
250
200
150
100
50
0
850 5C
NIM
OCUT-1
TPC1
CAL62
SW1736
B
TPC1
850 5C
SW1736
CAL62
NIM
NIM si Gas6
OCUT-1
OCUT-1 Gas6
Rec. Gas6
α-Gas6
α-Tubulin

FIGURE 3

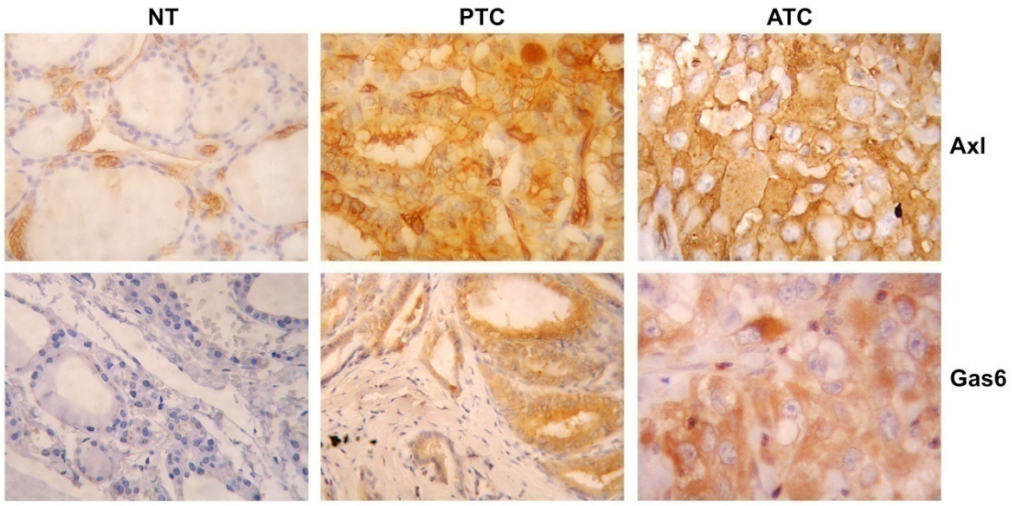

FIGURE 4

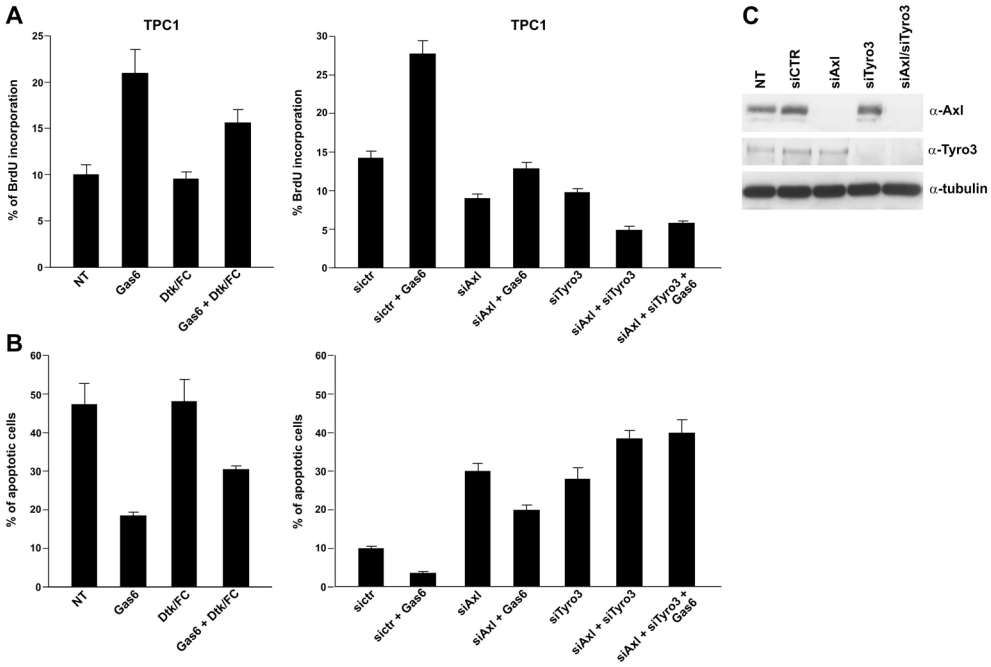
A
TPC1
% of BrdU incorporation
NT
Gas6
Dtk/FC
Gas6 + Dtk/FC
TPC1
% BrdU incorporation
sictr
sictr + Gas6
siAxl
siAxl + Gas6
siTyro3
siAxl + siTyro3
siAxl + siTyro3 + Gas6
B
% of apoptotic cells
NT
Gas6
Dtk/FC
Gas6 + Dtk/FC
% of apoptotic cells
sictr
sictr + Gas6
siAxl
siAxl + Gas6
siTyro3
siAxl + siTyro3
siAxl + siTyro3 + Gas6
C
NT
siCTR
siAxl
siTyro3
siAxl/siTyro3
α-Axl
α-Tyro3
α-tubulin

FIGURE 5

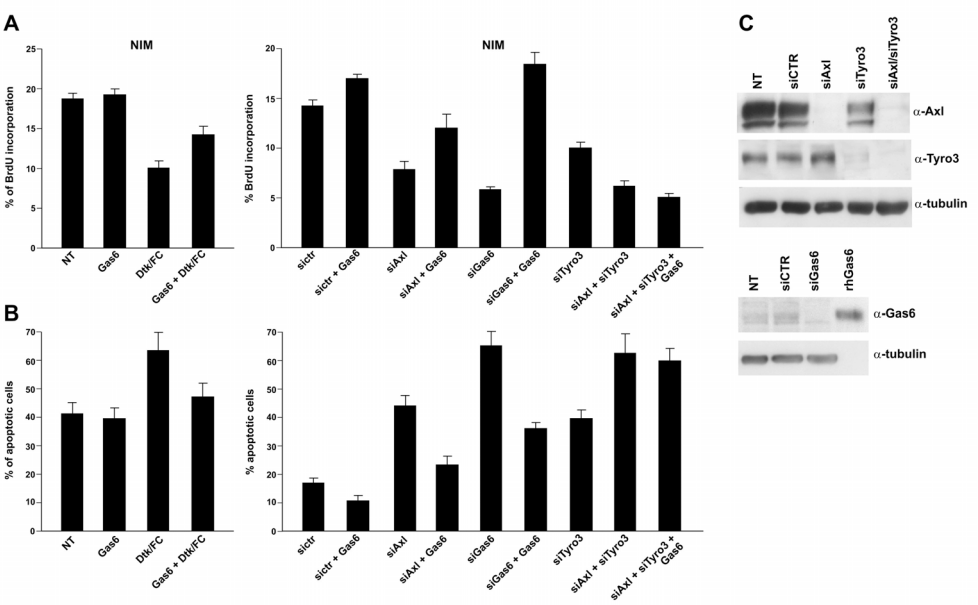
A
NIM
% of BrdU incorporation
NT
Gas6
Dtk/FC
Gas6 + Dtk/FC
NIM
% BrdU incorporation
siCtr
siCtr + Gas6
siAxl
siAxl + Gas6
siGas6
siGas6 + Gas6
siTyro3
siAxl + siTyro3
siAxl + siTyro3 + Gas6
B
% of apoptotic cells
% apoptotic cells
C
NT
siCTR
siAxl
siTyro3
siAxl/siTyro3
α-Axl
α-Tyro3
α-tubulin
NT
siCTR
siGas6
rhGas6
α-Gas6
α-tubulin

FIGURE 6

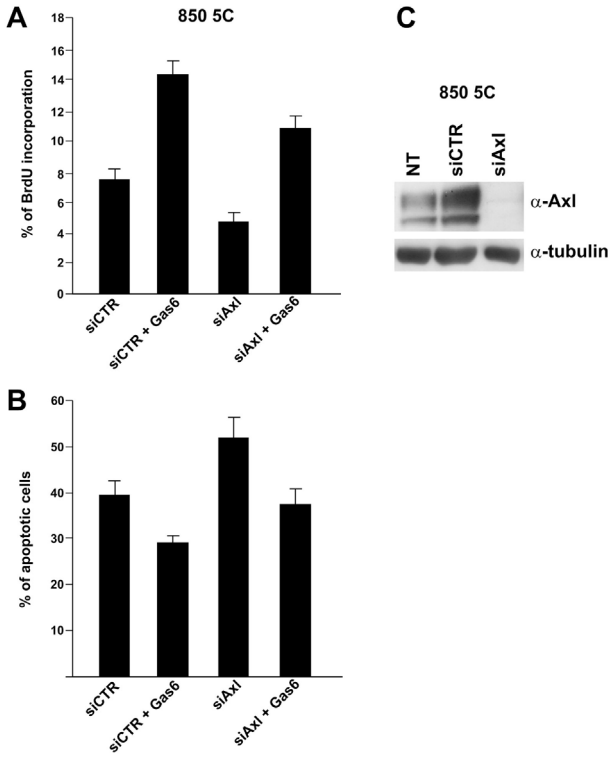
A
850 5C
% of BrdU incorporation
18
16
14
12
10
8
6
4
2
0
siCTR
siCTR + Gas6
siAxl
siAxl + Gas6
B
% of apoptotic cells
60
50
40
30
20
10
siCTR
siCTR + Gas6
siAxl
siAxl + Gas6
C
850 5C
NT
siCTR
siAxl
α-Axl
α-tubulin

FIGURE 7

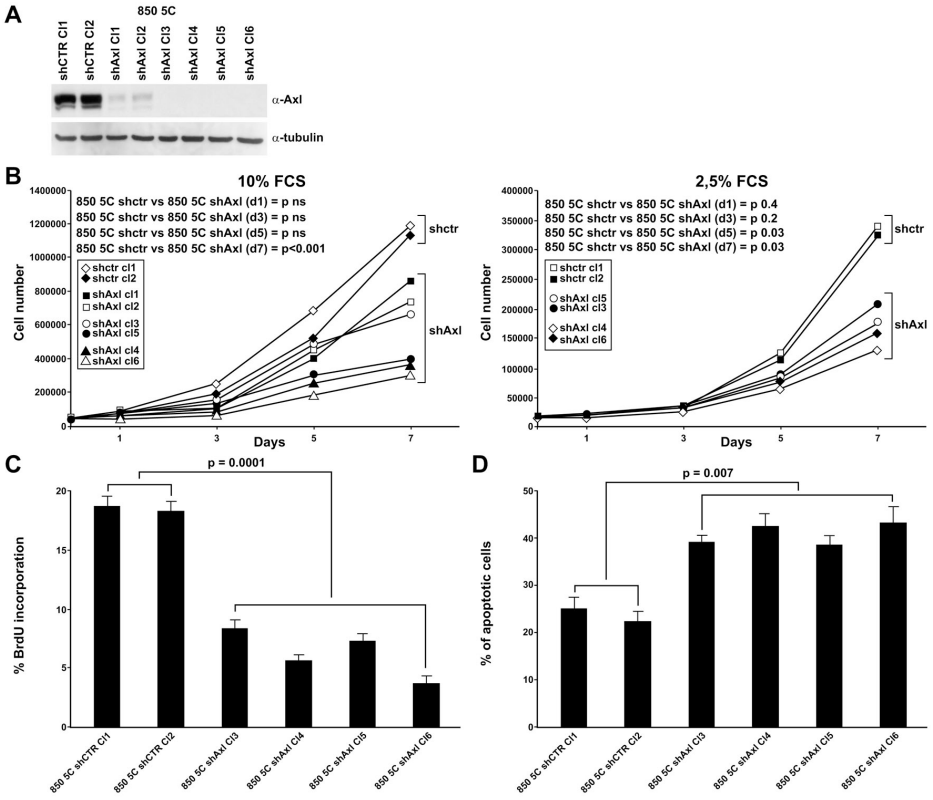
A
850 5C
shCTR Cl1
shCTR Cl2
shAxl Cl1
shAxl Cl2
shAxl Cl3
shAxl Cl4
shAxl Cl5
shAxl Cl6
α-Axl
α-tubulin
B
10% FCS
850 5C shctr vs 850 5C shAxl (d1) = p ns
850 5C shctr vs 850 5C shAxl (d3) = p ns
850 5C shctr vs 850 5C shAxl (d5) = p ns
850 5C shctr vs 850 5C shAxl (d7) = p<0.001
shctr cl1
shctr cl2
shAxl cl1
shAxl cl2
shAxl cl3
shAxl cl5
shAxl cl4
shAxl cl6
shctr
shAxl
Cell number
Days
2,5% FCS
850 5C shctr vs 850 5C shAxl (d1) = p 0.4
850 5C shctr vs 850 5C shAxl (d3) = p 0.2
850 5C shctr vs 850 5C shAxl (d5) = p 0.03
850 5C shctr vs 850 5C shAxl (d7) = p 0.03
C
p = 0.0001
% BrdU incorporation
D
p = 0.007
% of apoptotic cells
850 5C shCTR Cl1
850 5C shCTR Cl2
850 5C shAxl Cl3
850 5C shAxl Cl4
850 5C shAxl Cl5
850 5C shAxl Cl6

FIGURE 8

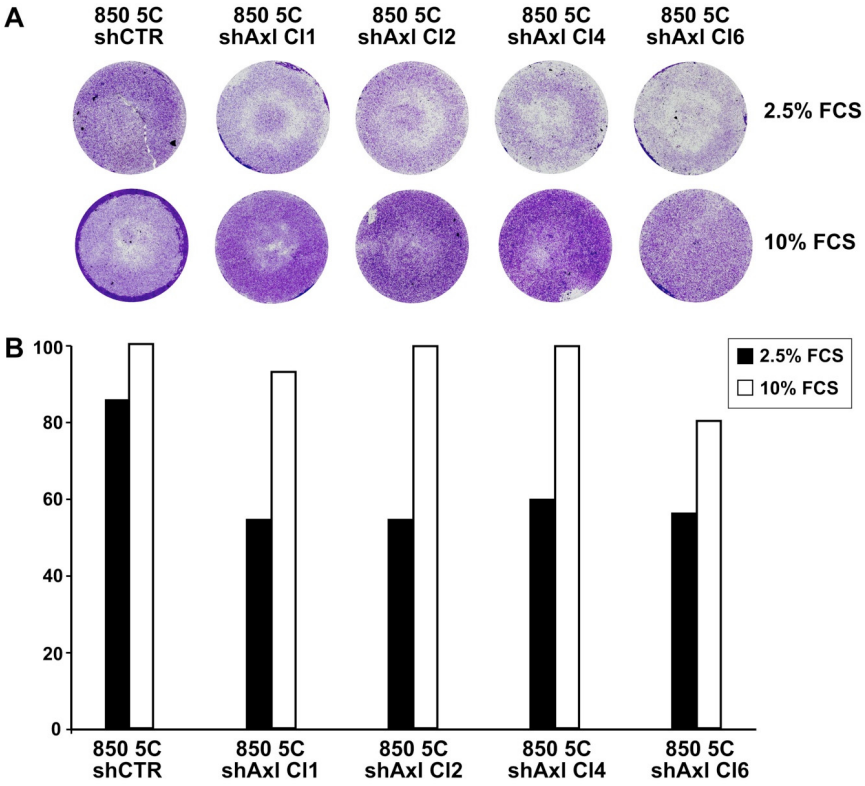
A
850 5C shCTR
850 5C shAxl Cl1
850 5C shAxl Cl2
850 5C shAxl Cl4
850 5C shAxl Cl6
2.5% FCS
10% FCS
B
100
80
60
40
20
0
2.5% FCS
10% FCS
850 5C shCTR
850 5C shAxl Cl1
850 5C shAxl Cl2
850 5C shAxl Cl4
850 5C shAxl Cl6

FIGURE 9

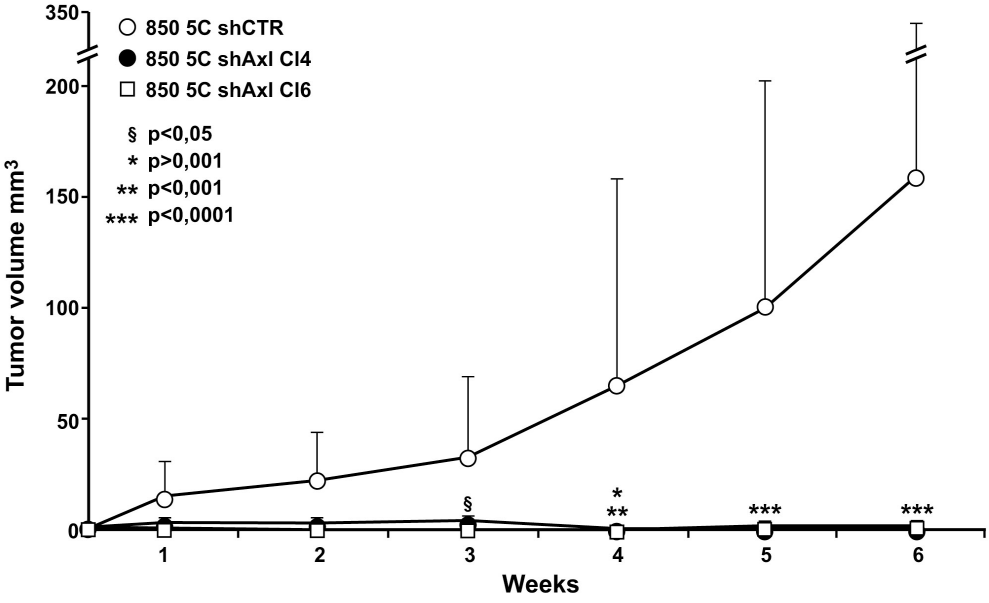
350
200
150
100
50
0
Tumor volume mm3
850 5C shCTR
850 5C shAxl Cl4
850 5C shAxl Cl6
§ p<0,05
* p>0,001
** p<0,001
*** p<0,0001
§
*
**
***
***
1
2
3
4
5
6
Weeks

TABLE 1

Sample	% Axl positivity	% Gas6 positivity
PTC	60%	ND
PTC	20%	20%
PTC	60%	40%
PTC	40%	10%
PTC	0%	10%
PTC	30%	40%
PTC	80%	30%
PTC	10%	10%
PTC	40%	0%
FTC	0%	0%
FTC	30%	0%
FTC	20%	0%
FTC	60%	20%
FTC	60%	10%
FTC	0%	0%
FTC	0%	20%
FTC	0%	20%
FTC	10%	10%
FTC	10%	10%
PDC	10%	30%
ATC	60%	50%
ATC	40%	60%
ATC	0%	30%
PDC	0%	40%
PDC	30%	0%
PDC	30%	30%
ATC	10%	60%